Anatomical and methodological descriptions leading to optimize corneal refractive surgery procedures

Imène Salah-Mabed

▶ **To cite this version:**

Imène Salah-Mabed. Anatomical and methodological descriptions leading to optimize corneal refractive surgery procedures. Bioengineering. Université Paris Saclay (COmUE), 2018. English. NNT : 2018SACLS164 . tel-01895622

HAL Id: tel-01895622

https://theses.hal.science/tel-01895622

Submitted on 15 Oct 2018

HAL is a multi-disciplinary open access archive for the deposit and dissemination of scientific research documents, whether they are published or not. The documents may come from teaching and research institutions in France or abroad, or from public or private research centers.

L'archive ouverte pluridisciplinaire **HAL**, est destinée au dépôt et à la diffusion de documents scientifiques de niveau recherche, publiés ou non, émanant des établissements d'enseignement et de recherche français ou étrangers, des laboratoires publics ou privés.

université PARIS-SACLAY

NNT: 2018SACLS164

Thèse de doctorat

Descriptions anatomiques et méthodologiques aux fins d'optimisation de techniques de chirurgie cornéenne à visée réfractive

Thèse de doctorat de l'Université Paris-Saclay
Préparée à l'université Paris Sud
Laboratoire d'Optique Appliquée (LOA)
ENSTA ParisTech, École Polytechnique, CNRS UMR 7639

École doctorale n°572 Ondes et Matière (EDOM)
Spécialité de doctorat : Milieux dilués et optique fondamentale

Thèse présentée et soutenue à Palaiseau, le 22 Juin 2018, par

Imène SALAH-MABED

Composition du Jury :

Nathalie WESTBROOK, Professeure. IOGS, Palaiseau	Président du jury
Florent APTEL, PU-PH. CHU Grenoble Alpes	Rapporteur
Holger LUBATSCHOWSKI, Professeur. Dr, CEO Rowiak, Hanovre	Rapporteur
Marie-Claire SCHANNE-KLEIN, Directeur de recherche. Ecole Polytechnique, Palaiseau	Examinateur
Karsten PLAMANN, Professeur de l'ENSTA ParisTech, Palaiseau	Directeur de thèse
Damien GATINEL, Docteur en médecine. Fondation Ophtalmologique Adolphe de Rothschild, Paris	Co-Directeur de thèse

Table of Contents

Acknowledgment

The day when I would be writing my thesis acknowledgment, seemed very far to me and even utopian, at the time when after having worked for three years in a private ophthalmological practice as an optometrist, I wanted to direct my professional paths towards clinical research.

I knocked on the door of Dr. Damien Gatinel, who encouraged me to pursue a PhD. The quest for a research allowance was challenging but proved possible thanks to some luck and perseverance. The choice to leave the known for the unknown was not easy, but today, I am very happy of the road I have taken. This thesis represented for me an exceptionally stimulating and enriching experience. I had a lot of fun trying to understand the laws of interaction between nature and technology, as well as to discover the world of researchers, so varied, rewarding and generous towards me.

Firstly, I would like to express my sincere gratitude to my supervisors, Dr. Damien Gatinel and Prof. Karsten Plamann, for sharing with me their immense knowledge and their rigorous and professional guidance.

Dr Gatinel, thank you for giving me the chance to join your team at the Rothchild Foundation, for your trust, patience and motivation. I could not have imagined having a better advisor and mentor for my PhD study.

Prof. Plamann, thank you for accepting to supervise my work during its latest phases. Your guidance, kindness and positive attitude were of an immense help during all the time of writing this thesis.

Besides my supervisors, I would also like to thank Prof. Florent Aptel, Prof. Dr. Holger Lubatschowski, Dr. Marie-Claire Schanne-Klein and Prof. Nathalie Westbrook, for accepting to join my thesis committee.

Thank you to my fellow lab mates, Kelly and David, for the stimulating discussions, for all the fun we had in the last couple of years and for their support during the more challenging times. I will always remember our lengthy discussions and political debates around the coffee machine…

Thank you to Lucie and Romain, my lab mates during the last couple of months of my thesis for their warm welcoming.

Thank you to my colleagues at the Rothschild Foundation, Alain, who guided me to discover the world of cornea, Emmanuel, for his humility, patience, kindness, and the great working experience I had with him. Christophe for his medical contribution to my work and for our funny conversations. Guillaume for his availability and the relevance

of his suggestions. Alice and Romain for their professionalism. Thank you to Evelyne and Hanna, who always kept their door open to me and whose kindness, availability and sympathy helped me to progress in this project. Hélène, Emmanuelle, Justine, Agnès, Marine, Mathilde, Isabelle H, Grégory, Sébastien, Sourilla, Stéphanie, Ludivine, Isabelle M and all the residents and interns. Your kindness and professionalism were very important in this project. Thank you to all the patients who participated in the different studies of my research, to the technical teams of the Rothschild Foundation, in particular to the IT department who contributed to the advancement and success of this project, being always very effective and patient with me.

Finally, I would like to thank my family. My parents and three sisters for their support. Nothing would have been possible without them; and last but not least to my husband Nabil, and our three boys, Camil, Amir and Elias, for their tremendous support throughout my research, the writing of this thesis and in my life in general.

Finally, I would like to thank in advance all the readers who will be interested in this work and its continuation.

Figures and Tables

Abbreviations

ATR: Against The Rule
CH: Corneal Hysteresis
CRF: Corneal Resistance Factor
CCS: Corrected Contrast Sensitivity
CS: Contrast Sensitivity
CSB: Corrected Sensitivity to Blur
D: Dioptre
DOF: Depth of Field
EX500: WaveLight® EX500 (Alcon® Laboratories Inc., USA)
FS200: WaveLight® FS200 (Alcon® Laboratories Inc., USA)
FT: Fourier Transform
GAG: Glycosaminoglycans
HOAs: High Order Aberrations
IOL: Intraocular Lense
IOP: Intraocular Pressure
IOP_{cc}: Corrected Intra Ocular Pressure
IOP_{g}: Goldman Intra Ocular Pressure
KC: Keratoconus Corneas
KCS: Keratoconus Suspected Corneas
LASIK: Laser-Assisted In-Situ Keratomileusis
LCA: Longitudinal Chromatic Aberration
LOAs: Low Order Aberrations
MAR: Minimum Angle of Resolution
MTF: Modulation Transfer Function
OPD: Optical Path Difference
OTF: Optical Transfer Function
PhD: Philosophiae Doctor
PRK: Photorefractive Keratectomy
PSF: Point Spread Function
PTF: Phase Transfer Function
RMS: Root Mean Square
Rothschild Foundation: Fondation Ophtalmologique Adolphe de Rothschild, 29 rue Manin 75019 Paris, France
SMILE: Small Incision Lenticule Extraction
TCA: Transverse Chromatic Aberration
UDVA: Uncorrected Distance Visual Acuity
UV: Ultraviolet
VA: Visual Acuity
CDVA: best Corrected Distance Visual Acuity
WTR: With The Rule

Introduction

Scientific context

Glasses and contact lenses are the most commonly-used correction tools for myopia and other optical aberrations. However, laser-assisted refractive surgery was introduced c. 30 years ago when Marguerite McDonald performed the first PRK and has since turned into a major field of ophthalmology in developed countries. It is expected to grow significantly because of the increasing prevalence of myopia.

The advent of femtosecond lasers represented a breakthrough in corneal refractive surgery. Nowadays, the most widely-used laser-assisted refractive surgery technique for correcting ametropia is the Laser-Assisted In-Situ Keratomileusis (LASIK) which is performed in three main steps: first a hinged flap is cut thanks to a femtosecond laser and folded back, revealing the corneal stroma; second, an excimer laser remodels the stromal layer tissue to correct focusing errors of the eye; finally, the flap is unfolded back.

The number of procedures of laser-assisted refractive surgery and phakic IOL implantation in the world is estimated at c. 3.6 million in 2017. It is expected to grow at a compounded annual rate of 5.2 percent until 2022 to reach 4.6 million (Refractive surgery report: a global market analysis for 2016 to 2022, 2017). The use of femtosecond laser is expected to grow with a rate of 15.5 percent to reflect the dominant place of LASIK and the increase in popularity of the newly emerged small incision lenticule extraction (SMILE) technique which has secured crucial approvals in the US and Europe and is gaining in popularity in India and China.

The increased number of procedures is accompanied by constant improvements in the surgical techniques as many issues are still to be addressed. The main challenge of our work is to better understand the evolution and role of factors affecting post-surgical visual quality. This would permit to enhance and customize operative techniques, and thus optimize the optical and visual results of refractive surgery.

To achieve this objective it is important to understand the various mechanisms and anatomical and ocular factors involved in refractive surgery and question the interactions between them. We can also ask ourselves, what effects do these parameters produce on the visual performance of the operated eye? Are there factors which are endogenous to the human eye that affect postoperative performance?

Objectives

The objective of this thesis is to provide practical recommendations to surgeons with the aim to optimize the performance of their surgical routines. The project has been executed by covering the following phases:

- The investigation of pupil dynamics in different contexts of refractive corneal surgeries;
- The assessment of the impact of the epithelium on the topography of normal, keratoconus (KC) and keratoconus suspected (KCS) corneas;
- The evaluation of changes in anatomical parameters of the eye, visual performances and subjective quality of vision after a myopic LASIK was performed with the WaveLight® Refractive Suite (Alcon® Laboratories Inc., USA).

The project included six clinical studies and was first directed by Dr. Richard Legras (Laboratoire Aimé Cotton), followed by Prof. Karsten Plamann, during its last six months. All the experiments were conducted in the Cataract and Refractive surgery department of the Rothschild Foundation under the direction of Dr. Damien Gatinel.

Organization

The dissertation is composed of two main parts. First, a literature review on the subject is provided, then the second part focuses on the experiments.

- **Chapter 1** provides a description of the anatomy of the eye and its optical properties. The nature of visible light and the physical process leading to the formation of the image and the associated aberrations are reviewed. It also explores the means of assessment of visual quality which is a combination of optical and neural factors and of subjective and psychological factors.
- **Chapter 2** defines refractive surgery and describes the key historic milestones in the development of this field of ophthalmology. A classification of the different techniques and a description of the current socio-economic importance and outlooks of laser-assisted techniques are also proposed.
- **Chapter 3** describes the general methodology and materials used in our six studies. The outcomes of these studies have been reported in scientific articles which have been published in ophthalmology publications or were under review by an editor when this thesis manuscript was finalised. Each article was included in this thesis as a separate (sub)-chapter with no modification

compared to the published version except the numbering of the tables, figures and references which has been amended to follow the order of this manuscript.

- **Chapter 4** addresses the pupil dynamics in refractive surgery through 3 studies. We first assessed prospectively the intra-session repeatability of pupillometric measurements using infrared pupillometry. Then, we tried to determine whether there is a systematic variation of the position of the pupil centre when the diameter of the pupil varies. The change in the position of the pupil centre in relation to other parameters (age, sex, refractive error, etc.) was also investigated. In this study, we used an infrared dynamic pupillometry device, the WaveLight® Topolyzer^{TM} VARIO (Alcon® Laboratories Inc., USA), in mesopic and photopic conditions. The measured distance between the corneal vertex (first Purkinje image) and the pupil centre in the two illumination conditions was also analyzed. Finally, we explored pupil dynamics in hyperopic and myopic eyes under mesopic and photopic conditions before, one month and 3 months after cataract surgery. Several parameters (pupil diameter, corneal astigmatism, anterior chamber depth, axial length and pachymetry) were analysed.
- **Chapter 5** includes a comparison of the epithelium and the Bowman's layer specular topographies in patients having low to moderate myopia corrected by PRK. The aim of this study was to explore the shape of the Bowman's layer by analysing three topographic components (keratometry, astigmatism and asphericity), with a Placido topographer - OPD-Scan® II (Nidek®, Japan) - on three concentric zones. In the second part of this chapter, we compared normal and keratoconic corneas with the same criteria. The purpose of this study was to explore the impact of the epithelium on the keratoconus (KC) and keratoconus suspected (KCS) corneas and to assess the existence of a potential predictive preoperative factors that differentiate the normal and the abnormal corneas before epithelium removal.
- In **Chapter 6,** we proposed to evaluate changes in anatomical parameters of the eye, visual performances and quality of vision after a LASIK refractive surgery performed with the WaveLight® Refractive Suite (Alcon® Laboratories Inc., USA). We present anatomical changes, biomechanical corneal response, visual performances (visual acuities, contrast sensitivities, depth of focus), total and corneal aberrations and patients' satisfaction before and after LASIK. We

also tried to correlate all these parameters to obtain a more exhaustive view of the present outcomes of moderate to high myopic LASIK surgery with the above-mentioned devices.

- The **Conclusion and perspectives** chapter provides a summary of the practical recommendations to surgeons resulting from this thesis as well as an overview of possible further investigations.

Chapter 1: Optics of the human eye

The human eye is an optical system which includes two refracting elements, the cornea and the lens, and a light receptor, the retina. When light enters the eye, refraction happens due to the step in refractive index at the two surfaces of the cornea (anterior and posterior), the two surfaces of the crystalline lense as well as the gradient in refractive index within the lens. The quality of the image at the retina is function of the transparency, curvature and refractive indices of these elements.

The eye is far from being a "perfect" optical system (with respect to typical quality criteria in optical engineering) and imperfections of the refractive surfaces are a source of ocular aberrations. Other phenomena such as the specular reflection, absorption, scattering and diffraction also influence the formation of the image. Visual acuity is also dependent on the performance of the photoreceptors of the retina.

In this chapter, we will discuss the nature of the visible light as well as the physical processes leading to the formation of the image and the associated aberrations. We will also explore the means of assessment of visual quality which is a combination of optical and neural factors and of subjective and psychological factors.

1.1 Overview of the human eye

1.1.1 Anatomy of the human eye

The structure of the human eye is shown in Figure 1.

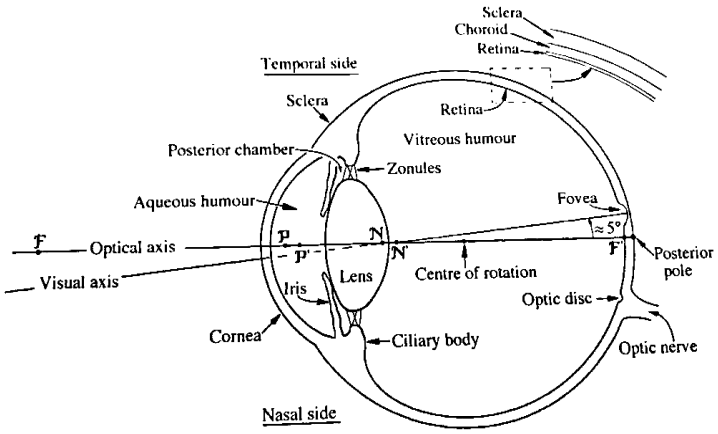

Figure 1 The structure of the human eye (Atchinson & Smith, Optics of the Human Eye, 2002)

The **cornea** represents the front part of the eye. It is transparent and has a quasi-spherical shape with a radius of curvature of c. 8 mm (Atchinson & Smith, Optics of

the Human Eye, 2002). The refractive power of the cornea accounts for c. 75% of the total refractive power of the eye (Atchinson & Smith, Optics of the Human Eye, 2002).
The **sclera** is a dense, white, opaque, fibrous tissue which protects the eye. It is the posterior casing of the eye, the cornea being the front one. The sclera is formed of collagen and other elastic fibre. It has a quasi-spherical form with a radius of curvature of c. 12 mm (Atchinson & Smith, Optics of the Human Eye, 2002).
The **iris** is the aperture stop of the eye. It is a circular shaped structure determining the level of light entering in the posterior part of the eye through the control of the size of the opening hole located in its centre which is called **pupil**.
The **anterior chamber** is the space between the posterior part of the cornea and the iris. It includes the **aqueous humour**.
The **crystalline lens** or lens is a transparent, biconvex structure which is responsible for the accommodation function of the eye. By changing its shape, the lens changes the focal distance of the eye so that it can focus on objects at various distances. The refractive power of the lens accounts for c. 25% of the total refractive power of the eye (Atchinson & Smith, Optics of the Human Eye, 2002).
The **posterior chamber** is located between the iris, the **ciliary body** and the crystalline lens.
The **retina** is the light-sensitive tissue forming the back of the eye as indicated in the Figure. It consists of cellular and pigmented layers and a nerve fibre layer.
The vitreous chamber is the space between the crystalline lens and the retina. It contains a transparent gelatinous material called the **vitreous humour**.

1.1.2 The cornea

Anatomical structure

The cornea is the avascular and transparent tissue representing the front part of the eye. It is in direct contact with the outside air. Its anterior face is covered by the tear film, while its posterior face is immersed in the aqueous humour which fills the anterior chamber.
The shape of the cornea is convex, which gives it a refractive power. The adult cornea measures 11 to12 mm horizontally and 9 to 11 mm vertically (Atchinson & Smith, Optics of the Human Eye, 2002). Its thickness is c. 0.5 mm at the centre and increases progressively towards the periphery to achieve 0.7 mm (Atchinson & Smith, Optics of the Human Eye, 2002). The main functions of the cornea are the protection of the eye, the transmission of light into the eye (transparency), and the refraction power to form

the image. Figure 2 describes the different layers of the cornea.

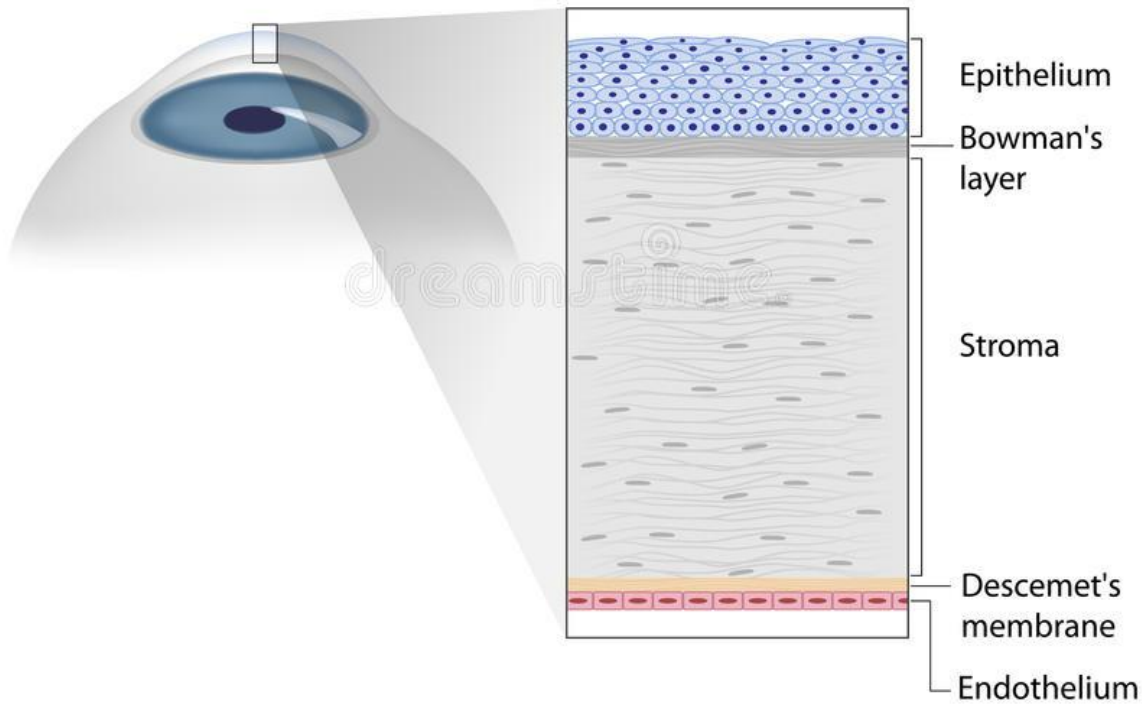

Figure 2 The structure of the cornea (www.dreamstime.com, 2018)

The **tear film** is 4-7 µm thick and composed of oily, mucous and aqueous layers, the later representing 98% of the thickness (Atchinson & Smith, Optics of the Human Eye, 2002). While it does not contribute significantly to the refractive power of the cornea, it is essential for clear vision as it moistens the cornea and constitutes a smooth and regular surface. When the tear film dries out, the transparency of the cornea decreases significantly (Atchinson & Smith, Optics of the Human Eye, 2002).

The tear film is inseparable from the **corneal epithelium**. It is c. 50 µm thick i.e. c. 10% of the total thickness of the cornea (Atchinson & Smith, Optics of the Human Eye, 2002) and consists of 6 layers of cells among which only the innermost layer can divide. It protects the rest of the cornea by providing a barrier against water and toxic substances and has important optical functions which are addressed later in this thesis.

Bowman's layer is 8 to 14 µm thick and consists of randomly arranged collagen fibrils. It does not regenerate after injury or rupture, leaving an opaque fibrous scar. Its absence in these cases does not appear to disturb the organization of the epithelial or stromal layers (Atchinson & Smith, Optics of the Human Eye, 2002).

The **stroma** is a c. 500 µm thick (c. 90 % of the corneal thickness) dense connective tissue of remarkable regularity which ensures the transparency and structural

strength of the cornea (Atchinson & Smith, Optics of the Human Eye, 2002). It is almost acellular as all the cells included in the stroma represent only 2 to 3 % of its total volume, the rest of this volume being occupied by collagen fibrils organized in lamellae. The corneal stroma consists predominantly of 2 µm thick, flattened, collagenous lamellae (200–250 layers) oriented parallel to the corneal surface and continuous with the sclera at the limbus. The collagen fibrils are predominantly of type I (30 nm diameter, 64–70 nm banding) with some type III, V and VI also present (Forrester, Dick, McMenamin, Roberts, & Pearlman, 2016). The transparency of the cornea is highly dependent on the regular diameter and spacing of the collagen fibrils, which is regulated by glycosaminoglycans (GAG) and proteoglycans forming bridges between the collagen fibrils (Forrester, Dick, McMenamin, Roberts, & Pearlman, 2016). The GAGs in the human cornea are predominantly keratan sulphate and chondroitin (dermatan) sulphates. Between the collagen lamellae lie extremely flattened, modified fibroblasts known as keratocytes.

Descemet's membrane supports and protects the **corneal endothelium,** which consists of a single layer composed essentially of collagen IV and laminin. It is 5 µm thick and its role is to regulate hydration of the stroma and therefore retain the transparency of the cornea (Atchinson & Smith, Optics of the Human Eye, 2002).

Optical considerations

The total refractive power of the cornea F can be approximated as the sum of the powers of its two surfaces (anterior and posterior), as per the below formula (Atchinson & Smith, Optics of the Human Eye, 2002):

$$(1 – n) / R \text{ (anterior)} + (n – 1) / R \text{ (posterior)}$$

where R (anterior) is the radii of curvature of the anterior surface and R (posterior) is the radii of curvature of the posterior surface and equals to 0.81 x R (anterior); and n is the refractive index of the cornea which is usually taken as 1.376 which is the average refractive index of the stroma. The total power of the cornea is reported to be between 41.2 D and 43.2 D in the literature (Atchinson & Smith, Optics of the Human Eye, 2002).

The shape of the corneal surfaces has been widely studied and is often characterized by its asphericity specified clinically by the Q factor which describes the flattening of the cornea away from its centre. The human cornea's Q factor is reported in the literature to range between -0.30 and +0.16 (Atchinson & Smith, Optics of the Human

Eye, 2002).

1.1.3 The pupil

Entrance pupil and exit pupil

The iris forms the diaphragm of the eye, known as the pupil[1]. The pupil size is determined by two antagonistic muscles under the control of the autonomic nervous system:

- The pupillary sphincter, which is a smooth muscle innervated by the parasympathetic fibres of the oculomotor nerve;
- The pupil dilator muscle, which is a muscle innervated by sympathetic fibres.

When looking at an eye, at the level of the diaphragm, what we can see is the image of the iris diaphragm formed by the cornea (entrance pupil). The exit pupil is the image of the iris diaphragm formed by the lens (Figure 3; Figure 4). In general, for simplification purpose, and depending on the context, the term pupil is used for the entrance pupil. Compared to the entrance pupil, the exit pupil of the eye has little significance in clinical practice. Thus, throughout this manuscript, the term pupil of the eye will mean the entrance pupil.

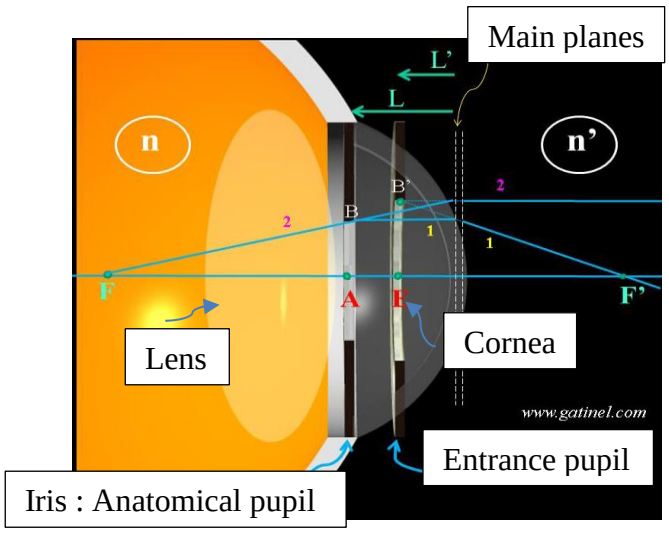

Figure 3 Formation of the entrance pupil (Gatinel, www.gatinel.com, 2018)

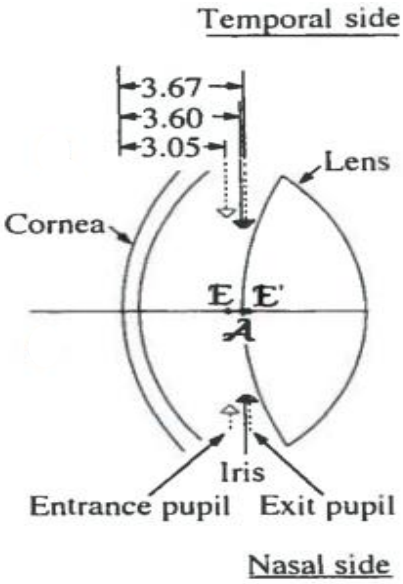

Figure 4 Entrance and exit pupil (in mm) (Atchinson & Smith, Optics of the Human Eye, 2002)

[1] In general, the diaphragm in the optical systems is not known as pupil. The word pupil is used for images of the diaphragm. The entrance pupil of an optical system is the image of the diaphragm formed in the object space. The image of the aperture formed in the image space is the exit pupil.

Pupil centre

In a perfect optical system symmetrically formed around an axis of revolution, the pupil would be centred. However, the eye is not a perfect optical system and the pupil of the eye is generally offset of 0.5 mm nasally compared to the optical axis (Wethmeimer, 1970). The position of the pupil controls the path of a light beam passing into the eye, and thus determines the amount and type of aberrations that affect the quality of the retinal image.

Walsh and Charman (Walsh & Charman, 1988) show that in natural and pharmacological expansion conditions, the pupillary centre appears to move with the change in pupil diameter (up to 0.4 mm for certain subjects). Wilson et al. (Wilson, Campbell, & Simonet, 1992) confirm the results of Walsh and Charman. In most subjects, this movement was temporal when the pupil dilated.

Pupillary diameter

Several factors influence the size of the pupil:

- The illumination level is the most crucial factor influencing the size of the pupil. The diameter thereof may range from 2.0 mm under high illumination to 8.0 mm under low illumination (Crawford, 1936). The pupillary response results in a reduction in the diameter thereof when the light intensity increases. When the light intensity is weak, there is a latency of 0.5 seconds before the constriction starts. When the luminous intensity increases, this latency becomes 0.2 to 0.3 seconds. There is less response when the light source moves from the centre of the visual field to the periphery thereof (Crawford, 1936).
- The constriction of the pupil due to direct light stimulation is called direct pupillary reflex. In a healthy visual system, there is also a consensual pupillary reflex which corresponds to an equal response of the two pupils when only one of them is stimulated. The pupil size also decreases when the eye converges and accommodates. This is called accommodation reflex in near vision (Atchinson & Smith, Optics of the Human Eye, 2002).
- The pupil diameter decreases with age, and the pupil reacts less to changes in light levels (Birren, Casperson, & Botwinick, 1950).
- Some chemicals have an influence on pupil diameter. Mydriatics (causing expansion) and miotics (causing constriction) may be sympathomimetic or parasympathetic (Kanski, 1969).

- The emotional state can play a role in pupil size. Hess (Hess, 1965) shows that the pupil size is dependent on brain activity. For example, pleasant mental images increase the pupil size, while unpleasant images decrease it.

1.1.4 The axis of the eye

The eye is an optical system consisting of various dioptres (the cornea and the lens), which allow the convergence of the rays on the fovea in the emmetropic eye. These anatomical structures are not aligned along the same axis of revolution. Therefore, we need different axes and angles to characterize this optical system (Pande & Hillman, 1993)- (Thibos, 1995) - (Arbelaez, Vidal, & Arba-Mosquera, 2008) - (Dunne, Davies, Mallen, Kirchkamp, & Barry, 2005). Figure 5 shows the different axes of the eye.

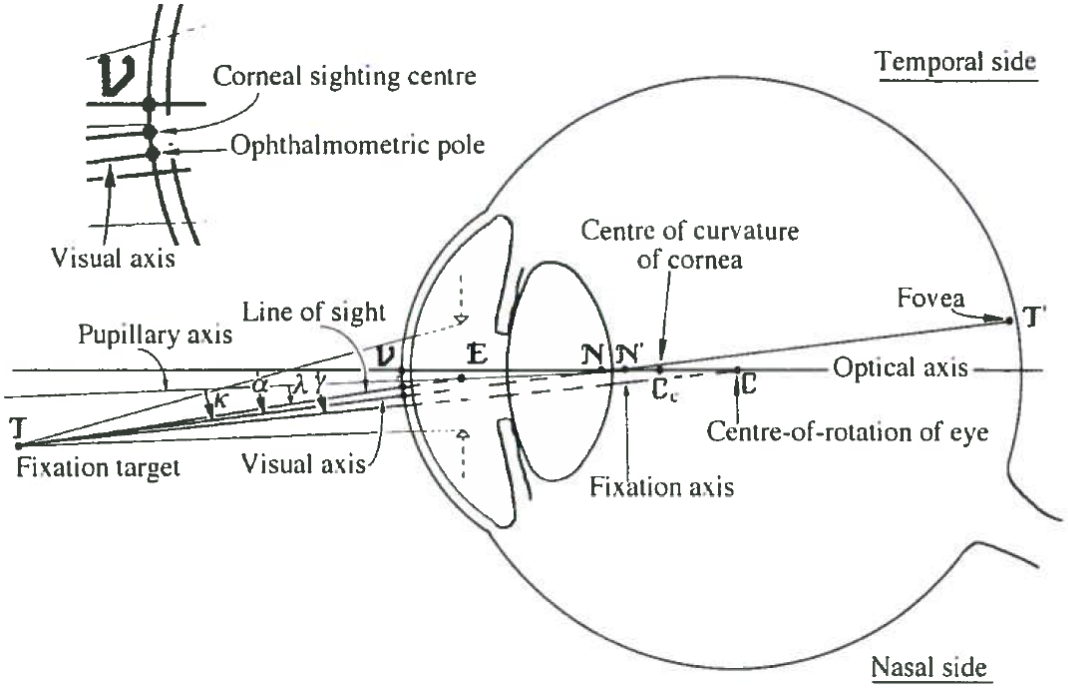

Figure 5 Right eye vertical sectional view. Representation of axes: median optical axis, pupillary axis, visual axis, line of sight. T attachment point. E centre of the entrance pupil. N and N' nodal points. Cc corneal centre of curvature. C centre of rotation of the eye. The object T has been shown very close to the eye to amplify the value of the angles formed by the visual axis, the line of sight and the mounting axis (Atchinson & Smith, Optics of the Human Eye, 2002)

The **optical axis** is the line joining the centres of curvature of the refractive surfaces of a centred optical system. It is used as a reference to define other axes of the eye. In a perfect optical system, the axes of the optical surfaces are common. The eye is not a centred optical system and has no real optical axis (the optical axes of the cornea and lens are different and are not centred). The concept of the optical axis can be

applied to the eye by defining it as the line of best fit through the centres of curvature of the best fit sphere of each surface (cornea and crystalline lens) (Cline, Hofstetter, & Griffin, 1989)- (Millodot, 1993).

The **visual axis** of the eye is the axis joining the fixation target point T, the nodal points and the fovea. The nodal points are those points through which the incidents and emerging rays pass and are parallel. The average nodal point of the eye is located 7.5 mm behind the corneal apex, approximately 17.0 mm in front of the fovea (Atchinson & Smith, Optics of the Human Eye, 2002). Since the dioptres of the eye do not have rotational symmetry, this visual axis is not a straight line but rather a curved one. The visual axis is a convenient reference for the study of visual functions, particularly because it does not depend on the diameter of the pupil. It is often located close to the line of sight at the intersection with the cornea and with the entrance pupil. The location of the intersection on the cornea of the visual axis is difficult to determine in clinical practice and does not correspond to an identifiable point (Cline, Hofstetter, & Griffin, 1989) - (Millodot, 1993).

The **pupillary axis** is the line passing through the geometric centre of the entrance pupil and is perpendicular to the cornea. If the eye were a centred optical system, the pupillary axis would correspond to the optical axis. But the pupil is often not centred with respect to the cornea, and it does not appear to have a regular shape. For these two reasons, the pupillary axis is in a direction other than that of the optical axis and does not cross the fixation target point T (Figure 5).

The **line of sight** is the line passing through the fixation target point T and the centre of the entrance pupil. It corresponds to the central ray of the incident light beam refracted by the cornea through the pupil. The line of sight is not fixed because the pupil centre can move when the diameter of the pupil changes. It therefore depends on the pupil diameter. Its intersection with the anterior surface of the cornea is called visual centre of the cornea (Cline, Hofstetter, & Griffin, 1989). In practice, this point is the projection of the centre of the pupil on the cornea (Cline, Hofstetter, & Griffin, 1989)- (Millodot, 1993).

The **keratometric axis** is the axis perpendicular to the cornea crossing the centre of curvature of the cornea and the fixation target point T. Its intersection with the cornea is called the **corneal vertex** or vertex or first Purkinje image (Maloney, 1990). The keratometric axis corresponds to the centre of the reflection of the Placido patterns which is used as a fixation target point in topography. The vertex is not a fixed point

but depends on the location of the fixation target point, and angle of the eye during the fixing (Arbelaez, Vidal, & Arba-Mosquera, 2008) (Figure 6).

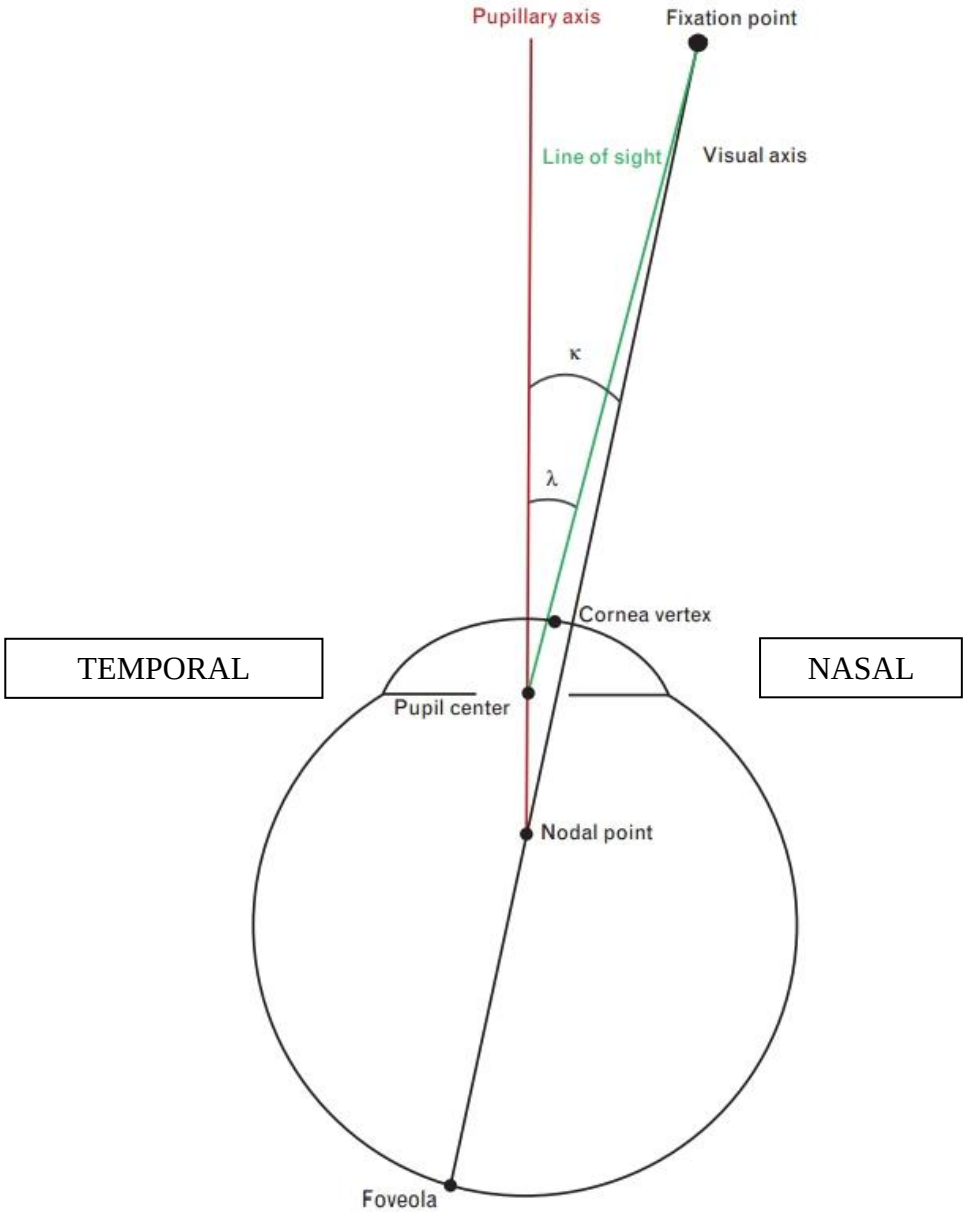

Figure 6 Representation of the kappa angle (κ) formed between the pupillary axis (red) and the visual axis (in black) and the lambda angle (λ) formed between the pupillary axis and the line of sight (green)

The **kappa angle** is defined as the angle between the visual axis and the pupillary axis (Figure 6) (Artal, Benito, & Tabernero, 2006)- (Berrio, Tabernero, & Artal, 2010)- (Basmak, Sahin, Yildirim, Saricecek, & Yurdakul, 2007). The **lambda angle** is formed by the pupillary axis and the line of sight. Because of the difficulty to clinically determine the visual axis, the kappa angle is often confused with the lambda angle in the literature. This approximation is even more valid as the fixation target point is located at infinity (Park, Oh, & Chuck, 2012).

Figure 6 shows that the corneal vertex is not exactly the visual centre of the cornea. Pande and Hillman showed on 50 eyes that the vertex was in average at 0.02 mm nasally from the intersection of the visual axis with the cornea. The pupil centre is located in average at 0.34 mm temporally from this point, and the geometric centre of the cornea is located in average at 0.55 mm temporally from this point (Pande & Hillman, 1993).

The fovea is located temporally to the intersection of the pupillary axis and the posterior pole. The angle formed is therefore positive in theory and the intersection point of the line of sight with the cornea is located nasally compared to the intersection of the cornea with the pupillary axis. Thus, Figure 6 shows that for an observer aligned with one light source, the corneal reflection is usually nasal to the centre of the pupil (positive kappa angle) and much more rarely temporal to the centre of the pupil (negative angle kappa).

1.1.5 The retina

The **retina** forms the back of the eye. Its thickness varies from 50 µm at the fovea centre to c. 600 µm near the optic disc (Atchinson & Smith, Optics of the Human Eye, 2002). It consists on multiple layers as described in Figure 7.

The key layer (number 2) is formed of photoreceptors. It is in the back of the retina and is the final part of the path taken by light rays passing through the eye. It is the interface between the optical system and the neural system which transmits the visual information to the brain and therefore is an essential element of the quality of image perceived by the brain.

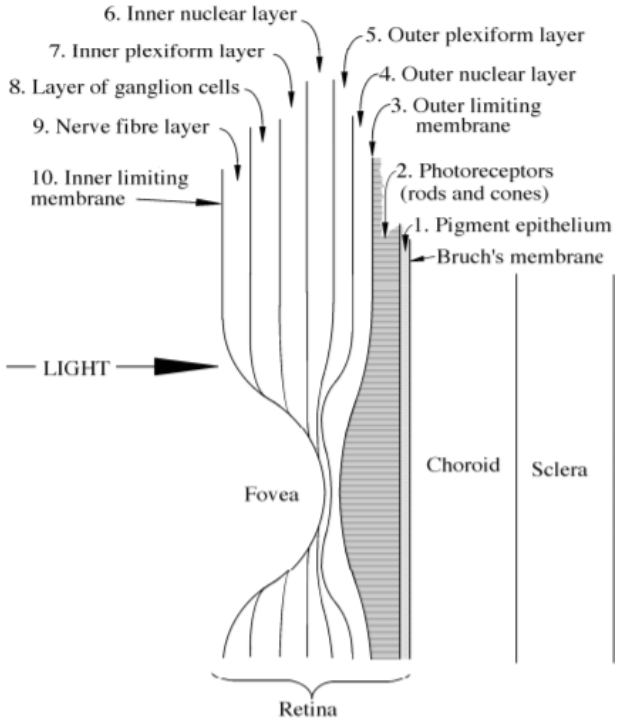

Figure 7 The structure of the retina (Atchinson & Smith, Optics of the Human Eye, 2002)

There are two types of photoreceptors called rods and cones because of their respective shapes. Rods are longer and narrower than cones, they are very sensitive to light but have a poor spatial resolution while cones function at higher levels of light but provide a better resolution (Atchinson & Smith, Optics of the Human Eye, 2002).

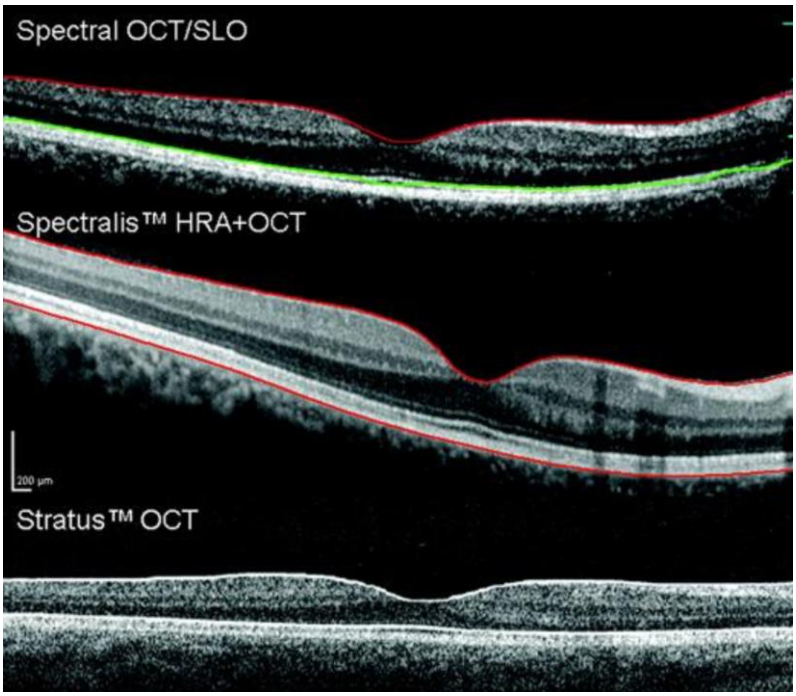

Figure 8 Image of retina photoreceptors obtained through tomography (Wolf-Schnurrbusch, et al., 2009)

The number of rods and cones in a typical retina is estimated at c. 100 million and 5 million respectively (Atchinson & Smith, Optics of the Human Eye, 2002). Rods and cones are not evenly distributed in the retina as shown in Figure 9.

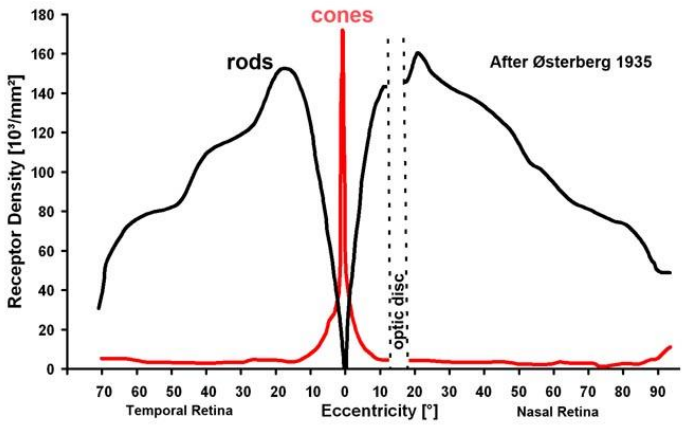

Figure 9 Density of cones and rods across the retina along the horizontal meridian (in temporal and nasal direction) (Osterberg, 1935)

The cones predominate at the fovea which is free of rods, while rods predominate in the periphery of the fovea (starting from an angle of 5° from the fovea) and reach their highest density at an angle of c. 20° from the fovea. Therefore, when the level of illumination is low the centre of the fovea is 'blind' and it is necessary to look eccentrically to be able to use the rods and see an object.

1.2 The light

We call visible light a part of the electromagnetic waves spectrum which produces a visual response in the human eye. Its wavelengths (λ) range between 390 and 780 nm.

The responsivity of the eye varies with the wavelight it receives. This observation is modelled by the luminosity function or luminous efficiency function of the human eye, which depends on the illumination condition. The *Commission Internationale de l'Eclairage* ("CIE") which is the international authority on light defines two commonly-used luminous efficiency functions corresponding to:

- the **photopic** illumination condition which corresponds to high light levels where the photoreception of the retina is dominated by cones. Luminance

limit of the photopic vision is c.3 cd/m^2 (Atchinson & Smith, Optics of the Human Eye, 2002);

- the **scotopic** illumination condition which corresponds to low light levels i.e. luminance below 0.03 cd/ m^3 (Atchinson & Smith, Optics of the Human Eye, 2002) where vision is mostly due to rods;

The **mesopic** illumination condition corresponds to medium light levels where both cones and rods are active. Luminance of the mesopic vision ranges from c. 0.03 to 3 cd/m^3.

The CIE defined the photopic luminous efficiency function V(λ) in 1924; It has a maximum value of 1 when λ equals 555 nm. It defined the scotopic luminous efficiency function V'(λ) in 1951; It has a maximum value of 1 when λ equals 507 nm (Atchinson & Smith, Optics of the Human Eye, 2002).

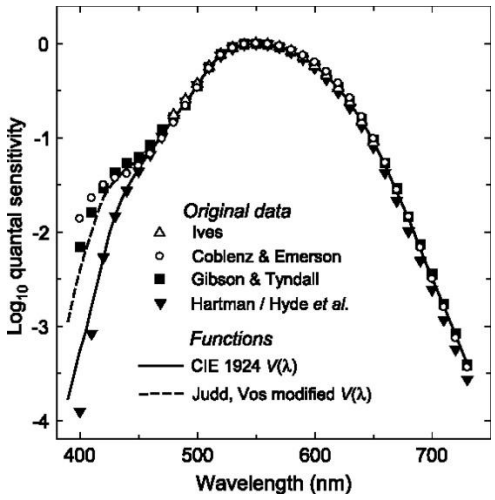

Figure 10 Examples of luminosity functions (Sharpe, Stockman, Jagla, & Jägle, 2005)

The luminosity function is used as a weighting in the formula determining the luminous flux (Φ_v), which is the measure of the perceived power of an electromagnetic beam. The unit of the luminous flux is the lumen and it is calculated by the below formula:

$$F = K_m \int_0^\infty F_R(\lambda) V(\lambda) d\lambda$$

where K_m is known as the maximum spectral luminous efficacy of radiation for photopic vision and has a value of 683.002 lm/W, $F_R(\lambda)$ is the spectral radiant flux and V(λ) is the photopic luminous efficiency function (Atchinson & Smith, Optics of the Human Eye, 2002).

1.3 Optical phenomena influencing the formation of the image

The images formed on the retina are blurred by many optical phenomena that occur during the light path through the eye, such as the **specular reflection**, **absorption**, **diffraction** and **scattering**. The quality of vision is also limited by the ocular aberrations, which the most significant are the refractive errors or **low order aberrations ("LOAs")** i.e. the myopia, hyperopia and astigmatism. The human eye also suffers from other aberrations which are called **high order aberrations ("HOAs")**. Finally, the quality of the image on the retina is also limited by the **resolution capacity** of this latter.

The following paragraphs aim at describing the above-mentioned phenomena and limits.

1.3.1 Specular reflection

In the eye, some light is reflected at each of the four major refractive surfaces.

The Fresnel equations defines the fraction of reflected (R) and transmitted (T) light passing through a smooth and regular surface located between two homogeneous materials. R and T depend on the refractive indices on the incident (n) and refracted (n') sides of a surface:

$$R = [(n' - n) / (n' + n)]^2$$

$$T = 4nn' / (n + n')^2$$

As the reflection happens at four main surfaces, we can clinically define four main reflected images called Purkinje images (P_i, P_{ii}, P_{iii}, P_{iv}). The position, size, and brightness of the Purkinje images depend on the position of the light source and the characteristics of the refractive surfaces of the eye. They give useful information about the lense and the cornea and are good reference points. In particular, P_i also called corneal vertex is an important clinical reference point.

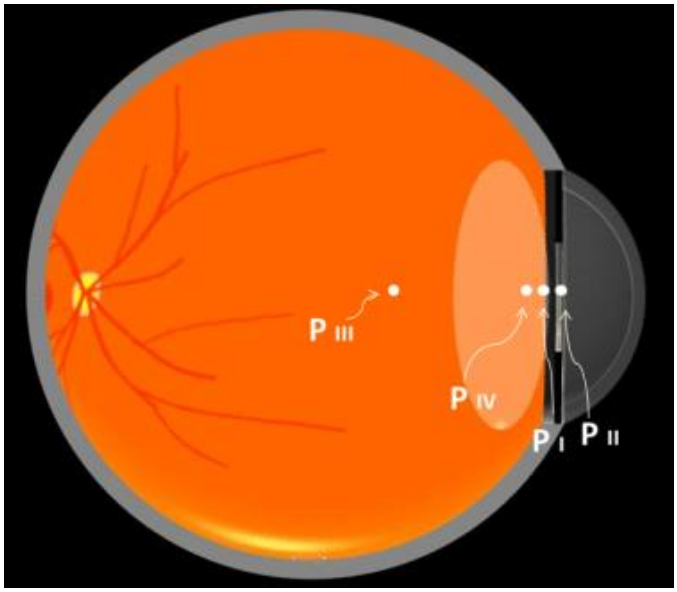

Figure 11 Positions of the Purkinje images (Gatinel, www.gatinel.com, 2018)

Figure 12 indicates the transmittance of the main components of the human eye for various wavelengths.

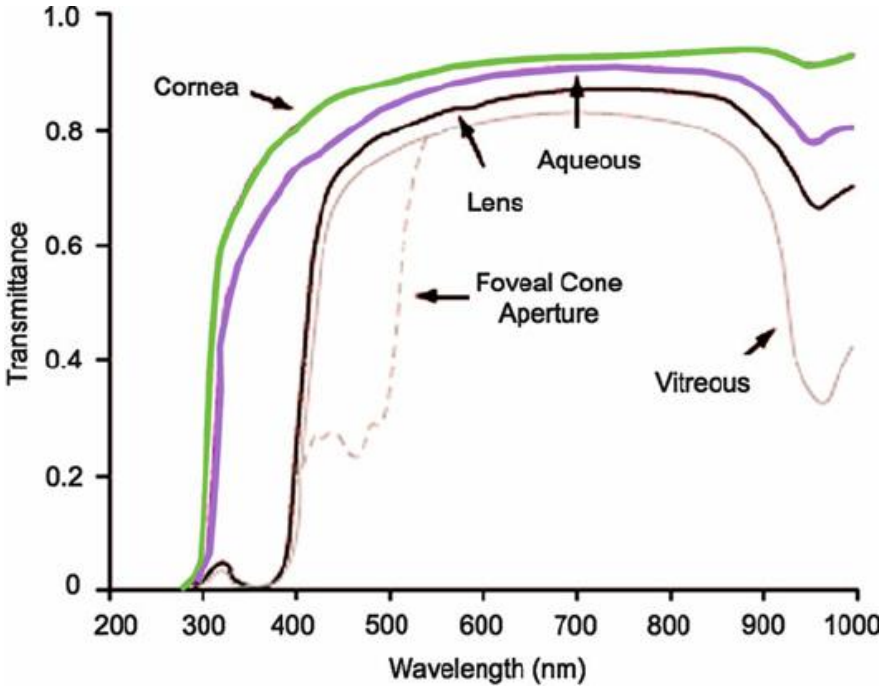

Figure 12 Transmittance at the posterior surface (Boettner & Wolter, 1962)

1.3.2 Absorption

We call absorption the attenuation of the intensity of an incident electromagnetic wave when passing through a medium. The absorbance of a medium is defined as the ratio of absorbed and incident intensities.

Absorption is due to a partial conversion of light energy via a resonance mechanism. When light reaches an absorbing material which molecules have the same vibrational frequency as the incident wavelength, those molecules will absorb the wave's energy and transform it into vibrational motion and then into thermal energy by transmitting the vibration to neighbouring molecules. Since different atoms and molecules have different natural frequencies of vibration, they will selectively absorb different frequencies of visible light

The ability of a medium to absorb electromagnetic radiation depends mostly of the electronic constitution of its atoms and molecules, the wavelength of radiation, the thickness of the absorbing layer as well as internal parameters such as the concentration of the absorbing agents and the temperature, as described by the Lambert-Beer law (Niemz, 2004):

$$I(z) = I_0 \exp(-\alpha z)$$

$$\text{where } \alpha = k' \times c$$

I(z) is the intensity at the distance z on the optical axis, I(0) is the incident intensity, α is the absorption coefficient of the medium, c is the concentration of absorbing agents and k' depends on internal parameters other than the concentration of absorbing agents.

The cornea mainly consists of water and therefore shows strong absorption and appear opaque at wavelengths higher than 600 nm (Atchinson & Smith, Optics of the Human Eye, 2002). On the other hand, proteins and other cellular components have a strong absorption coefficient in the UV segment of the spectrum; the cornea absorbs all wavelengths below 290 nm (Atchinson & Smith, Optics of the Human Eye, 2002).

The cornea is almost perfectly transparent in the visible region of the spectrum as shown in the figure below. The absorption coefficient of the skin is for instance 20-30 times higher than the absorption coefficient of the corneal tissue in the visible spectrum (Niemz, 2004).

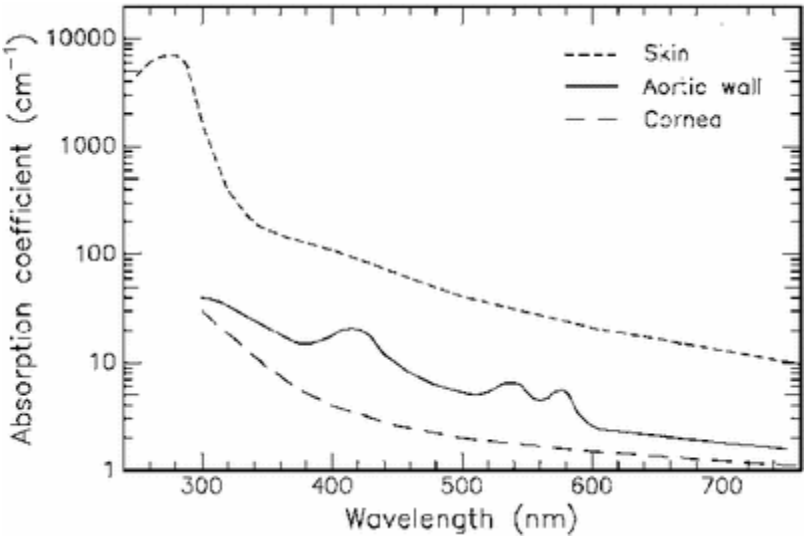

Figure 13 Absorption spectra of skin, aortic wall and cornea (Niemz, 2004)

1.3.3 Diffraction

Diffraction occurs when a propagating wave encounters a diffracting object which dimension is roughly comparable with its wavelength. Diffraction in the eye is influenced by the wavelength of the incident light and the diameter of the entrance pupil and plays a significant role in degrading the image quality at the retina.

The image of a light spot through an optical system only limited by diffraction is called Airy disk. The Rayleigh formula calculates the resolution limit of a given optical system due to the diffraction:

$$\theta_{min} = 1.22 \lambda / D \text{ (Atchison \& Smith, 2002)}$$

where θ_{min} is the angular resolution (in radians) also known as the angular radius of the Airy disc, λ the wavelength (in nm), and D is the pupil diameter in mm.

Thus, the greater the pupil diameter is, the lesser the effect of the diffraction materializes and better is the eye resolution. When the pupil diameter is 3 mm or above, the impact of diffraction on the quality of the image formed at the retina becomes negligible (Atchison & Smith, 2002).

1.3.4 Light scattering

Light scattering in the eye is due to the variation of the refractive index inside the eye at the microscopic level. It is due to a combination of refraction, reflection and diffraction.

Part of the light propagating through the eye is scattered. Approximately a quarter of the scattering is caused by the cornea (Vos & Boogard, 1963), approximately half is caused by the lens (Beckman, Thaung, & Sjöstrand) and circa a quarter is due to the

reflections on the retina (Vos, Contribution of the fundus oculi to entropic scatter, 1963). The consequence of the scattering is to add a background light on the retina. The impact of light scattering increases with age doubling from 20 to 70 years (IJspeert, de, van den Berg, & de, 1990).

1.3.5 Optical aberrations

Optical aberrations in the human eye are known since the 17th century. However, their description and measurement emerged in the late 19th century as a result of the development of the geometric aberrations theory by Philipp Ludwig von Seidel (1821 – 1896) and of the first aberrometer by Johannes Franz Hartmann (1865 - 1936) (Biedermann, 2002).

The Hartmann aberrometer was a screen perforated with numerous holes. In 1971, to analyse the wavefront exiting from an optical system, Shack and Platt replaced the holes of the Hartmann's screen by an array of micro lenses of same focal length arranged in a predetermined geometry, thereby developing the Hartmann-Shack wavefront sensor. The principle of this aberrometer is to create a point source in the object space at the fovea. Light from the eye reaching each lenslet is brought to a focus in the focal plane of the lens array. When an aberrated wavefront is measured, the image spot produced by each lenslet shifts with respect to the corresponding point in the reference, a distance proportional to the local phase distortion.

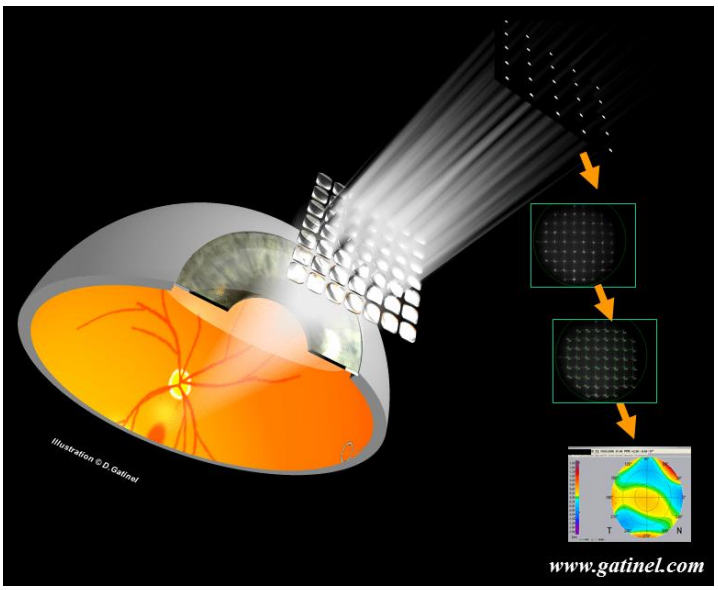

Figure 14 Principle of the Hartmann-Shack wavefront sensor (Gatinel, www.gatinel.com, 2018)

Many other reliable aberrometric techniques have been developed since and allow an accurate measurement of ocular aberrations using the concept of wave aberration, which describes the distortions of a wavefront (a surface of identical phase) in the pupil plane as it goes through the optical system.

Ocular aberrations are generally divided two types: monochromatic (or geometrical) aberrations and chromatic aberrations.

Monochromatic aberrations

The wavefront out of a perfect optical system would be spherical and the image of a point source through a circular pupil would be a point, only eventually limited by diffraction.

Monochromatic wave aberrations are a result of the geometric irregularities, tilts and decentrations of the eye's dioptres, which imply deviations in the wavefront from the ideal spherical shape. The wave aberration of an imperfect optical system such as the human eye is a complex surface represented by the wave aberration map *W(x, y)* defined as the difference between a perfect spherical wavefront and the aberrated wavefront at the exit pupil (Atchison & Smith, 2002).

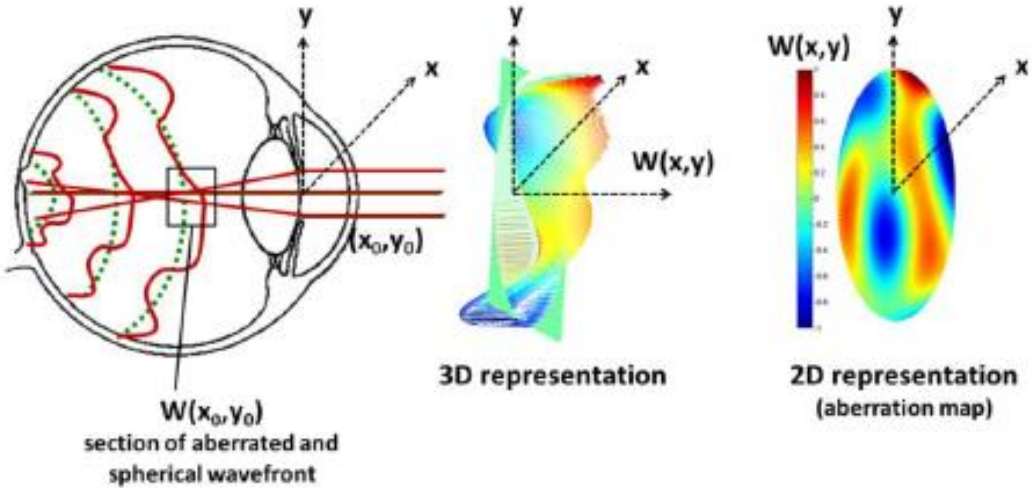

Figure 15 Schematic representation of the wave aberrations and wave aberration map (Vinas, 2015)

The wave aberration of an optical system is modelled mathematically by a sum of orthonormal polynomials. We use the Zernike polynomials, developed by physics Nobel prize winner Frits Zernike (1888 – 1966), which are a set of orthogonal functions. The wave aberration can be represented in polar coordinates (ρ, θ) of the pupillary

plan (American National Standard Institute recommendation) (Vinas, 2015), as follows:

$$W(\rho,\theta) = \sum_{i=0}^{\infty} c_n^m Z_n^m(\rho,\theta)$$

where, c_n^m are called Zernike coefficients and measure the magnitude of each aberration present in a human eye, and $Z_n^m(\rho,\theta)$ the Zernike polynomials of order n and frequency m is defined by:

$$Z_n^m(\rho,\theta) = \begin{cases} N_n^m R_n^{|m|}(\rho)\cos(m\theta); & for\ m \geq 0 \\ -N_n^m R_n^{|m|}(\rho)sin(m\theta); & for\ m < 0 \end{cases}$$

where,

$$\mathrm{R_n^{|m|}(\rho)} = \sum_{s=0}^{(n-|m|)/2} \frac{(-1)^s(n-s)!}{s![0.5(n+|m|)-s]![0.5(n-|m|)-s]!}\rho^{n-2s}$$

and,

$$\mathrm{N_n^{|m|}} = \left(\frac{2(n+1)}{1+\delta_{mo}}\right)^{1/2}$$

Figure 16 is the representation of the most common monochromatic aberrations (up to the 6th order) using the Zernike pyramid:

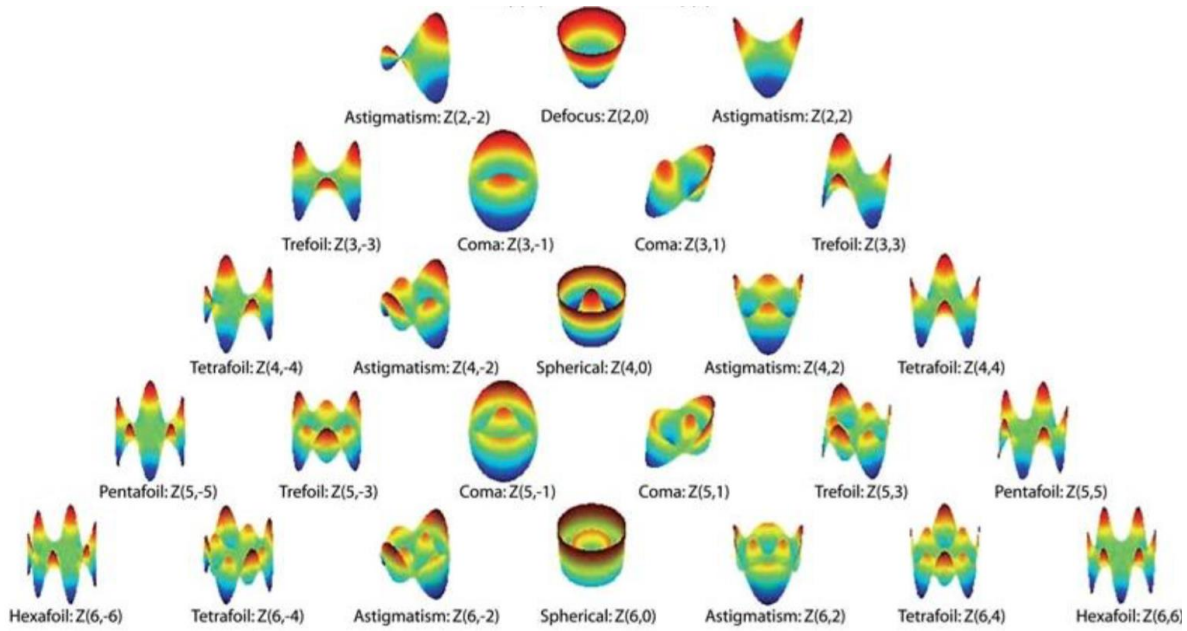

Figure 16 Zernike pyramid (Applegate, Wevefront sensing, ideal corrections, and visual performance, 2004)

The terms of order 0 and 1 are respectively those of piston and tilt. They represent a shift in the image which has no consequence on its quality and therefore are not ocular aberrations and not reflected in the pyramid above.

The second-order aberrations present on the first line of the pyramid are the LOAs i.e. Z (2,0) representing the defocus or sphere term (myopia and hyperopia).

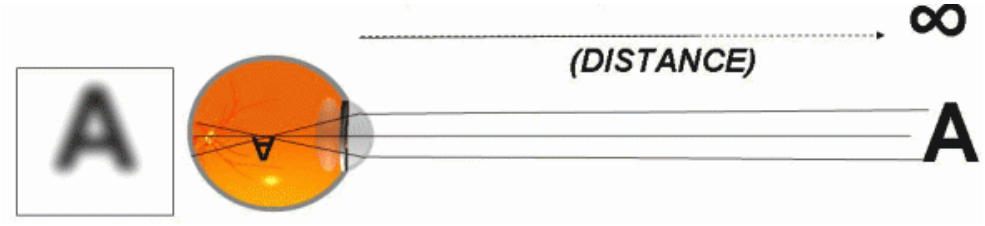

Figure 17 Schematic representation of a myopic eye (Gatinel, www.gatinel.com, 2018)

Z (2,-2) and Z (2,2) are related to astigmatism.

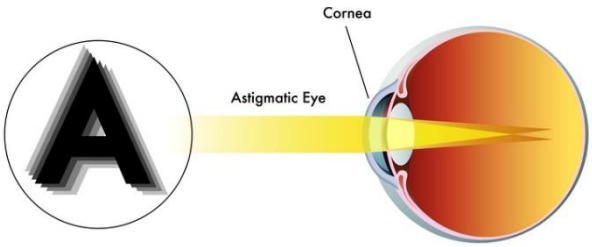

Figure 18 Schematic representation of 45° and 90° astigmatisms (Gatinel, www.gatinel.com, 2018)

The aberration of third order and above are the HOAs. Common HOAs are the coma aberrations, which result in off-axis point sources (such as stars in astronomy) appearing to have a tail (coma) like a comet; trefoil aberrations, which can be compared to astigmatisms of high order, responsible for a reduction of sensitivity to contrasts; and spherical aberrations which is due to an increased refraction of a light beam when it passes through the cornea near its edge. When spherical aberration is present, non-paraxial rays do not intersect at the paraxial focus. The further a ray is from the optical axis, the further its axial crossing point is from the paraxial focus?

Chromatic aberrations

Chromatic aberrations are a consequence of the chromatic dispersion i.e. the variation of the refractive index of the eye with the wavelength, which affects the diffraction, scattering and aberrations (Atchinson & Smith, Optics of the Human Eye, 2002). This

dispersion causes short wavelengths (such as the green light) to focus in front of long wavelengths (such as the red light), inducing a chromatic difference of focus between called **Longitudinal Chromatic Aberration ("LCA").**

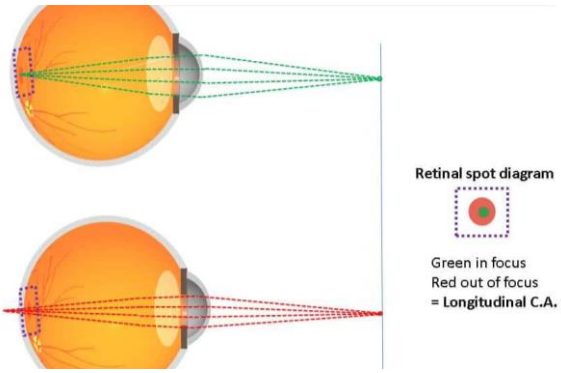

Figure 19 LCA in the eye (Gatinel, www.gatinel.com, 2018)

Besides, the misalignments between the different ocular dioptres and the off-axis position of the fovea result in a transversal shift of focus for different wavelengths, known as **Transverse Chromatic Aberration ("TCA")** (Atchinson & Smith, Optics of the Human Eye, 2002).

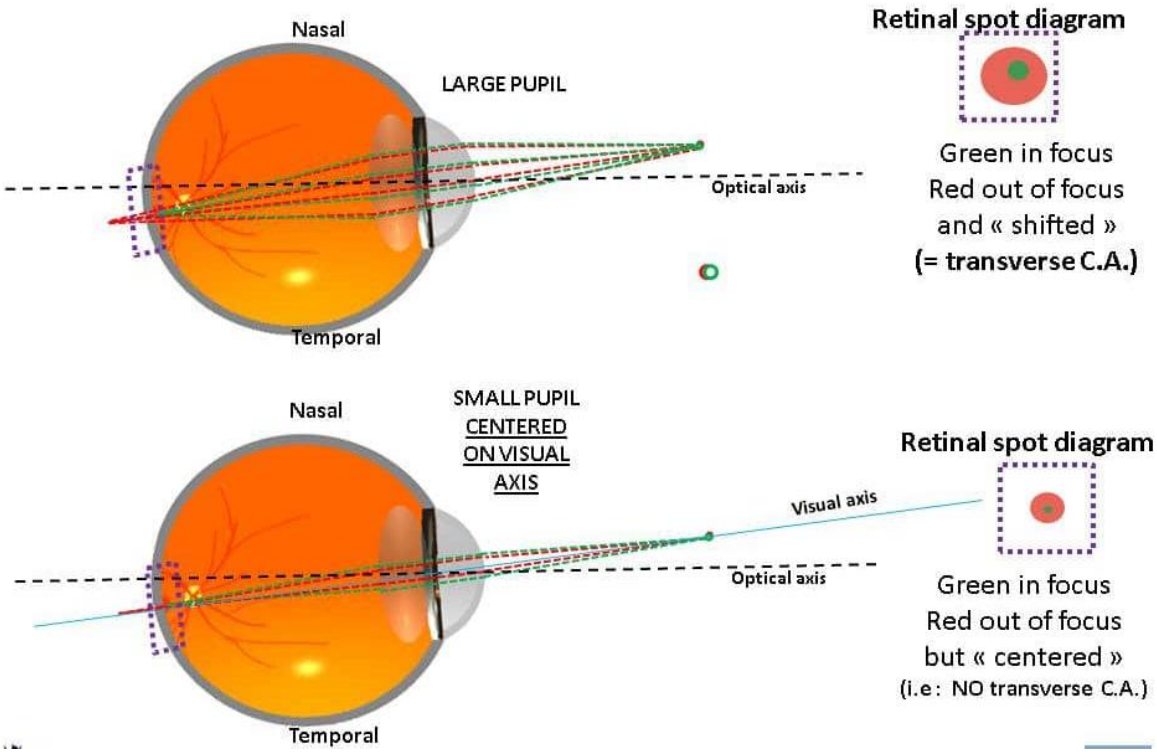

Figure 20 LCA in the eye (Gatinel, www.gatinel.com, 2018)

Because of LCA, the different wavelength images of the point are defocused by different amounts relative to the retina. Also, because the power of the eye is lower for long wavelengths than for short wavelengths, longer wavelength rays are deviated less than shorter wavelengths rays and meet the retina further from the optical axis.

1.3.6 Resolution limit of the retina

Visual Acuity ("VA") is also limited by the resolution capacity of the retina. The spatial organization and concentration of the photoreceptors on the retina is the limiting factor for the resolution ability of the human eye. Figure 21 describes the organization of the photoreceptors, and the implied calculation of the resolution also called Nyquist limit. The consequence of the resolution limit is a risk of poor cortical integration of the image, which can lead to an error of interpretation by the brain.

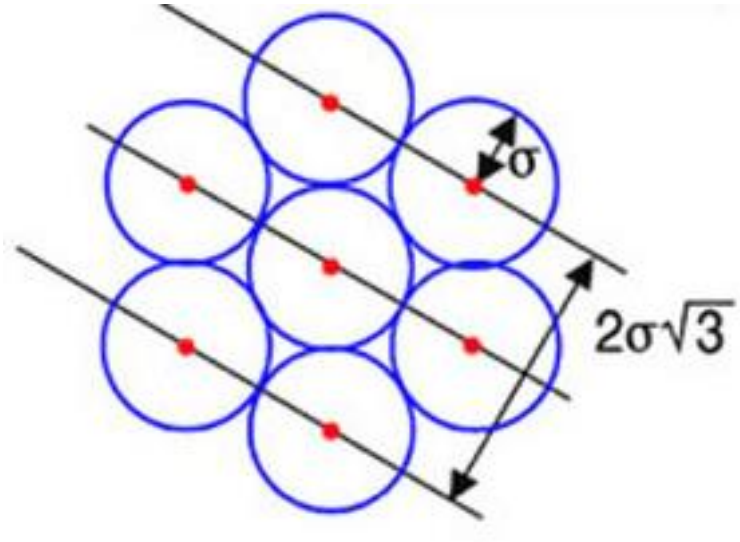

Calculation of Nyquist limit

$NL = 1 / (\sqrt{3} \times 2\sigma)$

Figure 21 Organization of the photoreceptors Nyquist limit (Devries & Baylor, 1997)

1.3.7 Stiles-Crawford effect

Stiles and Crawford discovered that the luminous efficiency of a beam of light entering the eye and incident on the fovea depends upon the entry point in the pupil. This phenomenon is known as the Stiles–Crawford effect (Westheimer, 2008). We call Stiles–Crawford effect of:

(i) the first kind the phenomenon where light entering the eye near the edge of the pupil producing a lower photoreceptor response compared to light of equal intensity entering near the centre of the pupil;

(ii) and of (ii) the second kind the phenomenon where the observed color of monochromatic light entering the eye near the edge of the pupil is different compared to that for the same wavelength light entering near the centre of the pupil, regardless of the overall intensities of the two lights. Both effects are highly wavelength-dependent, and more evident under photopic conditions (Westheimer, 2008).

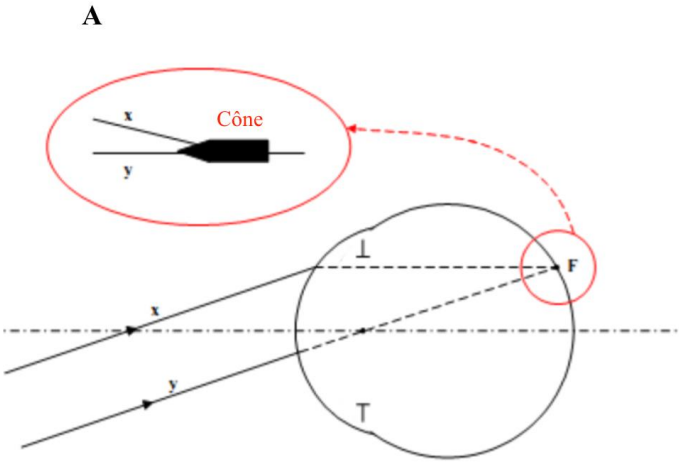

Figure 22 Illustration of the Stiles-Crawford effect

Because of the Stiles-Crawford effect, the rays coming from the periphery of the pupil have less influence on the quality of the retinal image less than the central rays. The Stiles-Crawford effect can be quantified using the below formula which calculates the luminous efficacy (EL) of a given ray entering the eye i.e. the luminance of this ray divided by the luminance of a ray entering the eye through the pupil center:

$$10^{-p(\lambda)(d-d_m)^2}$$

where d - d_m is the distance (in mm) calculated in the pupil's plan between the two rays; and p(λ) is a wavelength dependent parameter which represents the magnitude of the Stiles–Crawford effect, with larger values of p corresponding to a stronger falloff in the relative luminance efficiency as a function of distance from the centre of the pupil.

1.4 Assessment of the quality of vision

The most commonly used metric to assess the quality of vision is the Visual Acuity (VA). However, other psychophysical metrics such as the Contrast Sensitivity (CS) and the Depth of Field (DOF) are important. Besides, multiple other visual quality

metrics derive from the wave aberration theory, such as the Root Mean Square (RMS), and the retinal image quality-based metrics: Point Spread Function (PSF), and Optical Transfer Function (OTF). These later functions are based on Fourier transforms computed from wave aberration, and include the combined effects of diffraction and aberrations, but not scattering. The purpose of the below is to describe the key metrics used in this thesis.

1.4.1 Visual Acuity ("VA")

VA is the size of the smallest optotype (e.g. a letter) which an eye can solve at a given distance. At this distance, the angle underpinned by the detail of the optotype is called Minimum Angle of Resolution (MAR).

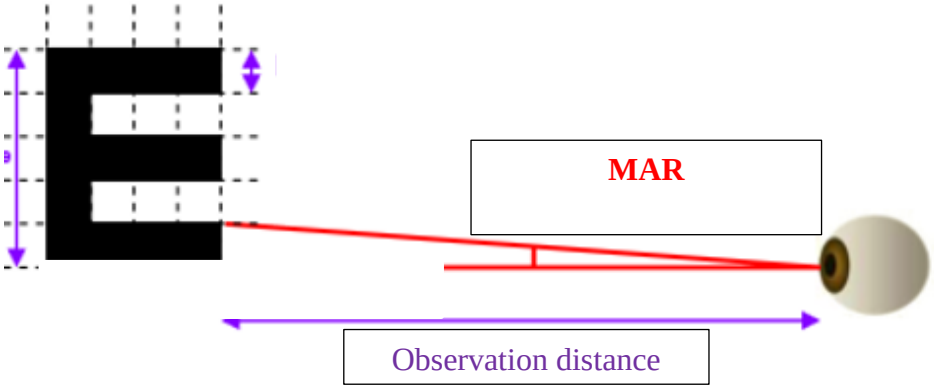

Figure 23 Minimum Angle of Resolution

VA is calculated as:

$$VA = 1 / MAR \text{ (expressed in minutes of arc)}$$

1.4.2 Contrast Sensitivity ("CS")

CS corresponds for a given spatial frequency to the inverse of the weakest contrast threshold detected by and eye. We can measure the contrast sensitivity curve by varying the spatial frequency.

Indeed, to distinguish between different objects or details within an object, the human eye requires a sufficient difference in luminance, or contrast which is calculated through the contrast formula of Michelson (Atchison & Smith, 2002):

$$L\ max – L\ min / (L\ max + L\ min)$$

The CS function is represented by a curve where the x-axis is the spatial frequency and the y-axis the CS. Neural and optical attenuations limit the high spatial frequency CS. The point where the CS function cuts the X axis is called cut off frequency.

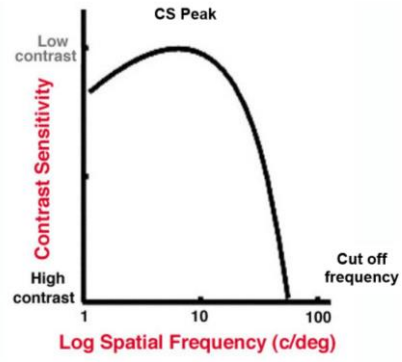

Figure 24 Photopic contrast sensitivity function

1.4.3 Depth of Field (“DOF”)

The depth of field (“DOF”) also called effective focus range, is the distance between the nearest and farthest object in that appear acceptably sharp in an image. In other terms, it is the range of distances over which an optical system such as the human eye cannot detect any change in focus.

The DOF decreases with increase in pupil diameter, increasing target luminance and correction of LCA of the eye.

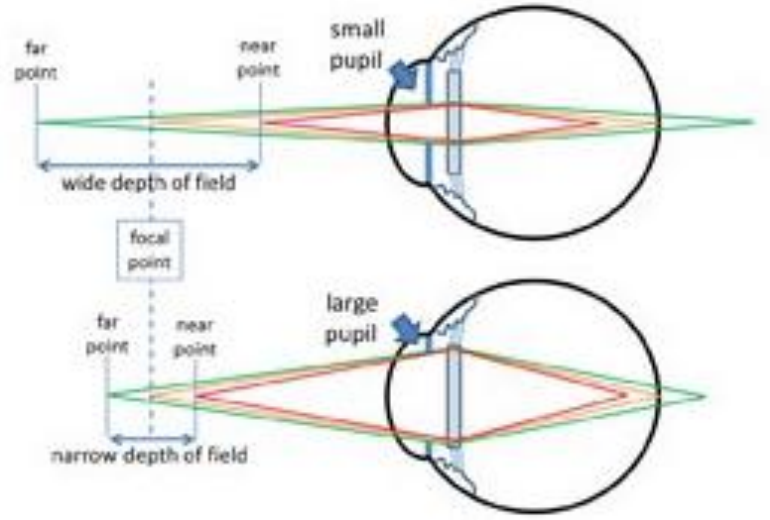

Figure 25 Decrease in DOF with an increased pupil size (Devgan, 2014)

1.4.4 Root Mean Square ("RMS")

A standard global pupil plane metric to evaluate the optical quality of the human eye is the RMS, which measures the deviation of the wavefront from a perfect reference spherical wavefront. RMS is defined as the root square of the sum of the squares of the optical path differences as measured from the reference spherical wavefront over the total wavefront area. It is computed directly from the Zernike coefficients.

$$RMS = \sqrt{\sum_{n.m} c_n^{m2}}$$

Where c_n^m is the Zernike coefficient of order **n** and frequency **m**.

The 2nd order optical aberrations represent 86 to 92% of the total RMS (Castejon-Mochon, Lopez-Gil, Benito, & P., 2002) - (Guirao, Porter, Williams, & Cox, 2002). The below table describes the contribution of lower degrees aberrations to total RMS.

	Castejon-Mochon et al. (2002) 5mm pupil / 108 eyes	Castejon-Mochon et al. (2002) 7mm pupil / 108 eyes	Guirao et al. (2002) 5.7mm pupil / 218 eyes
2nd order	90.8%	86.2%	92.0%
3rd order	6.4%	8.0%	4.4%
4th order	2.6%	3.9%	3.0%
5th order	0.2%	1.5%	0.6%

Table 1 Contribution of lower order optical aberrations to total RMS

1.4.5 Optical Transfer Function ("OTF")

The Point Spread Function (PSF) is the image of a point object through the optical System.

$$PSF(x,y) = K\left|FT\left[A(x,y)\,exp(i\frac{2\pi}{\lambda}W(x,y))\right]_{f_x=\frac{x}{z},f_y=\frac{y}{z}}\right|^2$$

where K is a constant, FT is the Fourier transform, z is the eye's length or pupil to image distance, A(x, y) is an apodization function when the waveguide nature of cones is considered and W(x, y) is the wave aberration function in Cartesian coordinates.
For example, the PSF of a point in an optical system only limited by the diffraction phenomenon is the Airy disk.

The Optical Transfer Function (“OTF”) is the Fourier transform of the PSF and measures the loss of contrast and phase shifts in the image of a sinusoidal target.

$$OTF = FT(PSF)$$

The Modulation Transfer Function (MTF), represents the decrease in the contrast as a function of the spatial frequency. It is calculated as:

$$MTF = |OTF|$$

The MTF indicates the ability of an optical system to transfer various levels of details (spatial frequencies) from the object to the image. Its units are the ratio of image contrast over the object contrast as a function of spatial frequency.

The Phase Transfer Function (PTF) is the phase of the OTF, and is associated with the presence of asymmetrical aberrations, such as coma and astigmatism.

Chapter 2: Overview and importance of refractive surgery techniques

Refractive surgery is a set of surgical techniques whose objective is to correct refractive errors of the eye such as near-sightedness (myopia), far-sightedness (hyperopia), astigmatism or presbyopia, in order to improve a patient's vision.

The purpose of this chapter is to describe the key historic milestones in the development of this field of ophthalmology, to classify the different techniques and to address the socio-economic importance of laser-assisted techniques.

2.1 History and development of laser-assisted refractive surgery

2.1.1 History of refractive surgery

In 2001, about 30 km south of Cairo, archaeologists discovered the tomb of Skar, the chief physician of one of Egypt's fifth dynasty of pharaohs. The tomb included on its walls drawings of ophthalmic surgery and about 30 bronze surgical tools. This tomb was dated bac c. 4,000 years which confirms the high surgical skill level achieved by old Egyptian which were performing the "couching operation" for dislodging the cataract away from the pupil.

This procedure was very simple. The physicians were using a lancet to push the clouded lens backward into the vitreous body (Huerva & Ascaso, 2013).

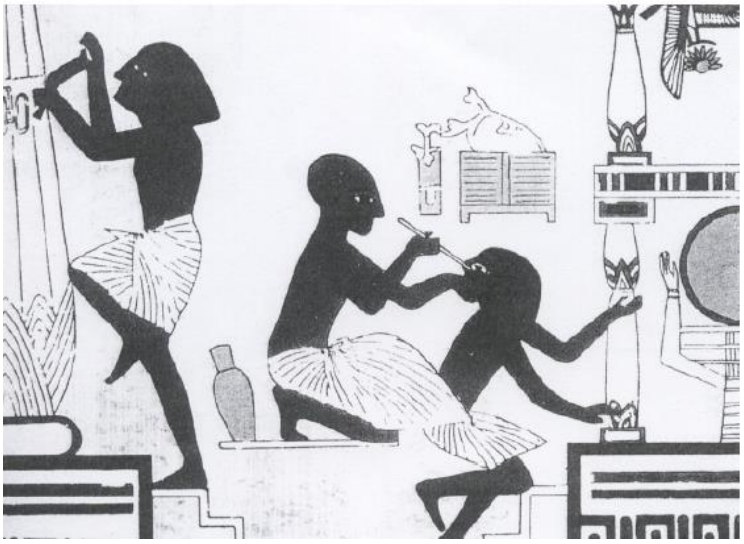

Figure 26 Wall painting in a tomb in Thebes dated about 1,200 BC (Huerva & Ascaso, 2013)

This technique which the ancestor of modern cataract surgery has been performed

until 1748, when the French doctor Daviel performed the first known modern cataract surgery (SNOF, s.d.).

While refractive surgery dates to the pharaonic ages, laser-assisted refractive surgery has only emerged as an established clinical discipline in the late 1980s. However, some of the principles behind current techniques were already known back in the 19th century. We will describe below the key steps of development of these techniques until the emergence of the Laser-Assisted In-Situ Keratomileusis (LASIK) technique.

The origins: Leendert January Lans (19th Century)

In 1850, Prussian ophthalmologist Albrecht von Graefe (1828 - 1870) developed a new cataract surgery based on a wide *ab externo* limbic incision. This new technique was the source of a very high incidence of post-operatively induced high astigmatisms (SNOF, s.d.). In 1898, Dutch ophthalmologist Leendert January Lans (1869 - 1941), published his PhD thesis which title was "Experimental studies of the treatment of astigmatism with non-perforating corneal incisions" (SNOF, s.d.). This thesis can be considered as the first scientific publication on refractive surgery. It described Lans' findings about the effect of non-perforating incision parallel to the limbus performed on rabbits in a laboratory i.e. that the flattening of the central cornea is increased by the depth of the corneal incisions and increases during healing.

The above is the basic principles of what will be known as the radial keratotomy (RK), the first refractive surgical methods to correct myopia, that were developed in 20th century.

The beginnings in Japan and the Soviet Union (1930s - 1970s)

More than 80 years after the works of Lans, Japanese ophthalmologist Tsutomu Sato (1902 - 1960) observed empirically the corneal flattening caused by acute keratoconus, which was the starting point for him to develop the first radial keratotomy technique to treat keratoconus and astigmatism. Sato was performing posterior corneal incisions using a knife blade. He treated more than 200 patients between the late 1930s and early 1940s.

In 1940s, Sato and his team added anterior corneal incisions to their technique and started during the 1950s to use the same principle to correct myopia performing an average of 40 incisions. Sato’s technique resulted in multiple complications (bullous keratopathy) which were reported more than 10 years after the surgical procedures

were performed to correct myopia and helped to understand the role in the endothelium for corneal transparency (SNOF, s.d.).

While Sato's technique was never used outside Japan, radial keratotomy reappeared in 1969 when Soviet military ophthalmologist Yenaliev adapted Sato technique by removing posterior incisions and maintaining only the anterior corneal's incisions. He operated 426 myopic eyes (myopia less than 12 dioptres) between 1969 and 1977, and used several incisions ranging between 4 and 24. He obtained an average correction of 3 to 4 dioptres (SNOF, s.d.).

In the 1970s, Soviet ophthalmologists Svyatoslav Fyodorov (1927 - 2000) and his team demonstrated the variation of the correction with the length of the incisions, as well as the peripheral curvature of the cornea to compensate the central flattening of the cornea. They defined the minimum optical zone diameter consistent with the absence of functional gene to 3 mm, then described the role of the ocular pressure, the keratometry, the depth of the incisions, and their ideal number (sixteen).

The emergence as an established clinical discipline in the Soviet Union, the US and Europe (1980s – 1990s)

Fyodorov established a considerable number of specialized surgical centres in the USSR treating a high number of patients. His technique was imported to the US and Europe during the late 1970s and the 1980s. The first RK was performed in the US by Leo Bores in Detroit in 1978.

Many clinical studies such as Deitz (Deitz & Sanders, 1985) - (Deitz, Sanders, & Marks, Radial keratotomy: An overview of the Kansas City study, 1984) - (Deitz, Sanders, & Raanan, Progressive hyperopia in radial keratotomy. Long-term follow-up of diamond-knife and metal-blade series, 1986) and Sawelson (Sawelson & Marks, 1987), helped to better understand the limits of efficiency of the technique and improve its limits in particular functional complications (irregular astigmatism), daytime refractive instability and progressive hypermetropisation.

Instrumentation evolved from steel to diamond blades which had a better precision of cutting, the maximum refractive correction limit was reduced from -4 to -12 dioptres, and the centripetal incisions were replaced by centrifugal incisions while the number of incisions was reduced from 16 to 4. The RK technique disappeared gradually in the mid-1990s with the emergence of the excimer laser-assisted techniques.

2.1.2 Development of laser-assisted refractive surgery techniques

In the 1960s, Catalan ophthalmologist Jose I. Barraquer has set most of the theoretical ground for the emergence of current laser-assisted refractive surgery techniques.

He worked on the development of the microkeratome, a surgical instrument able to achieve a regular keratectomy i.e. a superficial lamellar cut of the cornea with a controlled diameter and depth. The principles developed by Barraquer for the microkeratome are the basis of the femtosecond laser keratectomy which is the first phase a LASIK surgery.

Besides, Barraquer has also tried to develop secondary cutters in the microkeratome able to execute ablations in the posterior stromal bed which is the second phase of a Laser-Assisted In-Situ Keratomileusis (LASIK) (SNOF, s.d.). Barraquer's results were disappointing and he abandoned this workstream but the principles of in-situ keratomileusis were established.

In 1988, a new laser – the excimer- used in the industry since the 1970s was introduced in ophthalmology starting the age of photorefractive keratectomy (PRK). The excimer laser is a pulsed laser which emits in the far ultraviolet (193 nm). The high energy of the laser allows to break the intermolecular bonds without significant thermal effect. After various tests on blind eyes, Marguerite McDonald performed the first PRK on a seeing eye in 1988. While showing its effectiveness, the PRK results on visual quality and refractive performance were limited by centring and cornea healing issues due to the alteration of the anterior layers of the cornea.

To avoid the alteration of the anterior layers of the cornea due to the PRK, Pallikaris and Buratto developed in 1990-1991 a keratomileusis based on a photoablation in the corneal stroma using an excimer laser to treat high degree myopia. The improvement of the performance of lamellar keratectomy using an automated microkeratome (ACS) developed by Ruiz will help spreading Pallikaris' and Buratto's technique starting the age of Laser-Assisted In-Situ Keratomileusis (LASIK).

The further improvement of microkeratomes and optimisation of the issuance and control of laser beams, allowed for the use of LASIK to correct astigmatism, hyperopia and low degree myopia.

2.1 Classification of refractive surgery techniques

2.1.1 Interaction between laser and cornea

There are four types of possible interactions between a laser beam and the cornea:

absorption, transmission, reflection and dispersion. The proportion of the different effects observed depends on the respective characteristics of the laser and tissue, and more precisely of the energy absorbed by the molecules of the tissue.

The cornea transmits wavelengths between 300 and 1,300 nanometres. The phenomenon of dispersion of energy is especially observed when large surfaces are treated as thermal effects are strongest in the vicinity of the laser impact. The reflection of the laser beam at the anterior and posterior surfaces of the cornea is very small. The most important laser-cornea interaction is the absorption of the laser's energy by the cornea.

The absorption of the laser pulse energy within the cornea depends on the wavelength and pulse duration. For wavelengths lower than 300 nm, absorption is due to the macromolecules of the cornea while for wavelengths of 600 nm or more, it is mainly due to the water.

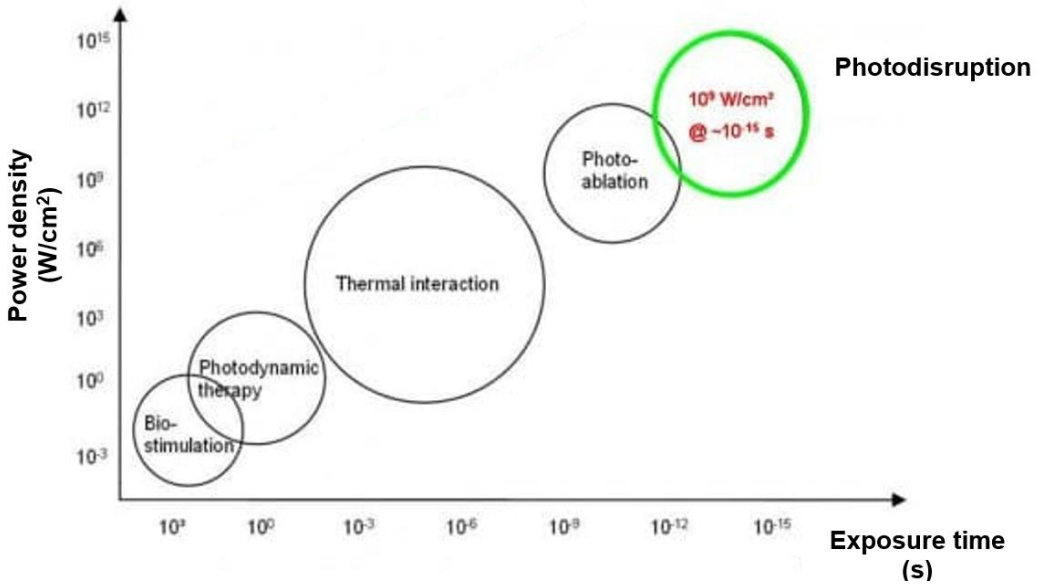

Figure 27 Map of laser-tissue interactions. The circles give only a rough estimate of the associated laser parameters. X axis is the duration of exposure to the laser radiation (inversely proportionate to the power density). Y axis is the power density. Modified from (Boulnois & JL, 1986)

For a maximum absorption, penetration of the laser inside the cornea must be minimal. In the **photothermal absorption** effect, the energy delivered by photons cause a molecular vibration which increases the tissue's temperature which may be sufficient to break low energy connections, such as hydrogens bonds and cause a protein denaturation.

In the **photodisruption absorption** effect, the mechanism of action is ionization which appears for very high concentrations of energy emitted through very short pulses (in

the range of the picosecond). This high energy intensity tears electrons of the atoms from their orbits and disintegrate the tissue in a mixture of ions and electrons called plasma, and a gas with similar electrical properties as metals. The femtosecond laser is based on this principle.

The **photochemical absorption** effect occurs with short wavelengths and low levels of energy.

The **photoablation** which is observed with ultraviolet radiation (for example with an excimer laser) is commonly used in corneal refractive surgery.

2.1.2 Classification

The general principle of refractive surgery is to modify the refractive power of a given eye. The classification of the different refractive surgery procedures can be done with several approaches. We have chosen to discriminate the major techniques in two groups according to the surgical site of action, corneal or intra-ocular.

Group 1: Corneal surgery techniques

This group encompasses various methods for adjusting an eye's focusing ability by reshaping the cornea to change the power of the corneal dioptre which represents two thirds of the total dioptric power of the eye. These methods are based on the substraction or addition of corneal tissues or biomaterials.

- **Photorefractive Keratectomy (PRK)**: A superficial photoablation using an excimer laser is executed on the Bowman's layer of the cornea. In this technique, the epithelium is removed manually by the surgeon prior to the photoablation and repairs itself after the surgery.

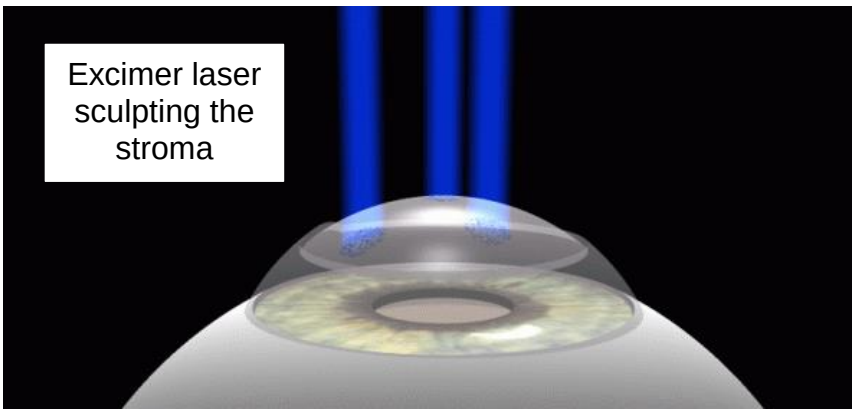

Figure 28 Principle of the PRK (Gatinel, www.gatinel.com, 2018)

Excimer lasers play a key role in refractive surgery as they can emit a high-energy radiation in the ultraviolet (UV) wavelengths. UV photons carry more energy than infrared or visible light photons and therefore have a photoablative effect on the corneal tissue with accuracy. UV photons may act in a targeted manner by breaking interatomic bonds. In the case of corneal refractive surgery, this interaction removes a very thin layer of corneal tissue with each impact. The excimer radiation used in refractive surgery (193 nm) is obtained from a mixture of Argon and Fluorine rare gazes (Ar-F) which are stored in the cavity of the laser under high pressure.

- **Keratomileusis:** keratomileusis means carving or sculpting the cornea. It is based on the subtraction of the corneal tissue of the stroma and achieved mostly through a Laser-Assisted In-Situ Keratomileusis (LASIK) surgery which is the most widely performed type of refractive surgery (c. 11 million procedure in the USA over the 1996-2014 period (Refractive surgery report: a global market analysis for 2016 to 2022, 2017)).

  The principle of LASIK is to realise a superficial keratectomy i.e. to create a flap by cutting through the corneal stroma. The flap creation was executed using a manual microkeratome until the end of 1990s and the emergence of femtosecond lasers. After this initial step, the correction itself is executed by an irreversible photoablation of tissue in the posterior stromal bed of the cornea using an excimer laser.

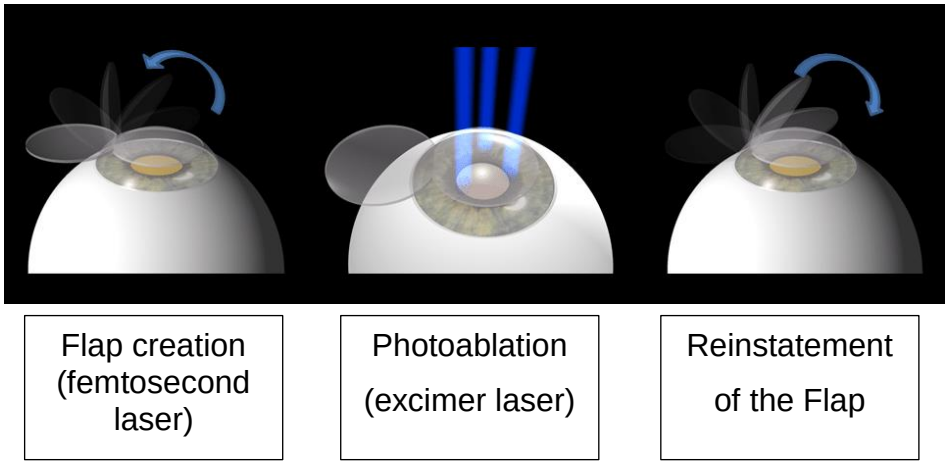

Figure 29 Principle of femto-LASIK (Gatinel, www.gatinel.com, 2018)

Femtosecond lasers emit pulses with relatively low pulse energies but with very high peak in the near infrared spectral range (800 nm to 1 micrometre). The duration of pulses delivered by a femtosecond laser used in ophthalmic surgery ranges between 200 and 800 femtoseconds according to the laser's model. The energy of the pulse is close to the Microjoule for LASIK applications.

For LASIK, the laser must issue approximately one million impacts which implies approximately 100,000 impacts per second. The time interval between two pulses (c. 10^{-5} second) is extremely long compared to the duration of a pulse. The spacing between pulses and line pulses is selected by the surgeon, as well as the energy delivered per pulse. Given the extremely short duration of femtosecond pulses, there is no thermal effect associated with this laser.

The advantages of the femtosecond lasers in refractive surgery especially compared with manual microkeratomes are the following:

- Low dependence vis-à-vis the keratometry of the cornea and its biomechanical characteristics when compared with manual microkeratomes;
- Better predictability of the cutting depth as the thickness obtained has a standard deviation of 5 microns with the latest generation of lasers vs. c. 20-30 microns with manual microkeratomes;
- Ability to refocus the route of the corneal flap on the centre of the pupil: prior to cutting, the control panel allows to preview the layout of the cut; refocussing is possible if the applanation discloses a shift of the pupil centre (effect of kappa angle or eccentricity of the pupil). This focus allows better optical quality after surgery;
- Surgery using femtosecond lasers induce less HOAs compared with manual microkeratomes (Yvon, Archer, Gobbe, & Reinstein, 2015)

The main disadvantage of femtosecond technology during the procedure is the possible occurrence of an opaque bubble layer during

cutting which is associated with the accumulation of degassing products of laser impacts in the corneal stroma and which sometimes requires waiting a few minutes before executing the subsequent excimer photoablation. Besides, another very rare and temporary adverse effect of the surgery is the so-called rainbow glare which is characterized by the perception of coloured halos around white light sources, whose distribution is generally a vertical rainbow (red inside towards blue outside). It is linked to a diffraction phenomenon by the regular network created by the successive impacts within the corneal stroma at the posterior face.

Keratomileusis can also be executed through a SMall Incision Lenticule Extraction (SMILE) procedure, which is a newer type of laser-assisted refractive surgery which differs from LASIK and is far less performed than this later for the time-being. During the intrastromal keratomileusis of a SMILE, a stromal lenticule is withdrawn from the corneal stroma without prior keratectomy. The femtosecond laser creates contiguous microcavitations and a secondary subsidence of the stroma. Excimer laser is not used.

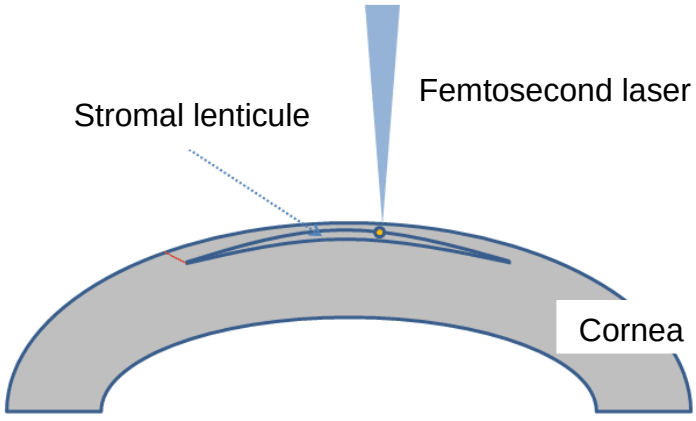

Figure 30 Principle of the SMILE keratomileusis (Gatinel, www.gatinel.com, 2018)

The two families of procedures above are based on the substraction of corneal tissue and are therefore irreversible.

- **Intracorneal Ring Segments:** This surgery is based on polymethylmethacrylate (PMMA) implants. These implants are inserted into a

peripheral corneal stroma tunnel created thanks to a femtosecond, which consequence is a flattening effect of the centre of the cornea. It is mostly used to correct low myopia and keratoconus.

Figure 31 Photograph of implanted intracorneal ring segments (Lotfi & Grandin, 2010)

- **Corneal Inlays:** Corneal inlays are implants designed to be inserted in the corneal stroma for the correction of presbyopia. They allow an increase in the DOF by a reduction of the diameter of the pupil of entry of the eye (pinhole).

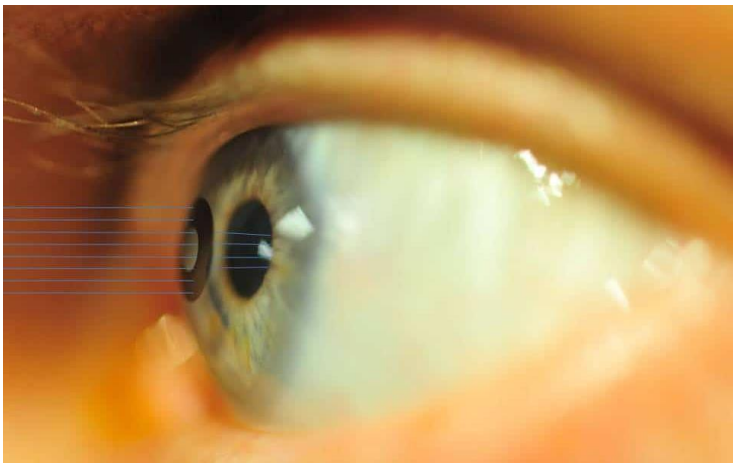

Figure 32 Principle of Corneal Inlays (Gatinel, www.gatinel.com, 2018)

The two above methods are based on the addition of biomaterials and are by construction potentially reversible.

Group 2: Intraocular Surgery techniques

These procedures are performed on the anterior segment of the eye: anterior

chamber and posterior chamber. These methods are based on the addition of synthetic refractive intraocular lenses to phakic eyes i.e. eyes with a natural crystalline lens, or on a replacement of the natural crystalline lens by a synthetic one.

- **Addition of refractive Intraocular Lenses (IOLs):** IOLs are implanted in phakic eyes. The IOLs can be made of Polymethyl methacrylate (PMMA), silicone, hydrophilic or hydrophobic acrylic or Collamer. They are always implanted in front of the crystalline lens but at varying distances.

  These techniques are reversible and are usually classified as follows according to (i) the positioning of the IOL in the anterior chamber (ACIOLs) or in the posterior chamber (PCIOLs); and (ii) the fixation method used.

  - Angle-Supported ACIOLs are implants placed in the anterior chamber of the eye. They are supported by the iridocorneal angle at the scleral spur which is an annular structure composed of collagen.
  - Iris-Supported ACIOLs are implants placed in the anterior chamber of the eye. They are fixed to the iris by a gripper mechanism.
  - PCIOLs are implants placed in the posterior chamber of the eye in the immediate proximity of the crystalline lens and bear in the ciliary sulcus.

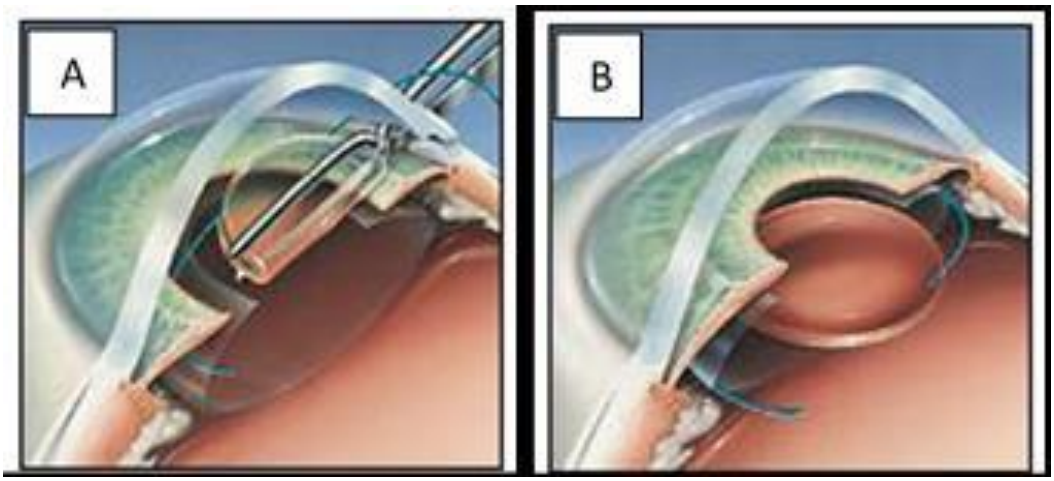

Figure 33 : Principle of microincision cataract surgery using acrylic or silicone foldable IOL implantation. A – The foldable IOL can be inserted through a <1.8mm microincision. B –The foldable IOL returns to original shape, and is put into place *(Lee, 2016)*

- **Exchange of crystalline lens:** this is an irreversible surgical method based on the replacement of the natural crystalline lens (clear or opaque) by a synthetic refractive lens and a removal of the natural accommodation of the eye. The refractive power of the lens is adapted to the targeted correction. The

crystalline lens is removed by phacoemulsification. The implant is positioned in the capsular bag. The implant is usually spherical and monofocal but can be multifocal or toric.

The table below summarizes the classification of the various refractive surgery techniques:

Group 1: Corneal surgery	
Principle of action	*Technique*
Substraction of corneal tissue (irreversible)	**Photorefractive Keratectomy (PRK)** **Keratomileusis** Laser-Assisted in SItu Keratomileusis (“LASIK”) SMall Incision Lenticule Extraction (“SMILE”)
Addition of biomaterials (reversible)	**Intracorneal Ring Segments** **Corneal Inlays**
Group 2: Intraocular Surgery	
Principle of action	*Technique*
Addition of phakic intraocular lenses (IOL)	**Anterior Chamber Phakic IOL** **Posterior Chamber Phakic IOL**
Exchange of crystalline	**Phacoemulsification**

Table 2 Classification of major refractive surgery techniques

2.2 Socio-economic weight and perspectives of laser-assisted refractive surgery

We will focus on this section on myopia which is the most widespread refractive error in the world. While no accurate prevalence numbers are provided by the World Health Organization, we estimate that short-sightedness affects c. 2.5 billion people i.e. one third of the world’s total population (Dolgin, 2015). Prevalence is usually high in the developed countries especially within the young adults, it is estimated to be c. 50% in the United States and Europe, and up to 90% in China (vs. 10-20% sixty years ago). Myopia has been a booming trend over the last 50 years reaching epidemiological levels in developed countries especially in the young populations. The prevalence of myopia in 20-year-old Hong Kong teenagers went from less than 10% in the 1940s to more than 80% in 2010.

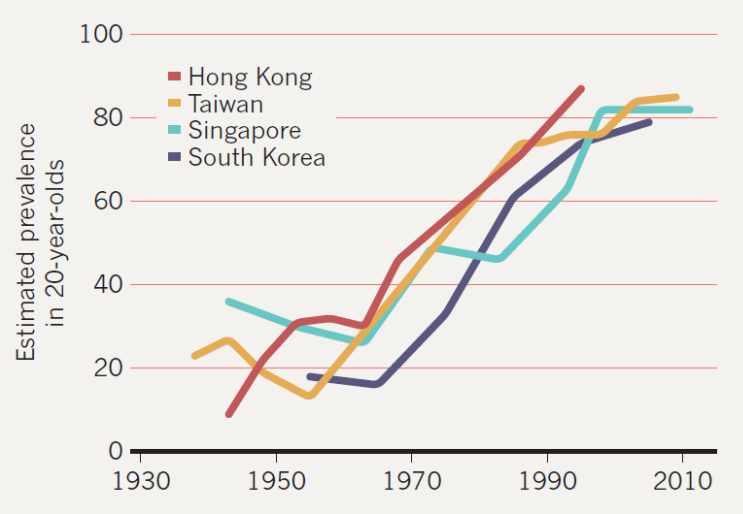

Figure 34 Estimated prevalence of myopia in 20-year-old Asians (Dolgin, 2015)

The boom in myopia accompanied the modern trend for children in developed countries to spend more time in studying and more recently working or playing with their computers and smartphone. This is particularly the case in East Asian countries as a report from the Organisation for Economic Co-operation and Development showed that the average 15-year-old in Shanghai now spends 14 hours per week on homework, compared with 5 hours in the United Kingdom and 6 hours in the United States.

While researchers in the 1990s, focused on the strong association between measures of education and the prevalence of myopia and explained that sustained close work could alter growth of the eyeball as it tries to accommodate the incoming light and focus close-up images squarely on the retina; more recent studies in the early 2000s, which looked at specific behaviours, such as books read per week or hours spent reading or using a computer, conclude that none appeared to be a major contributor to myopia risk (Saw, Carkeet, Chia, Stone, & Tan, 2002). However, it appears that children who spend less time outside have a greater risk of developing myopia. This observation may be related to the level of exposure to natural light of these children (Dolgin, 2015).

Glasses and contact lenses are the most common correction tools for myopia and other aberrations. However, laser-assisted refractive surgery which is born c. 30 years ago when Marguerite McDonald performed the first PRK, turned into a major sub-specialty of ophthalmology in developed countries and is expected to grow significantly following the boom of the myopia.

The number of procedures of laser-assisted refractive surgery and phakic IOL implantation in the world is estimated at c. 3.6 million in 2017. It is expected to grow at a compounded annual rate of 5.2 percent until 2022 to reach 4.6 million (Refractive surgery report: a global market analysis for 2016 to 2022, 2017).

Market Scope forecasts that the global refractive surgical industry will generate $7.6 billion in total patient fees in 2021 vs. $5.9 billion in 2016. Revenues at the manufacturer level as estimated at $803 million as of 2016 and are expected to grow by an average compounded annual rate of 8.8% to hit $1.2 billion in 2021. In particular, the femtosecond laser is expected to overperform with a growth rate of 15.5 percent to reflect the dominant place of LASIK and the increase in popularity with surgeons of the small incision lenticule extraction (SMILE) procedure which has secured crucial approvals in the US and Europe and is gaining in popularity in India and China.

China and the emerging markets - where non-surgical refractive correction are dominant - are the next frontier for the laser-assisted refractive surgery. The increase in purchase power in the developing world represents a very attractive growth opportunity for the industry.

Chapter 3: Materials and methods

As described the previous chapter, refractive surgery is a growing segment of ophthalmology. The increased number of procedures is accompanied by constant improvements in the surgical techniques where many issues are still to be addressed.

The main challenge of our work is to better understand the evolution and role of factors affecting post-surgical visual quality. This would permit to enhance and customize operative techniques, and thus optimize the optical and visual results of refractive surgery. To achieve this objective, it is important to understand the various mechanisms and anatomical and ocular factors involved in refractive surgery and question the interactions between them. We can also ask ourselves, what effects do these parameters produce on the visual performance of the operated eye? Are there factors which are endogenous to the human eye that affect postoperative performance?

To achieve our objective which is to provide practical recommendations for surgeons to optimize the performance of their routines, we conducted six studies. The outcomes of these studies have been reported in scientific articles which have been published in ophthalmology publications or were under review by a publication when this thesis manuscript was finalised. Each article was included in this thesis as a separate (sub)-chapter with no modification compared to the published version except the numbering of the tables, figures and references which have been amended to follow the order of this manuscript.

This chapter intends to explain in detail the general methodology and materials used in the six studies.

3.1 General methodology

We have sought to improve the predictability of certain postoperative results in the case of LASIK, PRK and cataract surgeries, to provide surgeons with practical recommendations that would contribute the development of more personalized treatment strategies. To achieve this, we have prospectively used "quality control" methodologies of on large samples of patients treated at the Rothschild Foundation. Informed consent was obtained from each patient after providing a detailed information about the purpose and procedure of the study in accordance with the declaration of Helsinki. Patients with a history of ocular surgery, corneal diseases or other eye

diseases (amblyopia, glaucoma, retinopathy, strabismus, etc.) were not included in the studies. Only adults (18-years old or more) were enrolled in our studies.

Exhaustive ophthalmologic examinations were performed on all patients preoperatively and postoperatively including manifest refraction, cycloplegic refraction, non-contact intraocular pressure assessment, slit lamp microscopic assessment of the anterior segment and dilated fundoscopy.

Anatomical and optical factors were measured using the Rothschild Foundation's equipment. Subjective visual quality was also assessed using questionnaires which were completed by patients before and after surgery.

The methods and equipment used in each study are described in the dedicated article/ chapter. However, we address below the characteristics of the most important measurements executed during our research.

We have performed **pupillometry** which is the measurement of pupil characteristics (pupil centre location, pupil diameter) and evolution.

Corneal topography corresponds to the graphic representation of certain geometric properties of the corneal surface. The measurement of corneal relief, curvature (keratometry), and thickness (pachymetry) are crucial steps in the diagnosis and detection of corneal diseases such as keratoconus, which is a priority in the preoperative examination. The Keratoconus causes a localized thinning and a deformation of the cornea. Corneal topography is also important for the development of vision correction methods such as contact lens adaptation and refractive surgery planning (LASIK in particular). Instruments that measured and described the topographic properties of the corneal surface (corneal topographs) are based on Placido discs technology which uses concentric reflective patterns. These systems are valuable tools in assessing keratometry and refraction, but they do not directly describe the actual spatial shape of the cornea. To obtain a "true" three-dimensional map of the shape of the anterior and posterior corneal surface, we use **corneal tomography** which is the measurement of corneal thickness in all the analysed surface. It is accomplished by scans (slots, Scheimpflug camera) or partial coherence tomography systems integrated in the new generation elevation topographs (Ambrósio & Belin, 2010).

Refractive errors (refractive spherical equivalent, corneal astigmatism) and biometry (axial length, anterior chamber depth) were also measured.

Also, we have performed **aberrometric measurements** based on the analysis of the

optical path difference (OPD) which outcome is the calculation of the RMS (quantifying of the level of optical aberrations in the eye).

Also, **biomechanical measurements** were considered to evaluate the mechanical stress of the cornea: the Corneal Hysteresis (CH) which is an assessment of the cornea's ability to absorb and dissipate energy that is significantly associated with the risk of glaucoma progression; the Corneal Resistance Factor (CRF) which is obtained by weighting the corneal hysteresis to reduce its correlation with the central thickness of the cornea; the Intraocular Pressure (IOP), Corrected Intra Ocular Pressure (IOPcc), and Goldman Intra Ocular Pressure (IOPg). Finally, **psychophysical measurements** (VA, CS, DOF) were performed.

3.2 Materials

3.2.1 Measurement instruments

WaveLight® Topolyzer™ VARIO (Alcon ® Laboratories Inc., USA)

This device has been used to perform pupillometries. It includes a dynamic pupil measurement software and is equipped with an infrared camera device which examines the changes in pupillary size during the transition from mesopic illumination conditions to photopic illumination conditions. All pupillary changes are recorded by a Charge Coupled Device (CCD) video camera system. During the dynamic pupillometry, a source of infrared light illuminates the surface of the iris in a grazing direction, thus, the pupillary edge is clearly identifiable by the camera device.

The WaveLight® Topolyzer™ VARIO (Alcon® Laboratories Inc., USA) also includes a topograph based on the Placido discs technology.

OPD-Scan® II and OPD-Scan® III (Nidek®, Japan)

The OPD-Scan® II and OPD-Scan® III (Nidek®, Japan) provide a comprehensive overview about the refractive status of the eye. These devices include an infrared pupilometer, a Placido disc corneal topographer and a wavefront aberrometer. The aberrometer is based on the analysis of the optical path difference (for which the name OPD stands) between a perfect wavefront and an aberrated wavefront.

Orbscan IIz® (Bausch & Lomb®, USA)

It is a Placido disk corneal topographer and Scheimpflug's based tomographer able to map the entire corneal surface and analyse elevation and curvature measurements

on both the anterior and posterior surfaces of the cornea.
The device uses 40 scanned slit images (9,000 data point) from throughout the cornea to measure the anterior and posterior corneal surfaces as well as a reflective image to measure the curvature of the anterior corneal surface.

Pentacam® AXL (Oculus Optikgeräte GmbH, Germany)

It is a corneal tomographer using a rotating Scheimpflug camera system that allows to measure elevations of the anterior and posterior surfaces of the cornea, as well as to measure point-by-point thickness.

IOLMaster® 700 with Swept Source OCT (Carl Zeiss Meditec AG®, Germany)

Optical biometer used it in our thesis to measure keratometry, axial length and anterior chamber depth. It is based on swept source Optical Coherence Tomography (OCT).

Optical Quality Analysing System (OQAS®) (Visiometrics®, Spain)

It is an instrument that provides the direct measure of the combined effect of HOAs and of the loss of transparency of the eye circles on the optical quality of the eye. It is of major interest in cataract surgery, but also in refractive surgery, because its use is about the many clinical situations or transparency of the cornea is altered: haze, scars, wrinkles and flaps micro-plis, transplants, etc.
The data provided by this instrument is derived from the analysis of the retinal image obtained with an infrared light beam. It was used in this work to assess the severity of the cataract on patients through the Objective Scatter Index (OSI).

Ocular Response Analyzer® or ORA (Reichert Technologies, USA)

It is a tonometer used in this thesis to measure the biomechanical properties of the cornea: CH, CRF, IOP, IOPcc, and IOPg.

3.2.2 Surgical instruments

LASIK surgery executed on patients enrolled in our studies was performed with the WaveLight® Refractive Suite (Alcon® Laboratories Inc., USA) composed of two lasers, the FS200 femtosecond laser and the EX500 excimer laser.

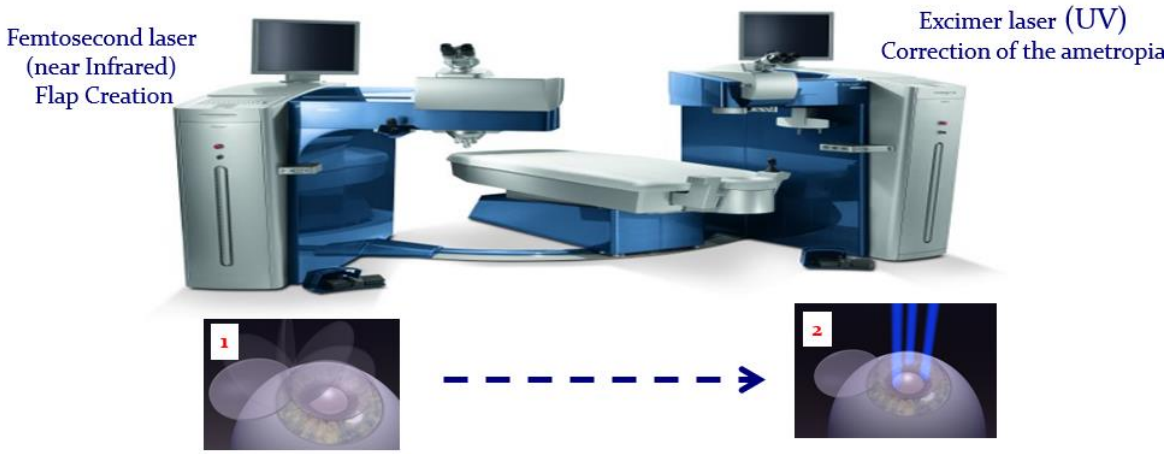

Figure 35 WaveLight® Refractive Suite (Alcon® Laboratories Inc., USA). Modified from (Gatinel, www.gatinel.com, 2018)

Femtosecond laser FS200

There are currently five commercialized femtosecond lasers used in ophthalmology for corneal surgery:

- the IntraLase® FS (Abbott Medical Optics®, USA) which operates at a wavelength of 1,05 µm and has a repetition rate of 60 kHZ;
- the Femtec® (Bausch & Lomb®, USA) which repetition rate is 40 kHZ;
- the Femto LDV® (Ziemer, Switzerland) with a repetition rate of approximately 1 MHz;
- the Visumax® (Carl Zeiss Meditec AG®, Germany) that operates at a repetition rate of 100 kHz;
- the FS 200 (Wavelight/Alcon, Germany - United States), which is available at the Rothschild Foundation and was used in the experiments of this thesis.

The FS200 femtosecond laser system is a low-energy and high pulse frequency laser that emits laser pulses with duration of 350 femtoseconds at a wavelength of 1,050 nm and pulse repetition rate of 200 kHz. It is able to execute the flap creation in a LASIK in 6 seconds (Kanellopoulos J. , 2010) - (Winkler von Mohrenfels, 2012). The figure below describes the optical path of this laser.

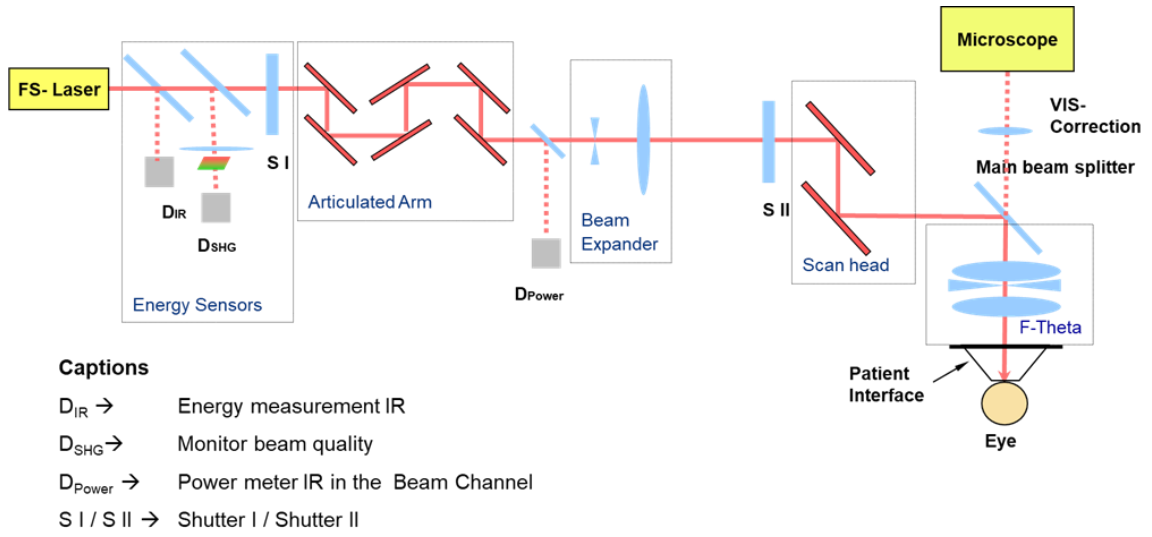

Figure 36 Optical path of the FS200 femtosecond laser. Courtesy of Alcon® Laboratories Inc., USA

Excimer EX500

There are currently nine excimer laser platforms which dominate the market. They all rely on the use of 193 nm excimer radiation (Argon - Fluorine) are listed in the figure below according to their date of launch (older to most recent one):

Figure 37 Excimer lasers available in the market (Gatinel, www.gatinel.com, 2018)

The most recent excimer lasers such as the EX500 use a technology called "flying spots": the energy of the laser light is distributed in the form of pulses, whose diameter is close to 1 mm. Each spot ablates some corneal tissue. The EX500 also includes an integral pachymetre for measuring corneal thickness in real time before, during and after the laser procedure.

The below table compares the key characteristics of the EX500 with other excimer laser devices available in the market:

Manufacturer	WaveLight® (Alcon®)	WaveLight® (Alcon®)	Carl Zeiss Meditec AG®	Abbott Medical Optics®
Model	Allegretto Wave	EX 500	MEL 80	VISX S4 IR
Working Distance (mm)	200	250	190	210
Frequency	200 Hz	500 Hz	250 Hz	6 Hz à 20Hz
Pulse duration	10 nanoseconds	< 7 nanoseconds	5 nanoseconds	20 nanoseconds
Ablation	Flying spot	Flying Spot	Flying Spot	Variable Size Spot
Mean Fluence	200 mJ/cm^2	200 mJ/cm^2	150 mJ/cm^2	160 mJ/cm^2
Mean Beam Diameter	0.68 mm	0.68 mm	0.7 ± 0.1mm	0.65mm
Spot size / Ablation Threshold	0.95 mm / max 1.0 mm	0.95 mm / max 1.0 mm	0,7 mm / max 1.1mm	0.65 mm
Ablation depth by Pulse	0.65 µm	0.65 µm	0.51 µm	0.38 µm
Ablation depth by Diopter Myopia (Optical Zone 6.5 mm)	15.5 µm	15.5 µm	16 µm	16 µm
Time/D Myopia (Optical Zone 6.0 mm)	3.5 seconds	1.4 seconds	3 seconds	6 seconds
Sampling Eyetracker Frequency	250 Hz	1,050 Hz	250 Hz / 1,050 HZ	60 Hz
Response Time Eye Tracker	6-8 Milliseconds	2-3 Milliseconds	<6 Milliseconds	16-24 Milliseconds
Optical Zone (OZ)	4.5-8 mm	4.5-8 mm	5-8 mm	6-6.5 mm

Table 3 Comparison of Excimer laser models

Chapter 4: Pupil dynamics in refractive surgery

4.1 Assessing repeatability of pupillometric measurements in the eyes of refractive surgery candidates using infrared pupillometer

Authors: Imene Salah Mabed, MSc; Alain Saad, MD; Damien Gatinel, MD

Department of Anterior Segment and Refractive Surgery, Rothschild Foundation, Paris, France

CEROC: Centre for Expertise and Research in Optics for Clinicians

None of the authors has any financial or proprietary interests in any product, method or material presented in this paper.

Published: J Refract Surg. 2017 Aug 1;33(8):552-557. doi: 10.3928/01913913-20170619-03

4.1.1 Abstract

Purpose: To assess the repeatability of measuring pupil dynamics using an infrared pupillometer.

Methods: 124 eyes of 124 patients scheduled for corneal laser refractive surgery were separated into 2 groups: a myopic and a hyperopic group under which 2 subgroups were assigned based on high or low levels of astigmatism. Measurements were taken using a dynamic pupillometry, WaveLight® Topolyzer^{TM} VARIO (Alcon® Laboratories Inc., USA). Main outcome measures were pupil diameter size, the distance between the pupil centre and the keratoscopic axis, and the spatial shift of the pupil center. Repeatability of measurements was assessed from test-retest repeatability (2.77 Sw), coefficient of variation (COV), and Intra-class Correlation Coefficient (ICC).

Results: The 2.77 Sw of all measured parameters was lower than 0.36 and 0.44 millimeters respectively for myopic and hyperopic eyes. The ICCs of the pupil diameter measurements were higher than 0.963 and 0.926 respectively in myopic and hyperopic eyes. ICCs of the distance between the pupil centre and the corneal vertex along the *x* axis were higher than 0.934 and 0.994 respectively in myopic and hyperopic eyes. Along the *y* axis, ICCs of this distance were higher than 0.417 in myopic eyes and higher than 0.504 in hyperopic eyes. The pupil centre shift

measurements ICCs were lower than 0.482 and 0.526, respectively for myopic and hyperopic eyes.

Conclusions: In all groups, WaveLight® Topolyzer^{TM} VARIO (Alcon® Laboratories Inc., USA) showed excellent repeatability when measuring pupil dynamic parameters except when measuring pupil centre shift and distance between the pupil centre and the corneal vertex along the vertical axis.

4.1.2 Introduction

The entrance pupil of the human eye is formed by the image of the aperture stop of the iris through the cornea (Atchinson & Smith, Optics of the Human Eye, 2002). Pupillary responses to multiple environmental factors (Lowenfeld, 1993) affect vision as with controlling how much light enters the eye, increasing or decreasing the depth of field, or changing the retinal light level (Atchinson & Smith, Optics of the Human Eye, 2002). Though it appears to be smooth, the human eye is an optical system with varying amounts of regular and irregular aberrations (Ivanoff, 1956) (Jenkins, 1963), whose effects become more exaggerated when the pupil dilates (Walsh & Charman, 1988) - (Martinez, et al., 1998) and potentially impact image quality for the retina (Artal & Navarro, 1994).

In light of recent developments for customized refractive surgery treatments, defining the pupil's size and the exact location of its centre has become increasingly important in clinical practice (Arbelaez, Vidal, & Arba-Mosquera, 2008) - (Kermani, Oberheide, Schmeidt, Gerten, & Bains, 2009) - (Park, Oh, & Chuck, 2012). Current practices in pupil tracking during refractive surgery rely on the assumption that the centre of the pupil will not shift even as the pupil moves (Lowenfeld, 1993) - (Ivanoff, 1956) - (Jenkins, 1963). Also, several research studies consider the centre of the pupil a good anatomical landmark for customized treatments because its shift is relatively small across different lighting conditions (Applegate, Thibos, Bradley, & al., 2000) - (Kermani, Oberheide, Schmeidt, Gerten, & Bains, 2009) - (Tabernero, Atchinson, & Markwell, 2009). Yet, some authors have recommended centering treatment based on the location of the corneal vertex, which they define as a stable landmark which may be closer to the visual axis (Okamoto, et al., 2011) - (Arbelaez, Vidal, & Arba-Mosquera, 2008) - (Reinstein, Gobbe, & Archer, Coaxially sighted corneal light reflex versus entrance pupil center centration of hyperopic corneal ablations in eyes with small and large angle kappa, 2013).

During cataract surgery, correct positioning is a standard concern, especially in

regard to the aspheric and multifocal intraocular lenses (Atchinson D. , 1991) - (Holladay, Piers, Koranyi, Van den Mooren, & Norrby, 2002). Intraocular lenses (IOL) are centered at the end of the cataract procedure when the pupils are still dilated. Importantly, a change in the location of the centre of the pupil when it constricts in normal lighting conditions may cause negative effects on the sight of the operated eye. Thus, the ability to determine pupil movements and the location of its centre with a high degree of accuracy and reliability is important in both clinical and academic settings.

Before the surgeon relies on measurements taken from pupillometric devices, it is necessary to ensure that repeated exams produce consistent results. Repeatability as defined by the International Organization for Standardization is a condition in which independent test results are obtained with the same method and equipment in the same subject by the same operator with the shortest possible time between successive readings (International Organisation for Standardization, 1994).

The WaveLight® Topolyzer^{TM} VARIO (Alcon® Laboratories Inc., USA) is a Placido corneal topograph which takes pupil measurements and high-resolution infrared images, thus capturing the shift of the pupil centre under different lighting conditions and with different pupil sizes.

To the best of our knowledge, only one study showed good repeatability and reliability of the WaveLight® Topolyzer^{TM} VARIO (Alcon® Laboratories Inc., USA) for keratometric data (Wang, et al., 2012). However, no comprehensive data on the repeatability of pupillometric measurements have been published. The present study sought to determine prospectively the intra-session repeatability of pupillometric dynamics using infrared pupillometry.

4.1.3 Patients and Methods

Subjects

Patients were prospectively recruited from the Department of Refractive Surgery at the Rothschild Foundation, Paris, France. All patients received complete pre-operative assessments, including cycloplegic refraction, slit lamp, and a fundus exam.

Patients with a history of ocular surgery, corneal disease, or other eye-related pathologies (i.e. amblyopia, glaucoma, cataracts, retinopathy, or strabismus) or suspected keratoconus after corneal topography were excluded. We excluded patients with dry eye disease to be sure to have high quality images. Patients older than 18 years with healthy eyes were approached and enrolled. The study and data

extraction plan were approved by the foundation's Institutional Review Board. Informed consent was obtained from each patient after they expressed understanding for the purpose and procedures of the study in accordance with the Declaration of Helsinki.

Data were organized into two groups of myopic or hyperopic eyes, then sub-grouped based on high or low levels of astigmatism. A low level of astigmatism was defined as (≤ -0.75 D), and medium to high levels of astigmatism were defined as (≥ -1.0 D).

Instruments

Pupillometry was performed on each eye using the dynamic pupil measurement module built into the videokeratoscope. Pupillometry and videokeratoscope devices are housed in the same workspace, so only one fixation target was required to perform both measurements.

The pupillometer is equipped with a combined infrared light and camera, which measures the changes in pupil size during the transition from mesopic to photopic conditions. All pupillary changes are recorded by a CCD camera system. During dynamic pupillometry, the infrared light shines onto the surface of the iris with a back and forth motion, while the camera lens records clear pupillary margins.

Recording begins automatically when the patient's eye is aligned with the target observation (a bright disc located 80 mm from the centre of the subject's eye). Three successive cycles are performed over 60 seconds (during each cycle, the 22 Placido discs turn off and on). Red and green points are used to show the pupil centre and the vertex (coaxially sighted corneal reflex) respectively (Figure 38).

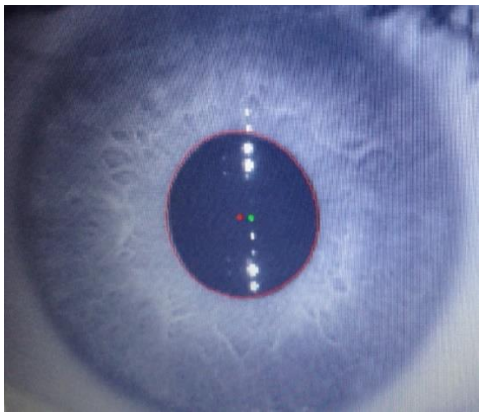

Figure 38 Image of the dynamic pupillometer showing the centre of the pupil (in red) and the corneal vertex (in green)

The software analyzes the images and provides a graphic representation of the

movement of the pupil centre between photopic and mesopic conditions. Additionally, the distance between the pupil centre and the keratometric axis (corneal vertex) in both mesopic and photopic conditions is provided.

Measurements and Procedures

The present study's definitions of repeatability and agreement were based on those adopted by the British Standards Institute and the International Organization for Standardization (British Standards Institution, 1994) - (International Organisation for Standardization, 1994).

Measurements were taken 3 hours or more after participants woke from sleep from 9am to 5pm for each one. Pupillometric exams were performed in a closed, dark room (lighting less than or equal to 1 lux). The head of each patient was covered with a thick black cloth, lowering the lighting from 1 lux to 0.4 lux. First measurements were taken without activating the Placido disc light in low mesopic conditions (0.4 lux), and then with the light on providing photopic lighting conditions (120 lux). Illuminance values were obtained using a BM3 TOPCON (TOPCON Medical Systems, Inc., Oakland, NJ) light meter. Three consecutive data captures were performed in which 3 cycles of mesopic and photopic conditions lasted for 60 seconds. Subjects were instructed to blink completely immediately before each measurement. The time lapse between scans was managed to be as fast as possible. Both eyes were tested consecutively, starting randomly with the right or left eye. All the measurements were performed by the same operator (IS). All the images were analyzed by computer software for data collection and data analysis. Pupil diameters, pupil centre shifts, and distances between pupil centers and corneal vertex measurements were represented in Cartesian coordinates (Figure 39).

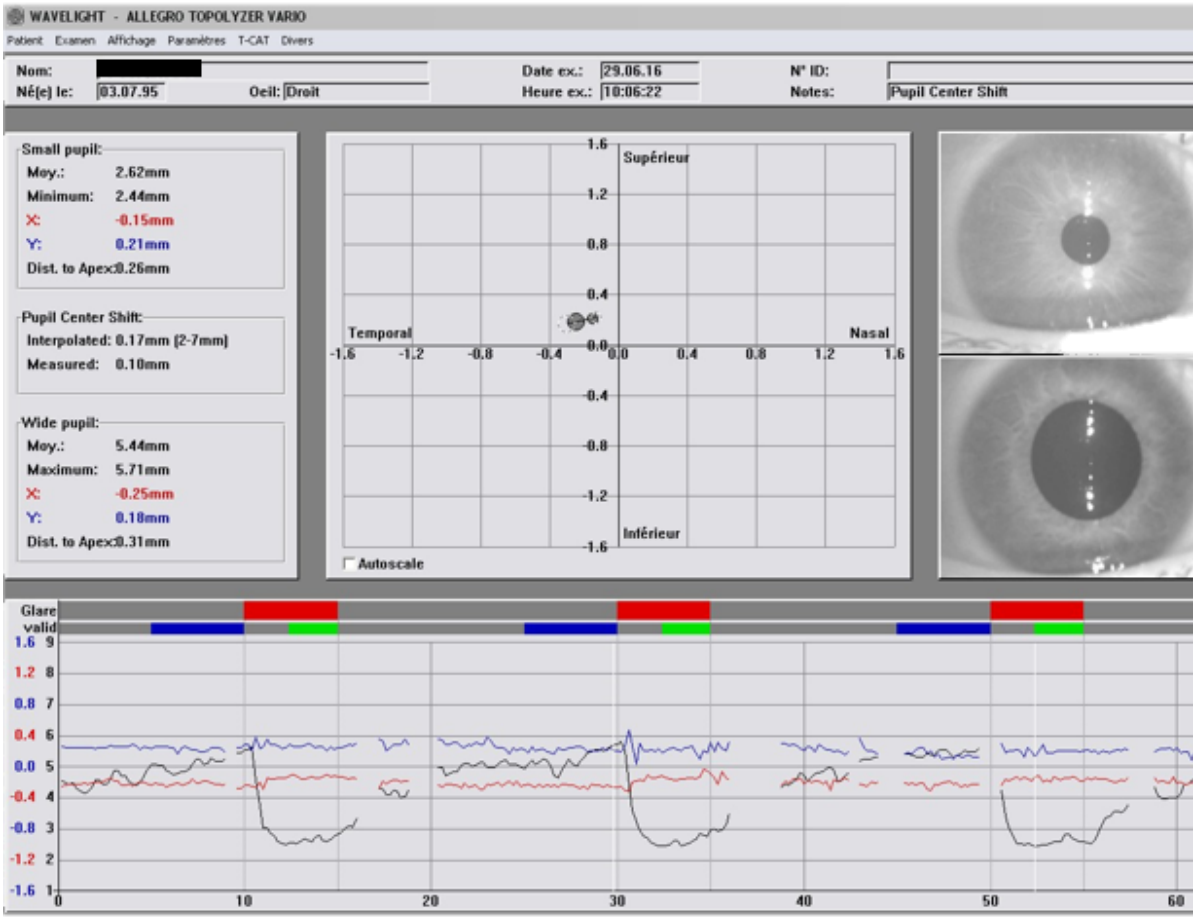

Figure 39 WaveLight® Topolyzer™ VARIO (Alcon® Laboratories Inc., USA) analysis software output screen, graphic representation of pupil dynamics

Statistics

Statistical analysis was performed with commercial software (SPSS for Windows v. 13.0; SPSS Inc., Chicago, IL, U.S.) and Microsoft Office Excel. A calculated *p* value less than 0.05 was considered to be statistically significant. The data was normally distributed (Shapiro-Wilk normality test *p*= 0.299 or more) and was presented in this study as the mean +/- standard deviation.

Intra-session Repeatability Calculation

Repeatability is the closeness of agreement between the results of successive measurements of an identical test material performed under defined conditions. Study conditions included the same operator, same apparatus, and a short time between analyses. To determine intra-session repeatability of the device, within-subject standard deviation (Sw), test-retest repeatability (TRT), the within-subject coefficient of variation (COV), and Intra-class Correlation Coefficients (ICC) were calculated for the three repeated measurements. [25] TRT was defined as 2.77 Sw, which means an

interval within which 95% of the differences between measurements are expected to lie. The COV was calculated as the ratio of the Sw to the overall mean. A lower COV is associated with higher repeatability.

The advantage of COV values is that they can be compared between data sets with different units or widely ranging means. The disadvantage is that when the mean value is near zero, the COV is sensitive to small changes in the mean, limiting its usefulness. The ICCs (ranging from 0 to 1) measure the consistency for data sets of repeated measurements. The closer the ICC is to 1, the more consistent the measurement is.

4.1.4 Results

Demographics

The relation of pupil between right and left eye is strong related. For assessing the repeatability, we included randomly only one eye of each patient. 124 eyes of 124 patients were included in the study. 92 myopic eyes (74% of the hall population) of 92 patients (mean age 35.2 ± 8.1 years, ranging from 23.2 to 59 years) and 32 hyperopic eyes (26% of the population) of 32 patients (mean age 52.3 ± 14.2 years from 24.8 to 73.3 years) were investigated. The data are detailed in Table 4.

	Total	Myopes		Hyperopes	
		Low Astigmatism (≤ -0.75 D)	High Astigmatism (≥ -1.0 D)	Low Astigmatism (≤ -0.75 D)	High Astigmatism (≥
Number of patients	124	92		32	
Number of eyes	124	59	33	25	7
Age (years)					
Average ± Standard deviation	39,6 ± 12,5	34,8 ± 8,0	35,9 ± 8,3	55,6 ± 12,6	40,2 ± 13,7
Minimum / Maximum	23,2 / 73,3	23,2 / 59,0	23,8 / 57,0	24,8 / 73,3	28,4 / 61,7
Refractive Spherical Equivalent (D)					
Average ± Standard deviation	-2,3 ± 3,4	-3,7 ± 2,0	-4,5 ± 2,3	2,7 ± 1,1	1,5 ± 2,3
Minimum / Maximum	-11,3 / 5,3	-9,1 / -0,5	-11,3 / -1,4	1,0 / 5,3	-0,5 / 5,1
Refractive Cylinder (D)					
Average ± Standard deviation	-1,0 ± 0,7	-0,5 ± 0,2	-1,6 ± 0,6	-0,6 ± 0,2	-1,7 ± 1,0
Minimum / Maximum	-0,25 / -4,00	-0,25 / -0,75	-1,00 / -3,50	-0,25 / -0,75	-1,00 / -4,00

Table 4 Demographic data

Intra-session Repeatability

For the whole population of eyes, the 2.77 Sw of all measured parameters were lower than 0.36 millimeters. The COV of the pupil diameters measurements were lower than 0.02% and the ICC higher than 0.971. The pupil centre Cartesian coordinates COV were lower than 0.5%, and ICCs of the distance between the pupil centre and the corneal vertex along the x axis higher than 0.972. Along the y axis, the ICC of this distance was lower than 0.658. The pupil centre shift measurements COV was equal to 0.36% and the ICC was equal to 0.431. These results are described in Table 5.

	Total				
Parameter	**Mean ± SD**	**Sw**	**2.77 Sw**	**COV (%)**	**ICC**
Mean Small Pupil	3,05 ± 0,56	0,07	0,19	0,02	0,979
Smallest Pupil	2,84 ± 0,55	0,07	0,19	0,02	0,971
SP-Vertex along x	0,04 ± 0,23	0,02	0,06	0,50	0,972
SP-Vertex along y	-0,04 ± 0,13	0,04	0,11	1,00	0,617
SP-Vertex chord length	0,25 ± 0,12	0,03	0,08	0,12	0,749
PCS	0,11 ± 0,07	0,04	0,11	0,36	0,431
Mean Wide Pupil	5,88 ± 0,95	0,13	0,36	0,02	0,973
Widest Pupil	6,14 ± 0,95	0,13	0,36	0,02	0,973
WP-Vertex along x	0,07 ± 0,27	0,02	0,06	0,29	0,994
WP-Vertex along y	-0,06 ± 0,12	0,03	0,08	0,50	0,658
WP-Vertex chord length	0,28 ± 0,14	0,03	0,08	0,11	0,832

Table 5 Intrasession Repeatability in Measuring pupillometric parameters in the whole population of eyes (N=124)

For myopic eyes, the 2.77 Sw of all measured parameters were lower than 0.36 millimeters. The COV of the pupil diameters measurements was lower than 0.03% and the ICC higher than 0.963. The pupil centre Cartesian coordinates COV were between 0.17% and 1% and the ICC of the distance between the pupil centre and the corneal vertex along the *x* axis higher than 0.934. Along the *y* axis, ICCs of this distance were higher than 0.417 in eyes with high astigmatism, and 0.637 in those with low astigmatism. The pupil centre shift measurements COV were equal to 0.36% and 0.27% and ICCs equal to 0.210 and 0.482 respectively in eyes with high astigmatism and in eyes with low astigmatism. Table 6 shows these data.

Parameter	Myopes									
	High Astigmatism					Low Astigmatism				
	Mean ± SD	Sw	2.77 Sw	COV (%)	ICC	Mean ± SD	Sw	2.77 Sw	COV (%)	ICC
Mean Small Pupil	3,17 ± 0,56	0,07	0,19	0,02	0,98	3,14 ± 0,53	0,07	0,1939	0,02	0,97
Smallest Pupil	2,95 ± 0,55	0,09	0,25	0,03	0,968	2,93 ± 0,51	0,07	0,1939	0,02	0,96
SP-Vertex along x	0,03 ± 0,25	0,01	0,03	0,33	0,991	0,02 ± 0,20	0,02	0,0554	1,00	0,93
SP-Vertex along y	-0,03 ± 0,15	0,05	0,14	1,67	0,676	-0,03 ± 0,11	0,04	0,1108	1,33	0,64
SP-Vertex chord length	0,26 ± 0,13	0,03	0,08	0,12	0,77	0,22 ± 0,10	0,02	0,0554	0,09	0,82
PCS	0,11 ± 0,06	0,04	0,11	0,36	0,21	0,11 ± 0,06	0,03	0,0831	0,27	0,48
Mean Wide Pupil	6,05 ± 0,87	0,13	0,36	0,02	0,965	6,12 ± 0,85	0,12	0,3324	0,02	0,97
Widest Pupil	6,31 ± 0,88	0,12	0,33	0,02	0,979	6,38 ± 0,85	0,12	0,3324	0,02	0,97
WP-Vertex along x	0,06 ± 0,28	0,01	0,03	0,17	0,997	0,05 ± 0,23	0,02	0,0554	0,40	0,99
WP-Vertex along y	-0,05 ± 0,13	0,05	0,14	1,00	0,417	-0,04 ± 0,10	0,02	0,0554	0,50	0,93
WP-Vertex chord length	0,29 ± 0,14	0,04	0,11	0,14	0,641	0,23 ± 0,12	0,02	0,0554	0,09	0,96

Table 6 Intra-session Repeatability in Measuring pupillometric parameters in myopic with high astigmatism eyes (N=33), and in myopic with low astigmatism eyes (N=59)[2]

[2] ***SP-Vertex along x***= *Distance between the small pupil center and the corneal vertex along x axis,*

For hyperopic eyes, the 2.77 Sw of all measured parameters was lower than 0.44 millimeters. The COV of the pupil diameters measurements was lower than 0.03%, while the ICC was higher than 0.926. The pupil centre Cartesian coordinates COVs were between 0.07% and 0.17% and ICCs of the distance between the pupil centre and the corneal vertex along the *x* axis higher than 0.994. Along the *y* axis, ICCs of this distance were higher than 0.805 in eyes with high astigmatism, and 0.504 in those with low astigmatism. The pupil centre shift measurements COVs were equal to 0.38% and 0.31% and ICCs were equal to 0.526 and 0.501 respectively in eyes with high astigmatism and in eyes with low astigmatism. These data are described in Table 7.

Parameter	Hyperopes									
	High Astigmatism					Low Astigmatism				
	Mean ± SD	Sw	2.77 Sw	COV (%)	ICC	Mean ± SD	Sw	2.77 Sw	COV (%)	ICC
Mean Small Pupil	2,87 ± 0,52	0,09	0,25	0,03	0,964	2,71 ± 0,54	0,04	0,11	0,01	0,991
Smallest Pupil	2,65 ± 0,52	0,09	0,25	0,03	0,972	2,53 ± 0,51	0,05	0,14	0,02	0,988
SP-Vertex along x	0,15 ± 0,36	0,01	0,03	0,07	0,999	0,10 ± 0,24	0,01	0,03	0,10	0,994
SP-Vertex along y	-0,04 ± 0,12	0,04	0,11	1,00	0,805	-0,07 ± 0,15	0,05	0,14	0,71	0,504
SP-Vertex chord length	0,36 ± 0,16	0,01	0,03	0,03	0,987	0,27 ± 0,15	0,04	0,11	0,15	0,579
PCS	0,08 ± 0,05	0,03	0,08	0,38	0,526	0,13 ± 0,11	0,04	0,11	0,31	0,501
Mean Wide Pupil	5,96 ± 0,59	0,16	0,44	0,03	0,929	5,07 ± 0,97	0,13	0,36	0,03	0,967
Widest Pupil	6,21 ± 0,58	0,16	0,44	0,03	0,926	5,34 ± 0,97	0,16	0,44	0,03	0,954
WP-Vertex along x	0,12 ± 0,39	0,02	0,06	0,17	0,997	0,12 ± 0,29	0,02	0,06	0,17	0,995
WP-Vertex along y	-0,03 ± 0,12	0,02	0,06	0,67	0,957	-0,11 ± 0,15	0,04	0,11	0,36	0,696
WP-Vertex chord length	0,38 ± 0,13	0,02	0,06	0,05	0,976	0,33 ± 0,15	0,03	0,08	0,09	0,85

Table 7 Intra-session Repeatability in Measuring pupillometric parameters in hyperopic with high astigmatism eyes (N=7), and in hyperopic with low astigmatism eyes (N=25)[3]

In all cases, ICCs of pupil centre Cartesian coordinates measurements along the *y* axis were higher for wide pupils than for small ones except for myopic eyes with a high amount degree of astigmatism. We did not find any correlation between the Sw and the amount of the spherical equivalent for all measured parameters (r^2<0.002,

***SP-Vertex along y**= Distance between the small pupil center and the corneal vertex along y axis, **SP-Vertex chord length**= Distance between the small pupil center and the corneal vertex, **PCS**= measured Pupil center shift between photopic and mesopic conditions, **WP-Vertex along x**= Distance between the wide pupil center and the corneal vertex along x axis, **WP-Vertex along y**= Distance between the wide pupil center and the corneal vertex along y axis, **WP-Vertex chord length**= Distance between the wide pupil center and the corneal vertex, **MM**= millimeters, **SD**= standard deviation, **Sw**= within-subject standard deviation, **COV**= within-subject coefficient of variation, **ICC**= intraclass correlation coefficient*

[3] ***SP-Vertex along x**= Distance between the small pupil center and the corneal vertex along x axis, **SP-Vertex along y**= Distance between the small pupil center and the corneal vertex along y axis, **SP-Vertex chord length**= Distance between the small pupil center and the corneal vertex, **PCS**= measured Pupil center shift between photopic and mesopic conditions, **WP-Vertex along x**= Distance between the wide pupil center and the corneal vertex along x axis, **WP-Vertex along y**= Distance between the wide pupil center and the corneal vertex along y axis, **WP-Vertex chord length**= Distance between the wide pupil center and the corneal vertex, **MM**= millimeters, **SD**= standard deviation, **Sw**= within-subject standard deviation, **COV**= within-subject coefficient of variation, **ICC**= intra-class correlation coefficient*

p<0.001).

4.1.5 Discussion

The validity of a measurement depends on two types of measurement uncertainties: systematic errors and random errors. An instrument produces valid measures when the average of several measures is close to the actual measured value for each parameter. Repeatability indicates the instrument's ability to repeat its own results (International Organization for Standardization, 1977). In this study, we have not studied the validity of the device. However, it depends on the repeatability that we studied. The calibration of an instrument compared to known standards eliminates a systematic error. Errors, such as the ones associated with routine use of an instrument are random and can be minimized by a detailed routine procedure and using repeated independent measurements. Determining random errors leads to the identification of instrument measurement repeatability (Saad, Saab, & Gatinel, 2010).

The measurements of pupil size in photopic and mesopic conditions showed excellent repeatability with ICCs more than 0.971. In refractive surgery practice, it is important to rely on a pupil diameter measurement for the determination of the optical zone of the treatment. The size of the optical zone must match the size of the pupil diameter. If not, the patient can experiment visually disabling side effects such as glare, ghosting, halos, loss of contrast, and monocular diplopia (Doane, Cavanaugh, Durrie, & Hassanein, 1995) - (Gatinel & Bains, 2010).

Measuring the distance between the pupil centre and the corneal vertex on the horizontal axis in both photopic and mesopic conditions can also be considered highly repeatable. However, measurements of this distance along the vertical axis, and measurements of the pupil centre shift showed a mild to poor repeatability in some cases, except in hyperopic eyes in which the vertical coordinates of the centre of the pupil showed good indicators of repeatability. The corneal vertex is the corneal projection of the centre of the Placido discs (i.e. the centre of the first Purkinje-Sanson image). The location of this image depends on the location of the light source and where the patient directs his gaze. The pupil centre is measured as the centroid of the pupil edges in infrared pupillometry. These two points returned in the same frontal plane describe a vector on which the distance between the vertex and the centre of the pupil is normed. The vertex is considered here as the origin of an orthonormal base.

We assume that the poor repeatability of pupil centre displacement measures was

due to poor repeatability of the measurements of pupillary centre-corneal vertex distance along the *y* axis because its calculation depends on it directly (i.e. difference between photopic distance from pupil centre to corneal vertex and mesopic distance from pupil centre to corneal vertex).

These reference points are important in corneal excimer laser-based surgery. Indeed, it has been debated whether to use the entrance pupil centre or the corneal vertex as the ideal reference upon which to centre ablation treatments (Applegate, Thibos, Bradley, & al., 2000) - (Salz & Stevens, 2002). Pande and Hillman (Pande & Hillman, 1993) have stated that the ideal physiologic centre for keratorefractive surgical procedures is the corneal intercept of the visual axis, but it is difficult to identify this in a clinical setting. Using a modified autokeratometer to photograph the corneas of 50 patients, they conclude that the coaxially sighted corneal light reflex was the closest to the corneal intercept along the visual axis.

Determining the exact location of the corneal light reflex (corneal vertex) is instrument dependant and may change between preoperative measurements and even postoperatively (Bueeler, Iseli, Jankov,, & Mrochen, 2005). However, Uozato and Guyon (Uozato & Guyon, 1987) consider that the corneal light reflex may not be used because of errors arising from the calculation of the angle lambda (i.e. the angle between the line of sight and the pupillary axis). Using the same instrument, the WaveLight® Topolyzer^{TM} VARIO (Alcon® Laboratories Inc., USA), we reported that the location of the pupil centre is very close (less than 200 microns) to the vertex position for eyes with low to moderate myopia, and almost superimposed for most high myopic eyes (Salah-Mabed, Saad, Guilbert, & Gatinel, 2014). Thus, for most myopic eyes, centring can be performed by default on the centre of the pupil. However, for hyperopic eyes and those with high amount of astigmatism, the distance between the pupil centre and the corneal vertex is often more pronounced (310 microns to 770 microns). For these eyes, it is best to choose a shifted centring towards the vertex (mid distance, or ⅔-⅓) to improve the visual quality of eyes which have undergone corneal refractive surgery (Reinstein, Gobbe, & Archer, Coaxially sighted corneal light reflex versus entrance pupil center centration of hyperopic corneal ablations in eyes with small and large angle kappa, 2013).

The values found in this study cannot be exactly compared to other values in the literature because no study to our knowledge has yet determined the repeatability of pupillometry measurement taken by this camera. However, Twa et al. compared

infrared video recording pupillometry with measurements by digital photography, ruler, semi-circular templates, and the Colvard pupillometer. They found that the repeatability of the measurements was the higher for infrared video recording, followed by digital photography, Colvard pupillometry, ruler, and templates (Twa, Bailey, Hayes, & Bullimore, 2004). Other authors achieved the same conclusion by comparing the repeatability of infrared pupillometry measurements with the repeatability of measurements with other devices (Wachler & Krueger, Agreement and repeatability of pupillometry using videokeratography and infrared devices, 2000) - (Wachler & Krueger, 1999).

Repeatability errors regarding the distance between the pupil centre and the corneal vertex on the vertical axis can be induced depending on operator or patient factors. We believe it would have been interesting to eliminate aberrant measurements among the three measures initially taken by the WaveLight® Topolyzer^{TM} VARIO (Alcon® Laboratories Inc., USA) to evaluate their effect on repeatability. It would also have been preferable to carry out more measures to better assess repeatability. We would have been able to study the repeatability by the method of limits. 27 Indeed, as we described it, the disadvantage of using the COV is that when the mean value is near zero, which is the case here, the COV is sensitive to very small changes in the mean, limiting what it can show. In addition, repeatability of pupil centre coordinates is better in hyperopic eyes as compared to myopic eyes. This may be due to the fact that the distance between the pupil centre and the vertex is greater for hyperopia, so the COV becomes less sensitive to small changes. It would also have been preferable to include more than 7 hyperope with high astigmatism eyes in the analysis to assess the repeatability more accurately. However, this number reflects the proportion of hyperopes with high astigmatism we had in our study population. Errors could also be due to poor eye fixation of the target. We can assume that vertical movements of the eye can easily happen when the patient breathes. This could make the corneal vertex “move” vertically.

Finally, errors may be due to different emotional states, fluctuations of accommodation or to a lack of concentration (Hess, 1965).

In conclusion, we have shown in this study that the measure of pupil diameters in photopic and mesopic condition provided by the WaveLight® Topolyzer^{TM} VARIO (Alcon® Laboratories Inc., USA) were highly repeatable. One measure would therefore be sufficient to provide a useful value. However, in the case of a large

distance between the pupil centre and the corneal vertex, we recommend repeating the measurements several times and removing aberrant ones to increase the reliability of the measures and the efficacy of finding the exact centre of the pupil.

4.2 Measurement of pupil centre shift in refractive surgery candidates Caucasian eyes using infrared pupillometry

Authors: Imene Salah Mabed, MSc; Alain Saad, MD; Emmanuel Guilbert, MD; Damien Gatinel, MD

Department of Anterior Segment and Refractive Surgery, Rothschild Foundation, Paris, France

CEROC: Centre of Expertise and Research in Optics for Clinicians

None of the authors have any financial or proprietary interests in any product, method or material presented in this paper.

Published: J Refract Surg. 2014;30(10):694-700. doi:10.3928/1081597X-20140903-07

4.2.1 Abstract

Purpose: To evaluate the effectiveness of the pupil centre shift with changes in the state of pupil size and with other ocular variables.

Methods: Dynamic pupillometry with the WaveLight® Topolyzer^{TM} VARIO (Alcon® Laboratories Inc., USA) was performed in 248 eyes of 124 patients scheduled for corneal laser refractive surgery. High-resolution images were obtained using the infrared-sensitive camera (incorporated in the vidéokeratoscope) under mesopic and photopic conditions. Measurements of pupil diameters, distance between the pupil centre and keratoscopic axis, and spatial shift of the pupil centre were obtained after analysis.

Results: The mean distance between the pupil centre and the corneal vertex in mesopic and photopic conditions of illumination in myopic eyes was 0.27 ± 0.14 mm (range: 0.02 to 0.70 mm) and 0.24 mm ± 0.12 mm (range: 0.06 to 0.65 mm), respectively whereas it was 0.36 ± 0.15 mm (range: 0.03 to 0.70 mm) and 0.31 ± 0.16 mm (range: 0.03 to 0.77 mm) in hyperopic eyes, respectively. The mean spatial pupil centre shift was significant: 0.11 ± 0.07 mm (range: 0.02 to 0.57 mm) in myopic eyes, and 0.12 ± 0.09 mm (range: 0.02 to 0.47 mm) in hyperopic eyes. The pupil centre shifted consistently temporally as the pupil dilated. The pupil centre shift was not significantly related to sex, age, eye (right or left) or refractive error.

Conclusions: The mean distance between the pupil centre and the corneal vertex is

greater in hyperopic eyes than in myopic eyes, whereas the spatial shift of this pupil centre has a temporal direction as the pupil dilates and is constantly small in all groups. However, pupil centre shift can be important in a few patients.

4.2.2 Introduction

The entrance pupil of the human eye is formed by the image of the aperture stop of the iris through the cornea (Atchinson & Smith, Optics of the Human Eye, 2002). By changing its size, due to multiple factors (Lowenfeld, 1993), the pupil has effects on vision, such as controlling the inflow of light entering the eye, the depth of field, or the retinal light level (Atchinson & Smith, Optics of the Human Eye, 2002). The human eye is an optical system affected by variable amounts of regular and irregular aberrations (Ivanoff, 1956) - (Jenkins, 1963) which effect is greater when the pupil dilates (Walsh & Charman, 1988) - (Martinez, et al., 1998) influencing the quality of the retinal image (Artal & Navarro, 1994).

With the emergence of customized refractive surgery treatments, the role of the size and location of the pupil with respect to the treatment centration strategy receives increasing attention (Arbelaez, Vidal, & Arba-Mosquera, 2008) - (Kermani, Oberheide, Schmeidt, Gerten, & Bains, 2009) - (Park, Oh, & Chuck, 2012). Pupil tracking in refractive surgery relies on the assumption that the pupil centre location does not shift during pupil movements (Gobbi, et al., 1995) - (Bueeler & Mrochen, 2004). Indeed, if the corneal ablation is well centered when the pupil is small and off centre when the pupil dilates, the patient can experiment light halos, complains of glare in low light conditions and present a decrease in visual acuity and contrast sensitivity (Fay, Trokel, & Myers, 1992). Precise centration and positioning is also important in cataract surgery, especially with regard to the aspheric and multifocal intraocular lenses (Atchinson D. , 1991) - (Holladay, Piers, Koranyi, Van den Mooren, & Norrby, 2002). Intraocular lenses (IOL) are centered at the end of the cataract procedure under dilated pupil conditions. A change in the pupil centre position as the pupil constricts in normal illumination conditions, may cause effects on the optical quality of the operated eye.

The purpose of this study was to determine whether there is a systematic variation of the position of the pupil centre when the diameter of the pupil varies. The change in the position of the pupil centre in relation to other parameters (age, sex, refractive error, etc.) was also investigated. In this study, we used an infrared dynamic pupillometry device, the WaveLight® Topolyzer^{TM} VARIO (Alcon® Laboratories Inc., USA), in mesopic and photopic conditions. The measured distance between the corneal

vertex (first Purkinje image) and the pupil centre in the two illumination conditions was also analyzed.

4.2.3 Patients and Methods

Subjects

This study included 248 eyes of 124 patients presenting for refractive surgery from February, to May 2013, at our facility. All patients received a complete ocular assessment prior to surgery, including cycloplegic refraction, slit lamp and fundus examination.

All patients with a history of ocular surgery, corneal diseases or other ocular pathologies (amblyopia, glaucoma, cataract, retinopathy, strabismus), and suspected keratoconus on corneal topography were excluded. We included patients older than 17 years old with healthy eyes. The study and data accumulation were achieved with approval from the Rothschild Foundation Institutional Review Board. Informed consent was obtained from each patient after information about the purpose and procedure of the study, in accordance with the Declaration of Helsinki.

Instrument and measurement procedure

Pupillometry of each eye was performed using the dynamic pupil measurement module, WaveLight® Topolyzer^{TM} VARIO (Alcon® Laboratories Inc., USA) software, incorporated in the videokeratoscope (Figure 40).

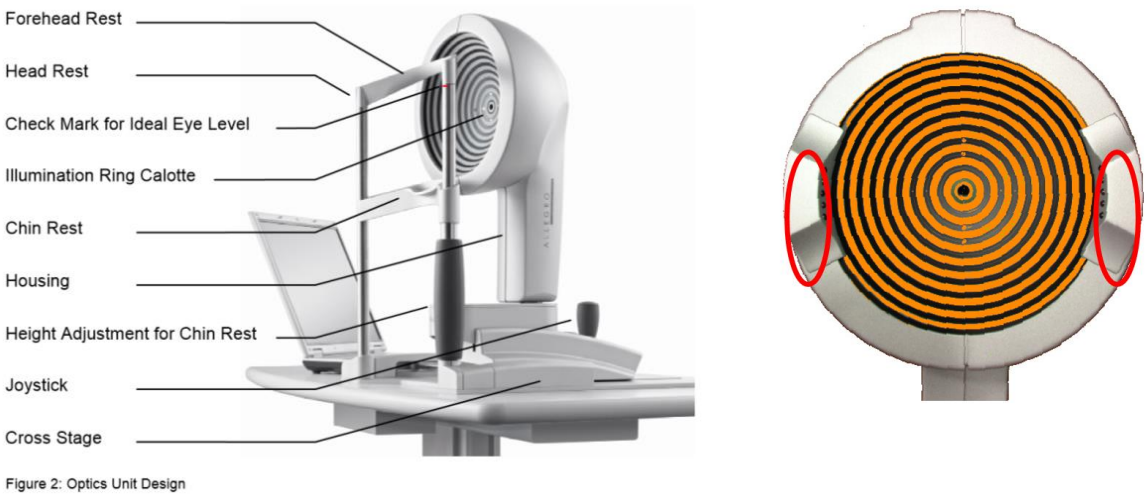

Figure 40 WaveLight® Topolyzer^{TM} VARIO (Alcon® Laboratories Inc., USA)

As the pupillometry and videokeratoscope modules are included in the same unit, only one fixation target is required to perform the measurements.

The pupillometer is equipped with an infrared illumination and camera device. The instrument measures the changes in pupil size during the transition from mesopic to photopic conditions. All pupillary changes are recorded by a CCD camera system. During the dynamic pupillometry, the infrared light illuminates the surface of the iris with a grazing direction, allowing the pupillary margin to be clearly identified by the camera device.

Recording begins automatically when the patient's eye is aligned with the target observation (bright central disc located 80 mm from the subject's eye). Three successive cycles are performed during 60 seconds (During each cycle, the 22 Placido discs turn off and on successively). A red and a green point are used to show the pupil centre and the vertex respectively (Figure 38).

The software analyzes the images and provides a graphical representation of the movement of the pupil centre between photopic and mesopic conditions. In addition, the distance between the pupil centre and the keratometric axis (corneal vertex) in both mesopic and photopic conditions is provided.

The pupillometries were performed in a closed, dark room (illumination lower than or equal to 1 lux illumination). The head of each patient was covered with a thick black clouding cloth, lowering the lighting conditions from 1 lux to 0.4 lux. The acquisitions were made first with Placido disc's light off in low mesopic conditions (0.4 lux), then with light on providing photopic lighting conditions (120 lux). Illuminance values were obtained thanks to a BM3 TOPCON light meter. Three consecutive acquisitions were performed (each acquisition included 3 cycles of mesopic and photopic conditions) per eye, in order to assess the repeatability of the instrument. Both eyes were tested consecutively, starting randomly with the right or left eye. All the measurements were performed by the same operator (IS). All the images were analyzed by computer software for data collection and data analysis. Pupil diameters, pupil centre shifts, and distances between pupil centers and corneal vertex measurements were represented in Cartesian coordinates (Figure 39).

Statistics

Statistical analyses were performed with a commercial software (SPSS v. 13.0; SPSS Inc., Chicago, IL). We used the following statistical analysis: paired *t* test, unpaired t test, general linear model (ANCOVA) and Pearson correlation analysis. A calculated P value <0.05 was considered statistically significant. Data are presented as the

mean +/- standard deviation.

4.2.4 Results

Demographics

One hundred eighty-three myopic eyes (74%) of 93 patients (36 men, mean age 32.2 years, ranging from 20.5 to 56.3 years), 64 hyperopic eyes (26%) of 34 patients (11 men, mean age 49.2 years from 22.1 to 70.6 years) and a simple myopic astigmatic eye were investigated. Among the included eyes, there were 59 eyes of 49 patients with low astigmatism (cylinder less than 0.75 D) and 35 eyes of 26 patients, with high astigmatism (cylinder higher than 1.50 D). In myopic eyes, the mean refractive sphere was -3.6 ± 2.0 D (SD) (ranging from -9.5 to -0.3 D), with an average cylinder of -0.8 ± 0.8 D (ranging from 0 to -4.5 D). The mean refractive spherical equivalent was -4.0 ± 2.0 D (ranging from -0.5 to -11.3 D). The mean refractive sphere in hyperopic eyes was 2.7 ± 1.4 D (ranging from 0 to 6.0 D), with an average cylinder of -0.6 ± 0.8 D (ranging from -4.3 to 0). The mean refractive spherical equivalent was 2.4 ± 1.5 D (ranging from -1.1 to 5.3 D). These data are represented in Table 8.

	Total	Myopes	Hyperopes	Weak Astigmatism (Cylinder<0.75D)	Strong Astigmatism (Cylinder>1.50D)
Number of patients	124	*93*	*34*	*49*	*26*
Number of eyes	248	183	64	59 (44 myopes / 15 hyper.)	35 (29 myopes / 6 hyper.)
R / L	124 / 124	93 / 90	32 / 32	26 / 33	19 / 16
Age (years)					
Average ± Standard deviation	36,9 ± 12,4	32,5 ± 8,1	49,2 ± 14,3	36,7 ± 11,9	34,1 ± 8,3
Minimum / Maximum	20,5 / 70,6	20,5 / 56,3	22,1 / 70,6	20,5 / 69,8	23,5 / 54,3
% male / % Female	36% / 64%	39% / 61%	32% / 68%	37% / 63%	54% / 46%
Mean Refractive Sphere (D)					
Average ± Standard deviation		-3,6 ± 2,0	2,7 ± 1,4		
Minimum / Maximum		-9,5 / -0,3	0,0 / 6,0		
Average Cylinder (D)					
Average ± Standard deviation		-0,8 ± 0,8	-0,6 ± 0,8		
Minimum / Maximum		-4,5 / 0,0	-4,3 / 0,0		
Mean Refractive Spherical Eq. (D)					
Average ± Standard deviation		-4,0 ± 2,0	2,4 ± 1,5		
Minimum / Maximum		-11,3 / -0,5	-1,1 / 5,3		

Table 8 Demographic data

Pupil diameter

The mean pupil diameters obtained on the studied population (all groups) in mesopic and photopic conditions were respectively 5.90 ± 0.95 mm and 3.06 ± 0.57 mm. There was a significant difference between the pupil diameters obtained in the two illumination conditions (paired t test, P <0.0001). Figure 41 shows the negative correlation between age and pupil diameter under both conditions of illumination (mesopic conditions r = -0.575, P < 0.01 and photopic conditions r = -0.418, P < 0.01).

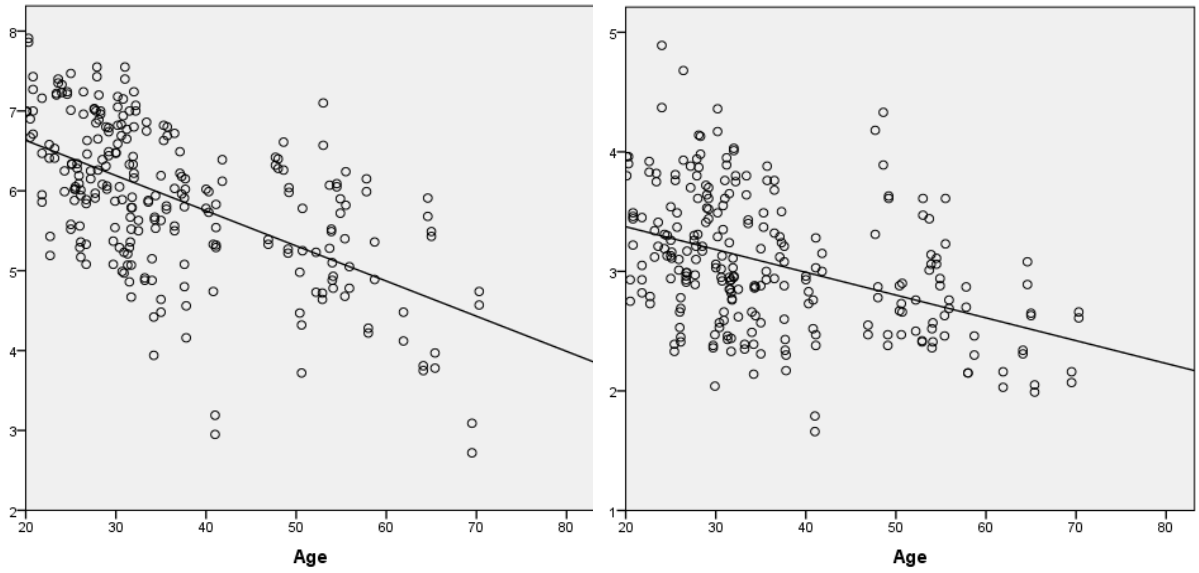

Figure 41 Pupil diameter (mm) as a function of age (years) in mesopic (left) and photopic (right) conditions

There was no significant difference in the pupil diameter between myopic and hyperopic eyes when age is taken into account whether in mesopic conditions (ANCOVA, P = 0.580) or in photopic conditions (ANCOVA, P = 0.424) or between highly astigmatic eyes and others (unpaired t-test, t = -0.819, P = 0.413 in mesopic conditions, t = -0.577, P = 0.564 in photopic conditions).There was no significant difference in pupil diameter between right eyes and left eyes in both illumination conditions (unpaired t test in mesopic conditions t = 0.618, P = 0.537 and in photopic conditions t = 0.479, P = 0.633). We did not find a significant difference between males' pupil diameters and females pupil diameters under photopic conditions (unpaired t-test, t = -1.602, P = 0.111).

Magnitude of the pupil dilatation

The magnitude of the pupil dilatation is defined as: (Pupil diameter in mesopic condition - Pupil diameter in photopic condition). In our sample, the mean magnitude of the pupil dilatation was 2.84 ± 0.59 mm (minimum 0.65, maximum 4.14 mm). Figure 42 shows the negative correlation between age and magnitude of pupil dilatation between the two conditions of illumination (r = -0.521, P < 0.01).

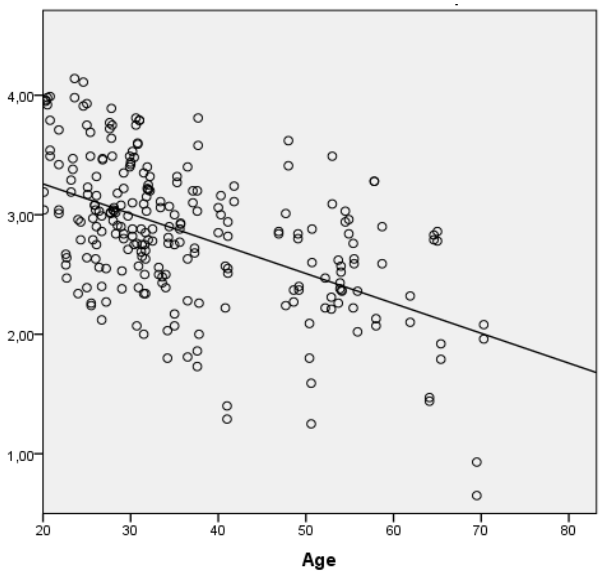

Figure 42 Magnitude of pupil dilatation (mm) as a function of age (years)

There was no significant difference in the magnitude of the pupil dilatation between myopic and hyperopic eyes when age is taken into account (ANCOVA, P = 0.972) or between highly astigmatic eyes and others (unpaired t-test, t = 0.749, P = 0.455).There was no significant difference in pupil dilatation between right eyes and left eyes (unpaired t test t = -0.526, P = 0.600). We did not find a significant difference between males and females when age was taken into account (ANCOVA, P = 0.827).

Pupil centre position

The pupil centre locations with respect to the corneal vertex are shown in Figure 43.

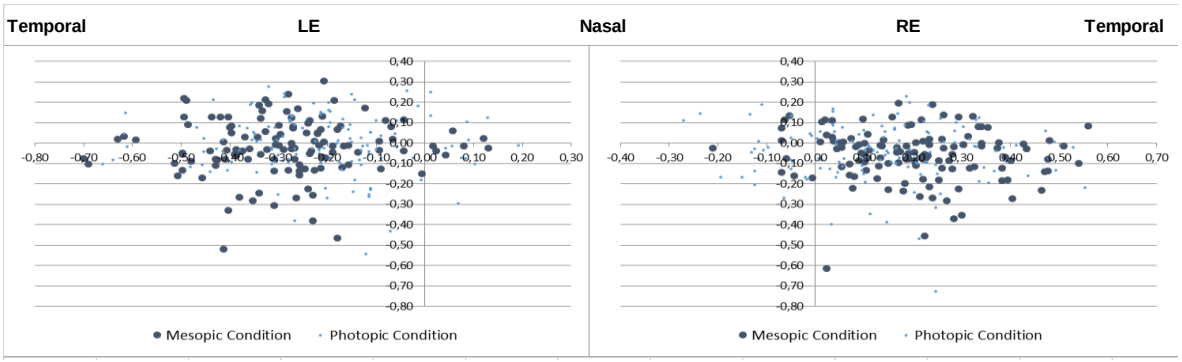

Figure 43 Pupil centre location in mesopic and photopic conditions

The mean distance between pupil centre and vertex in mesopic and photopic conditions were respectively 0.29 ± 0.14 mm and 0.26 ± 0.14 mm. There was a significant difference between the positions of the pupil centers in the two illumination conditions (paired t-test, P <0.0001). The pupil centre was located temporally in relation to the corneal vertex for the right (94% mesopic, 90% photopic conditions) and left (93% mesopic, 81% photopic conditions) eyes,

Figure 44 shows the mean distances between the pupil centre and the vertex in mesopic and photopic conditions as a function of age.

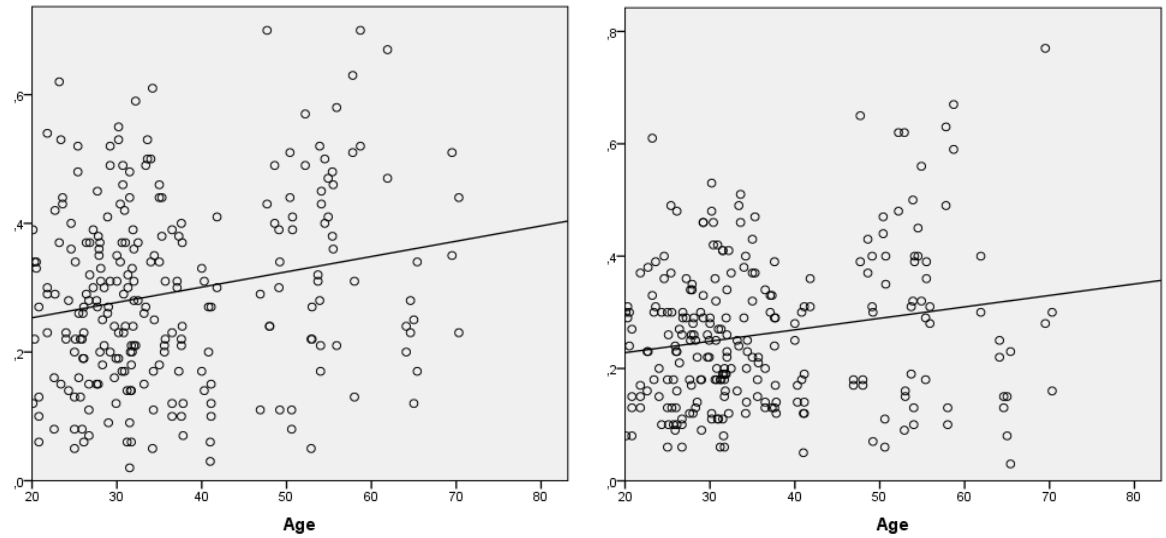

Figure 44 Distance between pupil centre and vertex (mm) as a function of age in mesopic (left) and photopic (right) conditions

There was a significant positive correlation between the distance between the pupil centre and the vertex and the age of patients in both mesopic (r = 0.206, P <0.01)

and photopic conditions (r = 0.188, P <0.01).

Table 9 shows the distances between pupil centers and vertex, in different ametropic groups.

	Total	Myopes	Hyperopes	Weak Astigmatism (Cylinder<0.75D)	Strong Astigmatism (Cylinder>1.50D)
Number of patients	124	*93*	*34*	*49*	*26*
Number of eyes	248	183	64	59 (44 myopes / 15 hyper.)	35 (29 myopes / 6 hyper.)
R / L	*124 / 124*	*93 / 90*	*32 / 32*	*26 / 33*	*19 / 16*
Distance pupil center - vertex in mesopic condition (in mm)					
Average ± Standard deviation	0,29 ± 0,14	0,27 ± 0,14	0,36 ± 0,15	0,28 ± 0,15	0,33 ± 0,15
Min / Max	0,02 / 0,70	0,02 / 0,70	0,03 / 0,70	0,02 / 0,59	0,09 / 0,70
Distance pupil center - vertex in photopic condition (in mm)					
Average ± Standard deviation	0,26 ± 0,14	0,24 ± 0,12	0,31 ± 0,16	0,25 ± 0,14	0,28 ± 0,14
Min / Max	0,03 / 0,77	0,06 / 0,65	0,03 / 0,77	0,03 / 0,77	0,10 / 0,65

Table 9 Distance between the pupil centre and the vertex according to ametropia

There was a significant difference in the distance between the pupil centre and the vertex between myopes and hyperopes when age is taken into account in mesopic (ANCOVA, P = 0.001) and photopic conditions (ANCOVA, P = 0.017).There was no significant difference in the distance between the pupil centre and the vertex between highly astigmatic eyes and others (unpaired t-test, t = -1.594, P = 0.112 in mesopic conditions, t = -0.966, P = 0.335 in photopic conditions).

There was no significant difference in the distance between pupil centre and vertex between the right and left eyes in both mesopic (unpaired t-test, t = 0.618, P = 0.537) and photopic conditions (unpaired t-test, t = 0.479, P = 0.633). We found no significant difference in the distance between the pupil centre and vertex between men and women (unpaired t-test, t = 1.571, P = 0.117).

The mean displacement of the pupil centre between mesopic and photopic conditions was 0.11 ± 0.08 mm. There was no correlation between the length of the pupil centre shift and the magnitude of the dilation of the pupil which averaged 2.84 ± 0.59 mm (r = -0.120). There was no significant difference of pupil centre shift between men and women (unpaired t-test, t = -1.126, P = 0.261). The pupil centre moved temporally as the pupil dilated, and this motion was not significantly different between the right and the left eyes (unpaired t-test, t = 0.729, P = 0.467). There was no correlation between pupil centre shift and age (r = 0.083).

Table 10 presents the results obtained for the pupil centre shift in the different ametropic groups.

	Total	Myopes	Hyperopes	Weak Astigmatism (Cylinder<0.75D)	Strong Astigmatism (Cylinder>1.50D)
Number of patients	124	*93*	*34*	*49*	*26*
% male / % Female	*36% / 64%*	*39% / 61%*	*32% / 68%*	*37% / 63%*	*54% / 46%*
Number of eyes	248	183	64	59 (44 myopes / 15 hyper.)	35 (29 myopes / 6 hyper.
R / L	*124 / 124*	*93 / 90*	*32 / 32*	*26 / 33*	*19 / 16*
Pupil center shift (in mm)					
Average ± Standard deviation	0,11 ± 0,08	0,11 ± 0,07	0,12 ± 0,09	0,13 ± 0,09	0,11 ± 0,05
Minimum / Maximum	0,02 / 0,57	0,02 / 0,57	0,02 / 0,47	0,02 / 0,47	0,02 / 0,24

Table 10 Pupil centre shift according to ametropia

We found no relationship between pupil centre shift and refraction (no significant difference between myopes and hyperopes (unpaired t test, t = 0.152, P = 0.879), between highly astigmatic eyes and others (unpaired t test, t = 0.177, P = 0.860).

4.2.5 Discussion

To our knowledge, we have studied the pupil centre location in the largest sample of eyes published to date. As in other studies (Yang, Thompson, & Burns, 2002) - (Tabernero, Atchinson, & Markwell, 2009), we found significant differences in the pupil diameter values obtained in the two illumination conditions, and a negative correlation between pupil size and age. The difference in the pupil diameter values between photopic and mesopic conditions is also reduced with age. These results confirm those published by Winn and al (Winn, Whitaker, Eliot, & Phillips, 1994). We did not find significant correlation between pupil diameter and refractive error when age was taken into account in both lighting conditions. These results are consistent with those found by Yang (Yang, Thompson, & Burns, 2002).

Since the pupil does not actually describe a perfect circular perimeter but rather possesses a slightly irregular elliptical geometry, its centre must be determined using some geometrical assumptions (Fedtke, Manns, & Ho, 2010). The corneal vertex (corneal light reflex) is the reflection of a light source by the anterior surface of the cornea and corresponds to a virtual image behind the cornea, also known as the first Purkinje-Sanson image. The location of this image depends on the location of the light source and the patient's direction of gaze. The distance between the pupil centre and vertex is a consequence of the kappa angle, which is formed by the intersection of the visual axis with the pupillary axis. As described by Artal and al (Artal, Benito, & Tabernero, 2006) this angle is smaller in myopic than in hyperopic eyes, which implies that the distance between the pupil centre and the vertex is smaller in myopic eyes

in comparison to hyperopic eyes. This study confirms the results of Artal and al (Artal, Benito, & Tabernero, 2006) as mean distance between the pupil centre and the vertex for myopic eyes was 0.27 ± 0.14 mm in mesopic conditions and 0.24 ± 0.12 mm in photopic conditions and for hyperopic eyes 0.36 ± 0.15 mm in mesopic conditions and 0.31 ± 0.16 mm in photopic conditions. Camellin and al. (Cammelin, Gambino, & Casaro, 2005) found a mean distance between the pupil centre and the keratoscopic axis greater in hyperopic eyes (0.45 ± 0.19 mm) than in myopic eyes (0.226 ± 0.13 mm). There is however a slight difference between the results of Camellin and al (Cammelin, Gambino, & Casaro, 2005) and those of the present study, which can probably be explained by the fact that Camellin and al. (Cammelin, Gambino, & Casaro, 2005) averaged the distance between the pupil centre and the vertex between the two lighting conditions, and therefore did not differentiate the pupil center-vertex distance in mesopic and photopic conditions.

To determine a possible displacement of the pupil center, there must be a fixed point of reference in the eye. The WaveLight® Topolyzer^{TM} VARIO (Alcon® Laboratories Inc., USA) uses the vertex, centre of reflecting patterns of Placido, as a fixed point. The first Purkinje image has often been considered as a landmark to align the eye of the optical systems. The image is formed by light reflection from the anterior surface of the cornea. When the cornea is illuminated by a light whose rays are parallel, the curvature causes the formation of an image at the focal point of the corneal diopter (Barry, Branmann, & Dunne, Catoptric properties of eyes with misaligned surfaces studied by exact ray tracing, 1997) - (Barry, Pongs, & Hillen, Algorithm for Purkinje images Iand IV and limbus centre localization, 1997) - (Cornsweet & Crane, 1973). The WaveLight® Topolyzer^{TM} VARIO (Alcon® Laboratories Inc., USA), as other instruments, uses the vertex to reference the pupil centre coordinates, while the pupil centre serves as a landmark for referring the laser ablation and tracking the eye, as current excimer lasers cannot track the target corneal zone. Theoretically, there should be no change in the position of the first Purkinje image (vertex) according to the centre of the limbus in the dilation of the pupil, if there is no change in the sighting direction with respect to the pupillometer optical axis. Yang and al. (Yang, Thompson, & Burns, 2002) showed that the vertex position referred from the centre of the cornea was substantially identical in mesopic and photopic conditions.

In corneal excimer laser-based surgery, the prevailing method for monitoring the eye movements is to use the centre of the entrance pupil, which corresponds to the line

of sight when the surgeon and patient are fixating coaxially. As the eye tracker tracks the centre of the pupil disk, any shift of the latter during the deliverance of the laser profile would cause the ablation to drift from its intended location.

It has been debated whether to use the entrance pupil centre or the corneal vertex as the ideal reference for ablation centration (Applegate, Thibos, Twa, & Sarver, 2009) - (Salz & Stevens, 2002) - (Schwiegerling, Aug, 2013). Pande and Hillman (Pande & Hillman, 1993) have stated that the ideal physiologic centration point for keratorefractive surgical procedures is the corneal intercept of the visual axis, but it is difficult to identify this in clinical practice. Using a modified autokeratometer to photograph the corneas of 50 patients, Pande and Hillman concluded that the coaxially sighted corneal light reflex (vertex) was the closest to the corneal intercept of the visual axis. They proposed the use of the vertex for centration instead of the entrance pupil. Some authors consider that the pupil centre is a good anatomical landmark for centering customized refractive surgery treatments (rather than the line of sight), since its movement is relatively small between the different illumination conditions (Tabernero, Atchinson, & Markwell, 2009) - (Applegate, Thibos, Bradley, & al., 2000) - (Reinstein & Cremonesi, 2002) - (Kermani, Oberheide, Schmeidt, Gerten, & Bains, 2009). Other authors have shown that even though it was small, the systematic displacement of the centre of the pupil, was sufficient to degrade the optical quality of the eye (Tabernero, Atchinson, & Markwell, 2009). According to Tabernero et al. (Tabernero, Atchinson, & Markwell, 2009) a pupil centre shift of 0.07 mm is sufficient to degrade the visual quality of an eye with a pupil mydriasis (7mm). The pupil centre shift degrading the visual quality of a pupil of 3 mm (in photopic conditions) is 0.2 mm. In our sample, 26% of the eyes described a movement less than 0.07 (66 eyes of 248, including 20 eyes presbyopic (over than 40 years), 42 non-presbyopic myopes and 2 eyes non presbyopic hyperopes).92% of our eyes described a pupil centre shift lower than 0.20 mm (21 eyes of 248 described a movement greater than 0.2 mm). Thus, according to our results and due to the pupil centre shift of the eye between photopic to mesopic conditions of illumination, we conclude that the quality of vision can be affected in 8% of cases in photopic conditions, and in 75% of cases in mesopic conditions. In addition, some authors recommend a treatment centered on the corneal vertex, which is a stable landmark and may be closer to the visual axis (Okamoto, et al., 2011) - (Arbelaez, Vidal, & Arba-Mosquera, 2008) - (Reinstein, Gobbe, & Archer, Coaxially sighted corneal light reflex versus entrance pupil center centration of

hyperopic corneal ablations in eyes with small and large angle kappa, 2013). Methods for centering ablation profiles considering pupil centre and corneal vertex information simultaneously have also been proposed.

Whenever the centre of the pupil is considered for centering wavefront -customized laser ablation, our results suggest that the surgeon should adjust the laser illumination system intensity until the pupil diameter value would be close to the pupil diameter measured at the time of wavefront acquisition, and that constant lighting intensity should be maintained throughout the excimer laser deliverance.

Our results confirm that regardless of the preferred centration strategy, using the photopic pupil centre to reference the treatment centration may incur the risk of a mismatch between the treated zone at the corneal plane and the entrance pupil in mesopic conditions, as the direction of the pupil centre shift is temporal during dilation. We found that the pupil centre is generally located temporally from the corneal vertex and describes a small but significant displacement of 0.11 ± 0.08 mm when the pupil dilates. The distance between the pupil centre and the vertex therefore increases when the pupil dilates. The average magnitude of the pupil centre shift during dilatation was 0.07 ± 0.05 mm horizontally and was directed temporally in 91% of 124 right eyes and 87% of 124 left eyes. Vertical movement was on average 0.06 ± 0.07 mm with no clear apparent direction (51% and 49% respectively in the upper and lower quadrant for the left eyes and 44% and 56% respectively in the upper and lower quadrant for the right eyes). The average absolute magnitude of the pupil centre that we measured falls between the values reported by Wyatt (Wyatt, 1995) and Walsh (Walsh, The effect of mydriasis on the pupillary centration of the human eye, 1988) but was lower than those reported by Tabernero and al (Tabernero, Atchinson, & Markwell, 2009) (significant movement of 0.21 ± 0.11 mm) and Wilson and al. (Wilson, Campbell, & Simonet, 1992) (significant movement, up to 0.6 mm). Yang and al. (Yang, Thompson, & Burns, 2002) measured a significant temporal displacement of 0.13 mm, which is similar to the result of our study. Camellin and al. (Cammelin, Gambino, & Casaro, 2005) measured a significant temporal movement of 0.086 mm (maximum 0,269 mm) in myopic and 0,095 mm (maximum 0,283 mm) in hyperopic eyes. Tabernero and al. (Tabernero, Atchinson, & Markwell, 2009) used two different devices for measuring the displacement of the pupil centre between mesopic and photopic conditions which may explain the differences with our results. They calculated the pupillary displacement and reported theoretical instead of measured values. Although we

found that very few eyes presented an important movement of the pupil centre between photopic and mesopic conditions, individual differences may explain the differences in values we have with Wilson and al (Wilson, Campbell, & Simonet, 1992). Indeed, we found only two eyes which pupil centre shifted more than 0.5 mm (maximum 0.57 mm). 92% of eyes described movement below or equal to 0.2 mm. Although the pupil centre tends to be farthest from the vertex for the hyperopic and presbyopic eyes (both lighting conditions), the change in its position during the transition from photopic to mesopic conditions is substantially similar in all subjects and appears not related to any factor studied. We found that the distance between the pupil centre and the vertex for highly astigmatic eyes was not significantly different from other groups, in both lighting conditions. There was a significant positive correlation between the pupil center-vertex distance and age of patients in both conditions of illumination. We cannot conclude whether age may play a role in increasing the distance between the pupil centre and the vertex, as this result could be explained by the fact that in our study, presbyopic (older) eyes were mostly hyperopic.

In conclusion, we found that the pupil centre described a small but significant shift between the two illumination conditions.

4.3 Assessment of pupil dynamics and biometry in eyes undergoing cataract surgery

Authors: Imene Salah Mabed, MSc; Alain Saad, MD; Hélène Rouger, PhD, Damien Gatinel, MD, PhD

Department of Anterior Segment and Refractive Surgery, Rothschild Foundation, Paris, France

CEROC: Centre of Expertise and Research in Optics for Clinicians

None of the authors has any financial or proprietary interests in any product, method or material presented in this paper.

Published: None. Submitted to J Refract Surg on April 12, 2018.

4.3.1 Abstract

Purpose: To assess pupil diameter dynamics and anterior segment changes in eyes undergoing cataract surgery.

Methods: Pupillometry was performed using OPD-Scan® III (Nidek®, Japan) in 95 eyes of 64 patients scheduled for cataract surgery. High-resolution images were obtained using the infrared-sensitive camera under mesopic and photopic conditions. Severity of the cataract (Objective Scatter Index-OSI), pachymetry, magnitude of the corneal and surgically-induced astigmatism, axial length and anterior chamber depth were measured using the OQAS® (Visiometrics®, Spain), the Pentacam® AXL (Oculus Optikgeräte GmbH, Germany) tomographer and IOLMaster® 700 with Swept Source OCT (Carl Zeiss Meditec AG®, Germany). All parameters were analyzed preoperatively and one and three months after surgery.

Results: The mean preoperative and three-month postoperative pupil diameters under mesopic conditions were of 4.7 ± 0.8 mm and 4.4 ± 0.7 mm, respectively. The mean preoperative and three-months postoperative pupil diameters under photopic conditions were of 3.3 ± 0.6 mm and 3.1 ± 0.5 mm, respectively. These differences were significant (paired t test, $P < 0.05$). There were no correlations between the three-months postoperative decrease in pupil diameter in mesopic and photopic conditions and preoperative OSI ($r^2=0.0017$, $p<0.05$ and $r^2=0.0008$, $p<0.05$ respectively). Three-months postoperative pupil diameter in mesopic and photopic conditions and preoperative pupil diameter were positively correlated ($r=0.852$, $p<0.001$; $r=0.717$,

p<0.001 respectively).

Conclusions: The mean pupil diameters in different illumination conditions decreased by approximately 300 µm three months postoperatively. The postoperative pupil diameter did not depend from the severity of the cataract and could be predicted preoperatively; which can be useful to identify patients appropriate for multifocal IOLs.

4.3.2 Introduction

The pupil of the human eye is formed by the image of the aperture stop of the iris seen through the cornea (Atchinson & Smith, Optics of the Human Eye, 2002). Through changes in its size due to multiple factors (Lowenfeld, 1993), the pupil has effects on the vision such as controlling the amount of light entering the eye, the depth of field, or the retinal light level (Atchinson & Smith, Optics of the Human Eye, 2002). The human eye is an optical system affected by variable amounts of regular and irregular aberrations (Ivanoff, 1956) - (Jenkins, 1963) whose effect is greater when the pupil dilates (Walsh & Charman, 1988) - (Martinez, et al., 1998) and influencing the quality of the retinal image (Artal & Navarro, 1994). With the emergence of customized cataract surgery treatments, the role of pupil size and location with respect to the treatment centration strategy has received increasing attention (Arbelaez, Vidal, & Arba-Mosquera, 2008) - (Kermani, Oberheide, Schmeidt, Gerten, & Bains, 2009) - (Park, Oh, & Chuck, 2012). It is well known that in pseudophakic patients, the pupil size is related to various visual parameters, including glare disability (Koch, Jardeleza, Emery, & Franklin, 1986) - (Masket, 1992), amplitude of apparent accommodation (Nakazawa & Ohtsuki, 1983) - (Nakazawa & Ohtsuki, Apparent accommodation in pseudophakic eyes after implantation of posterior chamber intraocular lenses: optical analysis, 1984) - (Elder, Murphy, & Sanderson, 1996), binocular function (Obara, Hashi, Tonaki, & Yoshida, 1989), and distance and near visual acuities with a multifocal intraocular lens (IOL) (Koch, Samuelson, Haft, & Merin, 1991) - (Ravalico, Baccara, & Bellavitis, 1992) - (Hayashi, Hayashi, Nakao, & Hayashi, 1995). The changes in pupil size induced by cataract surgery may impact vision quality in pseudophakic eyes. In particular, the postoperative pupil dynamics may influence the optical quality of pseudophakic eyes implanted with multifocal IOLs (Wang, Corpuz, Huseynova, & Tomita, 2016). When the pupil diameter of the pseudophakic eye is not large enough, the multifocal effect of the IOL is not optimal. In case of discrepancies between pupil dimensions and the optical design of zonal refractive or pupil-

dependent diffractive IOL optics, the visual performance may not be optimal, and the visual quality may be affected by halos and glare.

The aim of this study was to further explore pupil dynamics in hyperopic and myopic eyes under mesopic and photopic conditions before, one and 3 months after cataract surgery by analyzing several parameters (pupil diameter, corneal astigmatism, anterior chamber depth, axial length and pachymetry).

4.3.3 Patients and methods

Patients

This study included 95 eyes of 64 patients with moderate to severe cataract consulting for surgery between December 2016 and March 2017 in our facility. All patients underwent a complete ocular examination prior to surgery, including refraction and visual acuity, tonometry, pachymetry, IOL calculation, slit-lamp and fundus examination. We have decided to include the two eyes in 31 patients (62 eyes) based on the studies of Komatsu et al. (Komatsu, Oono, & Shimizu, 1997) and Moller et al. (Moller, Buchholz, & Huebscher, 2000), which conclude that no fellow eye effect on the pupil was induced by cataract surgery.

All patients with irregularly shaped or synechial pupil, with a history of ocular surgery, corneal diseases or other ocular pathologies except cataract (amblyopia, glaucoma, retinopathy, strabismus), or with suspected keratoconus on corneal topography were excluded. Besides, we excluded patients using systemic pharmacological agents which could influence the pupil size. We also excluded postoperatively all patients who experienced operative complications, including iris damage, asymmetrical or out-of-the-bag IOL, or for whom we had issues with data collection or analysis. Thus, patients with healthy eyes who only presented with cataract were included. This prospective clinical study and data collection were conducted after approval of the Rothschild Foundation Institutional Review Board. Informed consent was obtained from all patients after information on the study purpose and procedures, in accordance with the Tenets of the Declaration of Helsinki.

Instruments and measurement procedures

Preoperative pupillometry was performed in all eyes using the OPD-Scan® III (Nidek®, Japan) (Figure 45). The pupillometer is equipped with an infrared illumination and measures changes in pupil size during the transition from mesopic to photopic

conditions. The infrared light illuminates the iris surface with a grazing direction, allowing the pupillary margin to be clearly identified by the camera. The pupil diameters are recorded under photopic and mesopic conditions by a CCD camera system and pictures are displayed on the screen. All the pupil measurements were made when the patient eye was aligned with the fixation target (bright central spot located 75 mm from patient eye).

Preoprative pupillometry

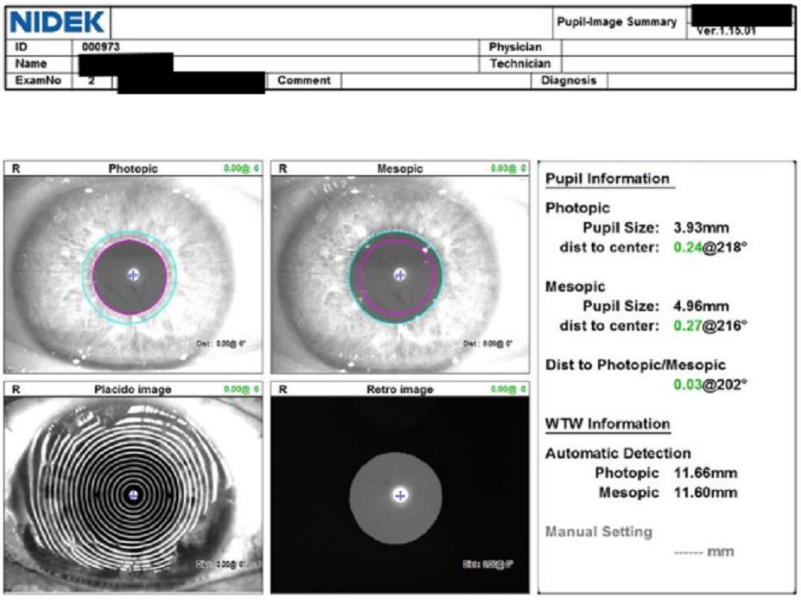

Pupillometry 3 months after surgery

Figure 45 Preoperative pupillometry under photopic and mesopic conditions (top), and pupillometry under photopic and mesopic conditions 3 months after surgery (bottom)

Preoperative corneal tomography was performed using the Pentacam® AXL (Oculus Optikgeräte GmbH, Germany) tomographer. Corneal tomography allows measuring the corneal thickness at any point of the corneal surface that is analyzed with Pentacam® AXL (Oculus Optikgeräte GmbH, Germany) Scheimpflug camera scanning systems. Central corneal pachymetry allows measuring the thickness in a single point, corresponding to the cornea center. In this study, we only analyzed pachymetry values. Keratometry, axial length and anterior chamber depth were obtained with the IOLMaster® 700 with Swept Source OCT (Carl Zeiss Meditec AG®, Germany) optical biometer. IOL power was then determined before surgery using the SRK/T formula for eyes with an axial length greater or equal to 22 mm and using the Haigis or Hoffer Q formulas for eyes with shorter axial lengths.

All measurements were performed in a closed, dark room (illumination lower than or equal to 1 lux). Patient head was covered with a thick black opacifying fabric, lowering the lighting conditions from 1 lux to 0.4 lux. Illuminance values were obtained using a BM3 TOPCON light meter (75-1 Hasunuma-Cho, Itabashi-Ku, Tokyo, 174-8580, Japan). The pupillometry values were first measured with the OPD-Scan® III (Nidek®, Japan) before subsequent acquisitions of the other parameters to avoid any influence of the biometer and topograph illumination systems on pupil dynamics. All the measurements were performed by the same operator (HR). All the data were analyzed using a data collection and analysis software.

Astigmatism is an optical aberration which is mainly caused by the toricity of a refractive surface (Harris, 2000). Although instruments measure the anterior corneal surface toricity (non-astigmatic), we will use the terms “astigmatism” and “toricity” interchangeably. Corneal and surgically-induced astigmatism (CSIA) magnitude was calculated as follows: the difference in keratometry (K) of the steepest and flattest hemi-meridians was calculated as the “cylinder” by the IOLMaster® 700 with Swept Source OCT (Carl Zeiss Meditec AG®, Germany) optical biometer software. CSIA magnitude was computed as the change between “K difference” values obtained after cataract surgery compared to baseline.

All studied parameters were also measured one and three months after cataract surgery by the same examiner with the same method, and the data were compared to preoperative ones.

Surgical technique

All the surgical procedures were performed by two experienced surgeons (DG and AS). After the application of topical anesthesia (0.5% oxybuprocaine), and pupil dilation with two-three drops of tropicamide (completer) repeated at 10-minute intervals, a 2.2-mm superotemporal (Right Eye) and superonasal (Left Eye) limbal incision was made along the steepest axis of the cornea. A continuous curvilinear capsulorhexis of 5.5 mm in diameter and hydro dissection of the crystalline cortex were then performed. Micro-axial phacoemulsification and polishing were performed. Our patients were implanted in the capsular bag with a good centration through the limbal incision as follows: 73% with monofocal IOLs (power of 19.8 ± 3.3 D), 15% with multifocal IOLs (power of 22.0 ± 2.5 D), and 12% with monofocal toric IOLs (power of 18.5 ± 4.0 D with cylinder of 3.3 ± 1.2 D). Surgery was completed without sutures. Stromal hydration of the incision site was performed as hydro-suture using a balanced salt solution. Post-operatively, 0.3% ciprofloxacin and 0.1% dexamethasone + 0.3% tobramycin eye drops were administered four times per day for one and four weeks, respectively.

Statistics

Normality of data distribution was tested using the Kolmogorov-Smirnov test. Statistical analyzes were performed with commercial software (SPSS v. 13.0; SPSS Inc., Chicago, IL). ANOVA tests, paired *t* tests, and Pearson correlations were used for statistical analysis. A calculated P value <0.05 was considered statistically significant. Data are presented as the mean +/- standard deviation.

4.3.4 Results

Demographics

95 eyes of 64 patients, including 52 myopic eyes (patient mean age: 68.9 ± 9.9 years, range: 48.5-84.2 years) and 43 hyperopic eyes (patient mean age: 72.6 ± 10.4 years, range: 45.5-92.9 years), were included. The mean Objective Scatter Index (OSI) measured preoperatively on the OQAS® (Visiometrics®, Spain) (Saad, Saab, & Gatinel, Repeatability of measurements with a double-pass system, 2010) was 3.22 ± 1.75 (range 1.0 to 11.0). In myopic eyes, the mean refractive spherical equivalent and axial length were of -3.4 ± 2.9 D (range: -14.6 - -0.1 D) and 24.67 ± 1.19 mm (range: 23-29.39 mm), respectively, with a mean cylinder of -1.3 ± 1.2 D (range: -6.3-0). In hyperopic eyes, the mean refractive spherical equivalent and axial length were of 1.8

± 1.1 D (range: 0.1-4.3 D) and 23.16 ± 1.02 mm (range: 21.56-25.44 mm), respectively, with a mean cylinder of -1.2 ± 1.0 D (range: -4.3-0).

The sample included 61% of female eyes and 39% of male eyes. There were no significant differences in terms of age (ANOVA, P = 0.185) and preoperative spherical equivalent (ANOVA, P = 0.862) between males and females. Patient demographics and baseline values are represented in Table 11.

	Hyperopic eyes	Myopic eyes	Total
Number of patients			64
Number of eyes	43	52	95
Right / Left	23 / 20	27 / 25	50 / 45
Age (years)			
Mean ± Standard deviation	72,6 ± 10,4	68,9 ± 9,9	70,6 ± 10,3
Minimum / Maximum	45,5 / 92,9	48,5 / 84,2	45,5 / 92,9
% Female / % Male	*60% / 40%*	*62% / 38%*	*61% / 39%*
Refractive Spherical Equivalent (D)			
Mean ± Standard deviation	1,8 ± 1,1	-3,4 ± 2,9	-1,0 ± 3,4
Minimum / Maximum	0,1 / 4,3	-14,6 / -0,1	-14,6 / 4,3
Refractive Cylinder (D)			
Mean ± Standard deviation	-1,2 ± 1,0	-1,3 ± 1,2	-1,2 ± 1,1
Minimum / Maximum	0,0 / -4,3	0,0 / -6,3	0,0 / -6,3
Axial Length (mm)			
Mean ± Standard deviation	23,16 ± 1,02	24,67 ± 1,19	23,99 ± 1,34
Minimum / Maximum	21,56 / 25,44	23,00 / 29,39	21,56 / 29,39

Table 11 Demographic data

Pupil diameter

The mean preoperative pupil diameters obtained in all eyes under mesopic and photopic conditions were respectively 4.7 ± 0.8 mm and 3.3 ± 0.6 mm. There was a significant difference between pupil diameters obtained under the two illumination conditions (paired t test, P <0.0001) before, one month and three months after surgery. We found a significant difference in preoperative pupil diameters under photopic conditions between male and female patients (ANOVA, P = 0.019). This difference was not significant preoperatively under mesopic conditions (ANOVA, P = 0.066), and one and 3 months post-surgery under both illumination conditions (ANOVA respectively, P = 0.249 and P = 0.117 at one month and P = 0.374 and P = 0.148 at three months).

The mean preoperative pupil diameters under mesopic and photopic conditions were significantly decreased one month and three months post-surgery in myopic and hyperopic eyes (paired t test, P <0.05; Table 12).

Parameter *(Mean ± Standard deviation)*	Pre-operative	One-month Post-operative	*p*	Three-months Post-operative	*p*
Mesopic Pupil Diameter (mm)					
Hyperopic Eyes	4,6 ± 1,0	4,4 ± 0,9	**0,002***	4,3 ± 0,8	**0,000***
Myopic Eyes	4,8 ± 0,7	4,5 ± 0,7	**0,000***	4,5 ± 0,7	**0,000***
All Eyes	4,7 ± 0,8	4,4 ± 0,8	**0,000***	4,4 ± 0,7	**0,000***
Photopic Pupil Diameter (mm)					
Hyperopic Eyes	3,3 ± 0,7	3,1 ± 0,6	**0,003***	3,1 ± 0,6	**0,001***
Myopic Eyes	3,3 ± 0,5	3,1 ± 0,5	**0,000***	3,1 ± 0,5	**0,000***
All Eyes	3,3 ± 0,6	3,1 ± 0,6	**0,000***	3,1 ± 0,5	**0,000***
Pupil Dilatation (mm)					
Hyperopic Eyes	1,29 ± 0,41	1,24 ± 0,44	0,267	1,24 ± 0,41	0,442
Myopic Eyes	1,42 ± 0,31	1,37 ± 0,36	0,163	1,44 ± 0,39	0,565
All Eyes	1,36 ± 0,36	1,31 ± 0,40	0,073	1,35 ± 0,41	0,833
Pachymetry (µm)					
Hyperopic Eyes	541 ± 34	548 ± 42	**0,016***	545 ± 42	0,073
Myopic Eyes	551 ± 43	554 ± 43	0,055	554 ± 42	0,058
All Eyes	546 ± 39	551 ± 42	**0,002***	550 ± 42	**0,009***
Anterior Chamber Depth (mm)					
Hyperopic Eyes	3,1 ± 0,4	4,3 ± 0,6	**0,000***	4,6 ± 0,4	**0,000***
Myopic Eyes	3,1 ± 0,4	4,4 ± 0,5	**0,000***	4,6 ± 0,5	**0,000***
All Eyes	3,1 ± 0,4	4,4 ± 0,5	**0,000***	4,6 ± 0,4	**0,000***
Axial Length (mm)					
Hyperopic Eyes	23,16 ± 1,02	23,11 ± 1,01	**0,000***	23,09 ± 1,01	**0,000***
Myopic Eyes	24,67 ± 1,19	24,60 ± 1,21	**0,000***	24,58 ± 1,19	**0,000***
All Eyes	23,99 ± 1,34	23,93 ± 1,34	**0,000***	23,91 ± 1,34	**0,000***
K Flat (Diopters)					
Hyperopic Eyes	43,5 ± 1,8	43,6 ± 1,7	0,085	43,5 ± 1,8	0,43
Myopic Eyes	42,8 ± 1,4	42,8 ± 1,4	0,524	42,7 ± 1,4	**0,019***
All Eyes	43,1 ± 1,6	43,2 ± 1,6	0,467	43,1 ± 1,6	**0,021***
K Steep (Diopters)					
Hyperopic Eyes	44,6 ± 1,7	44,9 ± 2,3	**0,037***	44,7 ± 1,7	0,267
Myopic Eyes	43,8 ± 1,5	43,8 ± 1,4	0,252	43,8 ± 1,5	0,655
All Eyes	44,1 ± 1,7	44,3 ± 2,0	**0,017***	44,2 ± 1,7	0,268

Table 12 Evolution of pupil parameters

Under any given illumination condition, no significant correlation was found between the difference in preoperative *versus* postoperative pupil diameters and the following variables: age, degree of Cataract (OSI value), preoperative spherical equivalent, anterior chamber depth and axial length. For instance, no correlation was found with age three months after surgery under mesopic conditions (r = 0.020, P = 0.847).

Strong and significant correlations were found between preoperative and postoperative pupil diameters under both illumination conditions (Table 13).

	Pupil Diameter 1-month Post-operative		Pupil Diameter 3-months Post-operative	
	r	p	r	p
Preoperative Mesopic Pupil Diameter	0,752	**0,000***	0,852	**0,000***
Preoperative Photopic Pupil Diameter	0,766	**0,000***	0,717	**0,000***

Table 13 Correlation between pupil diameter pre and post-operatively

Magnitude of pupil dilation

Pupil dilation magnitude is defined as: (Pupil diameter under mesopic condition - Pupil diameter under photopic condition). In our sample, the mean pupil dilation magnitude for all eyes was 1.36 ± 0.36 mm preoperatively, and 1.31 ± 0.40 mm and 1.35 ± 0.41 mm one and three months after surgery, respectively (Table 12).

No significant difference was found between males and females (ANOVA, P = 0.683, P = 0.552, P = 0.154, respectively for the preoperative, one-month and three-month postoperative values).

There was a significant difference in pupil dilation between myopic and hyperopic eyes three months after surgery (ANOVA, P = 0.016), while no significant difference was found preoperatively and one month after surgery (ANOVA respectively, P = 0.82 and P = 0.129).

Magnitude of corneal and surgically-induced astigmatism

Preoperatively, the mean K difference value was 0.30 D. One and three months after cataract surgery, these values measured on the cornea were 0.42 D and 0.33 D, respectively. Before and after surgery, the astigmatism was predominantly oriented in the with the rule (WTR) direction.

Figure 46 represents the magnitude and orientation of the anterior corneal astigmatism before and after cataract surgery.

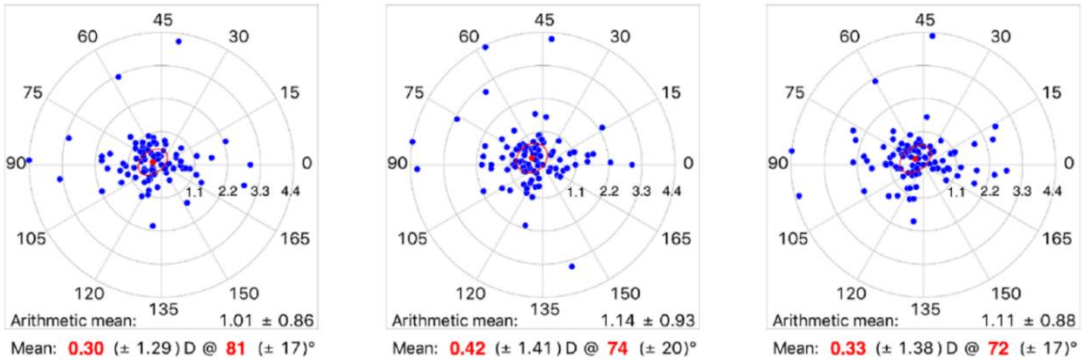

Figure 46 Preoperative corneal astigmatism (left), and CSIA at one month (centre) and three months (right)

A CSIA magnitude of 0.19 D and 0.10 D was found respectively one and three months after surgery. Figure 47 shows that the CSIA tended to decrease over time.

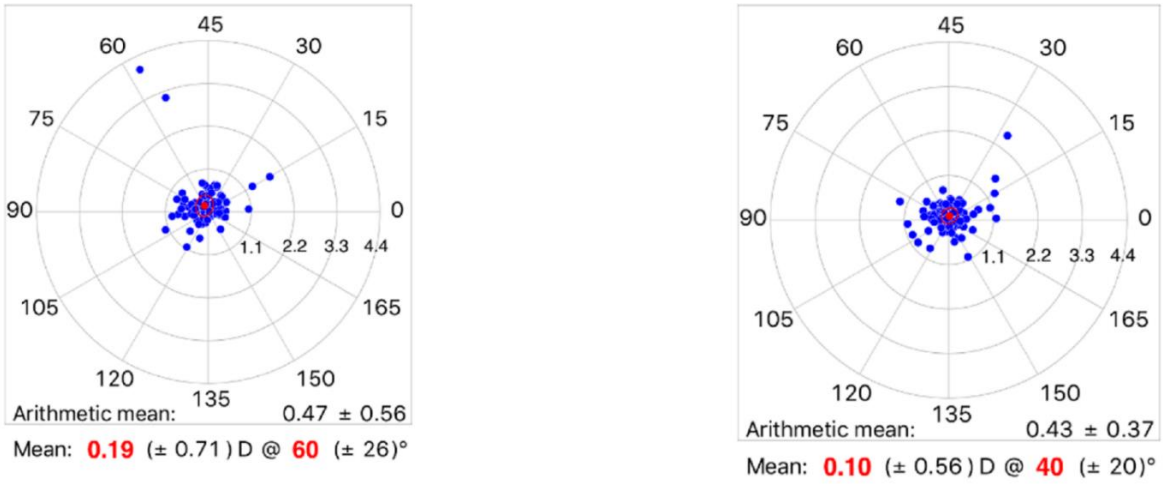

Figure 47 CSIA at one month (left) and three months post-operatively (right)

Pachymetry

The mean preoperative pachymetry values were of 541 ± 34 µm and 551 ± 43 µm respectively in hyperopic and myopic eyes. The mean postoperative pachymetry values were of 551 ± 42 µm and 550 ± 42 respectively at one and three months in all eyes. The differences between post- (both at one and three months) and preoperative pachymetry values were significant (paired t test, P =0.002 and P = 0.009, respectively, Table 12).

Anterior chamber depth

The mean preoperative anterior chamber depths were of 3.1 ± 0.4 mm and 3.1 ± 0.4 mm in hyperopic and myopic eyes, respectively. The mean postoperative anterior chamber depths in hyperopic and myopic eyes were of 4.3 ± 0.6 mm and 4.6 ± 0.4 mm at one month and 4.4 ± 0.5 mm and 4.6 ± 0.5 mm at three months, respectively (paired t test, P <0.0001 compared to baseline; Table 12).

There was a significant difference in preoperative anterior chamber depth between male and female eyes (ANOVA, P = 0.003) which disappeared one and 3 months after cataract surgery (ANOVA, P = 0.669 and P=0.095, respectively). There was no significant difference in preoperative or postoperative anterior chamber depths between hyperopic and myopic eyes (for instance ANOVA, P=0.932 three months after surgery).

Axial length

The mean preoperative axial lengths were of 23.16 ± 1.02 mm and 24.67 ± 1.19 mm respectively in hyperopic and myopic eyes. The mean postoperative axial lengths in hyperopic were of 23.11 ± 1.01 mm at one month and 23.09 ± 1.01 mm at three months (paired t test, P <0.0001 compared to baseline; Table 12). The mean postoperative axial lengths in myopic eyes were of 24.60 ± 1.21 mm at one month and 24.58 ± 1.19 mm at three months (paired t test, P <0.0001 compared to baseline; Table 12).

The mean decrease in axial length compared to the preoperative measurement was of 59.7 ± 56.5 µm one month after surgery and 78.2 ± 64.5 µm three months after surgery.

There was no significant difference in the decrease in axial length between hyperopic and myopic eyes (ANOVA, P = 0.334 and P = 0.369, respectively at one and three months) and between male and female eyes (ANOVA, P = 0.601 and P = 0.780, respectively at one and three months).

4.3.5 Discussion

In our study, we found significant differences in the pupil diameter values obtained under the two illumination conditions which is consistent with other studies (Yang, Thompson, & Burns, 2002) - (Tabernero, Atchinson, & Markwell, 2009). The mean pupil diameters obtained in all eyes under mesopic and photopic conditions were respectively 4.7 ± 0.8 mm and 3.3 ± 0.6 mm while they were 5.9 ± 1 mm and 3.1 ± 0.6 mm respectively in our previous study conducted in 248 eyes (Salah-Mabed, Saad, Guilbert, & Gatinel, 2014). The difference in pupil diameter under mesopic conditions between these two studies can be explained by the age factor. Indeed, patient mean age was 70.6 ± 10.3 years in the current study whereas it was 36.9 ± 12.4 years in our previous study. While the decrease in pupil diameter with age is well known (Winn, Whitaker, Eliot, & Phillips, 1994), it is interesting to note that our older sample had a higher mean pupil diameter under photopic conditions than that measured in our previous study. This finding could be explained either by a pupil stretching caused by an increased area of the anterior surface of the crystalline lens impaired by cataract or by the different measurement devices or protocols used in our two studies.

Although male and female patients were comparable in terms of number, age and preoperative spherical equivalent (ANOVA, P >0.185), their preoperative photopic pupil diameters were different. Indeed, the preoperative photopic pupil diameter was significantly smaller in men than in women and was associated with a significantly

higher preoperative anterior chamber depth. This difference disappeared three months after surgery. Besides, we did not find any significant difference in postoperative pupil dilation magnitude between men and women.

Given that (i) our sample showed no significant difference in terms of age and spherical equivalent between men and women, and (ii) such a difference was not observed in younger samples (Salah-Mabed, Saad, Guilbert, & Gatinel, 2014), a possible explanation could be the use of α-blockers in men for enlarged prostate treatments in our older sample. Indeed, α-blockers have been shown to induce pupil constriction (Handzel, Briesen, Rausch, & Kälble, 2012) - (Theodossiadis, et al., 2012) - (Chang, Campbell, Colin, & Schweitzer, 2014). Although we systematically excluded these patients from our study, some could have forgotten to disclose the previous use of such a medicine.

The mean pupil diameters in all eyes significantly decreased one and three months after surgery. Three months after surgery, it was 4.4 ± 0.7 mm (mesopic conditions) and 3.1 ± 0.5 mm (photopic conditions), vs respectively, 4.7 ± 0.8 mm and 3.3 ± 0.6 mm before surgery. The mean postoperative pupil diameter under photopic conditions was comparable to that measured in the younger population in our previous study (Salah-Mabed, Saad, Guilbert, & Gatinel, 2014). We believe that these results were not weakened by any fellow eye confounding issue for the 32 patients which two eyes were studies (Komatsu, Oono, & Shimizu, 1997) - (Moller, Buchholz, & Huebscher, 2000). This finding could be explained by the pupil stretching phenomenon described above. The lens thickness could contribute to a decreased pupil size as the IOL is much thinner, thus less protruding in the iris than larger cataract crystalline lens. To verify this hypothesis, it would be interesting to perform the same analysis in a younger sample with a lower degree of cataract, even if we found that the postoperative pupil decrease wasn’t related to the degree of cataract. Another explanation, may be an intraoperative damage to iris sphincter or inflammation. Finally, we could explain this result by a neuronal reaction of the pupil to a decreased performance of an opaquer crystalline due to cataract. Indeed, the eye pupil could dilate before surgery to allow a higher amount of light entering the eye in order to increase visual performances (Campbell & Gregory, 1960).

Moreover, age, preoperative spherical equivalent, preoperative anterior chamber depth and axial length did not correlate with the degree of reduction in postoperative pupil diameter.

Furthermore, phacoemulsification resulted in a mean reduction by 0.3 mm in preoperative pupil diameter both under mesopic and photopic conditions. In addition, a high correlation was observed between preoperative and postoperative pupil diameters, indicating that the postoperative pupil size could be predicted to range within 0.3 mm from the preoperative measurements. The sustained smaller postoperative pupil size we found is consistent with that reported in previous studies (it lasted up to 12 months in some studies) (Komatsu, Oono, & Shimizu, 1997) - (Moller, Buchholz, & Huebscher, 2000) - (Kanellopoulos & Asimellis, 2014).

However, other studies have reported a transient miotic effect of cataract surgery (Hayashi & Hayashi, Pupil size before and after phacoemulsification in nondiabetic and diabetic patients, 2004) - (Ba-Ali, Lund-Andersen, & Brøndsted, 2017). Indeed, Hayashi and Hayashi (Hayashi & Hayashi, Pupil size before and after phacoemulsification in nondiabetic and diabetic patients, 2004) have described the pupil size before and after (three days and one month) phacoemulsification in non-diabetic and diabetic patients. They have found a significant 0.5-mm decrease in pupil diameter 3 days after surgery. One month after surgery, the pupil diameter remained smaller but without reaching significance.

The differences in results could be due to different levels of inflammation, as postoperative inflammation has been shown to vary significantly. They have also found that the postoperative pupil size can be predicted from preoperative measurements. Therefore, the preoperative determination of pupil size is sufficiently meaningful to help for example to identify patients who are good candidates for multifocal implantation. Because of the magnification of the cornea, each examination measures the apparent pupil diameter, which differs by a ratio of about 15% from the actual “anatomical” pupil diameter. This consideration could be of importance to assess the impact of pupil dynamics on a particular optic design (Emsley, 1952).

Our sample included 52 myopic eyes and 43 hyperopic eyes. Before phacoemulsification, we did not find any significant difference in pupil diameters between myopic and hyperopic eyes under both illumination conditions, as in other studies (Salah-Mabed, Saad, Guilbert, & Gatinel, 2014). The same result was found for the preoperative magnitude of pupil dilation. However, we noted a significant difference in pupil dilation magnitude three months after surgery between the two groups. The myopic eyes appeared to have a significantly higher dilation ability. We have previously shown that cataract-free myopic eyes have a greater dilation ability

(Salah-Mabed, Saad, Guilbert, & Gatinel, 2014). Our results suggest that cataract could be a factor leading to reduce the differences in natural pupil dilation between myopic and hyperopic eyes.

Regarding the other parameters measured in our study, the central corneal pachymetry value was significantly higher one month after surgery compared to the baseline value. This difference remained significant three months after surgery. This could be due to the appearance of a surgically-induced edema, which usually disappears within three months (Aribaba, et al., 2015). Although the differences remained significant postoperatively, they were small (+4.8 ± 14.9 µm and +3.8 ± 13.7 µm, respectively one month and three months after surgery), and were not clinically relevant. We measured a CSIA magnitude of 0.19 D at the one-month examination, which decreased to a non-clinically significant level (0.10 D) at the three-month examination, supporting the results found in other studies (Febbraro, et al., 2015).

As expected, we measured an increase in anterior chamber depth by 1.40 ± 0.4 mm three months after surgery which is in line with the literature (Kanellopoulos & Asimellis, 2014).

Finally, like other studies, we measured a decrease in axial length by 59.7 ± 56.5 µm and 78.2 ± 64.5 µm, respectively one and three months after surgery which could be explained by the appearance of a macular edema which could persist at three months (Bilak, Simsek, Capkin, Guler, & Bilgin, 2015). We did not measure the pre- and postoperative retinal thickness with an OCT device to confirm the presence of this possible edema. This assumption should be tested in a further study.

In conclusion, we found, both under mesopic and photopic conditions, that the mean pupil diameters decreased three months after cataract surgery, while the anterior chamber depth and axial length increased. Moreover, the postoperative pupil diameter strongly correlated with the preoperative diameter, indicating that the postoperative pupil size could be predicted from preoperative measurements. As a result, the preoperative determination of the pupil diameter is clinically relevant for selecting IOL design. Further studies are needed to evaluate a potential correlation between surgically-induced pupil diameter and axial length evolution and the degree of cataract.

Chapter 5: Importance of the corneal epithelium in refractive surgery

5.1 Topography of the corneal epithelium and the bowman layer in low to moderately myopic eyes

Authors: Imene Salah-Mabed, MSc; Alain Saad, MD; Damien Gatinel, MD
Department of Anterior Segment and Refractive Surgery, Rothschild Foundation, Paris, France
CEROC: Centre of Expertise and Research in Optics for Clinicians
None of the authors have any financial or proprietary interests in any product, method or material presented in this paper.

Published: J Cataract Refract Surg 2016; 42:1190–1197 Q 2016. ASCRS & ESCRS.
doi: 10.1016/j.jcrs.2016.05.009

5.1.1 Abstract

Purpose: To compare the epithelium (air-tear film) and the Bowman layer's specular topographies in patients having low to moderate myopia corrected by photorefractive keratectomy (PRK).
Setting: Rothschild Foundation, Paris, France.
Design: Prospective interventional case series.
Methods: Anterior corneal specular Placido topography using the OPD-Scan® II (Nidek®, Japan) Placido-based topograph (NIDEK, Gammagori, Japan) was performed in 90 eyes of 51 patients undergoing PRK for myopia before and after the epithelium removal. The differences in axial keratometry, asphericity (Q value), astigmatism magnitude (toricity) and axis were computed in the first, third and fifth central corneal millimeter zones.
Results: The mean difference in axial mean keratometry was 0.56 ± 0.26 D, 0.56 ± 0.27 D and 0.56 ± 0.24 D in the first, third, and fifth central millimeter rings respectively. The mean difference in the magnitude of epithelial induced astigmatism was 0.42 ± 0.43 D x 90°, 0.41 ± 1.60 D x 78° and 0.02 ± 1.82 D x 83° (positive cylinder) respectively in the first, third and fifth central millimetre rings. Corneal astigmatism shifted toward increased with the rule orientation after epithelial removal. The mean

difference in asphericity (over central 6.0 mm) was - 0.07 ± 0.21. These differences were significant (p< 0.0001) and independent from age, sex, central pachymetry and spherical equivalent.

Conclusions: In low to moderately myopic eyes, the topography of the Bowman layer is significantly steeper than that of the epithelium. The epithelial layer tends to reduce the magnitude of the Bowman layer's astigmatism and prolateness.

5.1.2 Introduction

The Bowman layer is one constitutive layer of the cornea which separates the corneal epithelium from the anterior stroma. The corneal epithelium has an important contribution to the anterior corneal contour. During pre-operative evaluations of the cornea before refractive surgery, its effect on the anterior corneal contour impacts the topographical analysis of the air/tear film interface (Gatinel, Racine, & Hoang-Xuan, Contribution of the corneal epithelium to anterior corneal topography in patients having myopic photorefractive keratectomy, 2007).

The ability of the epithelium to reshape the anterior Bowman's layer surface has been established. Reinstein et al., showed that in PRK, the simple removal of the corneal epithelium can modify the geometric (and therefore refractive) properties of the cornea before excimer ablation (Reinstein, Silverman, & Coleman, High-frequency ultrasound measurement of the thickness of the corneal epithelium, 1993). The corneal epithelium has the ability to compensate the stromal surface distortions due to flap irregularities or abnormal stromal ablation in lamellar refractive surgery (DZ, RH, HFS, & SJ, 1999). Gatinel et al., in 2007, were the first to analyse the corneal shape of the Bowman layer in refractive surgery candidates after epithelial removal during a PRK procedure (Gatinel, Racine, & Hoang-Xuan, Contribution of the corneal epithelium to anterior corneal topography in patients having myopic photorefractive keratectomy, 2007). Using an Orbscan II topography system (Bausch & Lomb), they found that corneas from 44 myopic eyes treated with PRK had a more prolate shape after epithelial removal and before excimer ablation (the mean Q value was -0.44 ± 0.14 (SD) epi-on, and -0.65 ± 0.46 (SD) epi-off). They also concluded that in the central cornea, the keratometric power without the epithelium, was lower than the one with epithelium (mean value was 44.42 ± 1.59 (SD) epi-on and 43.46 ± 1.37 (SD) epi-off). These results were relatively consistent with those provided by other authors (Patel, Reinstein, Silverman, & Coleman, 1998) - (Zipper, Manns, & Fernandez, 2001) - (Simon, Ren, Kervick, & Parel, 1993).

The aim of this study was to explore the shape of the Bowman layer by analyzing three topographic components (keratometry, astigmatism and asphericity), with a Placido topographer - OPD-Scan® II (Nidek®, Japan) - on three concentric zones. The values obtained before and after epithelium removal were compared in normal low to moderately myopic eyes undergoing PRK.

5.1.3 Patients and methods

Subjects

This study included 90 eyes of 51 patients receiving PRK operations for myopia from January 2012 to July 2013 at the Rothschild Foundation. All patients received a complete ocular assessment prior to surgery, including cycloplegic refraction, slit lamp and fundus examination. Preoperative corneal topography was performed with the OPD-Scan® II (Nidek®, Japan), and the Orbscan IIz® (Bausch & Lomb®, USA).

Patients presenting with corneal diseases or other ocular pathologies (amblyopia, glaucoma, cataract, retinopathy, strabismus), or those with indications of subclinical keratoconus, or those with a history of ocular surgery were excluded from the study. We excluded patients whose eyes tested positive for Keratoconus (KC) or Keratoconus suspect (KCS) diagnosed by the Corneal Navigator Neural Network, which uses Klyce & Maeda indices on the OPD-Scan® II (Nidek®, Japan). Patients who had worn rigid gas-permeable lenses in the 12 months before the preoperative examination and those who had worn soft contact lenses in the 3 weeks before surgery were also excluded. We included patients older than 18 years with unremarkable ophthalmic histories besides low to moderate myopic refractive error. The reasons for choosing PRK were (1) the presence of a thin cornea (defined as a residual stromal bed less than 300 mm after subtracting the sum of the planned laser in situ keratomileusis [LASIK] flap and laser ablation thickness); (2) patient preference or the practice of activities which risk ocular trauma when both LASIK and PRK were proposed. All patients provided written informed consent.

The study and data acquisition were achieved with approval from the Rothschild Foundation Institutional Review Board. Informed consent was obtained from each patient after he/she voiced understanding about the purpose and the procedures in the study in accordance with the Declaration of Helsinki.

Instruments and Methods

Topography of each eye was performed using the OPD-Scan® II (Nidek®, Japan) Placido-based topograph (Figure 48).

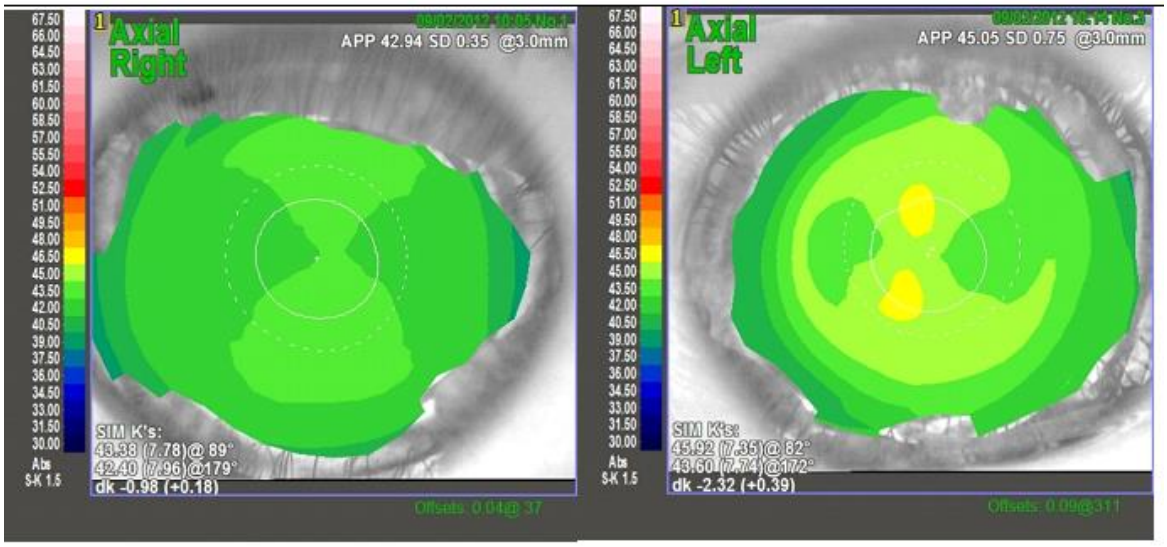

Figure 48 Refractive map before (left) and after (right) the epithelium removal

The specular corneal topography apparatus uses 19 vertical and 23 horizontal illuminated Placido disc segments in which anterior reflection covers a 0.5 mm to 11 mm area. This system captures the image of the reflected rings from the corneal surface to compute its axial and tangential curves using a proprietary algorithm.

Ten minutes before the activation of the PRK and the administration of topical anesthetic, the preoperative topography scan was performed using an OPD-Scan® II (Nidek®, Japan) located in the same room as the excimer laser unit on each eye. The patient was asked to blink several times before image acquisition. He was then instructed to focus on the centre disc of the Placido rings. To limit the influence of overnight corneal swelling, the PRK was performed at least 4 hours after the patient's awakening (Feng, Varikooty, & Simpson, 2001).

Next, 2 drops of lidocaine were administrated at 5-minute intervals. A lid- speculum was applied on the left eye of the patient. The epithelium was carefully peeled off with blunt forceps after the application of a 20% alcohol solution over 20 seconds on the 8 mm central corneal zone. The corneal surface was then rinsed with a balanced salt solution and inspected through the excimer laser microscope to ensure that all epithelial debris were removed. The speculum was then removed, and the patient was asked to sit at the topography instrument. Three consecutive postoperative topographies were performed, during which the patient was asked to blink several times. The examiner checked each image and its quality before recording it. The patient returned to the surgical bed and the excimer laser procedure was resumed and completed with the EX500 excimer laser. A bandage contact lens was placed over

the eye after completion of the surgical procedure. The procedure was repeated for the other eye (Gatinel, Racine, & Hoang-Xuan, Contribution of the corneal epithelium to anterior corneal topography in patients having myopic photorefractive keratectomy, 2007). All surgical procedures were performed by the same surgeon (DG).

All the topographic measurements were taken when the patient's eye fixated on the target (bright central spot located 75 mm from the subject's eye). Three consecutive acquisitions were performed for each eye and averaged for data analysis. All the measurements were performed by the same operator. The following data from each of the obtained topographies were recorded:

(1) Arithmetic mean between the steep and flat keratometry values (steep and flat simulated K-values) on the first, third, and fifth central millimeter rings.

(2) The amount and the axis of the surface toricity (keratometric astigmatism) on the first, third, and fifth central millimeter rings (difference between the respective steep and the flat K-values).

(3) Corneal Asphericity (mean Q value, mean Q steep value, and mean Q flat value) measured over the central 6.0 mm zone of the cornea.

Astigmatism Evaluation

We compared the amount of the corneal surface astigmatism with and without epithelium using a power vector method analysis. Power vectors are a geometrical representation of sphero-cylindrical refractive errors in 3 fundamental dioptric components (Thibos & Horner, Power vector analysis of the optical outcome of refractive surgery, 2001) - (Thibos, Wheeler, & Horner, Power vectors: an application of fourier analysis to the description and statistical analysis of refractive error, 1997).

The first component is a spherical lens with power M equal to the spherical equivalent of a given refractive error $\boldsymbol{M = S + C/2}$.

The two other components are the two Jackson crossed cylinder lenses, one with power $\boldsymbol{J_0 = (-C/2)\cos(2\alpha)}$ at axis α= 0°= 180° and the other one with power $\boldsymbol{J_{45} = (-C/2)\sin(2\alpha)}$ at axis α= 45°.

This analytical method allows to express a sphero-cylindrical refractive error by showing these three dioptric powers quantities (M, J_0, J_{45}). Harris (Harris, Dioptric strength: a scalar representation of dioptric power, 1994) and Raasch (Raasch, 1995) showed that these 3 numbers can be represented geometrically as the (x, y, z) coordinates of a point in a three-dimensional dioptric space. Accordingly, a power

vector is the vector drawn from the coordinate origin of this space to the point (M, J_0, J_{45}) which length is a measure of the overall blur strength $\mathbf{B= \sqrt{(M^2 + J_0^2 + J_{45}^2)}}$ of a sphero-cylindrical refractive error or lens.

In our study, these quantities did not correspond to refractive error but sphero-cylindrical axial power of the analysed corneal surface. The benefit of such a method is that the three fundamental components of the power vectors are independent of the others. This simplifies a lot the combination, the comparison and the statistical analysis of sphero-cylindrical power variations.

Statistical analysis

Statistical analyses were performed with a commercial software (SPSS v. 13.0; SPSS Inc., Chicago, IL). We used paired student *t* test to compare the corneal topography outcomes before and after removing the epithelium. Pearson correlation analyses were also used. A calculated *p*-value <0.05 was considered statistically significant. Data are presented as the mean +/- standard deviation.

Astigmatism plots were generated using the Astigplot® software (EB Eye). The average magnitude and axis of cylinders was computed using vector calculations. The astigmatism plots were represented with a positive cylinder magnitude convention.

5.1.4 Results

Demographics

Ninety myopic eyes of 51 patients (18 men and 33 females, mean age 34.81 ± 8.22 years, ranging from 19.74 to 50.51 to years) were included. Among the included eyes, there were 57 eyes with total refractive astigmatism of more than 0.25 D, and 33 eyes without refractive astigmatism. The mean preoperative refractive sphere was -3.03 ± 1.34 D (SD) (ranging from -7.00 to -0.75 D), with an average cylinder magnitude of -0.75 ± 0.51 D (ranging from -2.00 to -0.25 D). The mean refractive spherical equivalent was -3.28 ± 1.38 D (ranging from -7.00 / -0.88 D). These data are represented in Table 14.

Corneal tomography mas measured with the Orbscan IIz® (Bausch & Lomb®, USA) preoperatively: the mean central corneal thickness of the included eyes was 537µm ± 32.91 (SD) (range 479 µm to 616 µm).

Number of patients	*51*
Age (in years)	
Average ± Standard deviation	*34.81 ± 8.22*
Min / Max	*50.51 / 19.74*
Pachymetry (in µm)	
Average ± Standard deviation	*537.10 ± 32.91*
Min / Max	*616.00 / 479.00*
% male / % Female	*35% / 65%*
Number of eyes	*90*
Refractive Astigmatism >= 0.25	*57*
Refractive Astigmatism < 0.25	*33*
Sphere (in D)	
Average ± Standard deviation	*-3.03 ± 1.34*
Min / Max	*-7.00 / -0.75*
Cylinder (in D)	
Average ± Standard deviation	*-0.75 ± 0.51*
Min / Max	*-2.00 / -0.25*
Spherical Equivalent (in D)	
Average ± Standard deviation	*-3.28 ± 1.38*
Min / Max	*-7.00 / -0.88*

Table 14 Demographics data

Keratometry

The axial keratometric corneal power (sim-K average) was 44.22 ± 1.35 D, 44.29 ± 1.36 D and 44.05 ± 1.35 D in the first, third and fifth mm rings respectively. After the removal of the corneal epithelium, the axial corneal power measured on the Bowman layer was 44.78 ± 1.44 D, 44.86 ± 1.44 D and 44.61 ± 1.40 D in the first, third and fifth mm rings respectively (Table 15).

	Preoperative With Epithelium	Postoperative Without Epithelium	Postoperative - Preoperative	*P* Value
Keratometry (D) mean ± SD				
1 mm	44.22 ± 1.35 SD (Min 41.23 / Max 47.89)	44.78 ± 1.44 SD (Min 41.49 / Max 48.57)	0.56 ± 0.26 SD (Min 0.08 / Max 1.42)	p < 0,0001
3 mm	44.29 ± 1.36 SD (Min 41.24 / Max 47.88)	44.86 ± 1.44 SD (Min 41.51 / Max 48.73)	0.56 ± 0.27 SD (Min -0.08 / Max 1.40)	p < 0,0001
5 mm	44.05 ± 1.35 SD (Min 41.16 / Max 47.88)	44.61 ± 1.40 SD (Min 41.39 / Max 48.72)	0.56 ± 0.24 SD (Min -0.17 / Max 1.39)	p < 0,0001
Asphericity (Q Factor) mean ± SD				
Mean Q	-0.20 ± 0.13 (Min -0.60 / Max 0.09)	-0.27 ± 0.23 (Min -1.51 / Max 0.12)	-0.07 ± 0.21 SD (Min -1.25 / Max 0.45)	p < 0,001
Steep Q	-0.19 ± 0.21 (Min -0.73 / Max 0.39)	-0.26 ± 0.26 (Min -1.00 / Max 0.29)	-0.07 ± 0.25 SD (Min -0.65 / Max 0.47)	p < 0,013
Flat Q	-0.17 ± 0.13 (Min -0.42 / Max 0.36)	-0.18 ± 0.19 (Min -0.67 / Max 0.42)	-0.01 ± 0.20 SD (Min -0.37 / Max 0.56)	p < 0,682*

Table 15 Difference in keratometries and asphericities before and after the epithelium removal

** Non-significant*

There was a significant difference between the average corneal power before and after the epithelium removal on the 3 analyzed zones (paired t test, p<0.0001).

There was no significant difference of the average corneal power between men and women's eyes (before or after epithelium removal).

There was no correlation between the average keratometric power and the patient's age, refractive spherical equivalent and the initial central mean pachymetry, before and after the epithelium removal over the three ring zones of measurement (Table 16).

Correlation between the keratometry and the age, the initial spherical equivalent and the initial pachymetry		
	Preoperative With Epithelium	*Post epithelium ablation*
Age		
1 mm	*r= -0.242, p < 0.028*	*r= -0.248, p < 0.024*
3 mm	*r= -0.237, p < 0.031*	*r= -0.238, p < 0.030*
5 mm	*r= -0.241, p < 0.028*	*r= -0.243, p < 0.027*
Initial spherical equivalent		
1 mm	*r= 0.038, p < 0.729**	*r= 0.040, p < 0.246**
3 mm	*r= 0.038, p < 0.139**	*r= 0.020, p < 0.251**
5 mm	*r= 0.056, p < 0.047*	*r= 0.051, p < 0.943**
Initial pachymetry		
1 mm	*r= -0.023, p < 0.004*	*r= -0.051, p < 0.049*
3 mm	*r= -0.043, p < 0.051*	*r= -0.047, p < 0.019*
5 mm	*r= -0.032, p < 0.586**	*r= -0.065, p < 0.067*

Table 16 Correlations between keratometry and age, initial spherical equivalent and initial pachymetry before and after the epithelium removal

** Non-significant*

Magnitude of the epithelial induced astigmatism

Astigmatism is an optical aberration which is mainly caused by the toricity of a refractive surface. Although topography instruments measure toricity (not astigmatism) we will use the terms "astigmatism" and "toricity" interchangeably. The magnitude of the epithelial induced astigmatism (EIA) was calculated as follows.

In the considered ring zone, the difference in simulated keratometry (sim-K) of the steepest and the flattest hemi-meridians was calculated as the "sim-K difference" by the topography software. The magnitude of the EIA was computed as the variation between the "sim-K difference" values obtained after and before epithelial removal.

Preoperatively, the average sim-K difference values were 0.61 D, 0.41 D and 0.68 D in the first, third and fifth mm central zones respectively. After epithelial removal, the values of the (sim-K difference) measured on the Bowman layer were 1.03 D, 0.82 D and 0.70 D in the first, third and fifth mm rings, respectively. Before and after removal, the astigmatism was predominantly oriented with the rule (WTR).

The difference in the magnitude of the EIA was independent from age (r = -0.123, p = 0.26, r = -0.041, p = 0.713, and r = 0.054, p = 0.624 in the first, third and fifth rings respectively), sex (unpaired t-test, t = -0.674, p = 0.502, t = 1.182, p = 0.240, t = 0.617, p = 0.539 in the first, third and fifth rings respectively), the initial pachymetry (r = -0.085, p = 0.447 , r = -0.364, p = 0.001, and r = -0.176, p = 0.112 in the first, third and fifth rings respectively) and the initial spherical equivalent (r = -0.023, p = 0.833 , r = -0.037, p = 0.742, and r = 0.119, p = 0.286 in the first, third and fifth rings respectively).

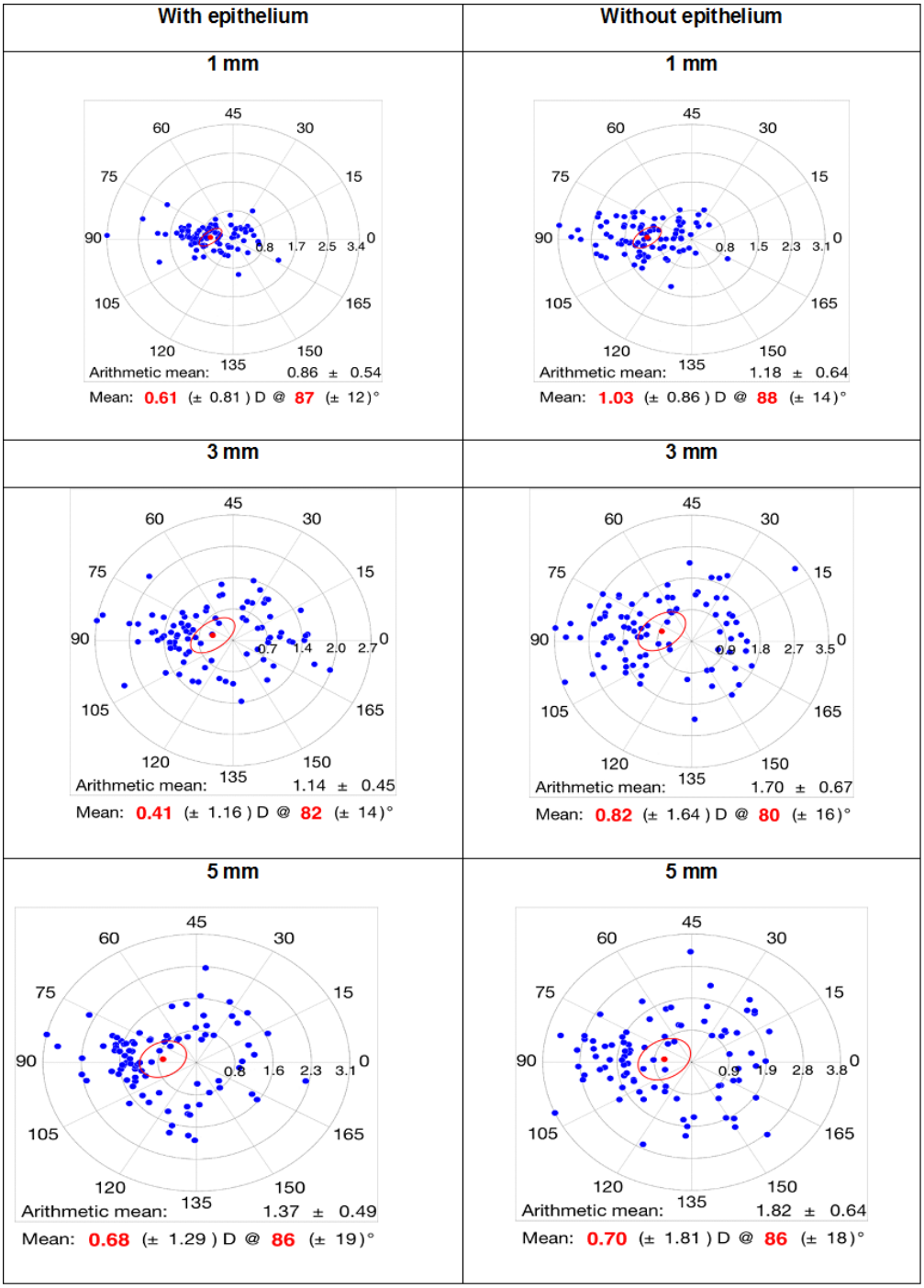

Figure 49 Corneal astigmatism with epithelium on (left) and with epithelium off (right)

The Figure 49 represents the magnitude and orientation of the anterior corneal astigmatism before and after the removal of the epithelium.

We found a difference of around 0.40 D in the 3 mm ring zone between the two analysed surfaces. It appears in Figure 50 that this difference tended to decrease toward the periphery.

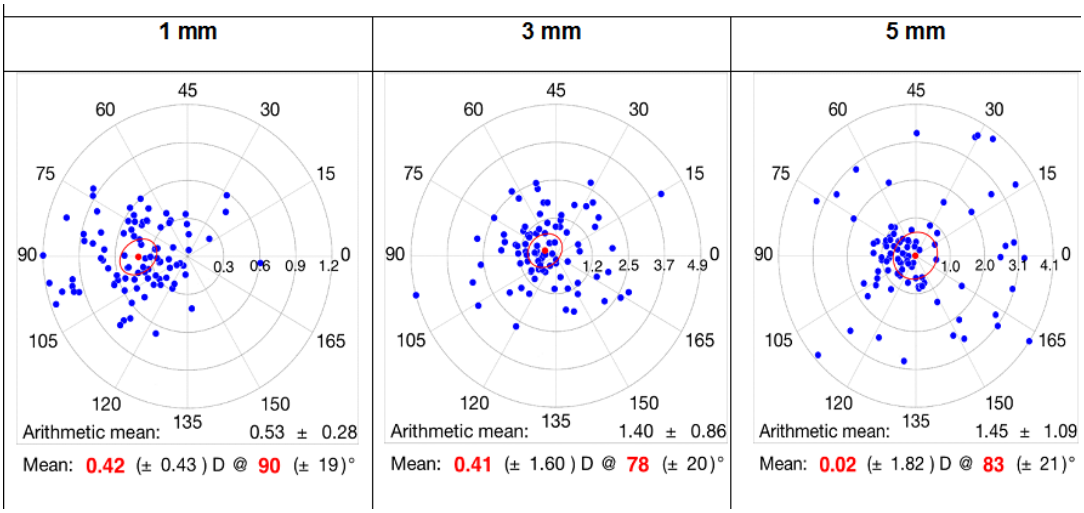

Figure 50 Epithelial astigmatism

In the 5 mm ring zone, we expressed the difference between epi-on and epi-off anterior corneal astigmatism as a power vector. We calculated the mean and standard deviation of each vector component, and the length ("Blur Strength") of the power vectors. Table 17 summarizes the results. All the differences were significant except in J_{45}.

	With Epithelium				Without Epithelium							
	M	J_0	J_{45}	B	M	*P* Value	J_0	*P* Value	J_{45}	*P* Value	B	*P* Value
Mean	-3.161	0.158	0.004	3	-4	p < 0,0001	0.317	p < 0,001	-0.001	p < 0,748 *	4	p < 0,0001
Minimum	-0.875	-0.625	-0.383	0.884	-1.875		-0.914		-0.470		1.879	
Maximum	-7	0.995	0.464	7	-9.375		1.345		0.585		9.416	
Standard Deviation	1.416	0.331	0.135	1.419	1.717		0.430		0.194		1.728	

Table 17 Distribution of manifest refraction before and after removal of the corneal epithelium

* *Non-significant*

Figure 51 shows that there was a wider difference in J_0 than in J_{45} between the epi-on state and the epi-off one.

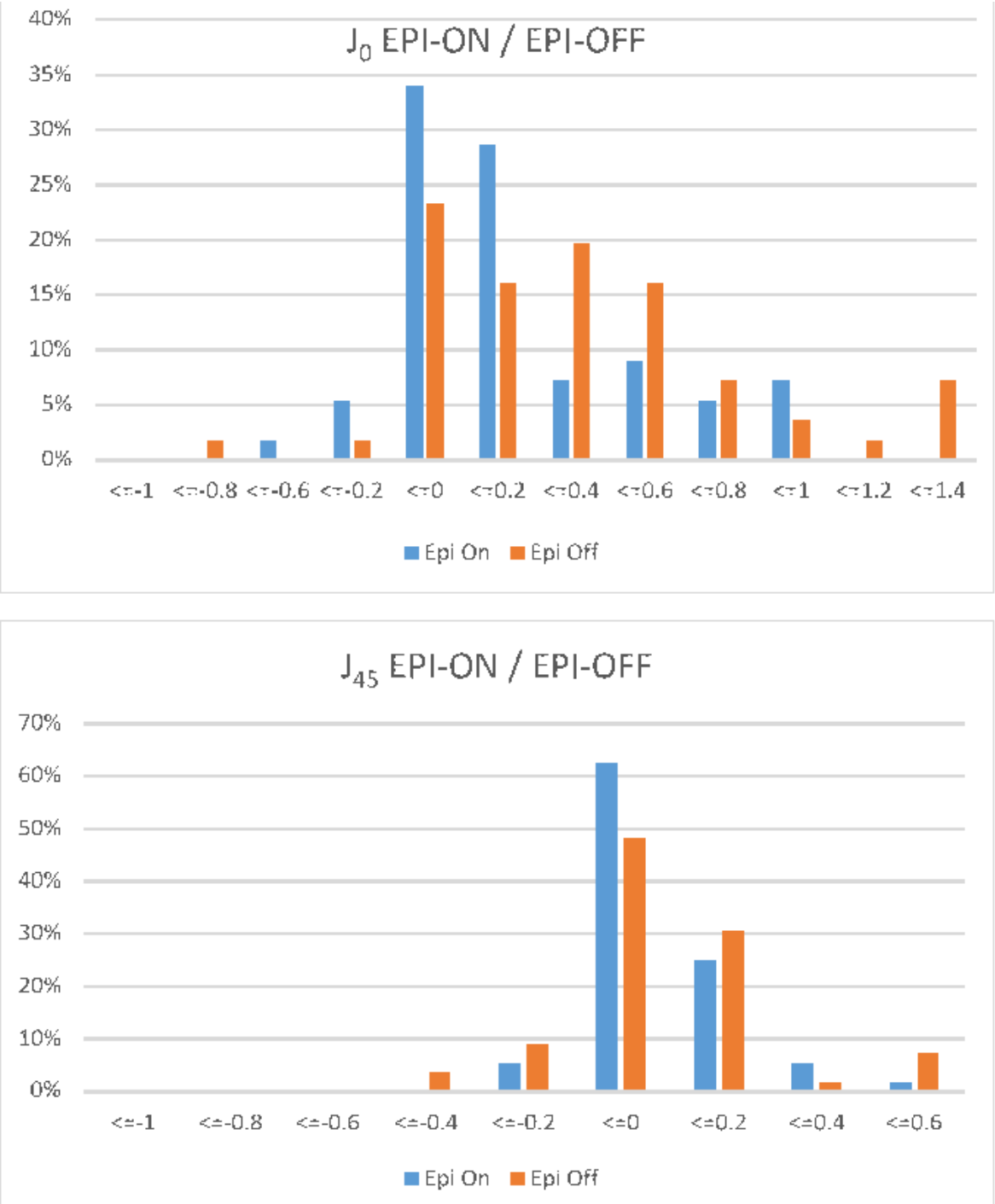

Figure 51 Distribution of the corneal astigmatism before and after the epithelium removal

Asphericity

The average corneal asphericity expressed by the Q-value was -0.20 ± 0.123 (SD) (range +0.09 to -0.60). It was of -0.27 ± 0.23 (SD) (range +0.07 to -1.51) after the removal of the corneal epithelium. The difference between these values was significant (p<0.001).

There was no significant difference in the anterior corneal asphericity between men and women (before removal of the corneal epithelium, unpaired t-test, t = -1.734, p = 0.162 and after removal of the corneal epithelium, unpaired t-test, t = 1.110, p = 0.333). Table 15 summarizes some of these results.

There was no correlation between age and asphericity before and after the epithelium removal (respectively r = 0.022, $p < 0.01$ and r = -0.03, $p < 0.01$).

There was no correlation between the preoperative spherical equivalent and the corneal asphericity measured with and without the epithelium (r = 0.304, $p < 0.01$ and r = 0.393, $p < 0.01$, respectively). There was no correlation between the initial mean central pachymetry and the corneal asphericity measured over the epithelium and the Bowman layer (r = 0.263, $p < 0.01$ and r = 0.075, $p < 0.01$, respectively).

5.1.5 Discussion

This study aims to extend the results of a previous study by Gatinel et al. (Gatinel, Racine, & Hoang-Xuan, Contribution of the corneal epithelium to anterior corneal topography in patients having myopic photorefractive keratectomy, 2007), who analyzed the topography of the Bowman layer by performing combined slit scanning and Placido topography after removal of the corneal epithelium in in-vivo normal myopic eyes.

We found that the epithelialized cornea had an average keratometric axial power slightly inferior to that of the Bowman layer in the first, third and fifth mm diameter ring zones. The corneal power measured when the epithelial layer was removed on the Bowman's membrane on the same zones was 44.78 ± 1.44 D, 44.86 ± 1.44 D and 44.61 ± 1.40 D respectively. These values weren't correlated with the age, the pachymetry and the refractive initial spherical equivalent. The topography of the Bowman membrane was on average significantly 0.56 D steeper in the central 1mm zone than the epithelial surface. This confirms that the epithelium acts like a convex/concave meniscus which reduces the paraxial keratometric corneal power by 0.56 D.

Patel et al. (Patel, Reinstein, Silverman, & Coleman, 1998) studied the central epithelial thickness distribution in 14 normal human corneas with in vivo measurements taken from high-frequency ultrasound digital signal processing with a measurement precision of 2 µm. They found that on average, the Bowman's layer had a higher keratometric power. They found a mean radius of Bowman's layer of 7.34 mm ± 0.17 (SE) which corresponded to a power of 45.37 D.

Our results are consistent with those reported by Zipper et al. (Zipper, Manns, & Fernandez, 2001). These authors studied topographic data from 16 fresh human cadaver eyes using a PAR corneal topography system (PAR Vision Systems Corp.) before and after removal of the epithelium with a blunt knife. They found that the difference in the apical radius of curvature between the two states corresponded to a power of approximately 0.5 D within the central 7.0 mm zone.

Simon et al. (Simon, Ren, Kervick, & Parel, 1993) reported slightly higher keratometric values for Bowman's layer. Using an automated keratometer in 10 fresh human eye-bank eyes with and without the epithelium, they found that the corneal epithelium accounts for an average of -1.03 D of the power of the eye at a central 2.0 mm zone. This power was -0.85 D at the 3.6 mm zone.

These differences, although minimal, might be explained by the different measurement methods used, the different corneal diameters studied, and finally, by the fact that the corneas were analysed ex-vivo in several surveys.

Curiously, our results contrast to those reported by Gatinel et al. (Gatinel, Racine, & Hoang-Xuan, Contribution of the corneal epithelium to anterior corneal topography in patients having myopic photorefractive keratectomy, 2007). This previous study concluded that the central cornea curvature was flatter after epithelial removal, as indicated by the change in the mean power of the cornea at 3.0 mm (44.42 ± 1.59 D in preoperative measurement and 43.46 ± 1.37 D without the epithelium). We found a difference of 0.56 D whereas they found a difference of 1 D in the opposite direction. A difference in measurement protocols may explain the contradiction between our results and those of our previous work (Gatinel, Racine, & Hoang-Xuan, Contribution of the corneal epithelium to anterior corneal topography in patients having myopic photorefractive keratectomy, 2007). The eyes included in the present study belonged to a population older than those in the previous study (Gatinel, Racine, & Hoang-Xuan, Contribution of the corneal epithelium to anterior corneal topography in patients having myopic photorefractive keratectomy, 2007).

Although we found that there was no correlation between the keratometry and the age before and after the epithelium removal, other surveys such as Hayashi et al. (Hayashi, Hayashi, & Hayashi, Topographic analysis of the changes in corneal shape due to aging, 1995) concluded that the mean refractive power of the cornea increases with age because the normal cornea becomes steeper and shifts from with-the-rule to against-the-rule astigmatism over time. The discrepancy between our two studies

could be explained by the difference in our sample's mean age.

The corneal surfaces had an increased gradient of flattening toward the periphery, as a more prolate shape was measured after the epithelium removal at the Bowman layer level. In this study, the average corneal asphericity expressed by the Q factor was -0.20 ± 0.13 (SD) (range +0.09 to -0.60) before and -0.27 ± 0.23 (SD) (range +0.07 to -1.51) after the removal of the corneal epithelium. The difference between these values was significant (p<0.001). In our previous study[1] the mean Q values measured by Orbscan II were -0.44 ± 0.14 before and -0.65 ± 0.46 after epithelial removal.

These differences may be explained by the fact that we measured the Q factor on the 7mm zone of the cornea, whereas our present results were obtained on a 5 mm zone. The use of different algorithms and instruments to measure the asphericity could also account for these differences. A trend toward more negative corneal asphericity on the Bowman's layer was found in both studies and was also similar to that reported by Patel et al.[4] and Zipper et al. (Zipper, Manns, & Fernandez, 2001). Our results are comparable to those of Read et al. (Read, Collins, Carney, & Franklin, 2006). Indeed, these authors found a Q-value of -0.19 on the epithelial corneal surface measured within the 6mm diameter zone (we found -0.20 on the 5 mm diameter zone).

Nevertheless, it could be interesting to note that during the interval of time between epithelium removal and OPD-Scan® II (Nidek®, Japan) measurements of Bowman surface, the anterior part of the stroma could swell in a certain amount. The contact between the bowman layer and the tear film could lead to a certain degree of prolateness and steepening. Which would mean that the keratometry and/or the prolateness were overestimated in the studies. The measurement of corneal thickness with the laser excimer platform or manually should have been contributive for that issue. It should be interesting to evaluate again those patients and, in case of retreatment, to see if under or over correction is due to epithelium rather than photoablation.

We didn't find any significant correlation between the age (r = 0.022, p < 0.01, r = -0.030, p < 0.01), the pachymetry (r = 0.263, p < 0.008, r = 0.075, p < 0.860), and the refractive initial spherical equivalent (r = 0.304, p < 0.040, r = 0.393, p < 0.002) and the asphericity (respectively before and after the epithelium removal).

On average, in accordance to Simon et al. (Simon, Ren, Kervick, & Parel, 1993), we showed that the corneal toricity tends to increase after epithelial removal. The mean magnitude of epithelium induced astigmatism (EIA) was approximately of 0.40 D.

However, Simon et al. (Simon, Ren, Kervick, & Parel, 1993) observed a change in the astigmatism axis between the epithelium and Bowman's layer surfaces, while we found a shift toward the WTR direction of astigmatism in the first and third central millimeters. The magnitude of the EIA appears to decrease as the distance to the corneal vertex increases and becomes non-significant at the fifth millimetre ring zone. Using very high-frequency digital ultrasound, Reinstein et al. (Reinstein, et al., 2009) - (Reinstein, Archer, Gobbe, Silvermann, & Coleman, 2010) had established the ability of the epithelium to reshape the anterior corneal surface, suggesting that the epithelium can remodel itself to compensate for stromal surface abnormalities created by flap irregularities or irregular stromal ablation after lamellar refractive surgery. The wound-healing process in PRK and rearrangement of the flap in LASIK may result in partial compensation of the sculpted pattern onto the corneal surface after laser ablation (Dausch, Klein, & Schröder, 1993) - (Flanagan & Binder, 2005). We confirmed in this study that the epithelium contributes to remodeling the corneal surface when limited to the Bowman layer.

Touboul et al. (Touboul, et al., 2012) suggested that the role of the epithelium and its contribution to corneal refractive power should be more important in keratoconus than in normal eyes.

The remodeling of the epithelial layer may cause the masking of some early corneal anomalies that might arise at the stromal level in early subclinical keratoconus (Reinstein & Silverman, Very high-frequency digital ultrasound: Artemis 2 scanning in LASIK, 2004).

In eyes scheduled for PRK, changes in keratometry, asphericity and toricity after the epithelium removal could negate the accuracy of the Placido-based custom ablation software. However, it appears reasonable to postulate that epithelial regrowth after surgery may also modify the geometry of the laser remodeled stromal surface. Although the epithelial and Bowman layer have slightly different topographic characteristics, the delivery of topography-guided custom ablation based on epi-on data may reduce the epi-off irregularity.

Our study allowed us to describe the shape of the epithelial and the Bowman layer surfaces in myopic eyes. Our findings suggest that in refractive procedures such as myopic photorefractive keratectomy, the refractive contribution of the epithelium could be taken into account to improve predictability. This approach may be particularly relevant for transepithelial PRK (Fadlallah, et al., 2011), where the mapping of the

epithelial layer may improve the precision of the procedure. Prediction of epithelial healing processes could be important to evaluate as well.

Our data was limited to the analysis of mean axial keratometry, toricity and asphericity of the Bowman layer. Further studies are necessary to investigate the role of the corneal epithelium in the quality of the retinal image by analyzing the effect of the corneal epithelium on high order aberrations of the eye.

5.2 Investigating the topographic effect of epithelium in myopic eyes with and without topographic preoperative abnormalities

Authors: Imene Salah Mabed, MSc (1,2), Alain Saad, MD (2), Karsten Plamann, PhD (1), Damien Gatinel, MD, PhD (2)

1. Laboratoire d'Optique Appliquée, CNRS, Université Paris-Saclay, ENSTA, Ecole Polytechnique, Orsay, France.
2. Department of Anterior Segment and Refractive Surgery, Rothschild Foundation, Paris, France.

None of the authors has any financial or proprietary interests in any product, method or material presented in this paper.

Published: None.

5.2.1 Abstract

Purpose: To investigate the epithelium topographic properties by comparing the epithelium (air-tear film) and the Bowman layer's specular topographies in normal (Group N) and keratoconus suspected (Group KCS) classified corneas having low to moderate myopia corrected by photorefractive keratectomy (PRK).

Setting: Rothschild Foundation, Paris, France.

Design: Prospective interventional case series.

Methods: Anterior corneal specular Placido topography using the OPD-Scan® II (Nidek®, Japan) Placido-based topograph (NIDEK, Gammagori, Japan) was performed in 97 eyes of 55 patients (Group N; 77 eyes, Group KCS; 20 eyes) undergoing PRK for myopia before and after the epithelium removal. The differences in axial keratometry, asphericity (Q value), astigmatism magnitude (toricity) and axis were computed in the first, third and fifth central corneal mm zones in both normal and keratoconus suspected corneas groups. High order aberrations have also been analyzed before and after epithelium removal and compared in the two groups.

Results: The mean difference in axial mean keratometry was 0.48 ± 0.20 D, 0.50 ± 0.24 D and 0.52 ± 0.20 D in the first, third, and fifth central millimeter rings respectively in the normal eyes group and 0.54 ± 0.29 D, 0.49 ± 0.35 D and 0.48 ± 0.27 D in the KCS group. The mean difference in the magnitude of epithelial induced astigmatism was 0.35 D x 89° (positive cylinder) in the first central millimetre rings in the normal eyes group and 0.55 D 86° in the KCS group. The mean difference in asphericity (on

the steep axe over central 6.0 mm) was - 0.04 ± 0.25 and - 0.17 ± 0.22 respectively in the normal eyes and KCS groups. These differences were significant (p< 0.0001).
In the normal corneas (Group 1) all studied aberrations increased significantly (p< 0.001) after the epithelium removal except spherical aberration. In the KC/KCS group (2), only the total corneal Aberration and the astigmatism increased significantly after the epithelium removal.
Conclusions: In low to moderately myopic eyes, the topography of the Bowman layer is significantly steeper than that of the epithelium in all groups. The epithelial layer tends to reduce the magnitude of the Bowman layer's astigmatism and prolateness and irregularities more in normal corneas than in keratoconic ones.

5.2.2 Introduction

Ectasia remains the most dreaded complication after refractive surgery. Hence, there is great interest in attempting to preoperatively identify patients at risk for this complication (Binder, 2008) - (Binder & Trattler, Evaluation of a risk factor scoring system for corneal ectasia after LASIK in eyes with normal topography, 2010) - (Randleman, Trattler, & Stulting, 2008) - (Randleman, Woodward, Lynn, & Stulting, 2008) - (Saad & Gatinel, Topographic and tomographic properties of forme fruste keratoconus corneas, 2010) - (Saad, Lteif, Azan, & Gatinel, 2010).
A major goal in preventing post laser in situ keratomileusis ectasia is to detect corneas with subclinical keratoconus (KCS) in its earliest and mildest form.
KC (Keratoconus) is an asymmetric (Zadnik, et al., 2002) progressive disorder that frequently affects both eyes.
The corneal epithelium has an important contribution to the anterior corneal contour (Salah-Mabed, Saad, & Gatinel, Topography of the corneal epithelium and Bowman layer in low to moderately myopic eyes, 2016). During pre-operative evaluations of the cornea before refractive surgery, its effect on the anterior corneal contour impacts the topographical analysis of the air/tear film interface (IJspeert, de, van den Berg, & de, 1990) - (Gatinel, Racine, & Hoang-Xuan, Contribution of the corneal epithelium to anterior corneal topography in patients having myopic photorefractive keratectomy, 2007).
The ability of the epithelium to reshape the anterior Bowman's layer surface has been established (Gatinel, Racine, & Hoang-Xuan, Contribution of the corneal epithelium to anterior corneal topography in patients having myopic photorefractive keratectomy, 2007) - (Salah-Mabed, Saad, & Gatinel, Topography of the corneal epithelium and

Bowman layer in low to moderately myopic eyes, 2016) - (Touboul, et al., 2012) - (Reinstein, Silverman, & Coleman, High-frequency ultrasound measurement of the thickness of the corneal epithelium, 1993).

Reinstein et al. (Reinstein, Silverman, & Coleman, High-frequency ultrasound measurement of the thickness of the corneal epithelium, 1993) , showed that in PRK, the simple removal of the corneal epithelium can modify the geometric (and therefore refractive) properties of the cornea before excimer ablation. The corneal epithelium has the ability to compensate the stromal surface distortions due to flap irregularities or abnormal stromal ablation in lamellar refractive surgery (Reinstein, Silverman, Sutton, & Coleman, 1999).

Gatinel et al., in 2007 (Gatinel, Racine, & Hoang-Xuan, Contribution of the corneal epithelium to anterior corneal topography in patients having myopic photorefractive keratectomy, 2007), were the first to analyse the corneal shape of the normal Bowman layer in refractive surgery candidates after epithelial removal during a PRK procedure. Using an Orbscan IIz® (Bausch & Lomb®, USA) topography system, they found that normal corneas from 44 myopic eyes treated with PRK had a more prolate shape after epithelial removal and before excimer ablation (the mean Q value was -0.44 ± 0.14 (SD) epi-on, and -0.65 ± 0.46 (SD) epi-off). They also concluded that in the central cornea, the keratometric power without the epithelium, was lower than the one with epithelium (mean value was 44.42 ± 1.59 (SD) epi-on and 43.46 ± 1.37 (SD) epi-off). These results were relatively consistent with those provided by other authors (Patel, Reinstein, Silverman, & Coleman, 1998) - (Zipper, Manns, & Fernandez, 2001) - (Simon, Ren, Kervick, & Parel, 1993).

Therefore, we can be led to wonder if the corneal epithelium could smooth enough the Bowman layers irregularities to be able to mask an early subclinical keratoconus.

Otherwise, the management by photorefractive keratectomy (PRK) of keratoconus (KC) eyes require an improvement in visual recovery and predictability of the outcomes. More or less efficient protocols were proposed to deliver a custom photoablative correction guided by preoperative topographic and aberrometric measurements (Bahar, Levinger, & Kremer, 2006) - (Kymionis, et al., 2009) - (Krueger & Kanellopoulos, Stability of simultaneous topography-guided photorefractive keratectomy and riboflavin/UVA cross-linking for progressive keratoconus: case reports, 2010).

To date, the most popular method for surface laser ablation in keratoconus is the

topography-guided process (Athens' protocol) (Kanellopoulos & Binder, Management of corneal ectasia after LASIK with combined, same-day, topography-guided partial transepithelial PRK and collagen cross-linking: the athens protocol, 2011). The corneal epithelium's thickness is very variable in keratoconus eyes. Thus, using a topography-guided correction may not be a so accurate way to correct vision in PRK. Touboul et al. (Touboul, et al., 2012) reported on keratoconus corneas that the Bowman topographies they have studied, were more curved and irregular after epithelial removal. These findings were consistent with the hypothesis that in hyperprolate keratoconic corneas, the epithelium was thinner in the steepest areas and thicker in the flattest ones and compensated for the negative asphericity and refractive asymmetry. Thus, they conclude to theoretical limits of topography-guided custom photoablation in keratoconic eyes given the keratometric variations observed after epithelium removal.

The aim of this study was to explore the impact of the epithelium on the KC and KCS corneas and to test if there are predictive preoperative factors that differentiate the normal and the abnormal corneas before epithelium removal. We have assessed the shape of the KC and KCS eyes Bowman's layer by analyzing three topographic components (keratometry, astigmatism and asphericity), with a Placido topographer - OPD-Scan® II (Nidek®, Japan) - on three concentric zones. The values obtained before and after epithelium removal were compared in normal, keratoconus suspected and keratoconus corneas groups with low to moderately myopia undergoing PRK. Studies have shown that wavefront technology may also be a useful adjunct to topography for diagnosing keratoconus (Bühren, Kook, Yoon, & Kohnen, 2010) - (Bühren, Kühne, & Kohnen, Defining subclinical keratoconus using corneal first-surface higher-order aberrations, 2007) - (Jafri, Li, Yang, & Rabinowitz, 2007).

This study compared also the anterior corneal epithelial wavefront data of KC and KCS eyes, and normal eyes, and the anterior corneal Bowman's layer wavefront data.

5.2.3 Patients and Methods

Subjects

This prospective study included 97 thin and irregular corneas of 67 patients receiving PRK operations for myopia from January 2012 to July 2014 at the Rothschild Foundation. All patients received a complete ocular assessment prior to surgery, including cycloplegic refraction, slit lamp and fundus examination. Preoperative corneal topography was performed with the OPD-Scan® II (Nidek®, Japan), and the

Orbscan IIz® (Bausch & Lomb®, USA).

Patients presenting with corneal diseases or other ocular pathologies (amblyopia, glaucoma, cataract, retinopathy, strabismus), or those with a history of ocular surgery were excluded from the study. Patients who had worn rigid gas-permeable lenses in the 12 months before the preoperative examination and those who had worn soft contact lenses in the 3 weeks before surgery were also excluded. We included patients older than 18 years with unremarkable ophthalmic histories besides low to moderate myopic refractive error. The reasons for choosing PRK in corneas were (1) the presence of a thin (defined as a residual stromal bed less than 300 mm after subtracting the sum of the planned laser in situ keratomileusis [LASIK] flap and laser ablation thickness) and irregular cornea (cornea tested positive for Keratoconus (KC) or Keratoconus suspect (KCS) diagnosed by the Corneal Navigator Neural Network, which uses Klyce & Maeda indices on the OPD-Scan® II (Nidek®, Japan)); (2) patient preference or the practice of activities which risk ocular trauma when both LASIK and PRK were proposed. All patients provided written informed consent.

The study and data acquisition were achieved with approval from the Rothschild Foundation Institutional Review Board. Informed consent was obtained from each patient after he/she voiced understanding about the purpose and the procedures in the study in accordance with the Declaration of Helsinki.

Instruments and Methods

Topography of each eye was performed using the OPD-Scan® II (Nidek®, Japan) Placido-based topograph (Figure 52). The specular corneal topography apparatus uses 19 vertical and 23 horizontal illuminated Placido disc segments in which anterior reflection covers a 0.5 mm to 11 mm area. This system captures the image of the reflected rings from the corneal surface to compute its axial and tangential curves using a proprietary algorithm.

Ten minutes before the activation of the PRK and the administration of topical anesthetic, the preoperative topography scan was performed using an OPD-Scan® II (Nidek®, Japan) located in the same room as the excimer laser unit on each eye. The patient was asked to blink several times before image acquisition. He was then instructed to focus on the centre disc of the Placido rings. To limit the influence of overnight corneal swelling, the PRK was performed at least 4 hours after the patient's awakening (Feng, Varikooty, & Simpson, Diurnal variation of corneal and corneal

epithelial thickness measured using optical coherence tomography., 2001).

A

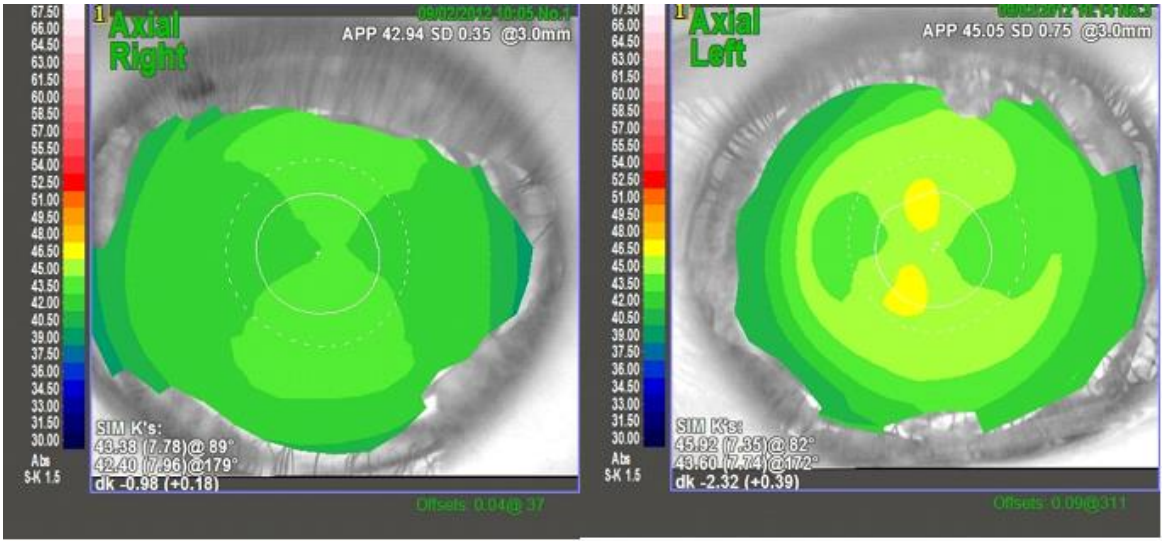

B

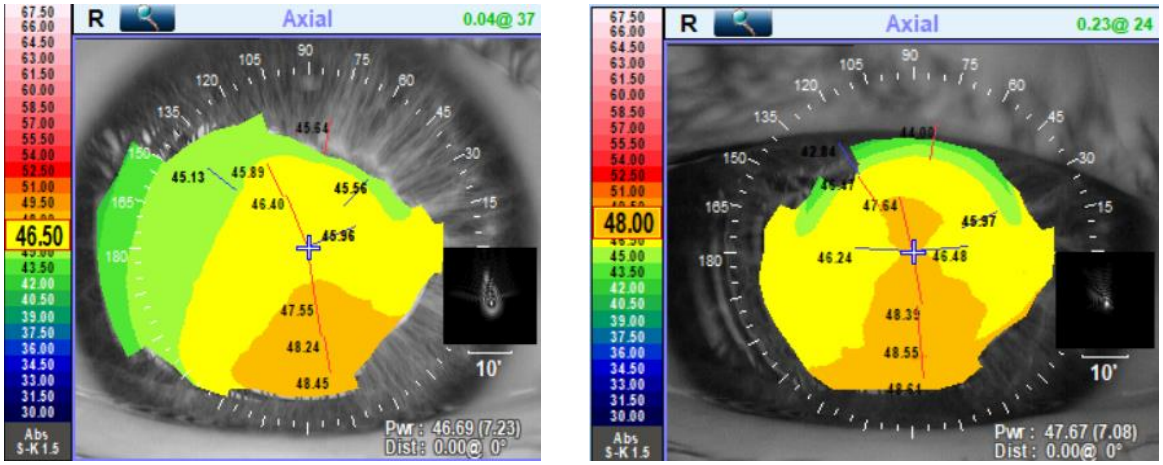

Figure 52 Refractive map before (left) and after (right) the normal (A) and keratoconic eye (B) epithelium removal

Next, 2 drops of lidocaine were administrated at 5 minutes intervals. A lid- speculum was applied on the left eye of the patient. The epithelium was carefully peeled off with blunt forceps after the application of a 20% alcohol solution over 20 seconds on the 8 mm central corneal zone. The corneal surface was then rinsed with a balanced salt solution and inspected through the excimer laser microscope to ensure that all epithelial debris were removed. The speculum was then removed, and the patient was asked to sit at the topography instrument. Three consecutive postoperative topographies were performed, during which the patient was asked to blink several

times. The examiner checked each image and its quality before recording it. The patient returned to the surgical bed and the excimer laser procedure was resumed and completed with the EX500 excimer laser. A bandage contact lens was placed over the eye after completion of the surgical procedure. The procedure was repeated for the other eye (Gatinel, Racine, & Hoang-Xuan, Contribution of the corneal epithelium to anterior corneal topography in patients having myopic photorefractive keratectomy, 2007).

All surgical procedures were performed by the same surgeon (DG).

All the topographic measurements were taken when the patient's eye fixated on the target (bright central spot located 75 mm from the subject's eye). Three consecutive acquisitions were performed for each eye and averaged for data analysis. The following data from each of the obtained topographies were recorded:

- Arithmetic mean between the steep and flat keratometry values (steep and flat simulated K-values) on the first, third, and fifth central millimeter rings.
- The amount and the axis of the surface toricity (keratometric astigmatism) on the first, third, and fifth central millimeter rings (difference between the respective steep and the flat K-values).
- Corneal Asphericity (mean Q value, mean Q steep value, and mean Q flat value) measured over the central 6.0 mm zone of the cornea.

Other than that, corneal aberrations measurements have been assessed. Indeed, the OPD-Scan® II (Nidek®, Japan) aberrometer is a combined automated retinoscopy and Placido disk videokeratoscope . (Muftuoglu & Erdem, 2008) - (Buscemi, 2002) - (MacRae & Fujieda, Slit skiascopic-guided ablation using the Nidek laser, 2000).

Corneal wavefront aberrations were reconstructed using a sixth order Zernike polynomial decomposition for a 5 mm pupil, centered on the vertex normal. The root mean squares (RMS in microns) for astigmatism, coma, trefoil and spherical aberration were analyzed.

Astigmatism Evaluation

We compared the amount of the corneal surface astigmatism with and without epithelium using a power vector method analysis. Power vectors are a geometrical representation of sphero-cylindrical refractive errors in 3 fundamental dioptric components (Thibos & Horner, Power vector analysis of the optical outcome of refractive surgery, 2001) - (Thibos, Wheeler, & Horner, Power vectors: an application

of fourier analysis to the description and statistical analysis of refractive error, 1997).
The first component is a spherical lens with power M equal to the spherical equivalent of a given refractive error M = S+ C/2.
The two other components are the two Jackson crossed cylinder lenses, one with power J_0 = (-C/2) cos (2 α) at axis α= 0°= 180° and the other one with power J_{45} = (-C/2) sin (2 α) at axis α= 45°.
This analytical method allows to express a sphero-cylindrical refractive error by showing these three dioptric powers quantities (M, J_0, J_{45}). Harris (Harris, Dioptric strength: a scalar representation of dioptric power, 1994) and Raasch (Raasch, 1995) showed that these 3 numbers can be represented geometrically as the (x, y, z) coordinates of a point in a three-dimensional dioptric space. Accordingly, a power vector is the vector drawn from the coordinate origin of this space to the point (M, J_0, J_{45}) which length is a measure of the overall blur strength $\mathbf{B= \sqrt{(M^2 + J_0^2 + J_{45}^2)}}$ of a sphero-cylindrical refractive error or lens.
In our study, these quantities did not correspond to refractive error but sphero-cylindrical axial power of the analysed corneal surface. The benefit of such a method is that the three fundamental components of the power vectors are independent of the others. This simplifies a lot the combination, the comparison and the statistical analysis of sphero-cylindrical power variations.

Statistical analysis

Statistical analyses were performed with a commercial software (SPSS v. 13.0; SPSS Inc., Chicago, IL). We used ANOVA test to compare the differences in parameters between groups before and after removing the epithelium. Wilcoxon (for non-normal distribution groups) and Student t tests have been used to compare studied parameters before and after removing the epithelium. Also, we used Kruskal-Wallis and Mann-Whitney tests for multiple nonparametric comparisons. The Pearson correlation analyses were also used. A calculated p-value <0.05 was considered statistically significant. Data are presented as the mean +/- standard deviation. Unpaired student t tests were used to compare the data between the two groups.
Astigmatism plots were generated using the AstigPlot® software (Borasio E. Eye Pro 2013).
The average magnitude and axis of cylinders was computed using vector calculations. The astigmatism plots were represented with a positive cylinder magnitude

convention.

5.2.4 Results

Demographics

In some eyes, the preoperative maps were labelled normal despite a thin cornea or subtle irregularities. These eyes constituted the normal group (group 1). In some eyes, the Placido topographer raised the possibility of a KCS or early KC. These eyes constituted the "KC/KCS" group (Group 2).

After the epithelial peeling, we have noticed that in the first group (Group 1) some preoperative normal classified corneas diagnosed by the OPD-Scan® II (Nidek®, Japan) Corneal Navigator Neural Network, became Keratoconus (KC) or Keratoconus suspect (KCS) classified. Therefore, we have subdivided the normal corneas group into two distinct groups: one of normal classified corneas which stayed normal after epithelium removal (group 1), and one of preoperative normal classified corneas that became KC or KCS classified after epithelium removal (Group1b).

	Normal Classified Corneas Before and after epithelium removal Group 1	**Normal Classified Corneas Before Epithelium Removal Group 1b**	**KC and KCS Classified Corneas Group 2**
Number of eyes	51	26	20
Number of patients	33	19	15
Age (in years)			
Average ± Standard deviation	35,48 ± 7,71	34,24 ± 8,56	38,02 ± 12,20
Min / Max	21,71 / 50,51	19,74 / 50,51	21,71 / 58,99
Pachymetry (in µm)			
Average ± Standard deviation	543,5 ± 35,3	523,2 ± 23,7	538,1 ± 27,8
Min / Max	482,0 / 616,0	483,0 / 565,0	504,0 / 597,0
% male / % Female	*36% / 45%*	*12% / 42%*	*53% / 47%*
Sphere (in D)			
Average ± Standard deviation	-3,05 ± 0,30	-2,93 ± 1,61	-3,15 ± 0,48
Min / Max	-0,75 / -5,00	-1,00 / -6,75	-1,50 / -7,00
Cylinder (in D)			
Average ± Standard deviation	-0,63 ± 0,48	-0,69 ± 0,46	-1,11 ± 0,81
Min / Max	-0,25 / -2,00	-0,25 / -1,75	0,00 / -3,25
Spherical Equivalent (in D)			
Average ± Standard deviation	-3,26 ± 1,22	-3,16 ± 1,58	-3,65 ± 1,51
Min / Max	-0,88 / -5,75	-1,63 / -6,75	-1,63 / -7,25

Table 18 Demographic data

Table 18 presents the demographic data for each group. The mean age was not

significantly different between groups (p = 0.363). The mean cylinder was significantly higher in the KC/KCS Group (Group 2) compared with the normal groups (Group 1 and Group 1b) (p< 0.001). Corneal tomography mas measured with the Orbscan IIz® (Bausch & Lomb®, USA) preoperatively. The mean central corneal thicknesses of the included eyes were respectively of 543.5 µm ± 35.3 (SD), 523.2m ± 23.7 (SD), 538.1µm ± 27.8 (SD), in the group 1, group 1b and group 2.

Keratometry

In normal corneas (Group 1), the axial keratometric corneal power (sim-K average) was 43,69 ± 1,09 D, 43,75 ± 1,10 D and 43,51 ± 1,07 D in the first, third and fifth mm rings respectively. After the removal of the corneal epithelium, the axial corneal power measured on the Bowman layer was 44,17 ± 1,18 D, 44,25 ± 1,20 D and 44,03 ± 1,10 D in the first, third and fifth mm rings respectively.

In the Group 1b, the axial keratometric corneal power (sim-K average) was 44,75 ± 1,08 D, 44,83 ± 1,09 D and 44,58 ± 1,10 D in the first, third and fifth mm rings respectively. After the removal of the corneal epithelium, the axial corneal power measured on the Bowman layer was 45,45 ± 1,10 D, 45,52 ± 1,09 D and 45,23 ± 1,11 D in the first, third and fifth mm rings respectively.

In the KC/KCS corneas (Group 2), the axial keratometric corneal power (sim-K average) was 45,87 ± 1,60 D, 45,98 ± 1,57 D and 45,67 ± 1,66 D in the first, third and fifth mm rings respectively. After the removal of the corneal epithelium, the axial corneal power measured on the Bowman layer was 46,42 ± 1,69 D, 46,47 ± 1,72 D and 46,15 ± 1,71 D in the first, third and fifth mm rings respectively.

There was a significant difference between the average corneal power before and after the epithelium removal on the 3 analyzed zones in all groups (Group 1: paired t test, p<0.001, Group 1b and 2: Wilcoxon, p<0.001). Table 19 presents these results.

Normal Classified Corneas Before and after epithelium removal (Group 1)	Preoperative With Epithelium	Postoperative Without Epithelium	*p Value*	Postoperative - Preoperative
Keratometry (D) mean ± SD				
1 mm	43,69 ± 1,09 (Min 41,23 / 46,08)	44,17 ± 1,18 (Min 41,49 / 46,84)	*p < 0,001**	0,48 ± 0,20 (Min 0,11 / 0,92)
3 mm	43,75 ± 1,10 (Min 41,24 / 46,24)	44,25 ± 1,20 (Min 41,51 / 46,96)	*p < 0,001**	0,50 ± 0,24 (Min 0,00 / 0,94)
5 mm	43,51 ± 1,07 (Min 41,16 / 45,86)	44,03 ± 1,10 (Min 41,39 / 46,58)	*p < 0,001**	0,52 ± 0,20 (Min 0,09 / 0,89)
Asphericity (Q Factor) mean ± SD				
Mean Q	-0,21 ± 0,12 (Min -0,54 / 0,09)	-0,27 ± 0,19 (Min -0,87 / 0,02)	*p = 0,012*	-0,06 ± 0,17 (Min -0,45 / 0,29)
Steep Q	-0,22 ± 0,19 (Min -0,65 / 0,39)	-0,26 ± 0,25 (Min -0,93 / 0,29)	*p = 0,279*	-0,04 ± 0,25 (Min -0,65 / 0,47)
Flat Q	*-0,15 ± 0,15 (Min -0,37 / 0,36)*	*-0,18 ± 0,16 (Min -0,50 / 0,28)*	*p = 0,215*	*-0,03 ± 0,17 (Min -0,37 / 0,36)*

Normal Classified Corneas Before Epithelium Removal (Group 1b)	Preoperative With Epithelium	Postoperative Without Epithelium	*p Value*	Postoperative - Preoperative
Keratometry (D) mean ± SD				
1 mm	44,75 ± 1,08 (Min 42,63 / 46,68)	45,45 ± 1,10 (Min 43,63 / 47,50)	*p < 0,001**	0,70 ± 0,32 (Min 0,08 / 1,42)
3 mm	44,83 ± 1,09 (Min 42,74 / 46,84)	45,52 ± 1,09 (Min 43,57 / 47,61)	*p < 0,001**	0,69 ± 0,31 (Min -0,08 / 1,40)
5 mm	44,58 ± 1,10 (Min 42,57 / 46,53)	45,23 ± 1,11 (Min 43,39 / 47,23)	*p < 0,001**	0,65 ± 0,26 (Min 0,17 / 1,39)
Asphericity (Q Factor) mean ± SD				
Mean Q	-0,20 ± 0,13 (Min -0,60 / 0,05)	-0,25 ± 0,18 (Min -0,58 / 0,12)	*p = 0,109*	-0,05 ± 0,14 (Min -0,32 / 0,26)
Steep Q	-0,17 ± 0,24 (Min -0,73 / 0,36)	-0,26 ± 0,28 (Min -1,00 / 0,24)	*p = 0,109*	-0,09 ± 0,26 (Min -0,62 / 0,46)
Flat Q	*-0,17 ± 0,24 (Min -0,73 / 0,36)*	*-0,17 ± 0,27 (Min -0,67 / 0,42)*	*p = 0,990*	*0,03 ± 0,26 (Min -0,31 / 0,56)*

KC and KCS Classified Corneas (Group 2)	Preoperative With Epithelium	Postoperative Without Epithelium	*p Value*	Postoperative - Preoperative
Keratometry (D) mean ± SD				
1 mm	45,87 ± 1,60 (Min 42,43 / 47,89)	46,42 ± 1,69 (Min 43,01 / 48,57)	*p < 0,001**	0,54 ± 0,29 (Min 0,02 / 0,99)
3 mm	45,98 ± 1,57 (Min 42,74 / 47,88)	46,47 ± 1,72 (Min 42,97 / 48,73)	*p < 0,001**	0,49 ± 0,35 (Min -0,14 / 1,01)
5 mm	45,67 ± 1,66 (Min 42,45 / 47,88)	46,15 ± 1,71 (Min 42,93 / 48,72)	*p < 0,001**	0,48 ± 0,27 (Min -0,02 / 0,89)
Asphericity (Q Factor) mean ± SD				
Mean Q	-0,17 ± 0,19 (Min -0,65 / 0,20)	-0,22 ± 0,22 (Min -0,65 / 0,16)	*p = 0,239*	-0,05 ± 0,20 (Min -0,49 / 0,32)
Steep Q	0,01 ± 0,38 (Min -0,32 / 0,92)	-0,15 ± 0,31 (Min -0,63 / 0,50)	*p = 0,006**	-0,17 ± 0,22 (Min -0,58 / 0,34)
Flat Q	*-0,20 ± 0,26 (Min -0,79 / 0,31)*	*-0,16 ± 0,23 (Min -0,68 / 0,38)*	*p = 0,102*	*0,04 ± 0,28 (Min -0,99 / 0,41)*

Table 19 Difference in keratometries and asphericities before and after the epithelium removal

** significant*

There was no correlation between the average keratometric power and the patient's age, refractive spherical equivalent and the initial central mean pachymetry, before and after the epithelium removal over the three ring zones of measurement in the three groups except for the KC/KC eyes (Group 2), even slight and non-significant, there was a negative correlation between the keratometry and the initial pachymetry (example in the 3 central mm, r= -0.416, P=0.068). Table 20 summarize these outcomes.

Normal Classified Corneas Before and after epithelium removal (Group1)	Preoperative With Epithelium		Postoperative Without Epithelium	
	r value	p value	r value	p value
Between Age and				
1 mm Keratometry	-0,091	0,524	-0,086	0,549
3 mm Keratometry	-0,078	0,588	-0,084	0,559
5 mm Keratometry	-0,100	0,487	-0,067	0,642
Between Initial Pachymetry				
1 mm Keratometry	-0,038	0,792	-0,046	0,747
3 mm Keratometry	-0,069	0,633	-0,038	0,794
5 mm Keratometry	-0,057	0,692	-0,091	0,523
Between Initial Spherical Equivalent				
1 mm Keratometry	0,002	0,987	0,046	0,748
3 mm Keratometry	0,012	0,934	0,012	0,935
5 mm Keratometry	0,028	0,847	0,081	0,571

Normal Classified Corneas Before Epithelium Removal (Group 1b)	Preoperative With Epithelium		Postoperative Without Epithelium	
	r value	p value	r value	p value
Between Age and				
1 mm Keratometry	-0,018	0,931	-0,071	0,729
3 mm Keratometry	-0,019	0,925	-0,051	0,804
5 mm Keratometry	-0,025	0,905	-0,050	0,807
Between Initial Pachymetry				
1 mm Keratometry	0,120	0,559	0,167	0,414
3 mm Keratometry	0,112	0,587	0,150	0,464
5 mm Keratometry	0,144	0,482	0,155	0,451
Between Initial Spherical Equivalent				
1 mm Keratometry	0,344	0,085	0,277	0,171
3 mm Keratometry	0,339	0,091	0,264	0,193
5 mm Keratometry	0,315	0,117	0,269	0,184

KC and KCS Classified Corneas (Group 2)	Preoperative With Epithelium		Postoperative Without Epithelium	
	r value	p value	r value	p value
Between Age and				
1 mm Keratometry	0,085	0,722	0,078	0,745
3 mm Keratometry	0,089	0,710	0,089	0,709
5 mm Keratometry	0,087	0,717	0,043	0,858
Between Initial Pachymetry				
1 mm Keratometry	**-0,386**	0,092	-0,405	0,076
3 mm Keratometry	**-0,416**	0,068	-0,420	0,066
5 mm Keratometry	**-0,363**	0,116	-0,378	0,101
Between Initial Spherical Equivalent				
1 mm Keratometry	0,114	0,633	0,143	0,546
3 mm Keratometry	0,088	0,711	0,118	0,620
5 mm Keratometry	0,141	0,554	0,137	0,566

Table 20 Correlations between keratometry and age, initial spherical equivalent and initial pachymetry before and after the epithelium removal

** significant*

Magnitude of the epithelial induced astigmatism

Astigmatism is an optical aberration which is mainly caused by the toricity of a refractive surface. Although topography instruments measure toricity (not astigmatism) we will use the terms “astigmatism” and “toricity” interchangeably. The magnitude of the epithelial induced astigmatism (EIA) was calculated as follows.

In the considered ring zone, the difference in simulated keratometry (sim-K) of the steepest and the flattest hemi-meridians was calculated as the “sim-K difference” by the topography software. The magnitude of the EIA was computed as the variation

between the “sim-K difference” values obtained after and before epithelial removal.

In normal corneas (Group 1), Preoperatively, the average sim-K difference values were 0.50 D, 0.32 D and 0.38 D in the first, third and fifth mm central zones respectively. After epithelial removal, the values of the (sim-K difference) measured on the Bowman layer were 0.87 D, 0.40 D and 0.35 D in the first, third and fifth mm rings, respectively. Before and after removal, the astigmatism was predominantly oriented with the rule (WTR).

Figures 53, 54, 55 represent the magnitude and orientation of the anterior corneal astigmatism before and after the removal of the epithelium respectively for the Group 1, 1b, and 2 respectively.

In the normal classified corneas (Group 1), We found a difference of around 0.35 D in the 1 mm ring zone between the two analysed surfaces. It appears in Figure 53 that this difference tends to decrease toward the periphery. This value was of 0.55 D in the Group 1b and 0.52 D in Group 2. Figure 54 shows that the difference tends to decrease toward the periphery as well in the preoperative normal classified corneas that became KC or KCS classified after epithelium removal (Group 1b).

In the 5-centre mm ring zone, we expressed the difference between epi-on and epi-off anterior corneal astigmatism as a power vector. We calculated the mean and standard deviation of each vector component, and the length (“Blur Strength”) of the power vectors. Table 21 summarizes the results. In all groups, all the differences were significant except in J_{45}. There was a wider difference in J_0 than in J_{45} between the epi-on state and the epi-off one.

With Epithelium	Without Epithelium
1mm	**1mm**
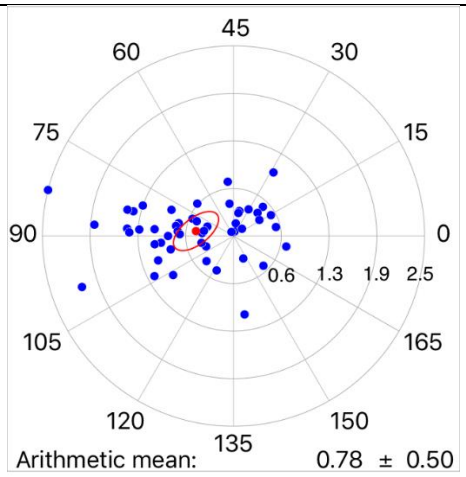 Mean: **0.50** (± 0.79) D @ **86** (± 13)°	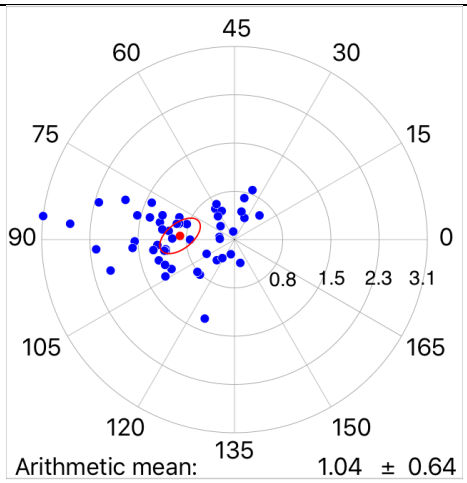 Mean: **0.87** (± 0.86) D @ **88** (± 14)°
3mm	**3mm**
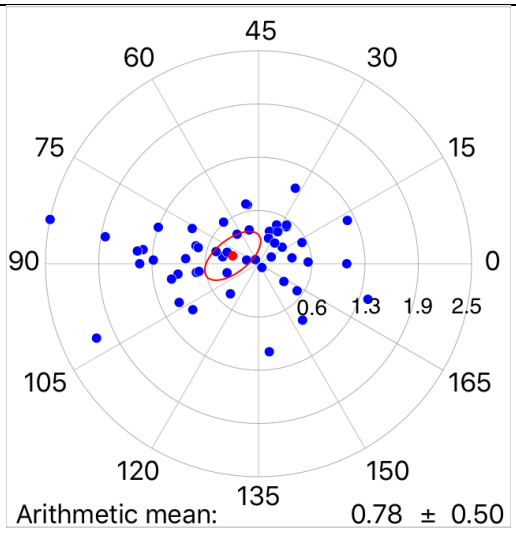 Mean: **0.32** (± 0.88) D @ **81** (± 13)°	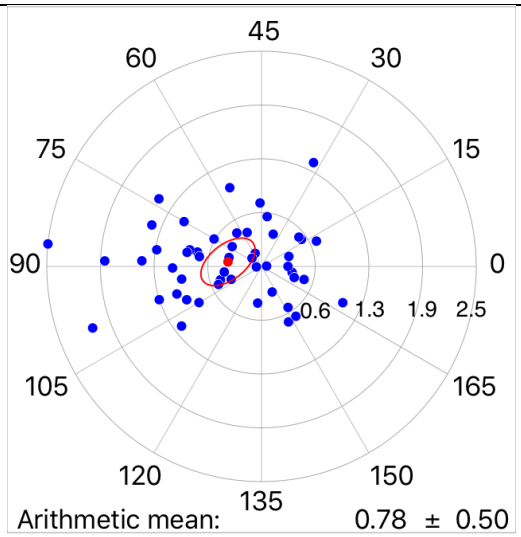 Mean: **0.40** (± 0.84) D @ **86** (± 15)°
5mm	**5mm**
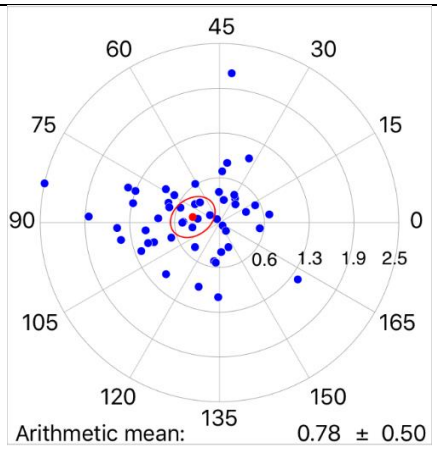 Mean: **0.38** (± 0.85) D @ **84** (± 19)°	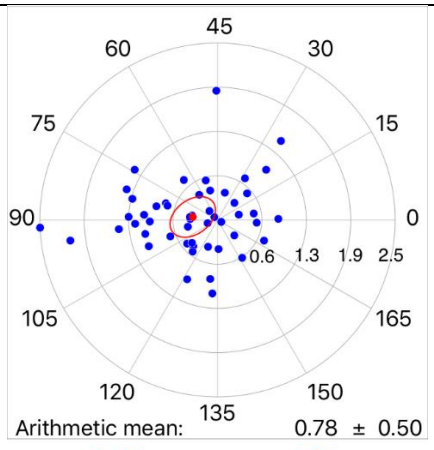 Mean: **0.35** (± 0.86) D @ **87** (± 17)°

Figure 53 Group 1 Corneal astigmatism with epithelium on (left) and off (right)

With Epithelium	Without Epithelium

1mm	1mm
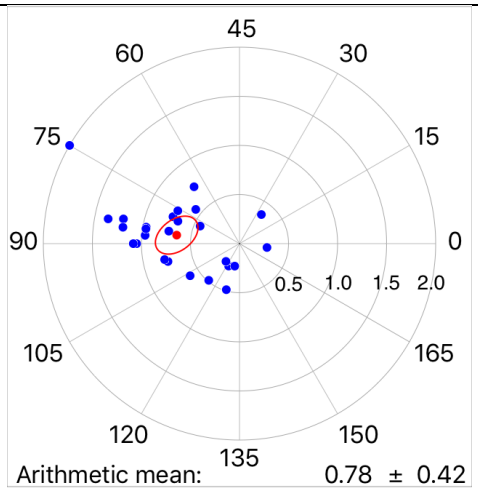 Mean: **0.66** (± 0.60) D @ **86** (± 17)°	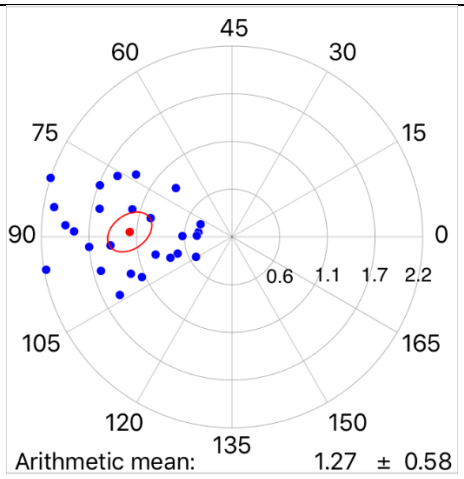 Mean: **1.21** (± 0.70) D @ **89** (± 17)°
3mm	**3mm**
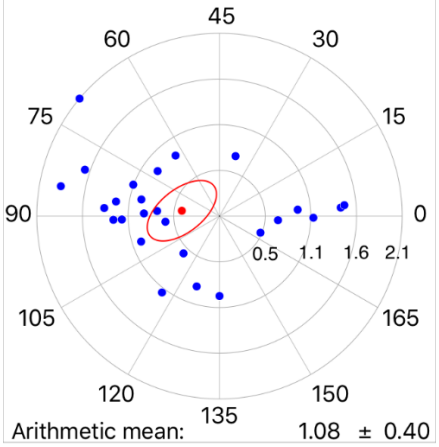 Mean: **0.45** (± 1.08) D @ **86** (± 14)°	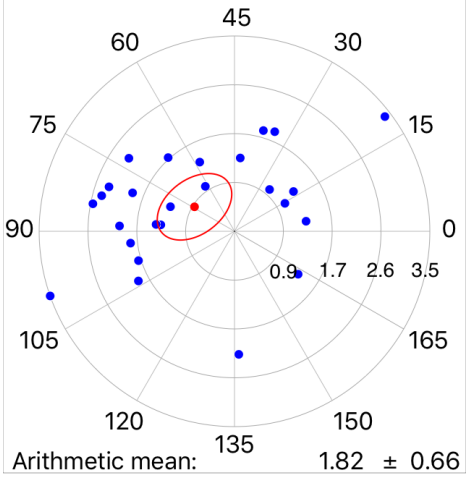 Mean: **0.83** (± 1.78) D @ **74** (± 17)°
5mm	**5mm**
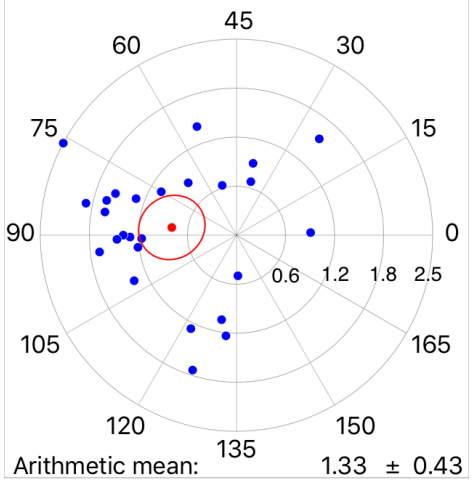 Mean: **0.82** (± 1.16) D @ **87** (± 21)°	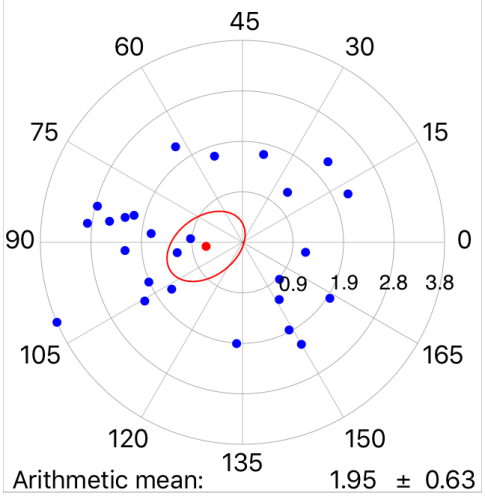 Mean: **0.69** (± 1.97) D @ **93** (± 17)°

Figure 54 Group 1b Corneal astigmatism with epithelium on (left) and off (right)

With Epithelium	Without Epithelium
1mm	**1mm**
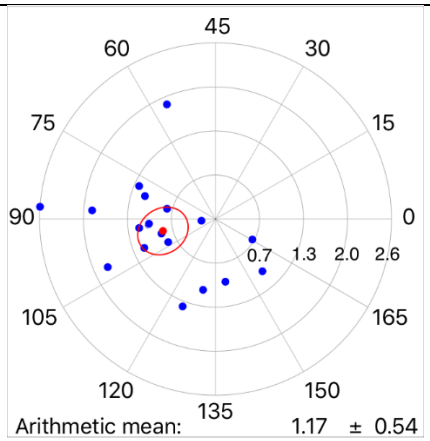 Mean: **0.80** (± 1.03) D @ **96** (± 20)°	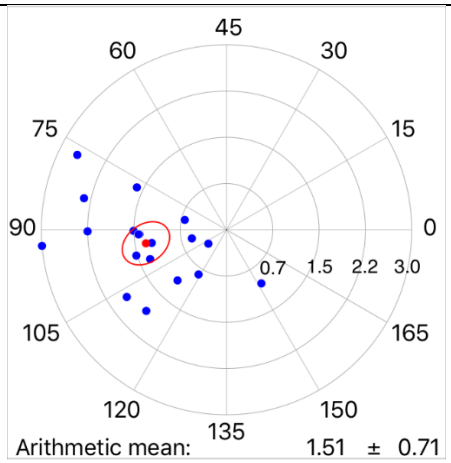 Mean: **1.32** (± 1.04) D @ **95** (± 18)°
3mm	**3mm**
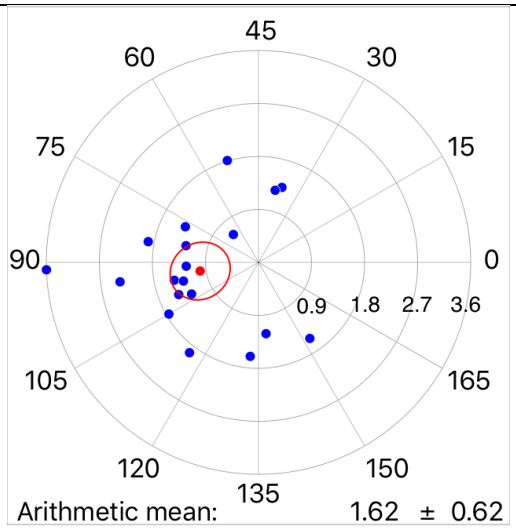 Mean: **1.01** (± 1.44) D @ **94** (± 21)°	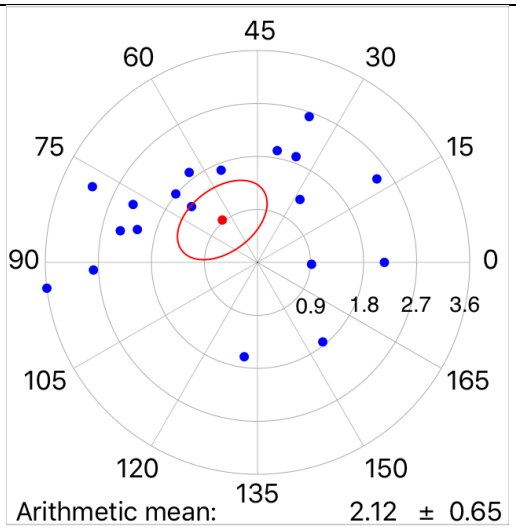 Mean: **0.95** (± 2.05) D @ **65** (± 16)°
5mm	**5mm**
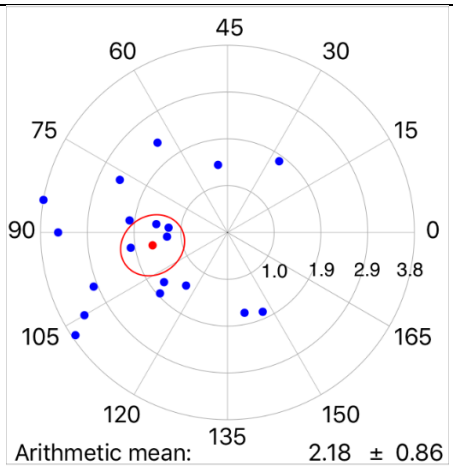 Mean: **1.55** (± 1.80) D @ **95** (± 21)°	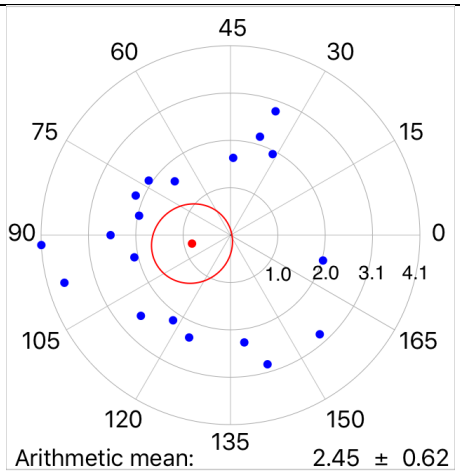 Mean: **0.85** (± 2.44) D @ **96** (± 22)°

Figure 55 Group 2 Corneal astigmatism with epithelium on (left) and off (right)

Normal Classified Corneas Before and after Epithelium Removal (Group1)	With Epithelium				Without Epithelium							
	M	J_0	J_{45}	B	M	*P Value*	J_0	*P* Value	J_{45}	*P Value*	B	*P Valu*
Mean	-2,978	0,113	0,026	2,996	-3,690	*p < 0,001**	0,299	p = 0,001*	0,027	*p = 0,688*	3,731	*p < 0,00*
Minimum	-5,500	-0,464	-0,312	0,884	-5,625		-0,766		-0,286		2,000	
Maximum	-0,875	0,940	0,464	5,523	-2,000		1,345		0,661		5,693	
Standard Deviation	1,124	0,302	0,154	1,132	1,138		0,455		0,240		1,158	

Normal Classified Corneas Before Epithelium Removal (Group 1b)	With Epithelium				Without Epithelium							
	M	J_0	J_{45}	B	M	*P Value*	J_0	*P* Value	J_{45}	*P Value*	B	*P Valu*
Mean	-3,159	0,122	-0,003	3,179	-4,072	*p < 0,001**	0,350	p < 0,001*	-0,056	*p = 0,191*	4,109	*p < 0,00*
Minimum	-6,75	-0,500	-0,383	1,630	-8,625		-0,364		-0,591		2,062	
Maximum	-1,625	0,862	0,375	6,750	-2,000		1,092		0,405		8,698	
Standard Deviation	1,581	0,285	0,285	1,574	1,793		0,359		0,199		1,789	

KC and KCS Classified Corneas (Group 2)	With Epithelium				Without Epithelium							
	M	J_0	J_{45}	B	M	*P Value*	J_0	*P* Value	J_{45}	*P Value*	B	*P Valu*
Mean	-3,650	0,226	0,041	4	-4,463	*p < 0,001**	0,470	p = 0,001*	0,078	*p = 0,433*	4,525	*p < 0,00*
Minimum	-7,25	-0,622	-1,125	1,630	-8,875		-0,449		-0,974		2,761	
Maximum	-1,625	1,600	0,739	7,254	-2,750		1,500		0,575		8,918	
Standard Deviation	1,512	0,480	0,392	1,511	1,626		0,484		0,334		1,623	

Table 21 Distribution of manifest refraction before and after removal of the corneal epithelium

* *significant*

Asphericity

In the normal corneas group (1), the average corneal asphericity expressed by the Q-value was -0.21 ± 0.12 (SD) (range +0.09 to -0.54). It was of -0.27 ± 0.19 (SD) (range +0.02 to -0.87) after the removal of the corneal epithelium. The difference between these values was not significant (p=0.012). These results were comparable in Group 1b and Group 2. In the KC/KCS group (Group 2), although the difference in Mean Q value was not significant between the epi-On and Epi-off measurements, it was significant along the Steep axis -0.17 ± 0.22 (SD) (range +0.34 to -0.58), P=0.006. Table 19 summarizes some of these results.

There was no correlation between the initial mean central pachymetry and the corneal asphericity measured over the epithelium and the Bowman layer (r = 0.168, p =0.1 and r = 0.041, p = 0.689, respectively).

Corneal Wavefront Data

The corneal wavefront data were analyzed on a 5 mm pupil diameter. In the normal corneas (Group 1) all studied aberrations were statistically different (p< 0.001) before and after the epithelium removal except spherical aberration that wasn't different after the epithelium removal (p=0.647). In preoperative normal classified corneas that became KC or KCS classified after epithelium removal (Group 1b), all studied aberrations were statistically different (p< 0.001) before and after the epithelium

removal except spherical aberration and Trefoil that weren't different after the epithelium removal (p=0.191, p=0.339 respectively). In the KC/KCS group (2), only the total corneal Aberration and the astigmatism were statistically different before and after the epithelium removal. Table 22 presents the different parameters in all groups.

	Normal Classified Corneas Before and after epithelium removal Group 1		Normal Classified Corneas Before Epithelium Removal Group 1b		KC and KCS Classified Corneas Group 2	
Aberrations difference (RMS in µm)	***Mean ± SD***	***p***	***Mean ± SD***	***p***	***Mean ± SD***	***p***
Total Corneal	0,21 ± 0,40	*p < 0,001**	0,42 ± 0,33	*p < 0,001**	0,32 ± 0,53	*p = 0,010**
Astigmatism	0,17 ± 0,24	*p < 0,001**	0,26 ± 0,21	*p < 0,001**	0,29 ± 0,28	*p = 0,001**
High Order Aberrations	0,11 ± 0,18	*p < 0,001**	0,12 ± 0,24	*p < 0,001**	0,00 ± 0,19	*p = 0,643*
Coma	0,06 ± 0,10	*p < 0,001**	0,07 ± 0,12	*p = 0,007**	-0,04 ± 0,18	*p = 0,469*
Trefoil	0,05 ± 0,11	*p < 0,001**	0,04 ± 0,14	*p = 0,339*	0,00 ± 0,15	*p = 0,778*
Spherical Aberrations (SA4)	0,00 ± 0,06	*p = 0,647*	0,01 ± 0,04	*p = 0,191*	0,01 ± 0,07	*p = 0,601*

Table 22 Corneal Aberrations differences before and after removal of the corneal epithelium

** significant*

OPD-Scan® II (Nidek®, Japan) irregularity indices

Some OPD-Scan® II (Nidek®, Japan) irregularity indices increased in all groups after the epithelium removal. Also, we noticed a more important increase of irregularities in the Group 1 and Group 1b than in the Group 2's corneas. (p<0.001).

Predictive factors differentiating Group 1 from Group 1b

Preoperative keratometry in the first, third and fifth mm rings is the only predictive factor differentiating Group 1 from Group 1b that we found (p<0.001). The mean preoperative keratometries in group 1 were of 43,69 ± 1,09 D, 43,75 ± 1,10 D and 43,51 ± 1,07 D in the first, third and fifth mm rings respectively. In the Group 1b, the axial keratometric corneal power (sim-K average) was 44,75 ± 1,08 D, 44,83 ± 1,09 D and 44,58 ± 1,10 D in the first, third and fifth mm rings respectively (Table 19).

5.2.5 Discussion

This study aims to extend the results of a previous study by Salah-Mabed et al. (Salah-Mabed, Saad, & Gatinel, Topography of the corneal epithelium and Bowman layer in low to moderately myopic eyes, 2016), who analyzed the topography of the Bowman layer by performing combined aberrometry and Placido topography after removal of the corneal epithelium in in-vivo normal myopic eyes.

We found that the epithelialized cornea had an average keratometric axial power slightly inferior to that of the Bowman layer in the first, third and fifth mm diameter ring zones in normal and KC/KCS classified groups. In the normal corneas Groups, the

corneal power measured when the epithelial layer was removed on the Bowman's membrane on the same zones was 44,17 ± 1,18 D, 44,25 ± 1,20 D and 44,03 ± 1,10 D respectively. These values weren't correlated with the age, the pachymetry and the refractive initial spherical equivalent. The topography of the Bowman membrane was on average significantly 0.48 D steeper in the central 1mm zone than the epithelial surface. This confirms that the epithelium acts like a convex/concave meniscus which reduces the paraxial keratometric corneal power by 0.48 D. This result confirms the one we found in our previous survey where it was of 0.56 D in the same zone.

In the Keratoconus/ Keratoconus suspected corneas, we found very close results of epithelial steepening. These results are completely different to those reported by Touboul.et al (Touboul, et al., 2012). Indeed, where we found a 0.48 D steepening of the cornea after epithelial removal, they reported a steepening of 2.04 D ± 0.95 in the central 1 mm. This enormous difference may be explained by the fact that they had included corneas with much higher stage of keratoconus than we did. Also, in our study, we confounded in the same group, the KC and KCS corneas; which can induce a difference as well. Our results showing that in the central keratoconus corneas, the epithelium hasn't the ability to flatten the Bowman layer more than in normal corneas, are consistent with the theory of the "epithelial doughnut pattern". Indeed, in eyes with keratoconus , Reinstein et al. (Reinstein, Archer, Gobbe, Silverman, & Coleman, Epithelial thickness in the normal cornea: three-dimensional display with Artemis very high-frequency digital ultrasound, 2008) - (Reinstein DZ & Gobbe, 2009) - (Reinstein, Gobbe, Archer, Silverman, & Coleman, Epithelial, stromal, and total corneal thickness in keratoconus: three-dimensional display with artemis very-high frequency digital ultrasound, 2010) found that the mean corneal vertex epithelial thickness was 45.7 ± 5.39 µm, with an "epithelial doughnut pattern" of epithelial thinning over the cone surrounded by an annulus of epithelial thickening, except in normal eyes, in which the mean corneal vertex epithelial thickness was 53.1 ± 4.5 µm and the epithelial pattern was slightly thinner superiorly. Similarly, Haque et al. (Haque, Simpson, & Jones, 2006) found with optical coherence tomography measurements that the central keratoconic epithelium was 4.7 µm thinner than in the normal cornea. Interestingly, this was along the lines of the changes occurred after hyperopic LASIK procedures, in which controlled central steepening occurs.

Reinstein et al. (Reinstein, Archer, Gobbe, Silvermann, & Coleman, Epithelial thickness after hyperopic LASIK: three-dimensional display with Artemis very high-

frequency digital ultrasound, 2010) conclude that the paracentral epithelial thickening compensated in part for the stromal tissue ablated by the hyperopic procedure, whereas the central epithelial thinning compensated for the localized increase in corneal curvature in keratoconic corneas.

Patel et al. (Patel, Reinstein, Silverman, & Coleman, 1998) studied the central epithelial thickness distribution in 14 normal human corneas with in vivo measurements taken from high-frequency ultrasound digital signal processing with a measurement precision of 2 µm. They found that on average, the Bowman's layer had a higher keratometric power. They found a mean radius of Bowman's layer of 7.34 mm ± 0.17 (SE) which corresponded to a power of 45.37 D.

Our results are consistent with those reported by Zipper et al. (Zipper, Manns, & Fernandez, 2001) on normal corneas. These authors studied topographic data from 16 fresh human cadaver eyes using a PAR corneal topography system (PAR Vision Systems Corp.) before and after removal of the epithelium with a blunt knife. They found that the difference in the apical radius of curvature between the two states corresponded to a power of approximately 0.5 D within the central 7.0 mm zone.

Simon et al. (Simon, Ren, Kervick, & Parel, 1993) reported slightly higher keratometric values for Bowman's layer. Using an automated keratometer in 10 fresh human eye-bank eyes with and without the epithelium, they found that the corneal epithelium accounts for an average of -1.03 D of the power of the eye at a central 2.0 mm zone. This power was -0.85 D at the 3.6 mm zone.

These differences, although minimal, might be explained by the different measurement methods used, the different corneal diameters studied, and finally, by the fact that the corneas were analysed ex-vivo in several surveys.

Curiously, our results contrast to those reported by Gatinel et al. (Gatinel, Racine, & Hoang-Xuan, Contribution of the corneal epithelium to anterior corneal topography in patients having myopic photorefractive keratectomy, 2007).

This previous study concluded that the central cornea curvature was flatter after epithelial removal, as indicated by the change in the mean power of the cornea at 3.0 mm (44.42 ± 1.59 D in preoperative measurement and 43.46 ± 1.37 D without the epithelium). We found a difference of 0.56 D whereas they found a difference of 1 D in the opposite direction. A difference in measurement protocols may explain the contradiction between our results and those of our previous work (Gatinel, Racine, & Hoang-Xuan, Contribution of the corneal epithelium to anterior corneal topography

in patients having myopic photorefractive keratectomy, 2007).

The eyes included in the present study belonged to a population older than those in the previous study (Gatinel, Racine, & Hoang-Xuan, Contribution of the corneal epithelium to anterior corneal topography in patients having myopic photorefractive keratectomy, 2007).

Although we found that there was no correlation between the keratometry and the age before and after the epithelium removal, other surveys such as Hayashi et al. (Hayashi, Hayashi, & Hayashi, Topographic analysis of the changes in corneal shape due to aging, 1995) concluded that the mean refractive power of the cornea increases with age because the normal cornea becomes steeper and shifts from with-the-rule to against-the-rule astigmatism over time. The discrepancy between our two studies could be explained by the difference in our sample's mean age.

The corneal surfaces had an increased gradient of flattening toward the periphery, as a more prolate shape was measured after the epithelium removal at the Bowman layer level. In this study, the average corneal asphericity expressed by the Q factor in the normal corneas (Group 1) was -0.21 ± 0.12 (SD) (range +0.09 to -0.54) before and -0.27 ± 0.19 (SD) (range +0.02 to -0.87) after the removal of the corneal epithelium. Even not statistically significant (p=0.012) the difference does exist and is very coherent to the one we found in our previous study (Salah-Mabed, Saad, & Gatinel, Topography of the corneal epithelium and Bowman layer in low to moderately myopic eyes, 2016). In our other previous study (Gatinel, Racine, & Hoang-Xuan, Contribution of the corneal epithelium to anterior corneal topography in patients having myopic photorefractive keratectomy, 2007), the mean Q values measured by Orbscan II were -0.44 ± 0.14 before and -0.65 ± 0.46 after epithelial removal.

These differences may be explained by the fact that we measured the Q factor on the 7mm zone of the cornea, whereas our present results were obtained on a 5 mm zone. The use of different algorithms and instruments to measure the asphericity could also account for these differences. A trend toward more negative corneal asphericity on the Bowman's layer was found in both studies and was also similar to what has been reported by Patel et al. (Patel, Reinstein, Silverman, & Coleman, 1998) and Zipper et al. (Zipper, Manns, & Fernandez, 2001). Our results are comparable to those of Read et al. (Read, Collins, Carney, & Franklin, 2006). Indeed, these authors found a Q-value of -0.19 on the epithelial corneal surface measured within the 6mm diameter zone (we found -0.20 on the 5 mm diameter zone).

Nevertheless, it could be interesting to note that during the interval of time between epithelium removal and OPD-Scan® II (Nidek®, Japan) measurements of Bowman surface, the anterior part of the stroma could swell in a certain amount. The contact between the bowman layer and the tear film could lead to a certain degree of prolateness and steepening. Which would mean that the keratometry and/or the prolateness were overestimated in the studies. The measurement of corneal thickness with the laser excimer platform or manually should have been contributive for that issue. It should be interesting to evaluate again those patients and, in case of retreatment, to see if under or over correction is due to epithelium rather than photoablation.

These results are the same in all three groups, except along the steep axis, where the difference in Q value was significant and approximately of -0.17 ± 0.22. (Table 19). This suggest that the epithelium compensated for the localized increase in corneal curvature changing. This is again consistent with the Reinstein doughnut theory (Reinstein, Archer, Gobbe, Silverman, & Coleman, Epithelial thickness in the normal cornea: three-dimensional display with Artemis very high-frequency digital ultrasound, 2008) - (Reinstein DZ & Gobbe, 2009) - (Reinstein, Gobbe, Archer, Silverman, & Coleman, Epithelial, stromal, and total corneal thickness in keratoconus: three-dimensional display with artemis very-high frequency digital ultrasound, 2010).

However, these values were different from those found by Touboul et al. (Touboul, et al., 2012), who reported an increase in prolateness of -0.76 ± 0.78. We notice in Touboul's sample that the standard deviation is that important that we cannot really conclude of the repeatability of the results.

Besides, on average, in accordance to Simon et al. (Simon, Ren, Kervick, & Parel, 1993) we showed that the corneal toricity tends to increase after epithelial removal. In normal corneas, the mean magnitude of epithelium induced astigmatism (EIA) was approximately of 0.35 D in the first central millimeter ring. This value reached approximately 0.55 D in group 1b and in early Keratoconus group (2). However, Touboul et al. found an EIA of approximately of 2.17 ± 1.90 D. These differences may be due to the fact that they might include in their survey higher stages decentered keratoconus. Besides, exactly like Simon et al. (Simon, Ren, Kervick, & Parel, 1993) report in normal corneas, we observed a change in the astigmatism axis between the epithelium and Bowman's layer surfaces, the magnitude of the EIA seems to decrease as the distance to the corneal vertex increases and becomes non-significant at the

fifth millimetre ring zone.

Otherwise, we studied the change in corneal aberrations pattern after the epithelial removal. In the normal corneas (Group 1) all studied aberrations were statistically increased ($p< 0.001$) before and after the epithelium removal except spherical aberration that wasn't different after the epithelium removal ($p=0.647$). In preoperative normal classified corneas that became KC or KCS classified after epithelium removal (Group 1b), all studied aberrations were statistically increased ($p< 0.001$) before and after the epithelium removal except spherical aberration and Trefoil that weren't different after the epithelium removal ($p=0.191$, $p=0.339$ respectively). In the KC/KCS group, only the total corneal Aberration and the astigmatism were statistically increased before and after the epithelium removal. This can suggest that in early keratoconic eyes, the most key role of the epithelium is to mask the EIA, and according to the "epithelial doughnut pattern" theory, the keratoconic epithelium might be too thin to mask the irregularities, even when the initial corneal aberrations level was high.

Also, according to OPD-Scan® II (Nidek®, Japan) irregularity indices, we noticed a more important increase in the group 1 and group 1b than in the Group 2. Finally, what preoperatively differentiated group1 corneas from group 1b corneas was only the preoperative keratometry. Indeed, in the group 1, the initial mean keratometry was approximately 43.5 D, where it was 44.5 D in group 1b. In other terms, starting from approximately 44.5 D, a cornea might be suspected of subclinical keratoconus. According to these findings, we can conclude that the remodeling of the epithelial layer may cause the masking of some early corneal anomalies that might arise at the stromal level in early subclinical keratoconus (Salah-Mabed, Saad, & Gatinel, Topography of the corneal epithelium and Bowman layer in low to moderately myopic eyes, 2016) (keratometries of approximately 44.5/45 D). We can suppose then, that the epithelium is able to mask Bowman's membrane irregularities until a certain degree of keratometry. When the keratometry is enhanced in the case of keratoconus, the epithelium become unable to mask enough the abnormalities.

Using very high-frequency digital ultrasound, Reinstein et al. (Reinstein, et al., Epithelial thickness profile changes induced by myopic LASIK as measured by Artemis very high-frequency digital ultrasound, 2009) - (Reinstein, Archer, Gobbe, Silvermann, & Coleman, Epithelial thickness after hyperopic LASIK: three-dimensional display with Artemis very high-frequency digital ultrasound, 2010) established the ability of the epithelium to reshape the anterior corneal surface, suggesting that the epithelium

can remodel itself to compensate for stromal surface abnormalities created by flap irregularities or irregular stromal ablation after lamellar refractive surgery. The wound-healing process in PRK and rearrangement of the flap in LASIK may result in partial compensation of the sculpted pattern onto the corneal surface after laser ablation (Dausch, Klein, & Schröder, 1993) - (Pietilä, Mäkinen, Pajari, & Uusitalo, 1997) - (Chen, Izadshenas, Rana, & Azar, 2002) - (Huang, Tang, & Shekhar, 2003) - (Flanagan & Binder, 2005).

We confirmed in this study that the epithelium contributes to remodeling the corneal surface when limited to the Bowman layer.

Touboul et al. (Touboul, et al., 2012) suggested that the role of the epithelium and its contribution to corneal refractive power should be more important in keratoconus than in normal eyes. All our results tend to conclude to a contrary theory that the epithelium in keratoconic corneas is unable to mask the irregularities. The corneas are too deformed and the epithelium, according to Reinstein is too thin to mask the important irregularities (Reinstein, Gobbe, Archer, Silverman, & Coleman, Epithelial, stromal, and total corneal thickness in keratoconus: three-dimensional display with artemis very-high frequency digital ultrasound, 2010).

In eyes scheduled for PRK, changes in keratometry, asphericity and toricity after the epithelium removal could negate the accuracy of the Placido-based custom ablation software. However, it seems reasonable to postulate that epithelial regrowth after surgery may also modify the geometry of the laser remodeled stromal surface. Although the epithelial and Bowman layer have slightly different topographic characteristics, the delivery of topography-guided custom ablation based on epi-on data may reduce the epi-off irregularity.

Our study allowed us to describe the shape of the epithelial and the Bowman layer surfaces in normal and keratoconic myopic eyes. Our findings suggest that in refractive procedures such as myopic photorefractive keratectomy, the refractive contribution of the epithelium could be taken into account to improve predictability. This approach may be particularly relevant for transepithelial PRK (Fadlallah, et al., 2011), where the mapping of the epithelial layer may improve the precision of the procedure. Prediction of epithelial healing processes could be important to evaluate as well.

Our data was limited to the analysis of mean axial keratometry, toricity and asphericity of the Bowman layer. We also studied the effect of the corneal epithelium on high

order aberrations of the eye. Further studies are necessary to confirm our results and to investigate the role of the corneal epithelium in the quality of the retinal image of the keratoconic eyes.

Chapter 6: Anatomical and visual outcomes after a LASIK performed in moderately to high myopic eyes with the WaveLight® Refractive Suite (Alcon® Laboratories Inc., USA)

Authors: Imene Salah Mabed, MSc (1,2), Guillaume Debellemanière, MD (2), Emmanuelle Perez, OD (2), Helene Rouger, OD (2), Karsten Plamann, PhD (1), Damien Gatinel, MD, PhD (2)

1. Laboratoire d'Optique Appliquée, CNRS, Université Paris-Saclay, ENSTA, Ecole Polytechnique, Orsay, France.
2. Department of Anterior Segment and Refractive Surgery, Rothschild Foundation, Paris, France.

None of the authors has any financial or proprietary interests in any product, method or material presented in this paper.

Published: None.

6.1 Abstract

Purpose: To evaluate changes in anatomical parameters of the eye, visual performances and quality of vision after a LASIK refractive surgery performed with the WaveLight® Refractive Suite (Alcon® Laboratories Inc., USA).

Setting: Rothschild Foundation, Paris, France.

Design: Prospective interventional case series.

Methods: We examined 60 myopic eyes (average Spherical Equivalent of -4.5D ranging from -9.3 to -0.75D) of 30 patients aged from 21.3 to 38.7 years. Anatomical parameters (pachymetry, corneal hysteresis (CH), resistance factor (CRF), Intra-Ocular Pressure (IOP), central keratometry, Q-factor, corneal and total aberrations on a 5.5 mm pupil), visual performances (high and low contrast visual acuity (VA), contrast sensitivity at 12 cycles per degree and tolerance/sensitivity to blur defined as the range of defocus for which high contrast letters of 20/50 was still perceived

acceptable), dry eye assessment (Break Up Time (BUT), OSDI questionnaire) and quality of vision (QoV) were measured prior to the surgery and 1 day (D1), 1 month (M1), 3 months (M3) and 6 months after.

Results: 6 months after surgery, keratometry became flatter and the Q-factor more oblate (from -0.18 ± 0.08 to +0.19 ± 0.06). CH and CRF significantly decreased respectively from 11.25 ± 1.4 mmHg to 9.24 ± 1.1mmHg and from 11.18 ± 1.4 mmHg to 7.66 ± 1.1 at M6. Pachymetry decreased by 117.9 ± 62.2µm at D1 and increased by 37.87 ± 32.6 µm between D1 and M6 probably due to epithelial remodeling, to posterior corneal surface reaction and/or to the low tomography detection at D1. Refraction became emmetropic at D1 and stayed stable. The most significant high-order aberration change postoperatively was an increase in 3rd order coma. 6 months after surgery, high and low contrast VA were slightly but non-significantly improved (<0.05 log MAR), whereas contrast sensitivity and tolerance/ sensitivity to blur remained unchanged. Quality of vision was not affected by surgery.

Conclusions: Some corneal and/or internal changes arising between D1 and M6 may limit the amount of residual refractive error to finally provide some good quality of vision 6 months after LASIK refractive surgery.

6.2 Introduction

LASIK (Pallikaris, Papatzanaki, Stathi, Frenschock, & Georgiadis, 1990) - (Farah, Azar, Gurdal, & Wong, 1998) became a very popular surgical option for the correction of myopia which is demonstrated by an increasing number of procedures. In this technique, a hinge flap is often created using a femtosecond laser and the folded back, the exposed stroma is photoablated using an excimer laser. In myopic LASIK, the stromal tissue is removed to flatten the curvature of the centre of the cornea which decreases the excessive refractive power or longer axial length of the eye.

In the past recent years, an increasing number of research focused on the assessment of quality of vision after LASIK refractive surgery (Bühren, et al., 2009) - (Kohnen, 2001) - (Mamalis, 2004) - (Pepose & Applegate, 2005) - (Piermarocchi, et al., Quality of vision: a consensus building initiative for a new ophthalmologic concept, 2006).

The aim of refractive surgery techniques is to improve visual outcomes. In the 1990s many studies were published on the correction of myopia with LASIK (Tsai, 1997) - (Knorz, Wiesinger, Liermann, Seiberth, & Liesenhoff, 1998) reporting low

predictability, significant regression and induced night vision disturbances (Corbett, et al., 1996) - (Chayet, et al., 1998). These issues were in large part due to the use of small optical zones (O'Brart, Corbett, Lohmann, Kerr Muir, & Marshall, 1995) - (O'Brart, et al., 1996), and the non-aspheric Munnerlyn ablation profiles leading to significantly inducing spherical aberrations (Seiler, Genth, Holschbach, & Derse, 1993). In the 2000s, other studies reported that LASIK was a safe and predictable method to correct moderate to high myopia (Kuang-mon & Liang, 2006) - (Reinstein, et al., 2016). Indeed, these studies show a high success rate, reflected by favourable functional outcomes (Kohnen, Bühren, Kühne, & Mirshahi, 2004) - (Twa, Lembach, Bullimore, & Roberts, 2005) - (Netto, Dupps, & Wilson, 2006) - (Kohnen, Kuhne, & Buhren,, The future role of wavefront-guided excimer ablation, 2007), and high physician and patient satisfaction (Solomon, et al., 2009).

Several studies report satisfaction rates of c. 90% after LASIK (Bailey, Mitchell, Dhaliwal, Boxer Wachler, & Zadnik, 2003) - (Tahzib, Bootsma, Eggink, Nabar, & Nuijts, 2005) - (Tuan, 2006), however other report dissatisfactions and point to possible improvements (McCormick, Porter, Cox, & MacRae, 2005).

Most of the published studies evaluated the visual clinical outcomes of LASIK in terms of visual performances (visual acuity, contrast sensitivity, depth of focus) (Nakamura, Bissen-Miyajima, & Toda,, 2001) - (Kuang-mon & Liang, 2006). Other studies described the microstructural changes induced in the stroma and Bowman’s layer in vivo using confocal microscopy (Vesaluoma, et al., 2000). However, many questions are still pending with regards to the biological response of the cornea to the ablation process (Roberts, 2000). These microstructural disturbances of the corneal stroma can be the cause wavefront aberrations (Marcos, Barbero, Llorente, & Merayo-Lloves, 2001). Recently, with the implementation of the techniques, we can measure the optical wavefront after refractive surgery. Studies have revealed that although conventional refractive errors (defocus and astigmatism) are reduced or cancelled, higher order aberrations are generally induced (Seiler, Kaemmerer, Mierdel, & Krinke, 2000) - (Thibos & Hong, Clinical applications of the Shack-Hartmann aberrometer, 1999). Along with other technical developments (eye trackers, small-spot lasers, …) the accurate measurement of ocular wave aberrations has opened doors for potential improvements of LASIK in particular through customized treatments for each patient cancelling low and high-order aberrations in the eye (MacRae, Schwiegerling, & Snyder, 1999) - (Schwiegerling & Snyder, 1998).

It was shown that the analysis of the total wavefront errors of the eye reflects the most complete measurement of retinal image quality, and then can be directly related to visual performances (Applegate, et al., 2000) - (Marcos, Aberrations and visual performance following standard laser vision correction, 2001). Although their impact on visual performance is not fully understood, wavefront-error data have been extensively used as objective parameters for quality of vision in theoretical models and in clinical trials (Kohnen, Bühren, Kühne, & Mirshahi, 2004) - (Twa, Lembach, Bullimore, & Roberts, 2005) - (Ortiz, et al., 2007) - (Bühren, Kühne, & Kohnen, Influence of pupil and optical zone diameter on higher-order aberrations after wavefront-guided myopic LASIK, 2005). That said, it is desirable to establish robust and clinically meaningful correlations between the results of wavefront analysis and subjective quality of vision.

This study describes the anatomical and visual outcomes of myopic LASIK performed with the WaveLight® Refractive Suite (Alcon® Laboratories Inc., USA) which includes a FS200 femtosecond laser and an EX500 excimer laser. We present anatomical changes, biomechanical corneal response (both anterior and posterior surfaces), visual performances (visual acuities, contrast sensitivities, depth of focus), total and corneal aberrations and patients satisfaction before and after LASIK. We also tried to correlate all these parameters to obtain a more exhaustive view of the present outcomes of moderate to high myopic LASIK surgery with the above-mentioned devices.

6.3 Patients and methods

Patients

This study included 60 eyes of 30 patients who undergone LASIK surgery for myopia treatment at the Rothschild Foundation from May 2015 until June 2016. All the patients received a complete ocular assessment prior to surgery, including cycloplegic refraction, slit lamp and fundus examination. Preoperative corneal topography was performed with the OPD-Scan® III (Nidek®, Japan), and the Orbscan IIz® (Bausch & Lomb®, USA).

Patients presenting with corneal diseases or other ocular pathologies (amblyopia, glaucoma, cataract, retinopathy, strabismus), those with indications of subclinical keratoconus, or those with a history of ocular surgery were excluded from the study. We also excluded patients whose eyes tested positive for Keratoconus (KC) or Keratoconus suspect (KCS) diagnosed by the Corneal Navigator Neural Network,

which uses Klyce & Maeda indices on the OPD-Scan® III (Nidek®, Japan). Patients who had worn rigid gas-permeable lenses in the 12 months prior to examination and those who had worn soft contact lenses in the 3 weeks prior to surgery were excluded as well.

We included patients older than 18 years with unremarkable ophthalmic histories besides myopic refractive error. The reasons for choosing LASIK were: the presence of a thick cornea (defined as a residual stromal bed higher than 300 mm after subtracting the sum of the planned LASIK flap and laser ablation thickness); the presence of a regular corneal surface diagnosed with an objective method based on Placido disk-derived data for the detection of eyes at risk of ectasia (Saad & Gatinel, Combining Placido and Corneal Wavefront Data for the Detection of Forme Fruste Keratoconus, 2016).

All patients provided written informed consent. The study and data acquisition were achieved with approval from the Rothschild Foundation's institutional review board. Informed consent was obtained from each patient after he/she voiced understanding about the purpose and the procedures in the study in accordance with the Declaration of Helsinki.

Surgical procedure and treatment planning

The 60 eyes enrolled in this prospective study underwent uncomplicated primary LASIK performed by the same experienced surgeon (DG) using the same refractive surgery platform (FS200 femtosecond laser and EX500 excimer laser). WaveLight FS200 femtosecond laser system is a low-energy and high pulse frequency laser that emits laser pulses with duration of 350 fs at a wavelength of 1,050 nm and pulse repetition rate of 200 kHz.

The laser's spots create a potential geometric shape or plane that is then manually dissected to complete the process. The flap creation was performed with the FS200 femtosecond laser, using standard treatment settings (9.2 mm flap diameter and 110 µm flap thickness).

A Mennerlyn algorithm based Photoablation (Chang, et al., 2003) was performed with the EX500 excimer (high pulse repetition rate of 500 Hz, fluence of 200 mJ/cm2). Each spot ablates 0.65 microns of stromal depth. For example, the correction of one diopter of myopia for an optical zone of 6.5 mm is performed in 1.4 seconds and induces a depth of ablation of 15.5 microns. During the photoablation, a 1050 Hz-type multi-

dimensional eye tracker, synchronized at 500 Hz (movement tracking with 2 milliseconds of latency) perform a dynamic pupil tracking from 1.5 mm to 8.0 mm.

A standard aspheric ablation profile was planned with a Plano target (at the corneal plane) refraction. The average optical zone was of 6.5 mm and the transition zone of 1.25 mm. For some subjects, because of a greater deviation between the pupillary axis and the visual axis (Kappa angle) (Salah-Mabed, Saad, Guilbert, & Gatinel, 2014), preoperative corneal vertex and pupillary axis were measured by the WaveLight® Topolyzer^{TM} VARIO (Alcon® Laboratories Inc., USA) linked with the EX500 excimer laser. A valid assumption is to consider that the optimal centration for corneal refractive surgical procedures may be located close to or midway between the corneal vertex (first Purkinje image) and the pupil centre (Manzanera, Prieto, Benito,, Tabernero,, & Artal,, 2015) - (Tabernero & Artal, 2012). However, in some eyes, the distance between these points can be as high as 400 µm. This reflects the presence of a large Kappa angle. Defining the proper axis for centration may become of critical importance in eyes that presenting a large distance between the pupil centre and the corneal vertex. The EX500 excimer laser software enables centration of the excimer profile of ablation from the pupil centre (0%) to the corneal reflex (100%) or in between, by a 10% step distance along the line joining the pupil centre to the corneal reflex. That's the reason why we planned to centre the ablation at equidistance between the pupil centre and the corneal vertex (50%) for all patients.

Preoperative and postoperative evaluation

Ophthalmologic examination performed on all patients preoperatively included manifest refraction, cycloplegic refraction, non-contact intraocular pressure evaluation, slit lamp microscopic evaluation of the anterior segment, and dilated fundoscopy. Preoperative examination included evaluation of biomechanical properties of the cornea (Corneal hysteresis (CH), Corneal Resistance Factor (CRF), Corrected Intra Ocular Pressure (IOPcc), and Goldman Intra Ocular Pressure (IOPg)) with the Ocular Response Analyzer® (Reichert Technologies, USA), pachymetry, keratometry, elevation and curvature topography analysis with Orbscan IIz® (Bausch & Lomb®, USA), wavefront aberrometry (Root Mean Square on 5.5 mm pupil) and corneal asphericity (at 6-mm diameter) analysis with OPD-Scan® III (Nidek®, Japan) topographer (Nidek, Inc., Fremont, CA). Corneal asphericity and Corneal and Total Ocular Aberrations were analysed according to Optical Society of America (OSA)

recommendations (Thibos, Applegate, Schwiegerling, Webb, & Members, 2002). Dry eye assessments were evaluated thanks to the corneal tear film Break Up Time (BUT) index.

10% and 90% contrast Uncorrected distance visual Acuity (UDVA) and best Corrected Distance Visual Acuity (CDVA) were assessed with the FrACT (Freiburg Visual Acuity and Contrast Test) 139 software at 4 meters monocularly and binocularly ref. This consists to the presentation of Landolt rings according to 8 orientations (Figure 56A). The size of the optotypes presented successively is calculated by a best-PEST 137 procedure, making it possible to estimate the threshold of acuity. Figure 56B shows the psychometric function relating the percentage of correct answers according to the size of the optotype. The visual acuity threshold corresponds to the minimum angle of resolution (MAR) for which 56.25% of the answers are correct. To determine visual acuity, we will use an 8-alternative forced choice method (8AFC) based on 30 trials. Because the patients would experience a minimizing effect from myopic correction of the trial lenses, magnification adjustment was made to the corneal plane so as to properly compare preoperative and postoperative vision. Visual acuities were adjusted according to the patient's refractive correction. The trial lens vertex distance of 17mm was used to calculate relative magnification (RM).

$$RM = 1 - hFs$$

Where h is the difference between the corneal and spectacle plane (vertex distance in meters) and Fs the back-vertex power of the corrective lens at the spectacle plane. The following equation was used to convert visual acuity from spectacle plane to corneal plane.

$$LogMAR_{cornea} = logMAR_{spec} - logRM \text{ (Kuang-mon \& Liang, 2006)}$$

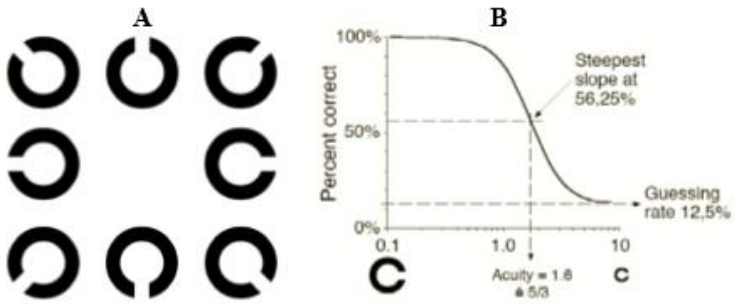

Figure 56 (A) Landolt rings displayed during the visual acuity test. 8 orientations were possible: left, top left, top, top right, right, bottom right, bottom, bottom left. (B) Psychometric function used by the Freiburg test. The probability of correct answers depends on the size of the optotype. Visual acuity is 16/10 (-0.2 logMAR) (Bach, 1996)

Photopic Corrected distance and Uncorrected Contrast Sensitivity (CCS and UCS) measurements were performed at 12 cycles per degree (cpd), using randomly oriented sinusoidal arrays at 4 meters. These networks have been computer-generated (on MATLAB), following a modified best-PEST 138 procedure, i.e. preceded by a psychophysical stairs method. To determine the contrast sensitivity, we used a 4-alternative forced choice method (4AFC) based on 30 trials. Photopic Best corrected and Uncorrected contrast sensitivity were also measured with introduction of glare. To generate glare, oncoming headlights were simulated by attaching 2.5-watt halogen floodlights to each side of the computer screen (Kuang-mon & Liang, 2006).

A “Tolerance to Blur” measurement was also performed (Corrected Sensitivity to Blur, CSB). The subjective depth of field criteria used was unacceptable blur. This is the level of blur that the patient would refuse to accept if he had to endure it permanently. The average generally observed is about 1.4 D (Atchison, Fisher, Pedersen, & Ridall, 2005) - (Atchison, Guo, & Fisher, Limits of spherical blur determined with an adaptive optics mirror, 2009) - (Ciuffreda, et al., 2006).

During the evaluation, the subjects wore their Sphero-cylindrical correction and held in front of their eyes an artificial pupil of 3 mm that subjectively adjusted to maximize the contrasts (and to decrease the level of ocular aberrations). The test, performed in monocular (in visual acuity), was located 4 meters away. The black-and-white (HEV) images were presented via a Keynote® presentation (Figure 57) at an angle of 80.38' (512x512 pixels image of 0.157' each), in shades of grey (monochromatic).

Starting systematically from the clear image as a reference, defocalization was added to each new slide (0.05µm or about 0.055D). The subject had to say stop as soon as the image was no longer acceptable according to the criterion of unacceptable blur described by Atchison (Atchison, Guo, & Fisher, Limits of spherical blur determined with an adaptive optics mirror, 2009).

An ascending and descending limit method was performed (i.e., an average of 3 clear-to-blur values and 3 blur-to-clear limit values). With a value in the positive and one in the negative, we have obtained an average depth of field value for each subject (Applegate, Sarver, & Khemsara, Are all aberrations equal ?, 2002) - (Benard, Lopez-Gil, & Legras, 2011).

Figure 57 Black-and-white (HEV) images presented for Tolerance/Sensitivity to Blur assessment

The illumination of the room where the tests were carried out is about 350 lux. The luminance of the screen that projects the contrast sensitivity, visual acuity and simulated images for the depth of field measurement has been systematically calibrated to about 100 candelas per m2.

All patients were also submitted to two French versions of vision quality questionnaires: (QOV) (McAlinden, Pesudovs, & Moore, 2010) (range 0 excellent quality of vision to 100 very poor quality of vision) and Ocular Surface Disease Index (OSDI) which was developed to quantify the specific impact of dry eye disease on vision-targeted health-related quality of life (range 0 normal to 100 severe dry eye) (Schiffman, Christianson, Jacobsen, Hirsch, & Reis, 2000) before and One, three and six Months postoperatively. The overall OSDI score defined the ocular surface as normal (0-12 points) or as having mild (13-22 points), moderate (23-32 points), or severe (33-100 points) disease

All these parameters were measured preoperatively and One day, One Month, 3 Months, and 6 Months postoperatively. The examiner checked each measure and its quality before recording it. All the measurements were performed by the same operator (IS).

Statistical analysis

Statistical analysis was performed with a commercial software (SPSS v. 13.0; SPSS Inc., Chicago, IL). We used paired and unpaired student *t* test to compare the outcomes in this population. ANOVA test were also used to compare means. Pearson correlation analyses were also used. A calculated *p*-value <0.05 was considered statistically significant. Data are presented as the mean +/- standard deviation.

Astigmatism plots were generated using the Astigplot® software (EB Eye). The average magnitude and axis of cylinders was computed using vector calculations. The astigmatism plots were represented with a positive cylinder magnitude convention.

6.4 Results

Demographics

60 myopic eyes of 30 patients were included in the study. The mean preoperative

spherical equivalent was -4.5 ± 2.2 D (ranging from -9.3 D to -0.8 D), and the mean age 30.4 ± 4.2 years (ranging from 21.3 to 38.7 years). The data are detailed in Table 23.

	Total	**Low Cylinder (<1.50 D)**	**High Cylinder (>=1.50 D)**
Number of patients	30	24	6
Number of eyes	60	*49*	*11*
Right / Left	30 / 30	24 / 25	6 / 5
Age (years)			
Mean ± Standard deviation	30,4 ± 4,2	30,8 ± 4,2	28,7 ± 4,4
Minimum / Maximum	21,3 / 38,7	21,3 / 38,7	21,3 / 36,6
% Female / % Male	*63% / 37%*	*67% / 33%*	*45% / 55%*
% of Contact Lense Carrier	*70%*	*78%*	*36%*
Refractive Spherical Equivalent (D)			
Mean ± Standard deviation	-4,5 ± 2,2	-4,6 ± 2,2	-3,8 ± 1,9
Minimum / Maximum	-9,3 / -0,8	-9,3 / -0,8	-6,6 / -1,3
Refractive Cylinder (D)			
Mean ± Standard deviation	-0,8 ± 0,8	-0,5 ± 0,3	-2,1 ± 0,7
Minimum / Maximum	0,0 / -3,3	0,0 / -1,3	-1,5 / -3,3

Table 23 Demographic data

Anatomical changes

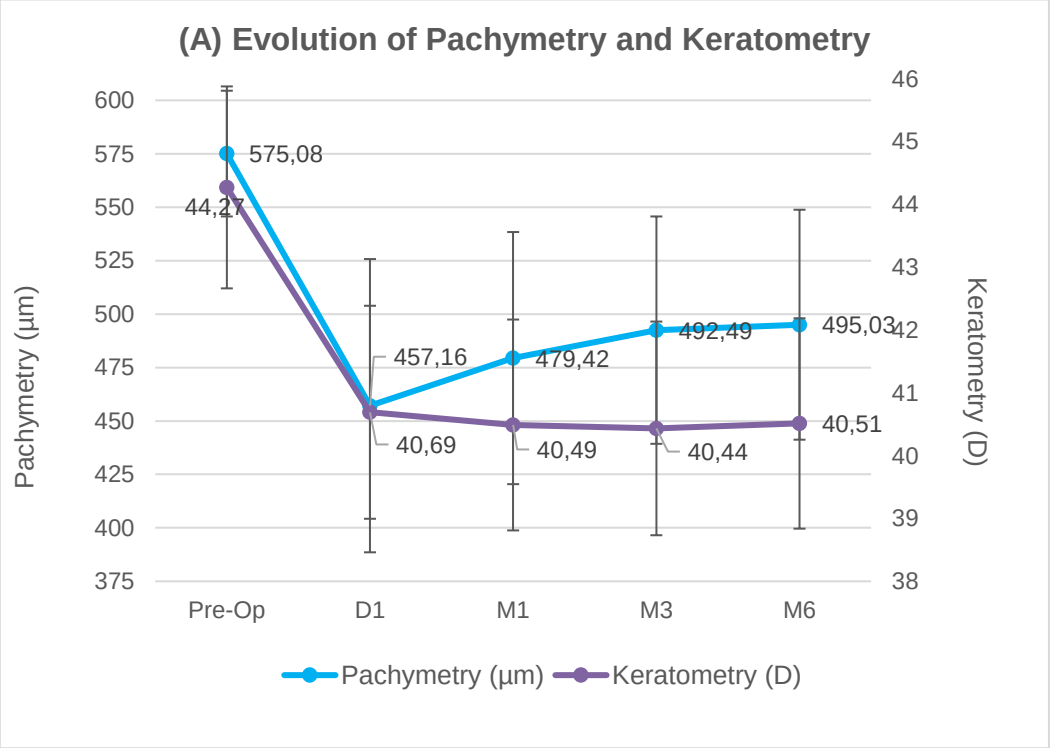

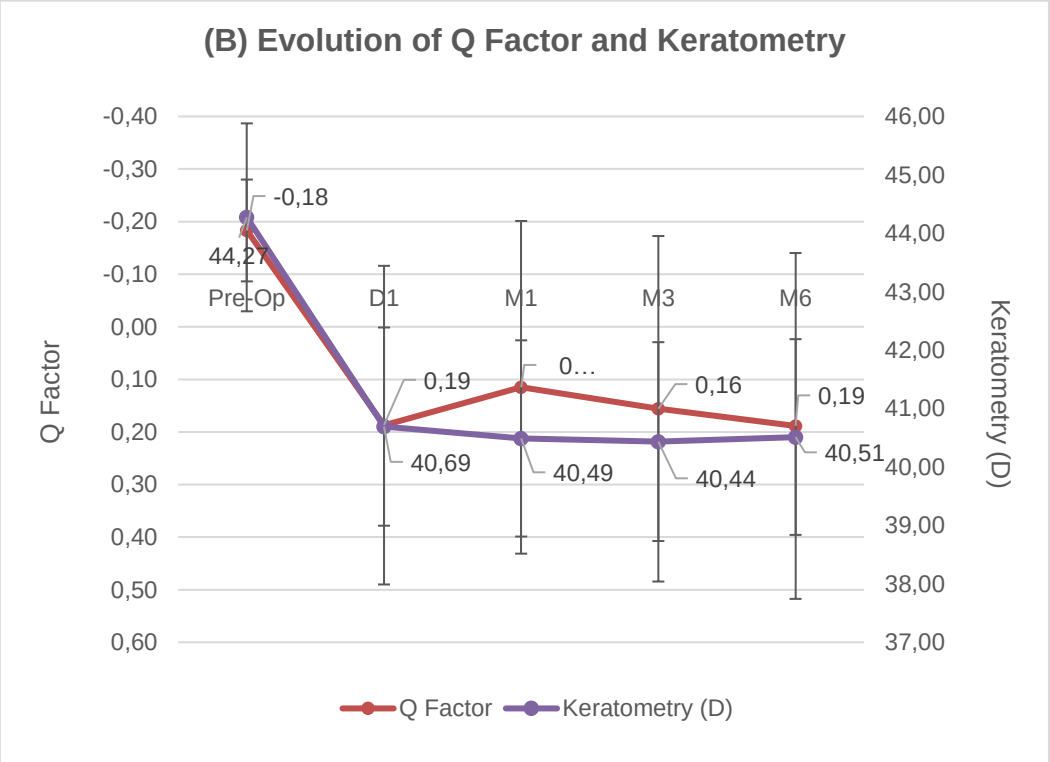

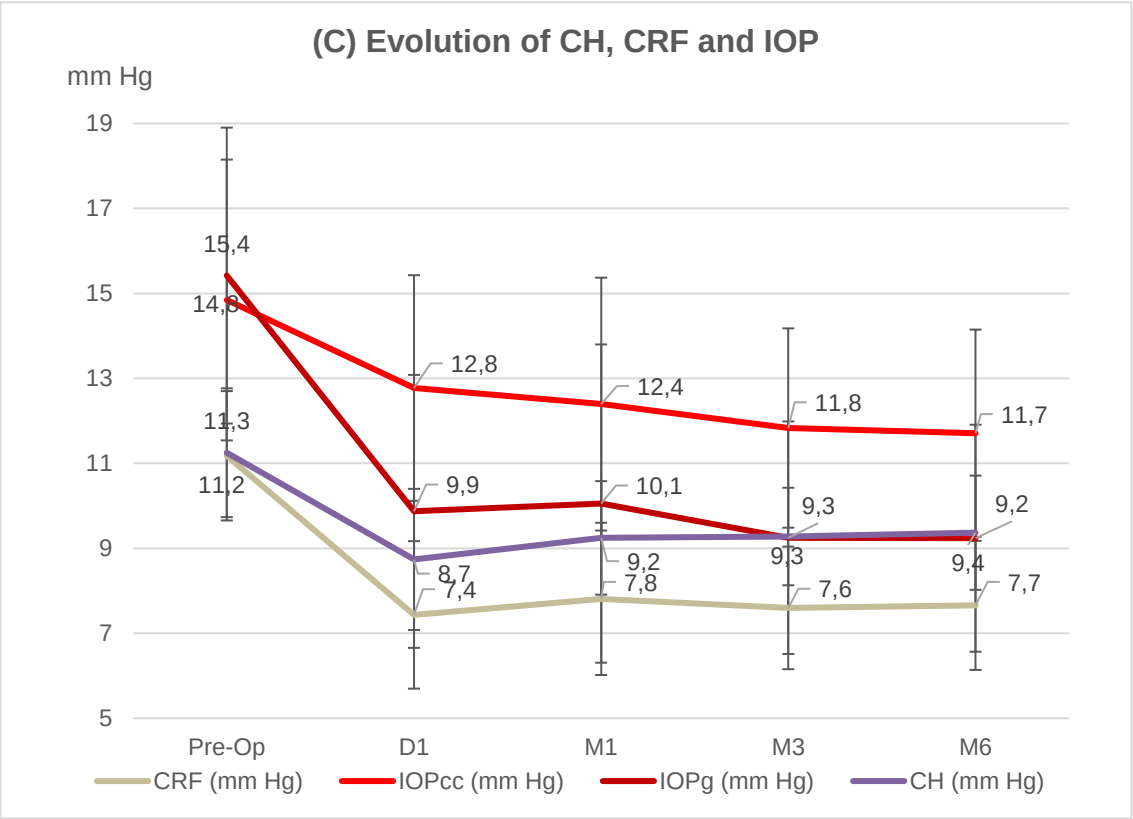

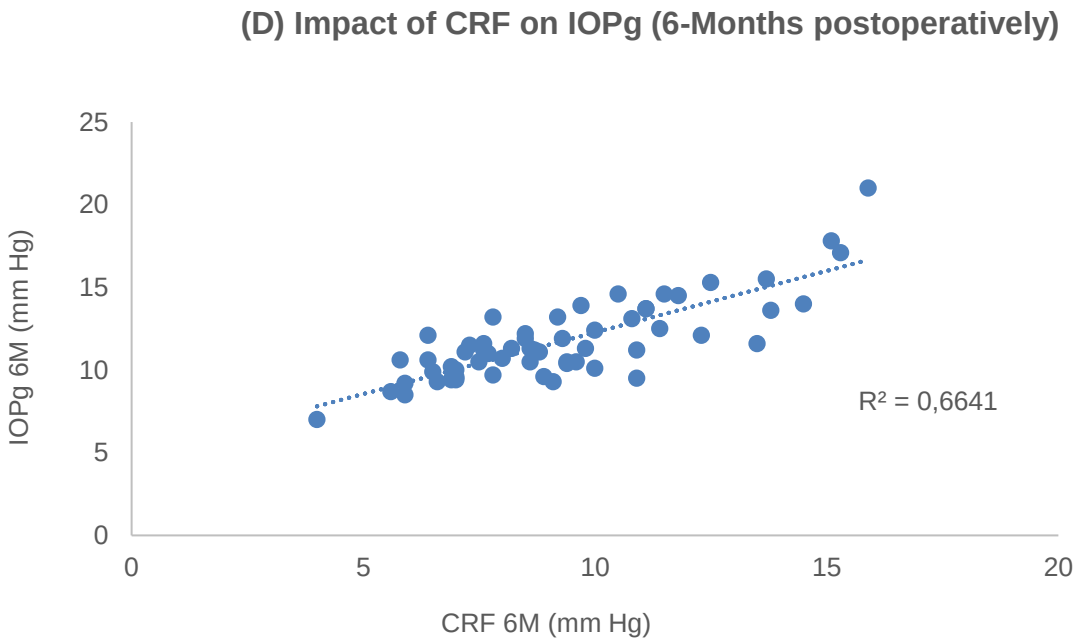

Figure 58 Evolution of anatomical parameters after myopic LASIK (A) Evolution of Pachymetry with regards to Keratometry, (B) Evolution of Keratometry with regards Asphericity, (C) Evolution of Biomechanics indices, (D) Correlation between Corneal resistance and IOP 6 Months after myopic LASIK

Six months post operatively, the cornea became flatter (44.27 ± 1.61 D preoperatively to 40.51 ± 1.67 D at 6- months postoperatively). There was a significant difference between the average corneal power before and after the LASIK (paired t test t = 17.50, *p*<0.001) (Figure 58A).

There was no correlation between the average keratometric power and the patient's age, refractive spherical equivalent and the initial central mean pachymetry, before and after the surgery (ex: correlation between pre-Op keratometry and age r^2=0.184, p=0.160).

The mean corneal pachymetries were 575.08 ± 29.41 µm, 457.16 ± 68.59 µm, 479.42 ± 58.97 µm, 492.49 ± 53.18 µm, 495.03 ± 53.79 µm respectively preoperatively, one day, 1 Month, 3 Months and 6 months postoperatively. 6 Months postoperatively, the pachymetry was significantly lower than preoperatively (paired t test t = 15.03, *p*<0.001).

Six months post operatively, the mean decrease in Keratometry was 3.76 ± 1.66 D while the mean decrease in pachymetry was 80.04 ± 41.26 µm. The difference in pachymetry at 6 Months postoperatively correlated positively (r^2=0.74, p<0.001) with the Mennerlyn Formula pachymetry estimation (Figure 59).

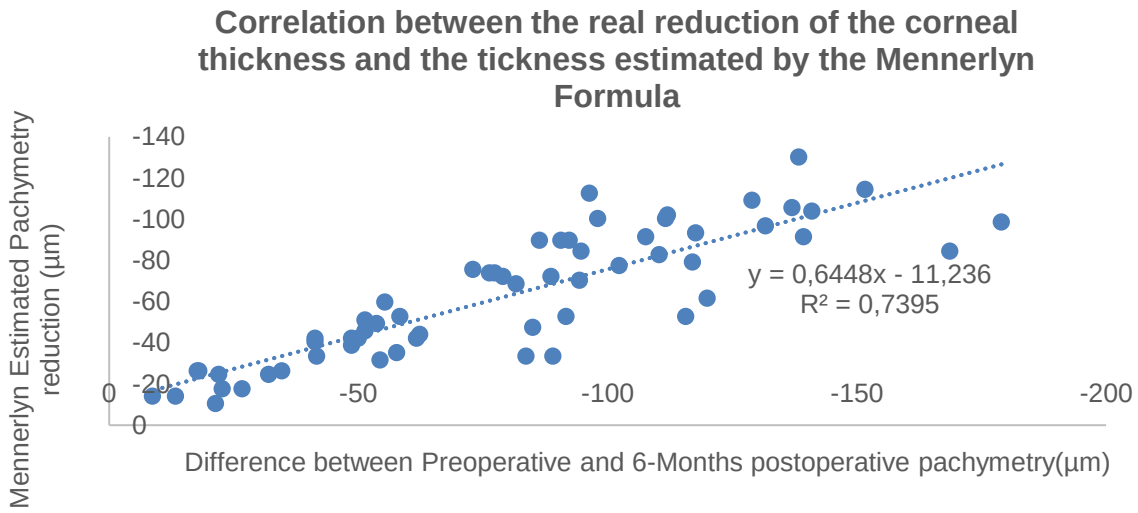

Figure 59 Positive correlation between the real reduction of the corneal thickness and the thickness estimated by the Mennerlyn Formula

One day after LASIK, the corneal asphericity expressed by the Q factor became significantly more oblate (Q = -0.18 ± 0.10 (SD) (range -0.38 to 0.05) preoperatively and Q = 0.19 ± 0.30 (SD) (range -0.29 to 0.98) one day after surgery (t = -9.52, P< 0.001). There was no significant difference in Q factor in different moments post-

surgery (t = -0.31, P = 0.98) (Figure 58B).

There was no correlation between the preoperative spherical equivalent and the preoperative corneal asphericity measured (r = -0.003, *p* = 0.98). There was no correlation between the initial mean central pachymetry and the corneal asphericity (r = 0.206, P = 0.18).

Figure 58C shows a decrease in IOPcc and IOPg from 14.84 ± 3.305 mmHg preoperatively to 11.71 ± 2.440 mmHg at 6-Months postoperative and from 15.42 ± 3.483 mmHg to 9.24 ± 2.671 mmHg respectively. The corneal indices of resistance and Hysteresis decreased significantly as shown in the same Figure 58C. There was a positive correlation between CRF and IOPg 6-Months postoperatively. (R^2 =0.74, p<0.001) (Figure 58D).

Safety and Predictability

Quality of Vision outcomes

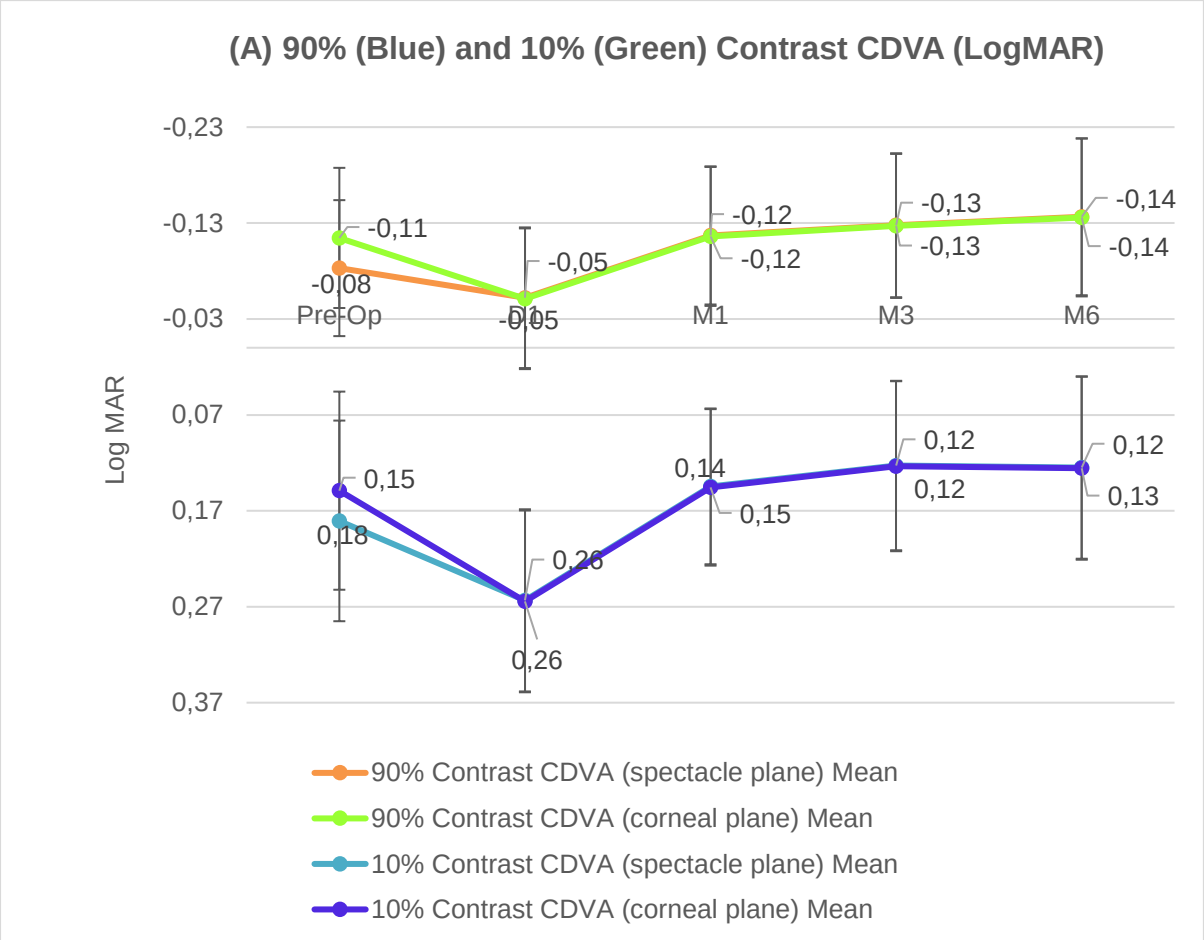

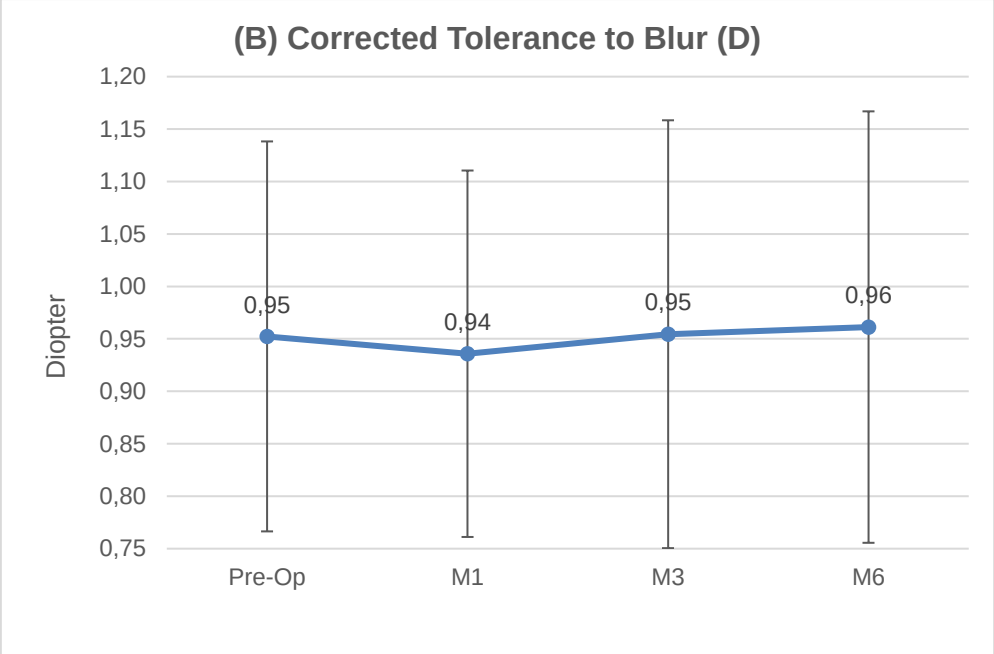

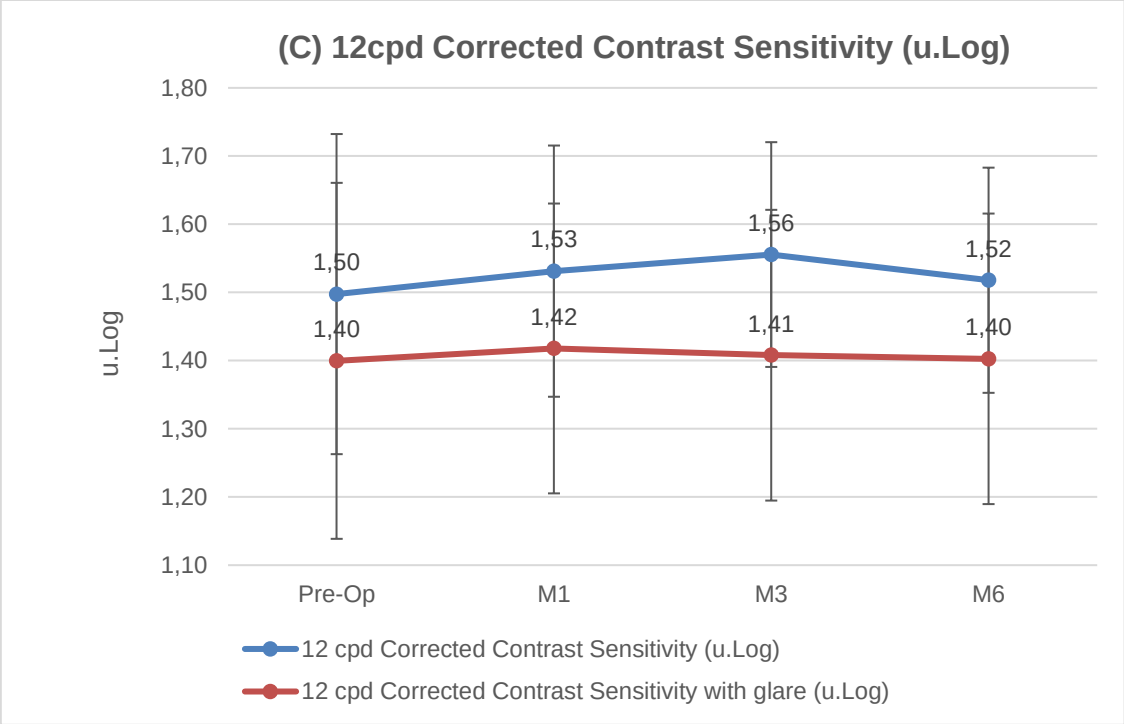

Figure 60 Evolution of Visual Outcomes after myopic LASIK: (A) Evolution of 90% and 10% Contrast CDVA in the spectacle and the corneal planes, (B) Evolution of the Corrected Sensitivity to Blur, (C) Evolution of 12 cpd Corrected Contrast Sensitivity and 12 cpd Corrected Contrast Sensitivity and 12 cpd Corrected Contrast Sensitivity with glare

Figure 60 shows that after LASIK, Monocular 90% and 10% CDVA increased slightly but not significantly (paired-test t = 2.07, p=0.053 and t = 1.62, p=0.11 respectively),

while Monocular Corrected contrast sensitivity and Corrected Sensitivity to Blur remained unchanged (paired-test t = -0.75, p=0.46 and t = -0.36, p=0.72 respectively). The CCS with glare was lower than the CCS by 0.1 u.log.

SAFETY	1 Day postoperative (n=60) Percentage (95% CI) High Astigmatism	Low Astigmatism	*p**	1 Month postoperative (n=60) Percentage (95% CI) High Astigmatism	Low Astigmatism	*p**	3 Months postoperative (n=60) Percentage (95% CI) High Astigmatism	Low Astigmatism	*p**	6 Months postoperative (n Percentage (95% CI) High Astigmatism	Low Astigmatism	*p**
CDVA												
Loss of 3 lines or more (90% contrast)	9%	4%	**0,039***			**0,037***			0,137			**0,005***
Loss of 2 lines (90% contrast)	27%	8%		9%				4%			2%	
Loss of 1 line (90% contrast)	36%	33%		27%	20%		36%	18%		55%	12%	
No loss or gain of lines (90% contrast)	18%	49%		45%	51%		55%	43%		45%	45%	
Gain of 1 line (90% contrast)	9%	6%		18%	27%		9%	29%			33%	
Gain of 2 lines (90% contrast)					2%			6%			8%	
Gain of 3 lines or more (90% contrast)												
Loss of 3 lines or more (10% contrast)	18%	14%	**0,008***	9%	2%	**0,035***		2%	0,751		2%	0,08
Loss of 2 lines (10% contrast)	36%	18%		9%				8%			4%	
Loss of 1 line (10% contrast)	36%	22%		18%	22%		18%	16%		36%	18%	
No loss or gain of lines (10% contrast)	9%	37%		36%	41%		36%	27%		18%	27%	
Gain of 1 line (10% contrast)		8%		18%	27%		36%	31%		45%	39%	
Gain of 2 lines (10% contrast)					8%		9%	16%			8%	
Gain of 3 lines or more (10% contrast)				9%							2%	
CCS (12cpd)												
Loss of 0.4 u.log or more	9%	31%	0,191	9%	6%	**0,001***	9%	4%	**0,001***	9%	2%	**0,001***
Loss of 0.1 to 0.4 u.log	64%	45%		27%	29%		9%	31%		18%	35%	
No loss or gain	9%	6%		27%	18%		18%	16%		36%	18%	
Gain of 0.1 to 0.4 u.log	18%	16%		27%	37%		55%	33%		27%	41%	
Gain of 0.4 u.log or more		2%		9%	10%		9%	16%		9%	4%	
Loss of 0.4 u.log or more (with glare)	-	-		9%	2%	**0,001***	9%	4%	**0,009***	9%	6%	**0,001***
Loss of 0.1 to 0.4 u.log (with glare)	-	-		36%	37%		18%	37%		36%	33%	
No loss or gain (with glare)	-	-		18%	18%		27%	14%		18%	12%	
Gain of 0.1 to 0.4 u.log (with glare)	-	-		18%	37%		27%	37%		27%	43%	
Gain of 0.4 u.log or more (with glare)				18%	6%		18%	8%		9%	6%	
CSB												
Loss of 0.3 D or more					10%	0,197		8%	0,108		8%	0,29
Loss of 0.1 to 0.3 D				9%	29%			39%		9%	45%	
No loss or gain				36%	31%		18%	14%		9%	12%	
Gain of 0.1 to 0.3 D				45%	29%		73%	35%		73%	22%	
Gain of 0.3 D or more				9%	2%		9%	4%		9%	12%	

Table 24 Differences between High (cylinder >=1.5D) and Low astigmatic eyes (cylinder <1.50 D) in 90% and 10% Corrected Distance Visual Acuity (CDVA), in Corrected Contrast Sensitivity and Corrected Contrast Sensitivity with glare (CCS at 12 cycles per degree), and in Corrected Sensitivity to Blur (CSB)

** significant*

Table 24 shows the safety and predictability of the LASIK in terms of quality of vision outcomes. Although there was no difference in quality of vision outcomes (CDVA, and CSB) preoperatively between High (cylinder >=1.5D) and Low astigmatic eyes (cylinder< 1.50D) except for the CCS (where the high astigmatic eyes CCS was smaller than the low astigmatic one, (ANOVA, p=0.016)), there were differences postoperatively. No significant difference was found between groups in CSB.

Refractive Spherical Equivalent Outcomes and Magnitude of astigmatism

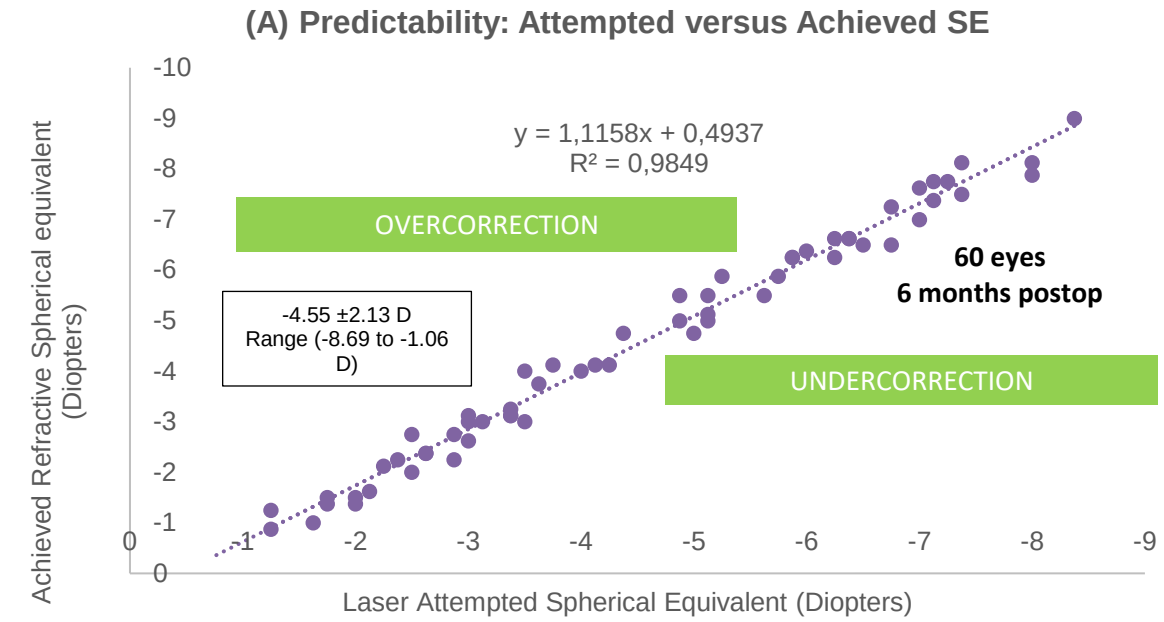

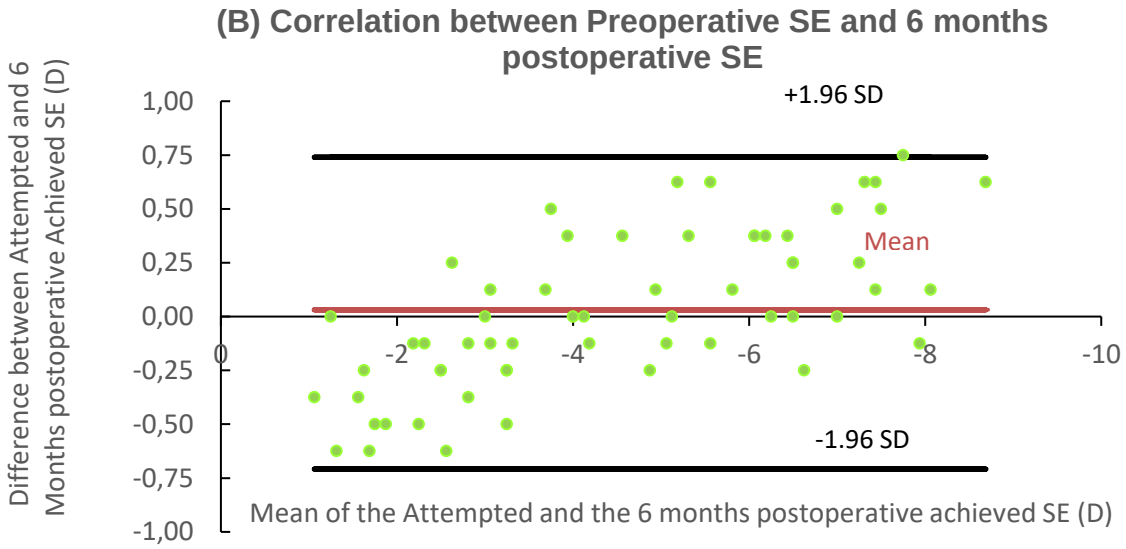

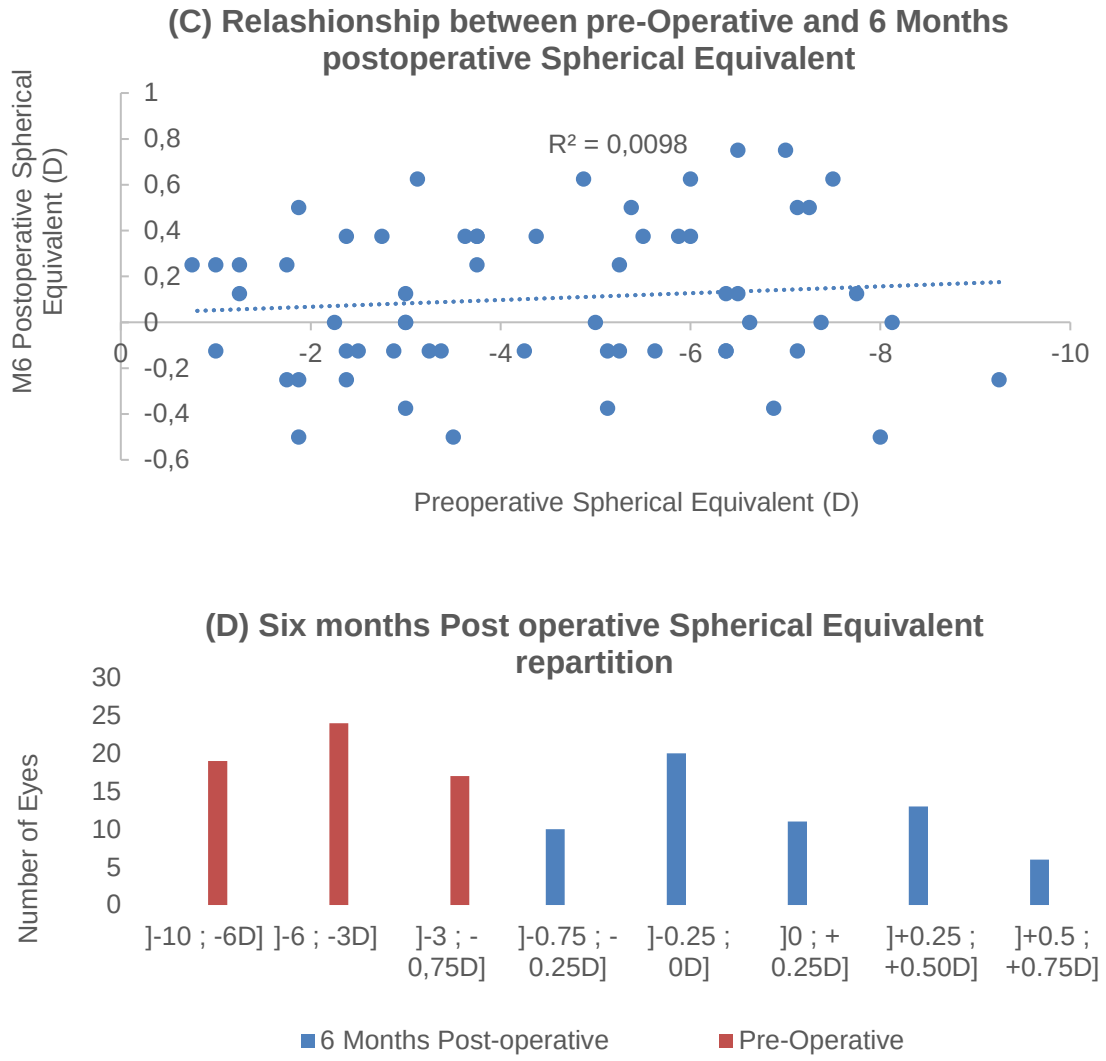

Figure 61 Refractive Spherical equivalent (SE) outcomes: Distribution of achieved SE outcomes after LASIK at 6 months (A), Bland-Altmann distribution of Attempted SE (B), Correlation between Preoperative SE and 6 months postoperative SE (C), Distribution of manifest SE preoperatively and 6 months postoperatively (D)

Figure 61A and 61B show predictability of the manifest SE (scattergram of attempted versus achieved manifest SE). There was a strong and statistically significant correlation between the laser attempted SE and the achieved SE (r^2= 0.98, p<0.001). The post-operative Spherical equivalent was independent from the preoperative one (r^2=0.0098, p<0.001) (Figure 61C), and there were no statistically difference in 6 months achieved SE between high astigmatic eyes and low astigmatic ones (ANOVA, p= 0.98). Figure 61D displays the distribution of preoperative and 6 months postoperative SE.

Astigmatism is an optical aberration which is mainly caused by the toricity of a refractive surface. Although topography instruments measure toricity (not

astigmatism) we will use the terms “astigmatism” and “toricity” interchangeably. The magnitude of the astigmatism was calculated as follows.

In the 5mm ring zone, the difference in simulated keratometry (sim-K) of the steepest and the flattest hemi-meridians was calculated as the “sim-K difference” by the topography software. The magnitude of the astigmatism was computed as the variation between the “sim-K difference” values. The average refractive astigmatism value decreased from 0.40 D preoperatively to 0.05 D 6 months postoperatively. And the corneal astigmatism decreased from 0.51 D to 0.19 D after LASIK. Before and after LASIK, the astigmatism was predominantly oriented with the rule (WTR) except for the total refractive astigmatism which was oriented against the rule at 6 months (Figure 62B).

The Figure 62 represents the magnitude and orientation of the refractive and anterior corneal astigmatism before and 6 months after the surgery. We found a difference of 0.58 D (for the refractive astigmatism) and 0.33 D (for the corneal astigmatism) between the two analysed periods.

There was no correlation between the 6 months postoperative cylinder value and preoperative cylinder. (r^2= 0.0013, p< 0.01).

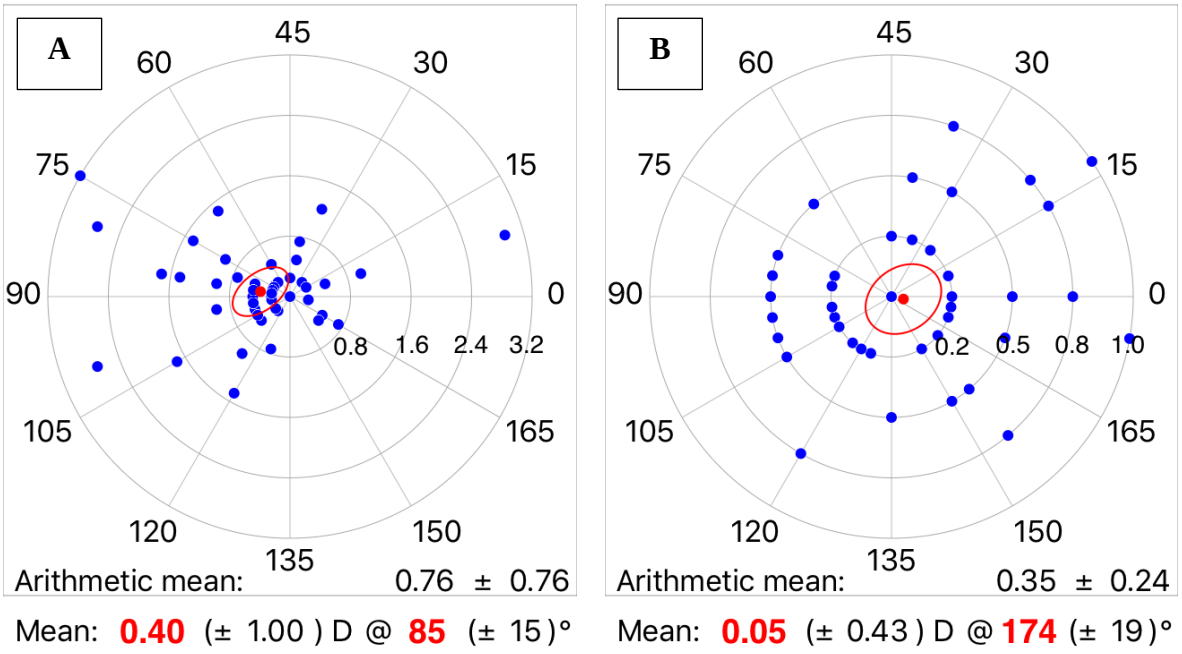

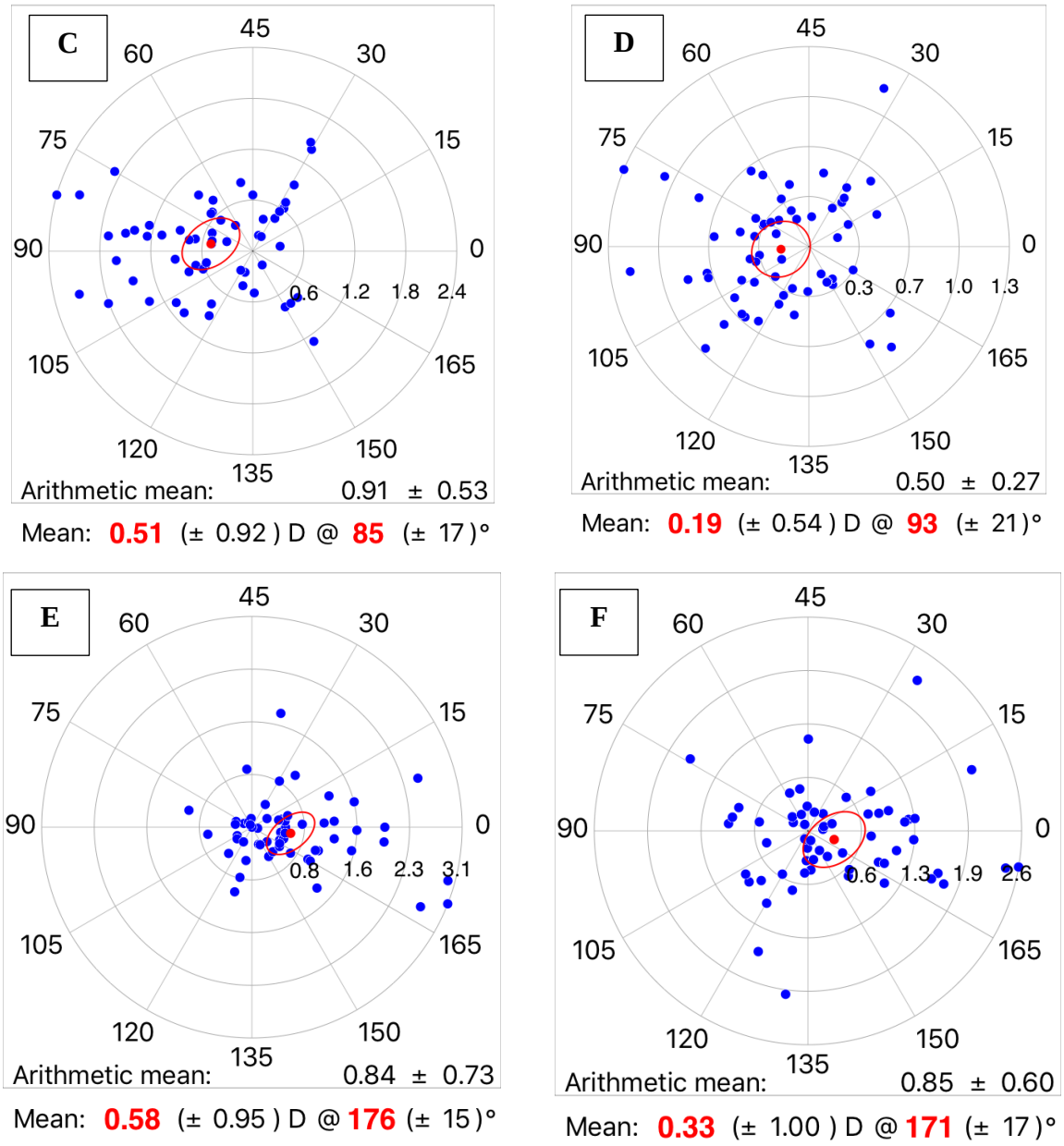

Figure 62 Figure 62 Preoperative Refractive astigmatism (A), 6 months postoperative Refractive astigmatism (B) Preoperative Corneal astigmatism (C), and 6 months postoperative Corneal astigmatism (D). Difference between preoperative and 6 months postoperative in in refractive astigmatism (E) and corneal astigmatism (F)

Corneal and Total Aberrations analysis on a 5.5 mm pupil

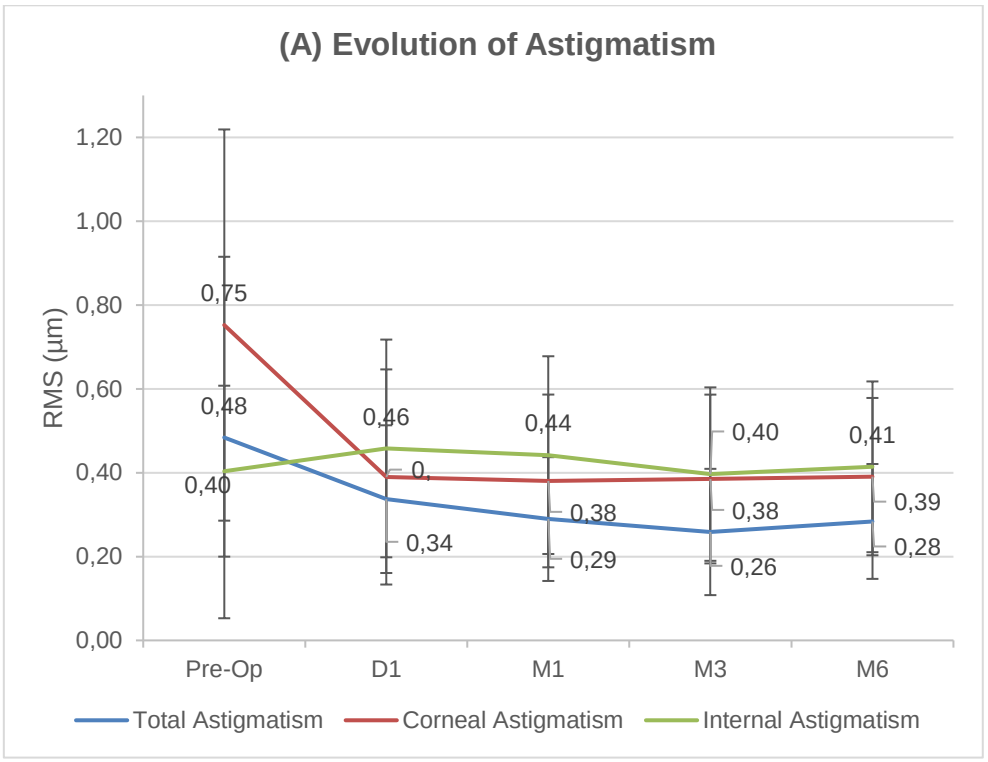

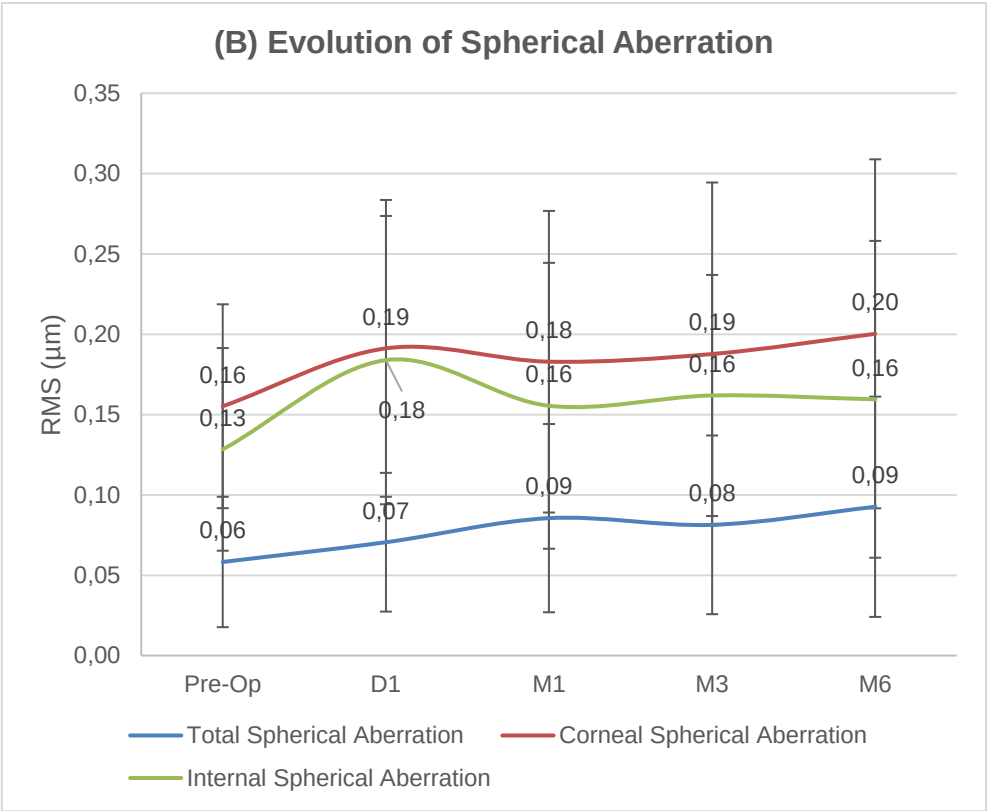

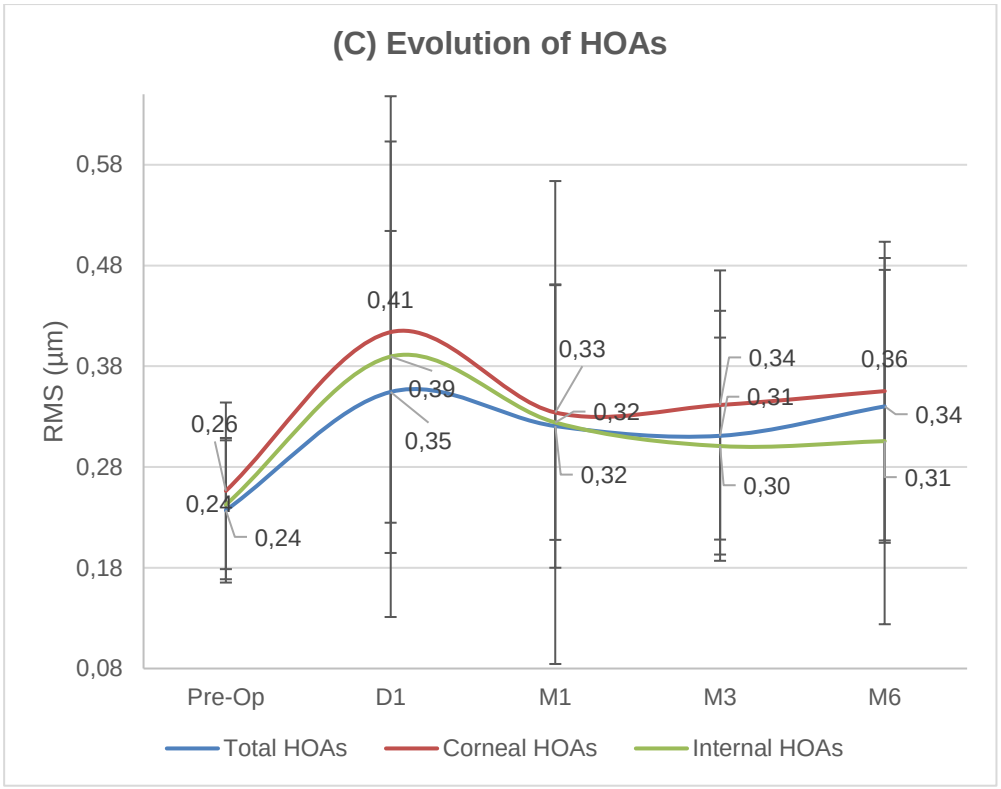

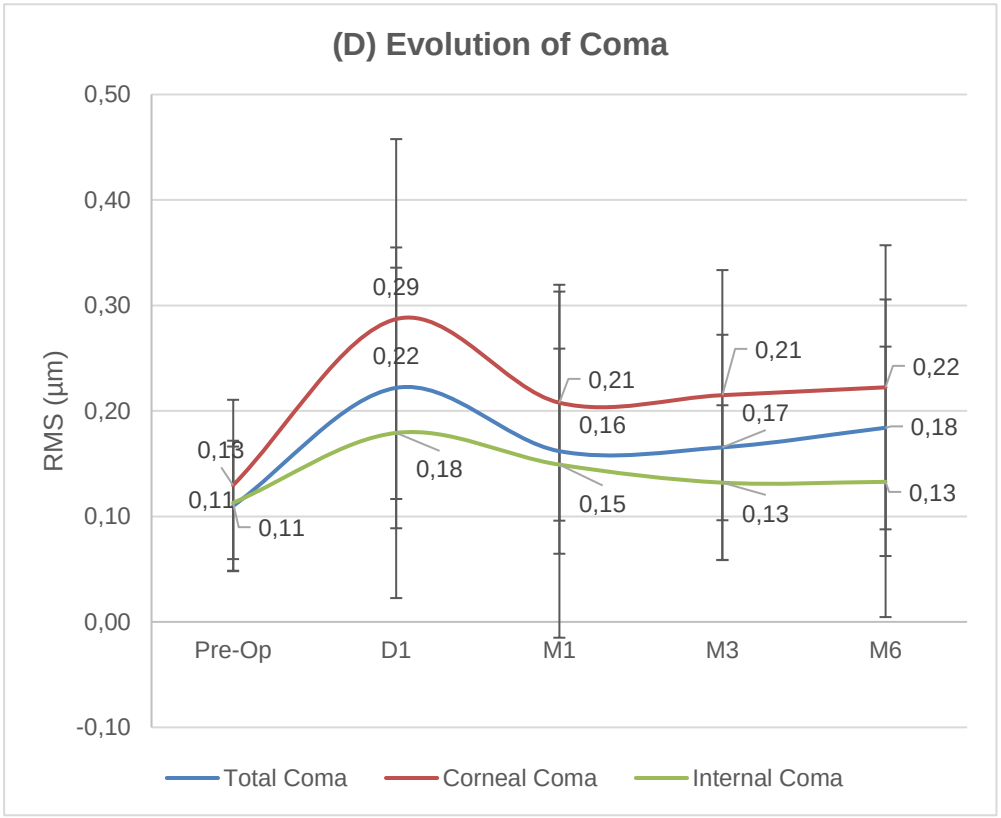

Figure 63 Evolution of RMS Ocular Total, Corneal and Internal Aberrations (µm): Astigmatism evolution (A), Spherical Aberration Evolution (Zernike SA4 + SA12) (B), High Order Aberrations (HOAs: 3rd order and higher) (C), and Coma evolution (D)

	Preoperative	6- Months postoperative	Difference	
Aberrations (RMS in µm)	***Mean ± SD***	***Mean ± SD***	***Mean ± SD***	***p***
Total High Order Aberrations (HOAs)	0,237 ±0,072	0,340 ±0,135	0,103 ±0,111	***p < 0,001****
Total Coma	0,11 ± 0,062	0,184 ± 0,121	0,074 ±0,108	***p < 0,001****
Total Spherical Aberrations (SA4+ SA12)	0,058 ± 0,04	0,093 ± 0,069	0,034 ±0,063	***p < 0,001****
Corneal High Order Aberrations (HOAs)	0,256 ± 0,088	0,355 ± 0,148	0,099 ± 0,115	***p < 0,001****
Corneal Coma	0,130 ± 0,081	0,222 ± 0,135	0,093 ± 0,118	***p < 0,001****
Corneal Spherical Aberrations (SA4+SA12)	0,155 ± 0,063	0,200 ± 0,109	0,045 ± 0,082	***p < 0,001****
Internal High Order Aberrations (HOAs)	0,243 ± 0,064	0,306 ± 0,182	0,063 ± 0,175	***p < 0,01****
Internal Coma	0,113 ± 0,053	0,133 ± 0,128	0,02 ± 0,128	*p = 0,26*
Internal Spherical Aberrations (SA4+SA12)	0,128 ± 0,063	0,159 ± 0,099	0,031 ± 0,10	***p = 0,027****

Table 25 Evolution of RMS Ocular Total, Corneal and Internal Aberrations (µm)

** significant*

Figure 63 and Table 25 show the very slight but significant increase in total, corneal and internal ocular aberrations after LASIK surgery. The most important increase in corneal and total HOAs seems to be attributed to the increase of corneal coma (Figure 64). The total spherical Aberration increased very slightly but significantly (0,034 ± 0,063, p<0.001).

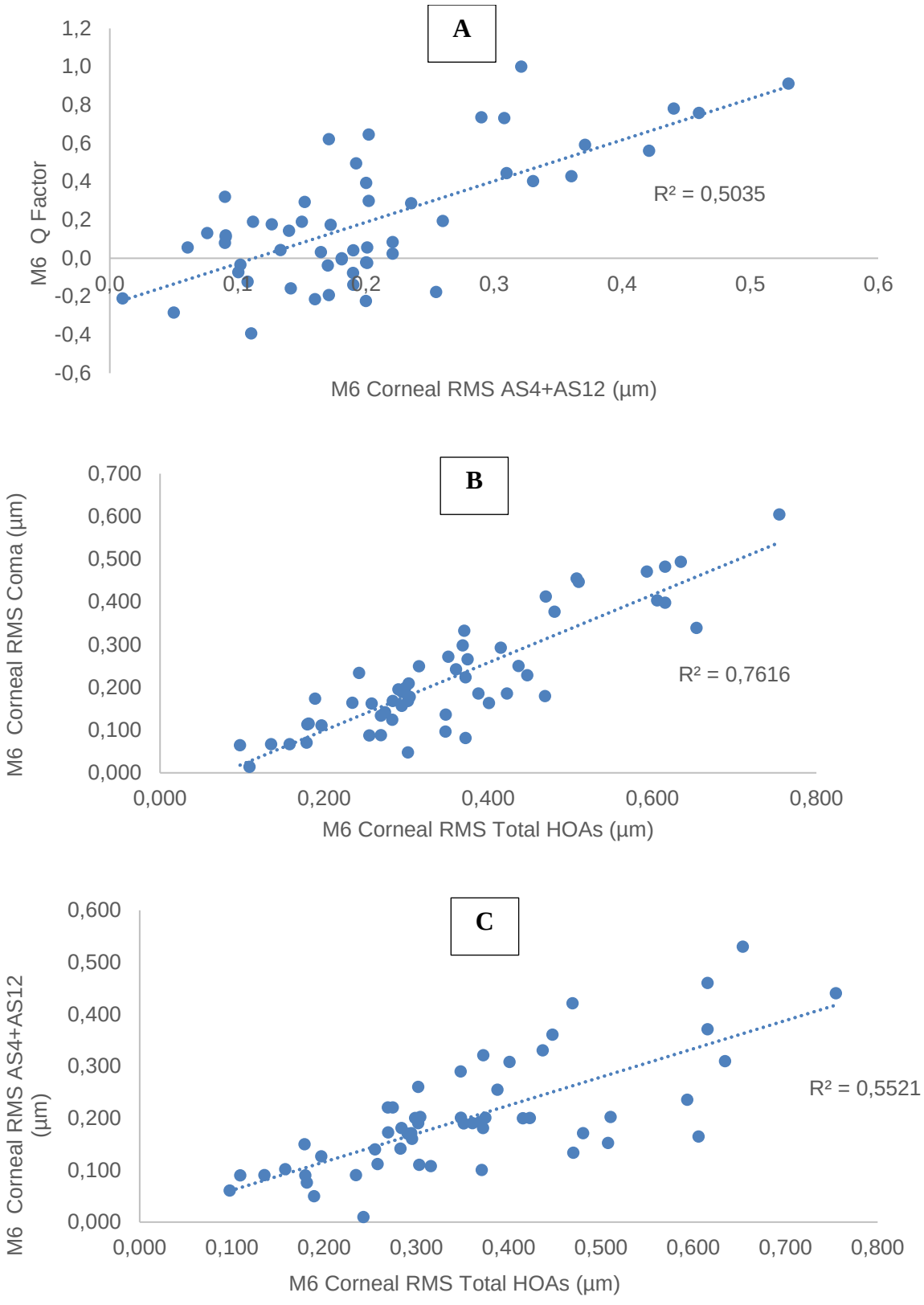

Figure 64 Relationship between spherical corneal aberrations and Q factor (A), between corneal HOAs and Corneal Coma (B) and between corneal HOAs and Corneal Spherical Aberrations (C)

We found no correlations between Total, corneal and Internal spherical aberrations after LASIK and preoperative Spherical equivalent (r^2=0.03, p<0.001, r^2=0.012, p<0.001 and r^2=0.009, p<0.001 respectively). No predictive factor for the increase in postoperative HOAs was found (low r^2, p> 0.05). However, we found a positive correlation between Total Preoperative HOAs and M6 postoperative HOAs (r^2=0.573, p<0.001).

Efficacy, Stability and Satisfaction

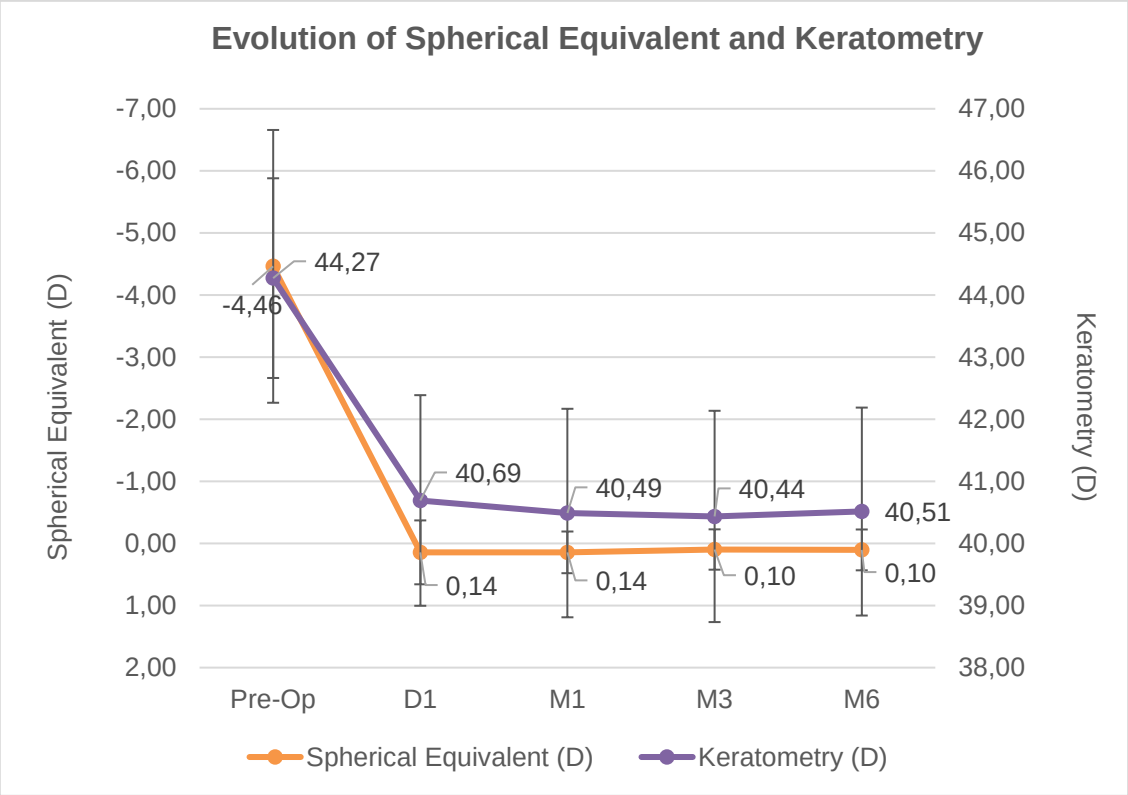

Figure 65 Stability of Keratometry and Spherical equivalent refraction after LASIK between 1 day and 6 months

One day after LASIK surgery, the mean refractive spherical equivalent and keratometry were +0.14 ± 0.52 D and 40.49 ± 1.70 D respectively and kept stable up to 6 months follow-up (Figure 65).

6 months after surgery, 62% of eyes achieved High contrast UDVA of -0.1 log MAR or better versus 42% CDVA before undergoing LASIK. Uncorrected CCS seemed to be unchanged 6months postoperatively, compared to the Corrected CCS in both normal and with glare illuminations conditions (Figure 66).

(A) Cumulative High Contrast Monocular Uncorrected Distance Visual Acuity (x Log MAR or better)

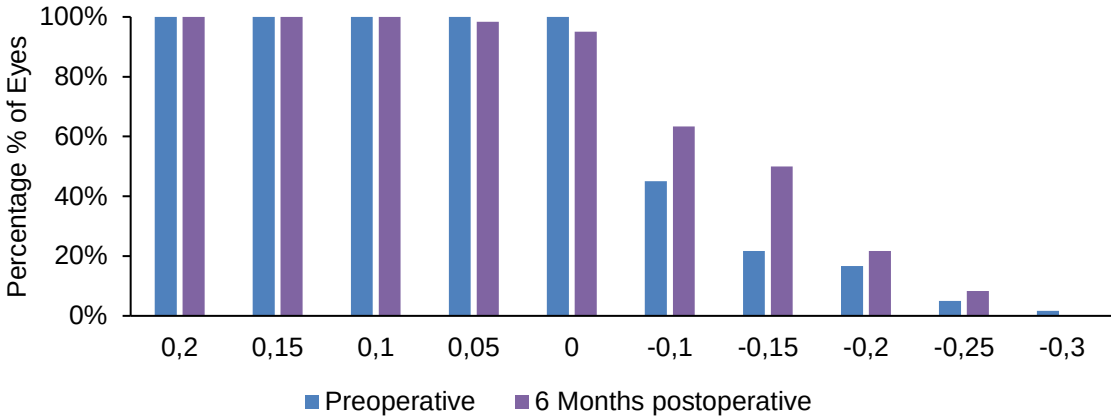

(B) Cumulative Low Contrast Monocular Uncorrected Distance Visual Acuity (x Log MAR or better)

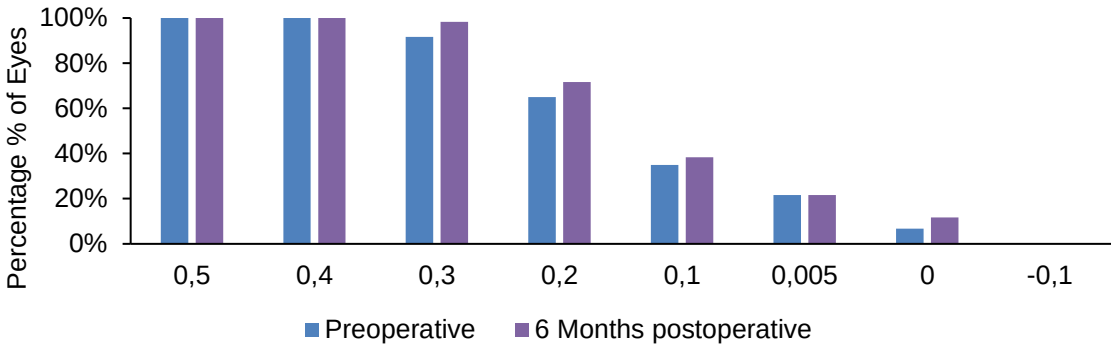

(C) Cumulative Monocular Uncorrected Distance Contrast Sensitivity (x u. Log or better)

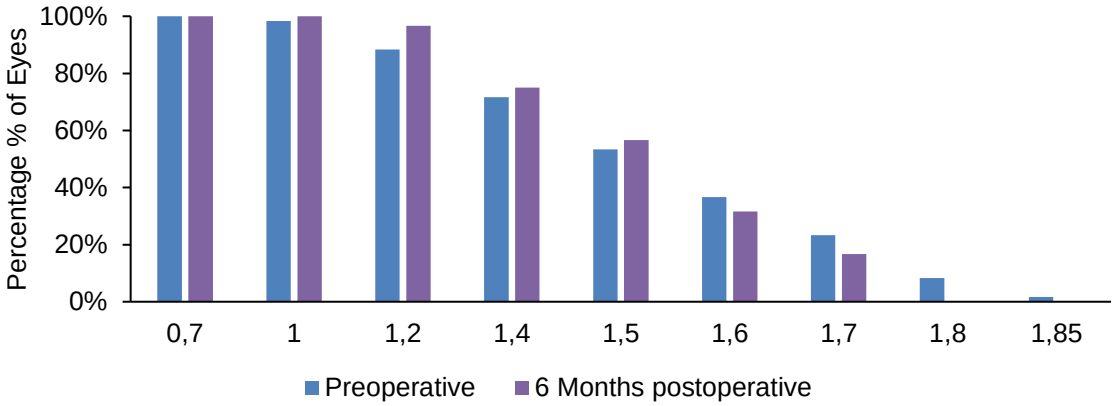

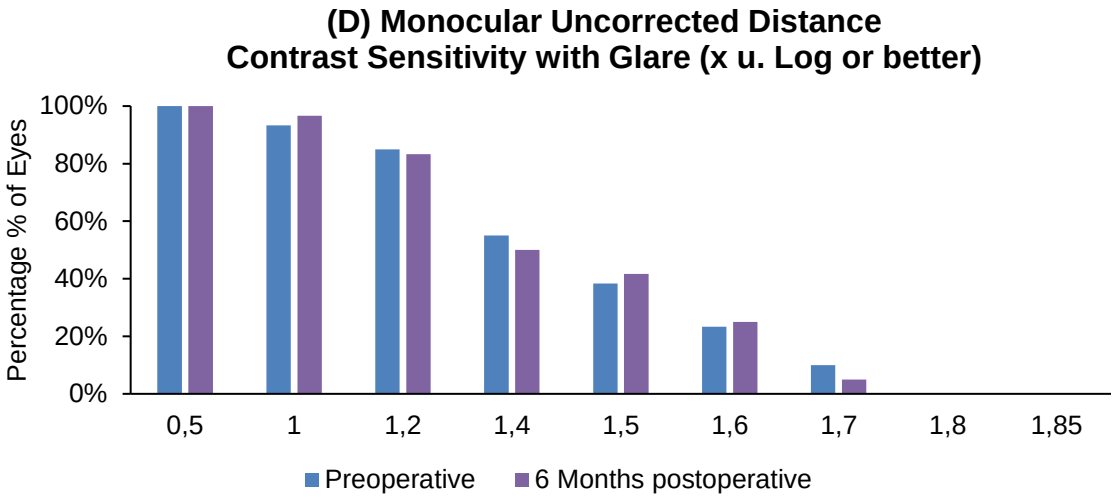

Figure 66 Changes in 90% contrast (A) and 10% (B) Uncorrected Distance Visual Acuity and Uncorrected Contrast sensitivity (C) and Uncorrected Contrast sensitivity with glare (D) at 6 months of follow-up after LASIK

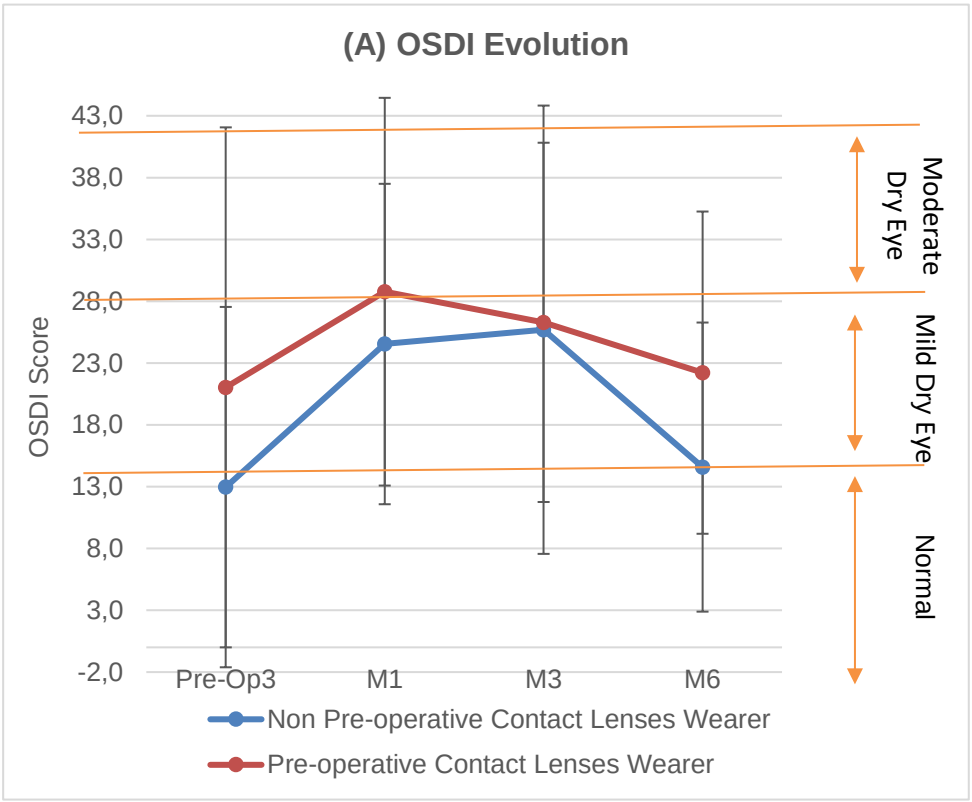

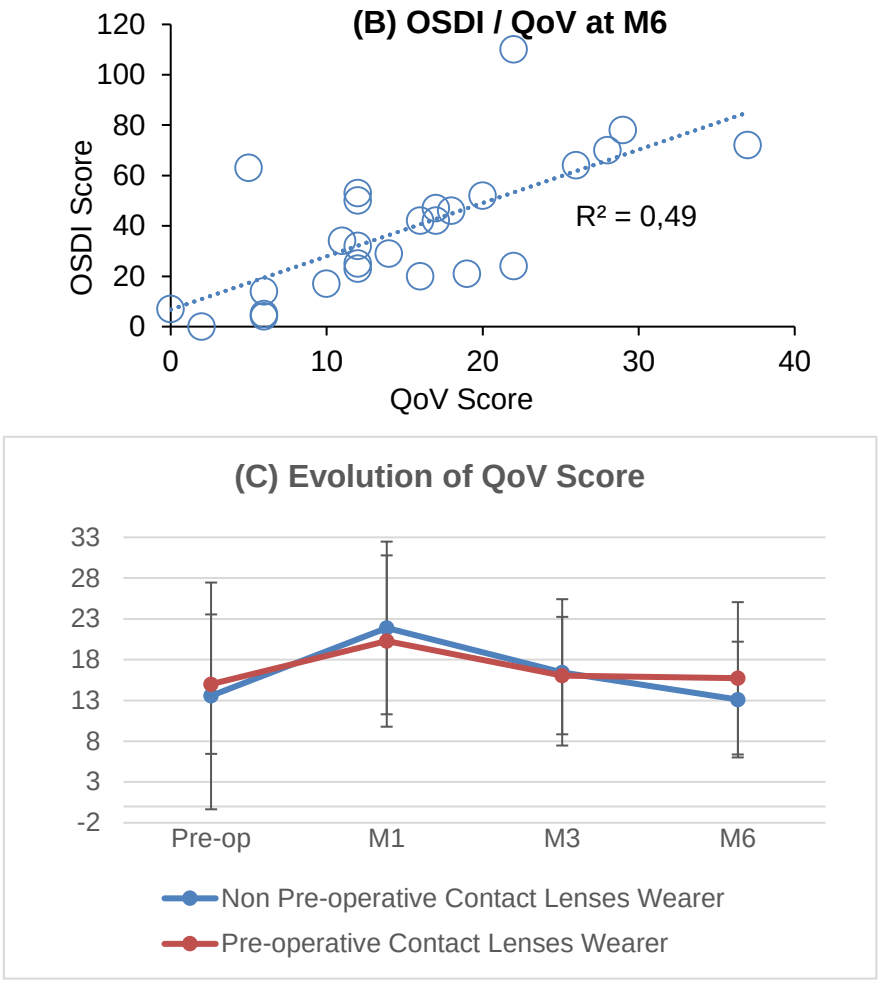

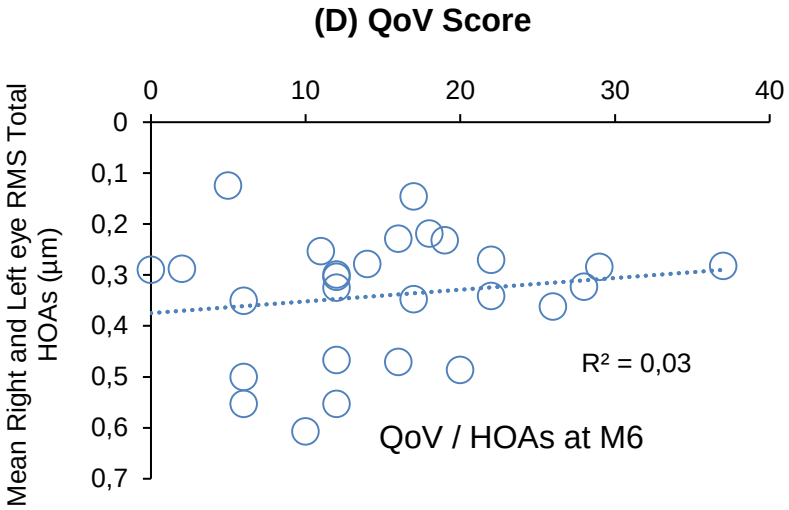

Figure 67 Evolution of QoV (A) and OSDI (C) scores and relationship between QoV score and OSDI score (B), and Total HOAs (D)

In both populations (preoperative contact lenses wearers and non-wearers) QoV score didn't change from preoperative level (paired t-test, p= 0.262). The same observation was made for the OSDI questionnaire although it increased, then decreased significantly between preoperative and 6 months postoperative foll ow-up (Figure 67A and 73C). Figure 67B and 67D show that 6 months after LASIK, dry eye symptoms were more related to the QoV score than corneal HOAs may explain the lower quality of vision. We found no correlation between the QoV score at 6 months follow-up and preoperative spherical equivalent (r^2= 0.0004, p<0.001).

6.5 Discussion

This study aims to explore the long-term post-myopic LASIK refractive surgery clinical results with the WaveLight® Refractive Suite (Alcon® Laboratories Inc., USA) by evaluating changes in anatomical parameters of the eye, visual performances and quality of vision. To the best of the author's knowledge, it does not exist much very exhaustive study that evaluates anatomical changes of the eye and reports outcomes for a myopic femtosecond LASIK performed with this Refractive Suite.

Anatomical changes

The mean corneal pachymetries were 575.08 ± 29.41 µm, 457.16 ± 68.59 µm, 479.42 ± 58.97 µm, 492.49 ± 53.18 µm, 495.03 ± 53.79 µm respectively preoperatively, one day, 1 Month, 3 Months and 6 months postoperatively. 6 Months postoperatively, the pachymetry was significantly lower than preoperatively (paired t test t = 15.03, *p*<0.001).

The pachymetry decreased noticeably on D1, then increased again until 6 months postoperatively. These results could be explained by the fact that the Orbscan IIz® (Bausch & Lomb®, USA) which allows the Scheimpflug system-based measurement of the corneal tomography largely underestimates the real thickness of the cornea at D1 because of the edema generated by the LASIK (Smadja, et al., 2012). Also, Smadja et al. (Smadja, et al., 2012) reported in 2012 that posterior steepening and a shift toward prolateness of the corneal posterior surface were observed very early after myopic LASIK, with a tendency to return toward the preoperative level between 1 month and 3 months. Finally, it is also described in the literature that there is an epithelial hyperplasia that occurs gradually a few weeks post LASIK (Reinstein, et al., Epithelial thickness profile changes induced by myopic LASIK as measured by

Artemis very high-frequency digital ultrasound, 2009) - (Reinstein, Archer, Gobbe, Silvermann, & Coleman, 2010), but actually, without impact on the keratometry in our study.

Six months after LASIK, the mean decrease in Keratometry was 3.76 ± 1.66 D while the mean decrease in pachymetry was 80.04 ± 41.26 µm. The difference in pachymetry at 6 Months postoperatively correlated positively ($r^2=0.74$, $p<0.001$) with the Mennerlyn Formula pachymetry estimation (Figure 59).

This means that the excimer laser dug in the centre more than the Mennerlyn formulae planes by a factor of 16% in our study. Indeed, as the Munnerlyn's formula does not consider possible variations in corneal asphericity; actual aspheric treatments induce a slightly different central ablation depth, allowing to maintain a level of post op Spherical aberration close to that preoperative (Krueger & Chan, 2012) - (Mrochen, Schelling, Wuellner, & Donitzky, 2009) - (Mrochen, et al., 2010) - (Mrochen, Donitzky, Wüllner, & Löffler, 2004).

One day after LASIK, the corneal asphericity expressed by the Q factor became significantly more oblate. (Q = -0.18 ± 0.10 (SD) (range -0.38 to 0.05) preoperatively and Q = 0.19 ± 0.30 (SD) (range -0.29 to 0.98) one day after surgery ($t = -9.52$, $P< 0.001$). There was no significant difference in Q factor in different moments post-surgery ($t = -0.31$, $P = 0.98$) (Figure 58B). Figure 64 show that even the asphericity changed, the spherical aberration calculated on a 5.5 mm pupil, increased very slightly (+0.034 ± 0,063). This result is very coherent with the higher digging of the central cornea to maintain a low level of positive spherical aberration induced by the surgery (Au & Krueger, 2012).

Otherwise, Figure 58C shows a decrease in IOPcc and IOPg from 14.84 ± 3.305 mmHg preoperatively to 11.71 ± 2.440 mmHg at 6-Months postoperative and from 15.42 ± 3.483 mmHg to 9.24 ± 2.671 mmHg respectively. The corneal indices of resistance and Hysteresis decreased significantly as shown in the same figure. There was a positive correlation between CRF and IOPg 6-Months postoperatively. ($R^2 =0.74$, $p<0.001$) (Figure 58D). IOPcc decreased by 3.13 mmHg 6 months postoperatively which is close to the standard deviation value (David, Stead, & Vernon, 2013).

Besides, Figure 58D shows that iop decrease seems de be related to the corneal resistance decrease due to the corneal flap cutting (Shin, Kim, Park, Yoon, & Lee, 2015).

This suggests that the measurement of the IOP post LASIK may be underestimated by approximately 3 mmHg compared to the real one.

The difficulty in this case is whether there is an effective decrease in the IOP or not. Indeed, it is possible that beside a decrease in the corneal resistance post Lasik, an effective (and partly) decrease of postoperative IOP may occur. In all cases, in ophthalmological practice, we recommend clinicians to systematically ask and check if their patients underwent LASIK. This may allow to better appreciate the underestimation of the IOP, especially for the follow-up and diagnosis of glaucomatous patients (Shin, Kim, Park, Yoon, & Lee, 2015).

Safety and Predictability

Quality of Vision outcomes

Figure 60 shows that after LASIK, Monocular 90% and 10% CDVA in corneal plane increased slightly but not significantly (paired-test t = 2.07, p=0.053 and t = 1.62, p=0.11 respectively), while Monocular Corrected contrast sensitivity and Corrected Sensitivity to Blur remained unchanged (paired-test t = -0.75, p=0.46 and t = -0.36, p=0.72 respectively). The CCS with glare was lower than the CCS by 0.1 u.log. These results were consistent with those in the literature (Kanellopoulos & Asimellis, Long-term bladeless LASIK outcomes with the FS200 Femtosecond and EX500 Excimer Laser workstation: the Refractive Suite, 2013) - (Tuan, 2006). However, regarding contrast sensitivity, it would have been preferable to study additional spatial frequencies. Indeed, Tuan et al. (Tuan, 2006) reported differences in outcomes between the different spatial frequencies. We have chosen to test only the one at 12 cpd to allow the patient to stay in comfortable conditions and not overly tired (and thus distort the results) due to the long examination sessions (2 hours).

Although there was no difference in quality of vision outcomes (CDVA and CSB) preoperatively between High (cylinder >=1.5D) and Low astigmatic eyes (cylinder< 1.50D) except for the CCS (where the high astigmatic eyes CCS was smaller than the low astigmatic one (ANOVA, p=0.016)), and no difference in 6 months postoperative residual SE, these eyes had a poorer postoperative CDVA and CCS. This may be due to under optimized astigmatism ablation profiles and/or nomogram of the excimer.

Refractive Spherical Equivalent Outcomes and astigmatism

The refractive spherical equivalent outcomes showed a very high predictability. Figure 61A and 61B display the accuracy of the laser nomogram (attempted corrected

spherical equivalent). It shows maximum residual SE of ± 0.75 D. These results are consistent with those reported previously by Kanellopoulos et al. (Kanellopoulos & Asimellis, Long-term bladeless LASIK outcomes with the FS200 Femtosecond and EX500 Excimer Laser workstation: the Refractive Suite, 2013). Besides, we found that the postoperative SE did not depend on the initial corrected SE, and that the High and low astigmatic eyes had the same residual SE. The 6 months post-operative refractive and corneal residual cylinder were low, and we did not find any correlation between preoperative refractive cylinder and 6 months post-operative cylinder. This suggest that this LASIK technique is predictable in all cases in our sample of eyes. However, we can notice that our sample did not include eyes with very high amount of astigmatism (maximum included -3.25 D).

Corneal and Total Aberrations analysis on a 5.5 mm pupil

Figure 63 and Table 25 show the very slight but significant increase in total, corneal and internal ocular aberrations after LASIK surgery. The most important increase in corneal and total HOAs seems to be attributed to the increase of corneal coma (Figure 64). Our results were comparable with those reported by Glydenkerne (Gyldenkerne, Ivarsen, & Hjortdal, 2015) on a 5 mm pupil. The increased amount of Coma may be induced by the 50% decentration towards the corneal vertex we planned for all patients. The total spherical Aberration increased very slightly but significantly (0,034 ± 0,063, $p<0.001$). These findings indicate that the WaveLight® Refractive Suite (Alcon® Laboratories Inc., USA) aspheric ablation profile seems to limit the increase in postoperative HOAs (Au & Krueger, 2012).

Again, our results were comparable with those described by Kruger et al. (Krueger & Chan, 2012), but highly different from those reported by Glydenkerne (Gyldenkerne, Ivarsen, & Hjortdal, 2015) and Buhren et al. (Bühren, et al., 2010), where the increase measured on a smaller pupil (5 mm) were respectively 0.15 ± 0,084 and 0.153 measured on a 6 mm pupil PMMA lenses that received excimer aspheric ablation profile. This is probably due to the less aspheric ablation profile of the used excimers. We found no correlations between total, corneal and Internal spherical aberrations after LASIK and preoperative spherical equivalent ($r^2=0.03$, $p<0.001$, $r^2=0.012$, $p<0.001$ and $r^2=0.009$, $p<0.001$ respectively), which is coherent with the optimized aspheric profile we mention previously.

However, we found a positive correlation between Total Preoperative HOAs and M6 postoperative HOAs (r2=0.573, p<0.001). Again, this is in favour of a minimal impact of excimer ablation on the increase of HOAs.

Finally, the internal aberrations can be computed by subtracting corneal from total aberration coefficients. Figure 63 and Table 25 show the internal aberrations before and after LASIK surgery. We found a very slight but significant increase in internal ocular aberrations studied (except for internal coma) after LASIK surgery. This increase was higher at D1 postoperatively, and then decreased between 1 and 6 months after surgery. In a previous study (Marcos, Barbero, Llorente, & Merayo-Lloves, 2001) - (Marcos, Barbero, Llorente, & Merayo-Lloves, 2001) made the same statement. They have then experienced in control subjects who had undergone a surgical procedure performed in two different experimental sessions (separated by at least 1 month, as in the surgical eyes) did not reveal statistically significant changes in the internal aberrations across sessions.

This indicated that possible changes across sessions in the accommodative state or decentrations of corneal topography data cannot account for the observed differences in the internal optics found between pre- and post-LASIK results. Therefore, we can conclude that these changes must be attributable to surgery, and specially to the changing shape of the posterior surface of the cornea (Marcos, Barbero, Llorente, & Merayo-Lloves, 2001) - (Smadja, et al., 2012).

Efficacy, Stability and Satisfaction

One day after LASIK surgery, the mean refractive spherical equivalent and keratometry were +0.14 ± 0.52 D and 40.49 ± 1.70 D respectively and kept stable up to 6 months follow-up (Figure 65).

6 months after surgery, 62% of eyes achieved High contrast UDVA of -0.1 log MAR or better versus 42% CDVA before undergoing LASIK. Uncorrected CCS seemed to be unchanged 6 months postoperatively, compared to the Corrected CCS in both normal and with glare illuminations conditions (Figure 66). Lasik surgery showed good outcomes in terms of efficacy and stability.

Besides, in both preoperative contact lenses wearers and non-wearers, QoV score didn’t change from preoperative level (paired t-test, p= 0.262). The same observation was made for the OSDI questionnaire although they increased, then decreased

significantly between preoperative and 6 months postoperative follow-up (Figure 67A and 67C). Figure 67B and 67D show that 6 months after LASIK, dry eye symptoms were more related to the QoV score than corneal HOAs and may explain the lower quality of vision. We found no correlation between the QoV score at 6 months follow-up and preoperative spherical equivalent ($r2= 0.0004$, $p<0.001$). Therefore, we can assume that the patients Quality of Vison depends more from the post-operative dry eye disease caused by LASIK than from the induced HOAs (which are low in this study) or the patients initial spherical equivalent correction.

We can then conclude that important anatomical changes in the eye occurred after LASIK surgery. Otherwise, LASIK surgery performed with FS200 femtosecond laser and EX500 excimer laser showed good outcomes. Therefore, we believe that some corneal and/or internal (posterior corneal surface) changes arising between D1 and M6 may limit the amount of residual refractive error to finally provide good vision 6 months after this refractive surgery. Our data was limited to the analysis of 6 months follow-up. Further studies are necessary to investigate the possible changing occurred after 6 months.

Conclusions and perspectives

Laser-assisted refractive surgery encompasses a set of surgical techniques aims at correcting refractive errors of the eye (myopia, hyperopia, astigmatism and presbyopia). It has recently established itself as a major sub-specialty of ophthalmology, the number of procedures being driven by the (i) significant increase in the prevalence of myopia in the world's population and (ii) the popularity of LASIK surgery which in its modern form is based on sophisticated femtosecond and excimer lasers.

Several studies in the 2000s reported satisfaction rates with patients of c. 90% after LASIK surgery. However, a number of recent studies report on dissatisfactions and point to issues to be addressed. The objective of this thesis was to provide practical recommendations to surgeons with the aim to optimize the outcome of their surgical routines and establish more personalized treatments. We have studied several little explored or unexplored topics:

- The pupil dynamics in different contexts of refractive corneal surgeries;
- The impact of the corneal epithelium on the topography of normal, keratoconus and keratoconus suspected corneas;
- The potential changes in the eye's anatomical parameters, visual performances and subjective quality of vision after a myopic LASIK surgery.

The most meaningful results achieved in our studies and implied practical recommendations are listed below:

- The measure of pupil diameters in photopic and mesopic condition provided by WaveLight® TopolyzerTM VARIO (Alcon ® Laboratories Inc., USA) were highly repeatable. One measure would therefore be sufficient to provide a useful value. However, in the case of a large distance between the pupil centre and the corneal vertex, we recommend repeating the measurements several times and removing aberrant results to increase the reliability of the measures and the efficacy of finding the exact centre of the pupil.
- Centration strategy is a crucial element for the success of a refractive surgery. Nowadays, some surgeons use the pupil center, which is visible under the laser during the photoablation as a reference to centre their treatment. We have found that the spatial shift of the pupil centre has a temporal direction as the

pupil dilates and is constantly small but can be important in a few patients. Whenever the centre of the pupil is considered for centering wavefront-customized laser ablation, our results suggest that the surgeon should adjust the laser illumination system's intensity until the pupil diameter value would be close to the pupil diameter measured at the time of wavefront acquisition. Constant lighting intensity should be maintained throughout the excimer laser deliverance.

Other surgeons centre their treatments on the corneal vertex (not visible by the surgeon during the procedure) or between the pupil centre and the corneal vertex. We have found that the mean distance between the pupil centre and the corneal vertex is greater in hyperopic eyes than in myopic eyes. This should be considered by the surgeon when determining his centration strategy.

- The mean pupil diameters under mesopic and photopic conditions decreased by approximately 300 µm three months after cataract surgery. The postoperative pupil diameter did not depend from the severity of cataract and could be predicted preoperatively, which can be useful to identify patients appropriate for specific types of multifocal IOLs.
- Our study allowed us to describe the shape of the epithelial and the Bowman layer surfaces in myopic eyes. Our findings suggest that in refractive procedures such as myopic PRK, the refractive contribution of the epithelium could be considered to improve predictability. This approach may be particularly relevant for trans epithelial PRK, where the mapping of the epithelial layer may improve the precision of the procedure. Prediction of epithelial healing processes could be important to evaluate as well.
- The epithelial layer tends to reduce more the magnitude of the Bowman layer's astigmatism, prolateness and irregularities in non keratoconic diagnosed corneas than in keratoconic ones.
- LASIK surgery performed with the WaveLight® Refractive Suite (Alcon® Laboratories Inc., USA) had good outcomes in our large sample of eyes. We believe that some corneal and/or internal (posterior corneal surface) changes arising between one day and 6 months may limit the amount of residual refractive error to finally provide good vision 6 months after LASIK surgery. Our data was limited to the analysis of 6 months follow-up.

This thesis opens the door to several follow-up studies. The centration strategy in LASIK is still a debated topic among surgeons, and a comparative study of the outcomes of the surgery performed on a large sample of eyes with different centration methods could prove interesting. Besides, regarding pupil dynamics in cataract surgery, further studies could focus on the optimal centration strategy for the IOL.

Also, further studies are necessary to investigate the role of the corneal epithelium in the quality of the retinal image. Besides, it could be useful to confirm our results regarding the role of the epithelium in refractive surgery on eyes with a more advanced stage of KC. Prediction of epithelial healing processes could be important to evaluate as well.

Finally, further studies are necessary to investigate the possible changes occurring 12 months or more after a myopic LASIK. We are currently analysing the outcomes of hyperopic LASIK surgery as well on a large sample of patients as a follow up to our study on the myopes.

Bibliography

(2018, April 28). Retrieved from www.dreamstime.com: fr.dreamstime.com/image-stock-structure-de-cornée-humaine-image29095451

Ambrósio, R., & Belin, M. (2010). Imaging of the Cornea: Topography vs Tomography. *J Refract Surg*, 26(11):847-849.

Applegate, R. (2004). Wevefront sensing, ideal corrections, and visual performance. *Optom Vis Sci*, 81: 167 - 77.

Applegate, R., Hilmantel, G., Howland, H., Tu, E., Starck, T., & Zayac, E. (2000). Corneal first surface optical aberrations and visual performance. *J Refract Surg*, 16(5):507-14.

Applegate, R., Sarver, E., & Khemsara, V. (2002). Are all aberrations equal ? *J Refract Surg*, 18:S556-62.

Applegate, R., Thibos, L., Bradley, A., & al., e. (2000). Reference axis selection: subcommittee report of the OSA working group to establish standards for measurement and reporting of optical aberrations of the eye. *J Refract Surg, 16(5)*(S656-S658).

Applegate, R., Thibos, L., Twa, M., & Sarver, E. (2009). Importance of fixation, pupil center, and reference axis in ocular wavefront sensing, videokeratography, and retinal image quality. *J Cataract Refract Surg, 35:139–152*.

Arbelaez, M., Vidal, C., & Arba-Mosquera, S. (2008). Clinical outcomes of corneal vertex versus central pupil references with aberration-free ablation strategies and LASIK. *Invest Ophthalmol Vis Sci, 49(12)*(5287-5294).

Aribaba, O., Adenekan, O., Onakoya, A., Rotimi-Samuel, A., Olatosi, J., Musa, K., . . . Akinsola, F. (2015, January). Central corneal thickness changes following manual small incision cataract surgery. *Clin Ophthalmol.*, 20;9:151-5.

Artal, P., & Navarro, R. (1994). Monochromatic modulation transfer function of the human eye for different pupil diameters: an analytical expression. *J Opt Soc Am A , 11(1)*(246-249).

Artal, P., Benito, A., & Tabernero, J. (2006). The human eye is an example of robust optical design. *J Vision, 6*(1-7).

Atchinson, D. (1991). Design of aspheric intraocular lenses. *Ophthalmic Physiol Opt, 11(2)*(137-146).

Atchinson, D., & Smith, G. (2002). *Optics of the Human Eye.* Edinburgh: Elsevier Science.

Atchison, D., & Smith, G. (2002). *Optics of the Human Eye.* Edinburgh: Elsevier Science.

Atchison, D., Fisher, S., Pedersen, C., & Ridall, P. (2005). Noticeable, troublesome and objectionable limits of blur. *Vision Res*, 45:1967-74.

Atchison, D., Guo, H., & Fisher, S. (2009). Limits of spherical blur determined with an adaptive optics mirror. *Ophthalmic Physiol Opt*, 29:300-11.

Au, J., & Krueger, R. (2012). Optimized Femto-LASIK Maintains Preexisting Spherical Aberration Independent of Refractive Error. *J Refract Surg*, 28(11):S821-S825.

Ba-Ali, S., Lund-Andersen, H., & Brøndsted, A. (2017, May). Cataract surgery affects the pupil size and pupil constrictions, but not the late post-illumination pupil response. *Acta Ophthalmol.*, 95(3):e252-e253.

Bach, M. (1996). The Freiburg Visual Acuity test--automatic measurement of visual acuity. *Optom Vis Sci*, 73(1):49-53.

Bahar, I., Levinger, S., & Kremer, I. (2006). Wavefront-supported photorefractive keratectomy with the Bausch & Lomb Zyoptix in patients with myopic astigmatism and suspected keratoconus. *J Refract Surg*, 22(6):533-8.

Bailey, M., Mitchell, G., Dhaliwal, D., Boxer Wachler, B., & Zadnik, K. (2003). Patient satisfaction and visual symptoms after laser in situ keratomileusis. *Ophthalmology*, 110(7):1371-8.

Barry, J., Branmann, K., & Dunne, M. (1997). Catoptric properties of eyes with misaligned surfaces studied by exact ray tracing. *Invest Ophtalmol Vis Sci, 38*(1476-1484).

Barry, J., Pongs, U., & Hillen, W. (1997). Algorithm for Purkinje images Iand IV and limbus centre localization. *Comput Biol Med, 27*(515-531).

Basmak, H., Sahin, A., Yildirim, N., Saricecek, T., & Yurdakul, S. (2007). The angle kappa in strabismic individuals. *Strabismus, 15(4)*(193-196).

Beckman, C., Thaung, J., & Sjöstrand, J. (n.d.). In-vitro lens scatter measurements and glare testing. *ARVO Annual Meeting .*

Benard, Y., Lopez-Gil, N., & Legras, R. (2011). Optimizing the subjective depth-of-focus with combinations of fourth- and sixth-order spherical aberration. *Vis Res*, 51:2471-7.

Berrio, E., Tabernero, J., & Artal, P. (2010). Optical aberrations and alignment of the eye with age. *J Vision, 10(14)*.

Biedermann, K. (2002). *Optical Information Processing: A Tribute to Adolf Lohmann, H. J. Caulfield,.* Bellingham, Washington, USA: SPIE PRESS.

Bilak, S., Simsek, A., Capkin, M., Guler, M., & Bilgin, B. (2015, April). Biometric and intraocular pressure change after cataract surgery. *Optom Vis Sci.*, 92(4):464-70.

Binder, P. (2008). Risk factors for ectasia after LASIK. *J Cataract Refract Surg*, 34(12):2010-1.

Binder, P., & Trattler, W. (2010). Evaluation of a risk factor scoring system for corneal ectasia after LASIK in eyes with normal topography. *J Refract Surg*, 26(4):241-50.

Birren, J., Casperson, R., & Botwinick, J. (1950). Age changes in pupil size. *J Gerontol , 5*(216-221).

Boettner, E., & Wolter, J. (1962). Transmission of the ocular media. *Invest. Ophtal.*, 1,776-83.

Boulnois, & JL. (1986, January). Photophysical processes in recent medical laser development: A review. *Lasers in ,edical science*, pp. 47-66.

British Standards Institution. (1994). *Accuracy (Trueness and Precision) of Measurement Methods and Results : General Principles and Definitions.* London: HMO BS ISO 5725 part 1.

Bueeler, M., & Mrochen, M. (2004). Limitations of pupil tracking in refractive surgery: systematic error in determination of corneal locations. *J Refract Surg, 20(4):371-8.*

Bueeler, M., Iseli, H., J. M., & Mrochen, M. (2005). Treatment-induced shifts of ocular reference axes used for measurement centration. *J Catarct Refract Surg.*, 31: 1986-1994.

Bühren, J., Kook, D., Yoon, G., & Kohnen, T. (2010). Detection of subclinical keratoconus by using corneal anterior and posterior surface aberrations and thickness spatial profiles. *Invest Ophthalmol Vis Sci*, 51(7):3424-32.

Bühren, J., Kühne, C., & Kohnen, T. (2005). Influence of pupil and optical zone diameter on higher-order aberrations after wavefront-guided myopic LASIK. *J Cataract Refract Surg*, 31(12):2272-80.

Bühren, J., Kühne, C., & Kohnen, T. (2007). Defining subclinical keratoconus using corneal first-surface higher-order aberrations. *Am J Ophthalmol*, 143(3):381-9.

Bühren, J., Nagy, L., Yoon, G., MacRae, S., Kohnen, T., & Huxlin, K. (2010). The Effect of the Asphericity of Myopic Laser Ablation Profiles on the Induction of Wavefront Aberrations. *Invest Ophthalmol Vis Sci*, 51(5): 2805–2812.

Bühren, J., Pesudovs, K., Martin, T., Strenger, A., Yoon, G., & Kohnen, T. (2009). Comparison of optical quality metrics to predict subjective quality of vision after laser in situ keratomileusis. *J Cataract Refract Surg*, 35(5):846-55.

Buscemi, P. (2002). Clinical applications of the OPD-Scan wavefront aberrometer/corneal topographer. *J Refract Surg*, 18(3 Suppl):S385-8.

Cammelin, M., Gambino, F., & Casaro, S. (2005). Measurement of the spatial shift of the pupil center. *J Cataract Refract Surg, 31*(1719-1721).

Campbell, F., & Gregory, A. (1960). Effect of pupil size on visual acuity. *Nature*, 187,1121-3.

Castejon-Mochon, J., Lopez-Gil, N., Benito, A., & P., A. (2002). Ocular wave-front aberration statistics in a normal young population. *Vision Res*, 42:1611-7.

Chang, A., Tsang, A., Contreras, J., Huynh, P., Calvano, C., Crnic-Rein, T., & Thall, E. (2003). Corneal tissue ablation depth and the Munnerlyn formula. *J Cataract Refract Surg*, 29(6):1204-10.

Chang, D., Campbell, J., Colin, J., & Schweitzer, C. (2014, April). Study Surgeon Group. Prospective masked comparison of intraoperative floppy iris syndrome severity with tamsulosin versus alfuzosin. *Ophthalmology*, 121(4):829-34.

Chayet, A., Assil, K., Montes, M., Espinosa-Lagana, M., Castellanos, A., & Tsioulias, G. (1998). Regression and its mechanisms after laser in situ keratomileusis in moderate and high myopia. *Ophthalmology*, 105(7):1194-9.

Chen, C., Izadshenas, A., Rana, M., & Azar, D. (2002). Corneal asphericity after hyperopic laser in situ keratomileusis. *J Cataract Refract Surg*, 28(9):1539-45.

Ciuffreda, K., Selenow, A., Wang, B., Vasudevan, B., Zikos, G., & Ali, S. (2006). “Bothersome blur”: A functional unit of blur perception. *Vision Res*, 46:895-901.

Cline, D., Hofstetter, H., & Griffin, J. (1989). *Dictionary of visual science.* Shilton Trade Book Publishing.

Corbett, M., Verma, S., O'Brart, D., Oliver, K., Heacock, G., & Marshall, J. (1996). Effect of ablation profile on wound healing and visual performance 1 year after excimer laser photorefractive keratectomy. *Br J Ophthalmol*, 80(3):224-34.

Cornsweet, T., & Crane, H. (1973). Accurate two dimensional eye tracker using first and fourth Purkinje images. *J Opt Soc Am A, 63*(921-928).

Crawford, B. (1936). The dependance of pupil size uppon external light stimulus under static and variable conditions. *Proc R Soc B, 121*(376-395).

Dausch, D., Klein, R., & Schröder, E. (1993). Excimer laser photorefractive keratectomy for hyperopia. *Refract Corneal Surg.*, 9:20-28.

David, V., Stead, R., & Vernon, S. (2013). Repeatability of ocular response analyzer metrics: a gender-based study. *Optom Vis Sci*, 90(7):691-9.

Deitz, M., & Sanders, D. (1985). Progressive hyperopia with long-term follow-up of radial keratotomy. *Arch Ophthalmol*, 103:782–784.

Deitz, M., Sanders, D., & Marks, R. (1984). Radial keratotomy: An overview of the Kansas City study. *Ophthalmology*, 91:467–478.

Deitz, M., Sanders, D., & Raanan, M. (1986). Progressive hyperopia in radial keratotomy. Long-term follow-up of diamond-knife and metal-blade series. *Ophthalmology*, 93:1284–1289.

Devgan, U. (2014). Target specific focal points to optimize refractive outcomes of cataract surgery. *Ocular Surgery News*.

Devries, S., & Baylor, D. (1997). Mosaic arrangement of ganglion cell receptive fields in rabbit retina. *J Neurophysiol*, 78(4):2048-60.

Doane, J., Cavanaugh, T., Durrie, D., & Hassanein, K. (1995). Relation of visual symptoms to topographic ablation zone decentration after excimer laser photorefractive keratectomy. *Ophthalmology*, 102:42-47.

Dolgin, E. (2015). The myopia boom. *Nature*, 276-278.

Dunaway, D., & Berger, I. (2007). Worldwide Distribution of Visual Refractive Errors and What to Expect at a Particular Location.

Dunne, M., Davies, L., Mallen, E., Kirchkamp, T., & Barry, J. (2005). Non invasive phakometric measurement of corneal and crystalline lens alignement in human eyes. *Ophthalmic Physiol Opt, 25(2)*(143-152).

DZ, R., RH, S., HFS, S., & SJ, C. (1999). Very high-frequency ultrasound corneal analysis identifies anatomic correlates of optical complications of lamellar refractive surgery; anatomic diagnosis in lamellar surgery. *Ophthalmology*, 106:474.

Elder, M., Murphy, C., & Sanderson, G. (1996). Apparent accommodation and depth of field in pseudophakia. *J Cataract Refract Surg.*, 22:615–619.

Emsley, H. (1952). *Visual Optics.* Butterworths.

Fadlallah, A., Fahed, D., Khalil, K., Dunia, I., Menassa, J., El Rami, H., . . . Fahed, S. (2011). Transepithelial photorefractive keratectomy: clinical results. *J Cataract Refract Surg.*, 37(10):1852-7.

Farah, S., Azar, D., Gurdal, C., & Wong, J. (1998). Laser in situ keratomileusis: Literature review of a developing technique. *J Cataract Refract Surg*, 24(7):989–1006.

Fay, A., Trokel, S., & Myers, J. (1992). Pupil diameter and the principal ray. *J Cataract Refract Surg, 18(4)*(348-351).

Febbraro, J., Wang, L., Borasio, E., Richiardi, L., Khan, H., Saad, A., . . . Koch, D. (2015, February). Astigmatic equivalence of 2.2-mm and 1.8-mm superior clear corneal cataract incision. *Graefes Arch Clin Exp Ophthalmol.*, 253(2):261-5.

Fedtke, C., Manns, F., & Ho, A. (2010). The entrance pupil of the human eye: a three dimensional model as a function of viewing angle. *Opt Soc Am, 18*(21).

Feng, Y., Varikooty, J., & Simpson, T. (2001). Diurnal variation of corneal and corneal epithelial thickness measured using optical coherence tomography. *Cornea*, 20:480-483.

Feng, Y., Varikooty, J., & Simpson, T. (2001). Diurnal variation of corneal and corneal epithelial thickness measured using optical coherence tomography. *Cornea*, 20(5):480-3.

Flanagan, G., & Binder, P. (2005). The theoretical vs. Measured laser resection for laser in situ keratomileusis. *J Refract Surg.*, 21:18-27.

Forrester, J., Dick, A., McMenamin, P., Roberts, F., & Pearlman, E. (2016). *The Eye.* Elsevier.

Fredrick, D. (2002). Myopia. *BMJ*.

Gatinel, D. (2018, April 28). Retrieved from www.gatinel.com.

Gatinel, D., & Bains, H. (2010). Treatment of highly aberrated eyes using the NIDEK CXIII excimer laser. *J Refract Surg.*, 26: 453-457.

Gatinel, D., Racine, L., & Hoang-Xuan, T. (2007). Contribution of the corneal epithelium to anterior corneal topography in patients having myopic photorefractive keratectomy. *J Cataract Refract Surg.*, 33:1860-1865.

Gobbi, P., Carones, F., Brancato, R., Carena, M., Fortini, A., Scagliotti, F., . . . Venturi, E. (1995). Automatic eye tracker for excimer laser photorefractive keratectomy. *Refract Surg, May-Jun;11(3 Suppl)*(S337-42).

Guirao, A., Porter, J., Williams, D., & Cox, I. (2002). Calculated impact of higher-order monochromatic aberrations on retinal image quality in a population of human eyes. *J Opt Soc Am A*, 19(1):1-9.

Gyldenkerne, A., Ivarsen, A., & Hjortdal, J. (2015). Comparison of corneal shape changes and aberrations induced By FS-LASIK and SMILE for myopia. *J Refract Surg*, 31(4):223-9.

Handzel, D., Briesen, S., Rausch, S., & Kälble, T. (2012, May). Cataract surgery in patients taking alpha-1 antagonists: know the risks, avoid the complications. *Dtsch Arztebl Int.*, 109(21):379-84.

Haque, S., Simpson, T., & Jones, L. (2006). Corneal and epithelial thickness in keratoconus: a comparison of ultrasonic pachymetry, Orbscan II, and optical coherence tomography. *J Refract Surg*, 22(5):486-93.

Harris, W. (1994). Dioptric strength: a scalar representation of dioptric power. *Ophthalmic Physiol Opt.*, 14: 216-218.

Harris, W. (2000, January). Astigmatism. *Ophthalmic Physiol Opt.*, 20(1):11-30.

Hayashi, K., & Hayashi, H. (2004, December). Pupil size before and after phacoemulsification in nondiabetic and diabetic patients. *J Cataract Refract Surg.*, 30(12):2543-50.

Hayashi, K., Hayashi, H., & Hayashi, F. (1995). Topographic analysis of the changes in corneal shape due to aging. *Cornea*, 14:527-532.

Hayashi, K., Hayashi, H., Nakao, F., & Hayashi, F. (1995). Correlation between pupillary size and intraocular lens decentration and visual acuity of a zonal-progressive multifocal lens and a monofocal lens. *Ophthalmology*, 108:2011–2017.

Hess, E. (1965). Attitude and pupil size. *Sci Am, 212(4)*(46-54).

Holladay, J., Piers, P., Koranyi, G., Van den Mooren, M., & Norrby, N. (2002). A new intraocular lens design to reduce spherical aberration of pseudophakic eyes. *J Refract Surg , 18*(683-692).

Huang, D., Tang, M., & Shekhar, R. (2003). Mathematical model of corneal surface smoothing after laser refractive surgery. *Am J Ophthalmol*, 135(3):267-78.

Huerva, F., & Ascaso, V. (2013). *The History of Cataract Surgery.*

IJspeert, J., d. W., van den Berg, T., & d. J. (1990). The intraocular straylight function in 129 healthy volunteers; dependence on angle, age and pigmentation. *Vision Research*, 699-707.

International Organisation for Standardization. (1994). *Accuracy (Trueness and Precision) of Measurement Methods and Results. Part 2. Basic Methods for the Determination of Repeatability and Reproducibility of a Standard Measurement Method.* Geneva, Switzerland.

International Organization for Standardization. (1977). *Statistics Vocabulary and Symbols.* Geneva, Switzerland: ISO 3534.

Ivanoff, A. (1956). About the Spherical Aberration of the Eye. *J Opt Soc Am, 46(10)*(901-903).

Jafri, B., Li, X., Yang, H., & Rabinowitz, Y. (2007). Higher order wavefront aberrations and topography in early and suspected keratoconus. *J Refract Surg*, 23(8):774-81.

Jenkins, T. (1963). Aberrations of the Eye and Their Effects on Vision. *Br J Physiol Opt, 20*(59-91).

Kanellopoulos, A., & Asimellis, G. (2013). Long-term bladeless LASIK outcomes with the FS200 Femtosecond and EX500 Excimer Laser workstation: the Refractive Suite. *Clin Ophthalmol*, 7: 261–269.

Kanellopoulos, A., & Asimellis, G. (2014, October). Clear-cornea cataract surgery: pupil size and shape changes, along with anterior chamber volume and depth changes. A Scheimpflug imaging study. *Clin Ophthalmol.*, 24;8:2141-50.

Kanellopoulos, A., & Binder, P. (2011). Management of corneal ectasia after LASIK with combined, same-day, topography-guided partial transepithelial PRK and collagen cross-linking: the athens protocol. *J Refract Surg*, 27(5):323-31.

Kanellopoulos, J. (2010). Innovations in femtosecond laser technology – the use of the WaveLight FS200 Laser for flap cutting during LASIK surgery. *European Ophthalmic Review*, 4:40-43.

Kanski, J. (1969). Mydriatics. *Br J Ophthalmol*, 53: 428-429.

Kermani, O., Oberheide, U., Schmeidt, K., Gerten, G., & Bains, H. (2009). Outcomes of hyperopic LASIK with the NIDEK NAVEX platform centered on the visual axis or line of sight. *J Refract Surg, 25 (1 Suppl)*(S98-S103).

Knorz, M., Wiesinger, B., Liermann, A., Seiberth, V., & Liesenhoff, H. (1998). Laser in situ keratomileusis for moderate and high myopia and myopic astigmatism. *Ophthalmology*, 105(5):932-40.

Koch, D., Jardeleza, T., Emery, J., & Franklin, D. (1986). Glare following posterior chamber intraocular lens implantation. *J Cataract Refract Surg.*, 12:480–484.

Koch, D., Samuelson, S., Haft, E., & Merin, L. (1991). Pupillary size and responsiveness; implications for selection of a bifocal intraocular lens. *Ophthalmology*, 98:1030–1035.

Kohnen, T. (2001). Measuring vision in refractive surgery. *J Cataract Refract Surg*, 27(12):1897-1898.

Kohnen, T., Bühren, J., Kühne, C., & Mirshahi, A. (2004). Wavefront-guided LASIK with the Zyoptix 3.1 system for the correction of myopia and compound myopic astigmatism with 1-year follow-up: clinical outcome and change in higher order aberrations. *Ophthalmology*, 111(12):2175-85.

Kohnen, T., Kuhne, C., & B. J. (2007). The future role of wavefront-guided excimer ablation. *Graefes Arch Clin Ophtalmol*, 245:189-194.

Komatsu, M., Oono, S., & Shimizu, K. (1997). The effects of phaco-emulsification-aspiration and intra-ocular lens implantation on the pupil: pupillographic and pharmacologic study. *Ophthalmologica*, 211(6):332-7.

Krueger, R., & Chan, P. (2012). Introduction to Commercially Approved Customized Ablation: Tenth Year in Review. *J Refract Surg*, 28(11):S813-S814.

Krueger, R., & Kanellopoulos, A. (2010). Stability of simultaneous topography-guided photorefractive keratectomy and riboflavin/UVA cross-linking for progressive keratoconus: case reports. *J Refract Surg*, 26(10):S827-32.

Kuang-mon, A., & Liang, J. (2006). Improved contrast sensitivity and visual acuity after wavefront-guided laser in situ keratomileusis: in-depth statistical analysis[J].Journal of cataract and refractive surgery. *J Cataract Refract Surg*, 32(2):215-220.

Kymionis, G., Kontadakis, G., Kounis, G., Portaliou, D., Karavitaki, A., Magarakis, M., . . . Pallikaris, I. (2009). Simultaneous topography-guided PRK followed by corneal collagen cross-linking for keratoconus. *J Refract Surg*, 25(9):S807-11.

Lee, A. (2016). Explain how intraocular lens design can influence progression of posterior capsule opacification following cataract surgery.

Lieberman, H., & Pentland, A. (1982). Microcomputer-based estimation of psychophysical thresholds: The bestPest. *Behavior Research Methods, Instruments & Computers*, 21-25.

Lotfi, A., & Grandin, J. (2010). Intracorneal ring segments implanted with femtosecond laser can treat keratoconus. *Ocular Surgery News*.

Lowenfeld, I. (1993). *The Pupil. Anatomy, Physiology, and Clinical Applications,* (Vol. 1 and 2). Iowa State University Press.

Lubatschowski, H. (2008). Overview of commercially available fem¬tosecond lasers in refractive surgery. *J Refract Surg*, 24(1): S102–S107.

MacRae, S., & Fujieda, M. (2000). Slit skiascopic-guided ablation using the Nidek laser. *J Refract Surg*, 16(5):S576-80.

MacRae, S., Schwiegerling, J., & Snyder, R. (1999). Customized and low spherical aberration corneal ablation design. *J Refract Surg*, 15(2 Suppl):S246-8.

Maloney, R. (1990). Corneal topography and optical zone location in photorefractive keractectomy. *Refract Corneal Surg, 6*(363-371).

Mamalis, N. (2004). Quality of vision. *J Cataract Refract Surg*, 30(3):529-530.

Mandell, R., Chiang, C., & Klein, S. (1995). Location of the major corneal reference points. *Optom Vis Sci, 72*(776-784).

Manzanera, S., Prieto, P., B. A., T. J., & A. P. (2015). Location of achromatizing pupil position and first Purkinje reflection in a normal population. *Invest Ophthalmol Vis Sci*, 56(2):962-6.

Marcos, S. (2001). Aberrations and visual performance following standard laser vision correction. *J Refract Surg*, 17(5):S596-601.

Marcos, S., Barbero, S., Llorente, L., & Merayo-Lloves, J. (2001). Optical Response to LASIK Surgery for Myopia from Total and Corneal Aberration Measurements. *IOVS*, 42.

Martinez, C., Applegate, R., Klyce, S., McDonald, M., Medina, J., & Howland, H. (1998). Effect of pupillary dilation on corneal optical aberrations after photorefractive keratectomy. *Arch Ophtalmol , 116*(1053-1062).

Masket, S. (1992). Relationship between postoperative pupil size and disability glare. *J Cataract Refract Surg.*, 18:506–507.

McAlinden, C., Pesudovs, K., & Moore, J. (2010). The development of an instrument to measure quality of vision: the Quality of Vision (QoV) questionnaire. *Invest Ophthalmol Vis Sci*, 51(11):5537-45.

McCormick, G., Porter, J., Cox, I., & MacRae, S. (2005). Higher Order Aberrations in Eyes with Irregular Corneas After Laser Refractive Surgery . *Ophtalmology*, 112: 1699-1709.

Millodot, M. (1993). *Dictionary of Optometry and Visual Science.* Butterworth-Heinmann.

Moller, D., Buchholz, I., & Huebscher, H. (2000). Pupil physiology after cataract surgery. *Ophthalmologe*, 97: 264–267.

Mrochen, M., Donitzky, C., Wüllner, C., & Löffler, J. (2004). Wavefront-optimized ablation profiles: theoretical background. *J Cataract Refract Surg*, 30(4):775-85.

Mrochen, M., Schelling, U., Wuellner, C., & Donitzky, C. (2009). Influence of spatial and temporal spot distribution on the ocular surface quality and maximum ablation depth after photoablation with a 1050 Hz excimer laser system. *J Cataract Refract Surg*, 35(2): 363-373.

Mrochen, M., Wüllner, C., Krause, J., Klafke, M., Donitzky, C., & Seiler, T. (2010). Technical aspects of the WaveLight FS200 femtosecond laser. *J Refract Surg*, 26(10):S833-40.

Muftuoglu, O., & Erdem, U. (2008). Evaluation of internal refraction with the optical path difference scan. *Ophthalmology*, 115(1):57-66.

Nakamura, K., Bissen-Miyajima, H., & T. I. (2001). Effect of laser in situ keratomileusis correction on contrast visual acuity. *J Cataract Refract Surg*, 27:357–361.

Nakazawa, M., & Ohtsuki, K. (1983). Apparent accommodation in pseudophakic eyes after implantation of posterior chamber intraocular lenses. *Am J Ophthalmol.*, 96:435–438.

Nakazawa, M., & Ohtsuki, K. (1984). Apparent accommodation in pseudophakic eyes after implantation of posterior chamber intraocular lenses: optical analysis. *Invest Ophthalmol Vis Sci*, 25:1458–1460.

Netto, M., Dupps, W., & Wilson, S. (2006). Wavefront-guided ablation: evidence for efficacy compared to traditional ablation. *Am J Ophtalmol*, 141(2):360-368.

Niemz, M. (2004). *Laser-Tissue Interactions.* Berlin: Springer.

Obara, Y., Hashi, H., Tonaki, M., & Yoshida, S. (1989). Causes of binocular dysfunction in pseudophakic eyes [Japanese]. *Jpn IOL Soc. J.*, 3:59–63.

O'Brart, D., Corbett, M., Lohmann, C., Kerr Muir, M., & Marshall, J. (1995). The effects of ablation diameter on the outcome of excimer laser photorefractive keratectomy. A prospective, randomized, double-blind study. *Arch Ophthalmol*, 113(4):438-43.

O'Brart, D., Corbett, M., Verma, S., Heacock, G., Oliver, K., Lohmann, C., . . . Marshall, J. (1996). Effects of ablation diameter, depth, and edge contour on the outcome of photorefractive keratectomy. *J Refract Surg*, 12(1):50-60.

Okamoto, S., Kimura, K., Funakura, M., Ikeda, N., Hiramatsu, H., & Bains, H. (2011). Comparison of avefront guided aspheric laser in situ keratomilesis for myopia: coaxially sighted corneal-ligh-reflex versus line-of-sight centration. *J Cataract Refract Surg, 37(11)*(1951-1960).

Ortiz, D., Alió, J., Illueca, C., Mas, D., Sala, E., Pérez, J., & Espinosa, J. (2007). Optical analysis of presbyLASIK treatment by a light propagation algorithm. *J Refract Surg*, 23(1):39-44.

Osterberg, G. (1935). Topography of the layer of rods and cones in the human retina. *Acta Ophthalmologica Supplement*, 6:1-103.

Pallikaris, I., Papatzanaki, M., Stathi, E., Frenschock, O., & Georgiadis, A. (1990). Laser in situ keratomileusis. *Lasers Surg Med*, 10(5):463-8.

Pande, M., & Hillman, J. (1993). Optical zone centration in keratorefractive surgery. Entrance pupil center, visual axis, coaxially sighted corneal reflex, or geometric corneal center? *Ophtalmology , 100*(1230-1237).

Park, C., Oh, S., & Chuck, R. (2012). Measurement of angle kappa and centration in refractive surgery. *Curre Opin Ophtalmol, 23(4)*(269-275).

Patel, S., Reinstein, D., Silverman, R., & Coleman, D. (1998). The shape of Bowman's layer in the human cornea. *J Refract Surg.*, 14:636-640.

Pepose, J., & Applegate, R. (2005). Making sense out of wavefront sensing. *Am J Ophthalmol*, 139(2):335-343.

Piermarocchi, S., Sartore, M., Bandello, F., Lanzetta, P., & Brancato, R. (n.d.).

Piermarocchi, S., Sartore, M., Bandello, F., Lanzetta, P., Brancato, R., Garattini, L., . . . Varano, M. (2006). Quality of vision: a consensus building initiative for a new ophthalmologic concept. *Eur J Ophtalmol*, 16: 851-860.

Pietilä, J., Mäkinen, P., Pajari, S., & Uusitalo, H. (1997). Excimer laser photorefractive keratectomy for hyperopia. *J Refract Surg*, 13(6):504-10.

Raasch, T. (1995). Spherocylindrical refractive errors and visual acuity. *Optom Vis Sci.*, 72:272-275.

Randleman, J., Trattler, W., & Stulting, R. (2008). Validation of the Ectasia Risk Score System for preoperative laser in situ keratomileusis screening. *Am J Ophthalmol*, 145(5):813-8.

Randleman, J., Woodward, M., Lynn, M., & Stulting, R. (2008). Risk assessment for ectasia after corneal refractive surgery. *Ophthalmology*, 115(1):37-50.

Ravalico, G., Baccara, F., & Bellavitis, A. (1992). Refractive bifocal intraocular lens and pupillary diameter. *J Cataract Refract Surg.*, 18:594–597.

Read, S., Collins, M., Carney, L., & Franklin, R. (2006). The topography of the central and peripheral cornea. *Invest Ophthalmol Vis Sci.*, 47:1404-1415.

(2017). *Refractive surgery report: a global market analysis for 2016 to 2022.* Market Scope.

Reinstein DZ, ,. A., & Gobbe, M. (2009). Corneal epithelial thickness profile in the diagnosis of keratoconus. *J Refract Surg*, 25(7):604-10.

Reinstein, D., & Cremonesi, E. (2002). Should LASIK sphero-cylindrcal treatments be centred on the pupil? Presented at: International Society of Refractive Surgery Annual Meeting. Orlando FL.

Reinstein, D., & Silverman, R. (2004). Very high-frequency digital ultrasound: Artemis 2 scanning in LASIK. *Probst LE, ed, LASIK; Advances, Controversies, and Custom*, pp. 23-41.

Reinstein, D., Archer, T., Gobbe, M., Silverman, R., & Coleman, D. (2008). Epithelial thickness in the normal cornea: three-dimensional display with Artemis very high-frequency digital ultrasound. *J Refract Surg*, 24(6):571-81.

Reinstein, D., Archer, T., Gobbe, M., Silvermann, R., & Coleman, D. (2010). Epithelial thickness after hyperopic LASIK: three-dimensional display with Artemis very high-frequency digital ultrasound. *J Refract Surg.*, 26:555-564.

Reinstein, D., Carp, G., Archer, T., Lewis, T., Gobbe, M., Moore, J., & Moore, T. (2016). Long-term Visual and Refractive Outcomes After LASIK for High Myopia and Astigmatism From -8.00 to -14.25 D. *J Refract Surg*, 32(5):290-7.

Reinstein, D., Gobbe, M., & Archer, T. (2013). Coaxially sighted corneal light reflex versus entrance pupil center centration of hyperopic corneal ablations in eyes with small and large angle kappa. *J Refract Surg, Aug; 29 (8) : 518-525*.

Reinstein, D., Gobbe, M., Archer, T., Silverman, R., & Coleman, D. (2010). Epithelial, stromal, and total corneal thickness in keratoconus: three-dimensional display with artemis very-high frequency digital ultrasound. *J Refract Surg*, 26(4):259-71.

Reinstein, D., Silverman, R., & Coleman, D. (1993). High-frequency ultrasound measurement of the thickness of the corneal epithelium. *Refract Corneal Surg.* , 9:385-387.

Reinstein, D., Silverman, R., & Coleman, D. (1993). High-frequency ultrasound measurement of the thickness of the corneal epithelium. *Refract Corneal Surg*, 9(5):385-7.

Reinstein, D., Silverman, R., Sutton, H., & Coleman, D. (1999). Very high-frequency ultrasound corneal analysis identifies anatomic correlates of optical complications of lamellar refractive surgery: anatomic diagnosis in lamellar surgery. *Ophthalmology*, 106(3):474-82.

Reinstein, D., Srivannaboon, S., Gobbe, M., Archer, T., Silvermann, R., & Coleman, D. (2009). Epithelial thickness profile changes induced by myopic LASIK as measured by Artemis very high-frequency digital ultrasound. *J Refract Surg.*, 25:444-450.

Reinstein, D., Srivannaboon, S., Gobbe, M., Archer, T., Silvermann, R., & Coleman, D. (2009). Epithelial thickness profile changes induced by myopic LASIK as measured by Artemis very high-frequency digital ultrasound. *J Refract Surg*, 25:444-450.

Rio, D. (2016). Optimisation des optiques bifocales destinées à la correction de la presbytie.

Roberts, C. (2000). The cornea is not a piece of plastic. *J Refract Surg*, 16: 407-413.

Saad, A., & Gatinel, D. (2010). Topographic and tomographic properties of forme fruste keratoconus corneas. *Invest Ophthalmol Vis Sci*, 51(11):5546-55.

Saad, A., & Gatinel, D. (2016). Combining Placido and Corneal Wavefront Data for the Detection of Forme Fruste Keratoconus. *J Refract Surg*, 32(8):510-6.

Saad, A., Lteif, Y., Azan, E., & Gatinel, D. (2010). Biomechanical properties of keratoconus suspect eyes. *Invest Ophthalmol Vis Sci*, 51(6):2912-6.

Saad, A., Saab, M., & Gatinel, D. (2010). Repeatability of measurements with a double-pass system. *J Catarct Refract Surg.*, Vol. 36, 28-33.

Salah-Mabed, I., Saad, A., & Gatinel, D. (2016). Topography of the corneal epithelium and Bowman layer in low to moderately myopic eyes. *J Cataract Refract Surg*, 42(8):1190-7.

Salah-Mabed, I., Saad, A., Guilbert, E., & Gatinel, D. (2014). Measurement of pupil center shift in refractive surgery candidates with caucasian eyes using infrared pupillometry. *J Refract Surg.*, 30(10): 694-700.

Salz, J., & Stevens, C. (2002). LASIK correction of spherical hyperopia, hyperopic astigmatism, and mixed astigmatism with the LADARVision excimer laser system. *Ophthalmology, 109:1647–1656*.

Saw, S., Carkeet, A., Chia, K., Stone, R., & Tan. (2002). *D. T. Ophthalmology*, 109,2065-2071.

Sawelson, H., & Marks, R. (1987). Three-year results of radial keratotomy. *Arch Ophthalmol*, 105:81–85.

Schiffman, R., Christianson, M., Jacobsen, G., Hirsch, J., & Reis, B. (2000). Reliability and validity of the Ocular Surface Disease Index. *Arch Ophthalmol*, 118(5):615-21.

Schwiegerling, J. (Aug, 2013). Eye Axes and Their Relevance to Alignment of Corneal Refractive Procedures. *J Refract Surg*(29(8):515-6).

Schwiegerling, J., & Snyder, R. (1998). Custom photorefractive keratectomy ablations for the correction of spherical and cylindrical refractive error and higher-order aberration. *J Opt Soc Am A Opt Image Sci Vis*, 15(9):2572-9.

Seiler, T., Genth, U., Holschbach, A., & Derse, M. (1993). Aspheric photorefractive keratectomy with excimer laser. *Refract Corneal Surg*, 9(3):166-72.

Seiler, T., Kaemmerer, M., Mierdel, P., & Krinke, H. (2000). Ocular optical aberrations after photorefractive keratectomy for myopia and myopic astigmatism. *Arch Ophthalmol*, 118(1):17-21.

Sharpe, L. T., Stockman, A., Jagla, W., & Jägle, H. (2005). A luminous efficiency function, V*(λ), for daylight adaptation. *Journal of Vision*, Vol.5, 3. doi:10.1167/5.11.3 .

Shin, J., Kim, T., Park, S., Yoon, M., & Lee, J. (2015). Changes in Biomechanical Properties of the Cornea and Intraocular Pressure After Myopic Laser In Situ Keratomileusis Using a Femtosecond Laser for Flap Creation Determined Using Ocular Response Analyzer and Goldmann Applanation Tonometry. *J Glaucoma.*, 24(3):195-201.

Simon, G., Ren, Q., Kervick, G., & Parel, J.-M. (1993). Optics of the corneal epithelium. *Refract Corneal Surg.*, 9:42-50.

Smadja, D., Santhiago, M., Mello, G., Roberts, J., Dupps, W., & Krueger, R. (2012). Response of the posterior corneal surface to myopic laser in situ keratomileusis with different ablation depths. *J Cataract Refract Surg*, 38(7): 1222-1231.

SNOF. (n.d.). Retrieved from www.snof.org.

Solomon, K., Fernández de Castro, L., Sandoval, H., Biber, J., Groat, B., Neff, K., . . . Force, J. L. (2009). LASIK world literature review: quality of life and patient satisfaction. *Ophthalmology*, 116(4):691-701.

Tabernero, J., & Artal, P. (2012). Optical modeling of a corneal inlay in real eyes to increase depth of focus: optimum centration and residual defocus. *J Cataract Refract Surg*, 38(2):270-7.

Tabernero, J., Atchinson, D., & Markwell, E. (2009). Aberrations and pupil location under corneal topography and Hartmann-Shack illumination conditions. *Invest Ophtalmol Vis Sci, 50(4)*(1964-1970).

Tahzib, N., Bootsma, S., Eggink, F., Nabar, V., & Nuijts, R. (2005). Functional outcomes and patient satisfaction after laser in situ keratomileusis for correction of myopia. *J Cataract Refract Surg*, 31(10):1943-51.

Theodossiadis, P., Achtsidis, V., Theodoropoulou, S., Tentolouris, N., Komninos, C., & Fountas, K. (2012, April). The effect of alpha antagonists on pupil dynamics: implications for the diagnosis of intraoperative floppy iris syndrome. *Am J Ophthalmol.*, 153(4):620-6.

Thibos, L. (1995). How to Measure Chromatic Aberration and Locate Useful Reference Axes of the Human Eye. Presented at OSA '95 meeting. Portland, OR.

Thibos, L., & Hong, X. (1999). Clinical applications of the Shack-Hartmann aberrometer. *Optom Vis Sci*, 76(12):817-25.

Thibos, L., & Horner, D. (2001). Power vector analysis of the optical outcome of refractive surgery. *J Cataract Refract Surg.*, 27:80-85.

Thibos, L., Applegate, R., Schwiegerling, J., Webb, R., & Members, V. S. (2002). Standards for reporting the optical aberrations of eyes. *J Refract Surg*, 18(5):S652-60.

Thibos, L., Wheeler, W., & Horner, D. (1997). Power vectors: an application of fourier analysis to the description and statistical analysis of refractive error. *Optom Vis Sci.*, 74:367-375.

Touboul, D., Trichet, E., Binder, P., Praud, D., Seguy, C., & Colin, J. (2012). Comparison of front-surface corneal topography and Bowman membrane specular topography in keratoconus. *J Cataract Refract Surg.*, 38:1043-1049.

Tsai, R. (1997). Laser in situ keratomileusis for myopia of -2 to -25 diopters. *J Refract Surg*, 13(5 Suppl):S427-9.

Tuan, K. (2006). Visual experience and patient satisfaction with wavefront-guided laser in situ keratomileusis. *J Cataract Refract Surg*, 32(4):577-83.

Twa, M., Bailey, M., Hayes, J., & Bullimore, M. (2004, February). Estimation of pupil size by digital photography. *J Cataract Refract Surg.*, 30(2):381-9.

Twa, M., Lembach, R., Bullimore, M., & Roberts, C. (2005). A prospective randomized clinical trial of laser in situ keratomileusis with two different lasers. *Am J Ophthalmol*, 140(2):173-83.

Uozato, H., & Guyon, D. (1987). Centering corneal surgical procedures. *Am J Ophthalmol.*, 103:264-275; correction, 852.

Venkateswaran, K., Roorda, A., & Romero-Borja, F. (2004 Jan-Feb). Theoretical modeling and evaluation of the axial resolution of the adaptive optics scanning laser ophthalmoscope. *J Biomed Opt*, 9(1):132-8.

Vesaluoma, M., Pérez-Santonja, J., Petroll, W., Linna, T., Alió, J., & Tervo, T. (2000). Corneal stromal changes induced by myopic LASIK. *Invest Ophthalmol Vis Sci*, 41(2):369-76.

Vinas, M. (2015). Polychromatic Adaptive Optics to evaluate the impact of manipulated optics on vision.

Vos, J. (1963). Contribution of the fundus oculi to entropic scatter. *J. Opt. Soc. Am.*, 53: 1449-1451.

Vos, J., & Boogard, J. (1963). Contribution of the cornea to entropic scatter. *J. Opt. Soc. Am*, 53: 869-873.

Wachler, B., & Krueger, R. (1999, February). Agreement and repeatability of infrared pupillometry and the comparison method. *Ophthalmology*, 106(2):319-23.

Wachler, B., & Krueger, R. (2000, January). Agreement and repeatability of pupillometry using videokeratography and infrared devices. *J Cataract Refract Surg.*, 26(1):35-40.

Walsh, G. (1988). The effect of mydriasis on the pupillary centration of the human eye. *Ophtalmic Physiol. Opt., 8*(178 - 182).

Walsh, G., & Charman, W. (1988). The effect of pupil centration and diameter on ocular performance. *Vision Res, 28*(659-665).

Walsh, G., & Charman, W. N. (1988). The effect of pupil centration and diameter on ocular performance. *Vision Res, 28*(659-665).

Wang, M., Corpuz, C., Huseynova, T., & Tomita, M. (2016, February). Pupil Influence on the Visual Outcomes of a New-Generation Multifocal Toric Intraocular Lens With a Surface-Embedded Near Segment. *J Refract Surg.*, 32(2):90-5.

Wang, Q., S. G., H. K., Xu, Z., Feng, Y., Wen, D., . . . Huang, J. (2012). A comprehensive assessment of the precision and agreement of of anterior corneal power measurements obtained using 8 different devices. PLoS One. *PLoS One*.

Westheimer, G. (2008). Directional sensitivity of the retina: 75 year of Stiles-Crawford effect. *Proc. R. Soc. B*, 275: 2777–2786.

Wethmeimer, G. (1970). Image quality in the human eye. *Optica Acta, 17*(641-658).

Wilson, M., Campbell, M., & Simonet, P. (1992). Change of pupil centration with change of illumination and pupil size. *Optom. Vis. Sci., 69*(129-136).

Winkler von Mohrenfels, C. (2012). First clinical results with a new 200 kHz femtosecond laser system. *Br J Ophthalmol*, 96:788-792.

Winn, B., Whitaker, D., Eliot, D., & Phillips, N. (1994). Factors affecting light-adapted pupil size in normal human subjects. *Invest Ophtal Vis Sci, 35*(1132-1137).

Wolf-Schnurrbusch, U., Ceklic, L., Brinkmann, C., Iliev, M., Frey, M., Rothenbuehler, S., . . . Wolf, S. (2009). Macular Thickness Measurements in Healthy Eyes Using Six Different Optical Coherence Tomography Instruments. *IOVS*.

Wyatt, H. (1995). The form of the human pupil. *Vision Res, 35*(2021-2036).

Yang, Y., Thompson, K., & Burns, S. (2002). Pupil location under medopic, photopic and pharmacologically dilated conditions. *Invest Ophtalmol Vis Sci, 43*(2508-2512).

Yoon, G., & Williams, D. (2002). Visual performance after correcting the monochromatic and chromatic aberrations of the eye. *Journal of Optical Society of America A, Optics, Image Science, and Vision*, 19:266–275.

Yvon, C., Archer, T., Gobbe, M., & Reinstein, D. (2015). Comparison of higher-order aberration induction between manual microkeratome and femtosecond laser flap creation. *J Refract Surg*, 31(2): 130-135.

Zadnik, K., Steger-May, K., Fink, B., Joslin, C., Nichols, J., Rosenstiel, C., . . . Schechtman, K. (2002). Between-eye asymmetry in keratoconus. *Cornea*, 21(7):671-9.

Zipper, S., Manns, F., & Fernandez, V. (2001). Corneal modelling using conic section fits of PAR corneal topography system measurements. *Ophthalmic Technologies XI, Proceedings SPIE 4245*, pp. 107-112.

SYNTHESE

Titre : Descriptions anatomiques et méthodologiques aux fins d'optimisation de techniques de chirurgie cornéenne à visée Réfractive

Mots clés : Chirurgie réfractive, Cornée, LASIK, PKR, Pupille, Epithélium, Myopie

La chirurgie réfractive laser assistée englobe un ensemble de techniques chirurgicales visant à corriger les erreurs de réfraction de l'œil. Elle s'est récemment imposée comme une sous-spécialité majeure de l'ophtalmologie, notamment grâce à l'utilisation de lasers sophistiqués femtoseconde et excimer. Plusieurs études dans les années 2000 ont rapporté des taux de satisfaction chez les patients de c. 90% après chirurgie LASIK. Toutefois, de nombreuses études récentes font état d'insatisfactions et signalent des problèmes à résoudre. L'objectif de cette thèse était de fournir des recommandations pratiques aux chirurgiens dans le but d'optimiser les résultats de leurs routines chirurgicales et d'établir des traitements plus personnalisés. Nous avons étudié plusieurs sujets peu ou inexplorés dans la littérature :

• la dynamique pupillaire dans différents contextes de chirurgie réfractive ;

• L'impact de l'épithélium cornéen sur la topographie de la cornée normale, kératoconique ou kératoconique suspecte ;

• Les changements potentiels dans les paramètres anatomiques, les performances visuelles et la qualité subjective de l'œil après une chirurgie de LASIK myopique.

Les résultats les plus significatifs obtenus dans nos études et les recommandations pratiques qui en découlent sont énumérés ci-dessous :

• La mesure des diamètres de pupille dans des conditions photopiques et mésopiques fournies par WaveLight® TopolyzerTM VARIO (Alcon® Laboratories Inc., États-Unis) était hautement répétable. Une mesure suffirait donc à fournir une valeur utile.

Cependant, dans le cas où il existe une grande distance entre le centre de la pupille et le sommet de la cornée, nous recommandons de répéter les mesures plusieurs fois et d'éliminer les résultats aberrants pour accroître la fiabilité des mesures et l'efficacité de la recherche du centre exact de la pupille.

• La stratégie de centrage est un élément crucial pour le succès d'une chirurgie réfractive. A ce jour, certains chirurgiens utilisent le centre de la pupille, qui est visible sous le laser lors de la photoablation comme référence pour centrer leur traitement. Nous avons montré que le centre de la pupille se déplacait selon la direction temporale lorsque la pupille se dilate. Ce déplacement est mince mais peut être important chez certains patients.

A chaque fois que le centre de la pupille est choisi pour centrer un traitement « wavefront-customized », nos résultats suggèrent que le chirurgien doit ajuster l'intensité du système d'éclairement jusqu'à ce que le diamètre de la pupille soit proche de celui mesuré au moment de l'aquisition du front d'onde. Une intensité lumineuse constante doit être maintenue tout au long de la délivrance du laser excimer. D'autres chirurgiens centrent leurs traitements sur le vertex cornéen (non visible par le chirurgien au cours de l'intervention) ou entre le centre de la pupille et le vertx. Nous avons trouvé que la distance moyenne entre le centre de la pupille et le vertex est plus grande chez les yeux hyperopes que chez les yeux myopes. Le chirurgien doit en tenir compte lors de la détermination de sa stratégie de centrage.

• Trois mois après une chirurgie de la cataracte, les diamètres pupillaires moyens en conditions mésopiques et photopiques ont diminué d'environ 300 µm. Le diamètre pupillaire postopératoire ne dépend pas de la sévérité de la cataracte et pourrait être prédit en pré-opératoire ; ce qui peut être utile pour identifier l'indication de certains types d'implants intra oculaires multifocaux.

• Notre étude nous a permis de décrire la forme des surfaces épithéliale et de la membrane de Bowman dans les yeux myopes. Nos résultats suggèrent que dans les procédures réfractives telles que la PRK myopique, la contribution réfractive de l'épithélium pourrait être envisagée pour améliorer la prévisibilité des resultats refractifs. Cette approche peut être particulièrement pertinente pour la PRK transépithéliale, où la cartographie de la couche épithéliale peut

améliorer la précision de la procédure. La prévision des processus de cicatrisation épithéliale pourrait également être importante.

• L'épithélium tend à réduire davantage la magnitude de l'astigmatisme, la prolacité et les irrégularités de la membrane de Bowman dans les cornées diagnostiquées non kératoconiques que dans les cornées kératoconiques.

• La chirurgie LASIK effectuée avec la suite réfractive WaveLight® (Alcon® Laboratories Inc., États-Unis) a montré de bons résultats dans notre large échantillon d'yeux. Nous pensons que certains changements cornéens et / ou internes (surface cornéenne postérieure) survenant entre un jour et 6 mois post-opératoire, peuvent limiter la valeur de l'erreur réfractive résiduelle.

université PARIS-SACLAY | ÉCOLE DOCTORALE Ondes et Matière (EDOM)

Titre : Descriptions anatomiques et méthodologiques aux fins d'optimisation de techniques de chirurgie cornéenne à visée Réfractive

Mots clés : Chirurgie réfractive, Cornée, LASIK, PKR, Pupille, Epithélium, Myopie

Résumé : Dans un contexte d'augmentation du nombre d'amétropes dans la population mondiale, et en conséquence, de l'accroissement du recours aux techniques de corrections chirurgicales, la compréhension et l'amélioration de celles-ci est un enjeu crucial. Nous avons cherché à améliorer la prédictibilité de certains résultats postopératoires dans le cas d'un LASIK (Laser-Assisted In-Situ Keratomileusis), d'une PKR (Photorefractive Keratectomy) ou d'une chirurgie de la cataracte, et ainsi de formuler des recommandations pratiques qui contribueraient au développement de stratégies de traitement davantage personnalisés.
Pour cela, nous avons utilisé prospectivement des méthodologies de « contrôle de qualité » des chirurgies sur de larges échantillons de patients.
Dans un premier temps, nous avons étudié la dynamique pupillaire dans le cadre de chirurgies au LASIK et notamment le rôle du centre pupillaire, point de référence important dans les stratégies de centrage.
Nous avons également évalué la dynamique du diamètre pupillaire et les modifications du segment antérieur sur des yeux subissant une chirurgie de la cataracte. La seconde partie du travail s'est focalisée sur le rôle de l'épithélium dans la topographique cornéenne. Nous avons comparé les topographies spéculaires de l'épithélium et de la couche de Bowman sur des cornée saines et des cornées kératoconiques, présentant une myopie faible à modérée corrigée par PKR. Enfin, dans la dernière partie de notre recherche, nous nous sommes intéressés aux changements de paramètres anatomiques de l'œil, des performances visuelles et de la qualité de vision subjective survenant dans un échantillon d'yeux myopes après un LASIK réalisé avec le laser WaveLight® Refractive Suite (Alcon® Laboratories Inc., USA).

Title: Anatomical and methodological descriptions leading to optimize corneal refractive surgery procedures

Keywords: Refractive surgery, Cornea, LASIK, PRK, Pupil, Epithelium, Myopia

Abstract: While the number of ametropic eyes in the world's population and consequently the use of surgical correction techniques is increasing, understanding and improving these techniques is a crucial issue. We sought to improve the predictability of certain postoperative results in the case of LASIK (Laser-Assisted In-Situ Keratomileusis), PRK (Photorefractive Keratectomy) and cataract surgery, and thus to formulate practical recommendations that would contribute to the development of more personalized treatment strategies.
To achieve this objective, we have prospectively used "quality control" methodologies to assess surgeries performed on large samples of patients.
First, we studied the pupillary dynamics in LASIK surgery and in particular the role of the pupillary centre, an important point of reference in the centration strategies.
We also assessed the dynamics of pupillary diameter and anterior segment changes on eyes undergoing cataract surgery. The second part of the work focused on the role of the epithelium in the corneal topography. We compared specular topographies of the epithelium and Bowman's layer in healthy and keratoconus corneas with mild to moderate myopia corrected by PRK. Finally, in the last part of our research, we were interested in the changes in anatomical parameters of the eye, visual performance and subjective quality of vision occurring in a sample of myopic eyes after LASIK performed with the WaveLight® Refractive Suite (Alcon® Laboratories Inc., USA).